UNIVERSIDAD COMPLUTENSE DE MADRID
FACULTAD DE CIENCIAS QUÍMICAS

TESIS DOCTORAL

New strategies for the treatment of cellular senescence

Nuevas estrategias para el tratamiento de la senescencia celular

MEMORIA PARA OPTAR AL GRADO DE DOCTORA

PRESENTADA POR

Ana Gil Ordóñez

DIRECTORAS

María Luz López Rodríguez
Silvia Ortega Gutiérrez
María del Mar Martín-Fontecha Corrales

Madrid

UNIVERSIDAD COMPLUTENSE DE MADRID

FACULTAD DE CIENCIAS QUÍMICAS

Departamento de Química Orgánica

NEW STRATEGIES FOR THE TREATMENT

OF CELLULAR SENESCENCE

NUEVAS ESTRATEGIAS PARA EL TRATAMIENTO DE LA SENESCENCIA CELULAR

PhD candidate

Ana Gil Ordóñez

Advisors:

Dra. María Luz López Rodríguez

Dra. Silvia Ortega Gutiérrez

Dra. María del Mar Martín-Fontecha Corrales

MADRID, 2019

UNIVERSIDAD COMPLUTENSE MADRID

DECLARACIÓN DE AUTORÍA Y ORIGINALIDAD DE LA TESIS PRESENTADA PARA OBTENER EL TÍTULO DE DOCTOR

D./Dña. Ana Gil Ordóñez,

estudiante en el Programa de Doctorado en Química Orgánica RD 99/2011,

de la Facultad de Ciencias Químicas de la Universidad Complutense de Madrid, como autor/a de la tesis presentada para la obtención del título de Doctor y titulada:

New strategies for the treatment of cellular senescence /

Nuevas estrategias para el tratamiento de la senescencia celular

y dirigida por: María Luz López Rodríguez

Silvia Ortega Gutiérrez

María del Mar Martín-Fontecha Corrales

DECLARO QUE:

La tesis es una obra original que no infringe los derechos de propiedad intelectual ni los derechos de propiedad industrial u otros, de acuerdo con el ordenamiento jurídico vigente, en particular, la Ley de Propiedad Intelectual (R.D. legislativo 1/1996, de 12 de abril, por el que se aprueba el texto refundido de la Ley de Propiedad Intelectual, modificado por la Ley 2/2019, de 1 de marzo, regularizando, aclarando y armonizando las disposiciones legales vigentes sobre la materia), en particular, las disposiciones referidas al derecho de cita.

Del mismo modo, asumo frente a la Universidad cualquier responsabilidad que pudiera derivarse de la autoría o falta de originalidad del contenido de la tesis presentada de conformidad con el ordenamiento jurídico vigente.

En Madrid, a 12 de julio de 2019

Fdo.: ANA GIL ORDÓÑEZ.

Esta DECLARACIÓN DE AUTORÍA Y ORIGINALIDAD debe ser insertada en la primera página de la tesis presentada para la obtención del título de Doctor.

"Much of life can be understood in rational terms if expressed in the language of chemistry"

Arthur Kornberg

A mi abuelo

El presente trabajo ha sido realizado en el laboratorio de Química Médica en el Departamento de Química Orgánica de la Facultad de Ciencias Químicas de la Universidad Complutense de Madrid (UCM), bajo la supervisión de la ***Catedrática Dra. Mª Luz López Rodríguez*** *y las* ***Dras. Silvia Ortega Gutiérrez*** *y* ***Mª del Mar Martín-Fontecha Corrales****, a quienes deseo expresar mi afecto y mi más profundo agradecimiento por su acogida en este grupo de investigación, por sus continuas enseñanzas, y por todo el ánimo, apoyo y confianza depositados en mí para la realización de este proyecto.*

Asimismo, quiero expresar mi agradecimiento:

Al Dr. Carles Úbeda y a Alejandra Flor del Centro Superior en Salud Pública de Valencia por la realización de los experimentos de crecimiento bacteriano.

To Prof. Jean-Charles Portais from Metatoul Centre (Metabolomics & Fluxomics Platform, Toulouse, France) for his warm reception in his laboratory. Likewise, I would like to extend this gratitude to all the people of the research group, especially to Floriant Bellver, Lindsay Peyriga and Maud Heuillet for their assistance and training during my internship.

A la Fundación "La Caixa" por darme la oportunidad de continuar mi formación científica gracias a su beca predoctoral.

Al personal del Centro de Apoyo a la Investigación (CAI) de Resonancia Magnética Nuclear, de Espectrometría de Masas, y de Citometría y Microscopía de Fluorescencia de la UCM por su ayuda y asesoramiento.

A todos los compañeros de laboratorio que han compartido conmigo estos años, con los que he vivido tan buenos momentos y de los que tantos conocimientos he adquirido: Ainoa, Adrián, Ángeles, Antonio, David, Estefanía, Fernando, Nagore y Paco. A Bellinda y Henar, por su cercanía y su constante ayuda e interés. A Andrea, por todos estos años mano a mano en el laboratorio. A Mónica, por su ayuda en mi última etapa. A Débora y Javi, por su acogida en el grupo, por inculcarme el espíritu medchem y por su ayuda y amistad. A Bea, por revolucionarnos biológicamente hablando. Y especialmente a Iván, Nora y Sergio, por convertirse en imprescindibles.

A Iván, por su completa dedicación y ayuda a los demás, por su alegría y positivismo con el que consigue alegrarnos los días. A Sergio, por su apoyo y por tantísimos momentos dentro y fuera del laboratorio, por acompañarme en el equipo microbiota, por tantas risas y viajes. A Nora, por ser 24/7, por su fiel amistad y apoyo todos estos años, por tantas conversaciones arreglando el mundo, por convertirse en mi mitad madrileña.

A todos los compañeros y amigos de los diferentes grupos de investigación del departamento. A los que estuvieron desde mis comienzos, Alfonso, Javi Ramos, Miki, Rosa y Sonia por tantas cenas, cafés y comidas de domingos. Y a los que llegaron en mi última etapa, Alejandro, Diego, Mª Carmen y Sergio, por descubrirme el mundo cluster (y su olor) y por tantísimas tardes, salidas y momentos llenos de risas y anécdotas.

Gracias a todos por ponérmelo fácil y hacerme sentir en casa estos cuatro años.

A toda la gente que a lo largo de estos años me ha acompañado en este recorrido. No puedo sentirme más afortunada de estar así rodeada, apoyada y cuidada. Gracias por estar siempre ahí y hacerme feliz, sin vosotros nada de esto hubiera sido posible. A los que llevan desde la infancia (Bea, Elena y Mikel) y a los que la vida ha ido poniendo en mi camino palentino-pucelano (Adri, Ángel, Elena, Jéssica, Quique y Noelia) y madrileño (Alba, Elena, Elvira, Paula, Raúl y Sergio). Al equipo Toulouse (Ana, David, Eliseo, Gorka, Iranzu, Jordan, los Pablos y Violeta), por hacer de mi estancia una experiencia inmejorable.

A mi familia, en especial a mis padres y mi hermana, por su apoyo, paciencia, ayuda, ánimo y confianza incondicional, por los valores que me han inculcado y sin los cuales no hubiera sido capaz de llegar hasta aquí. Espero que algún día lleguen a estar tan orgullosos de mí como lo estoy yo de ellos.

GRACIAS.

TABLE OF CONTENTS

ABBREVIATIONS AND ACRONYMS

Throughout this manuscript, abbreviations and acronyms recommended by the *American Chemical Society* for the areas of Organic and Medicinal Chemistry, revised by the *Journal of Organic Chemistry*[i] and *Journal of Medicinal Chemistry*[ii] in December 2018 have been used. We have further employed those indicated below.

ACN	Acetonitrile
AFC	*N*-acetyl-*S*-farnesyl-L-cysteine
App	Apparent
Br	Broad
BFC	Biotinyl-*S*-farnesyl-L-cysteine
BSA	Bovine serum albumin
CAI	Centro de asistencia a la investigación
DIAD	Diisopropyl azodicarboxylate
DIPEA	*N*,*N*-Diisopropylethanamine
DMEM	Dulbecco´s modified eagle m
DTT	Dithiothreitol
EDC	1-Ethyl-3-(3-dimethylaminopropyl)carbodiimide
FACS	Fluorescence activated cell sorting
FBS	Fetal bovine serum
FTase	Farnesyltransferase
FTI	Farnesyltransferase inhibitor
H2AX	Histone 2AX
HGPS	Hutchinson-Gilford progeria syndrome
HLM	Human liver microsomes
HOBt	1-Hydroxybenzotriazol
HRMS	High resolution mass spectrometry
HSA	Human serum albumin
ICMT	Isoprenylcysteine carboxyl methyltransferase
LAH	Lithium aluminium hydride
MLM	Mouse liver microsomes
MTT	3-(4,5-dimethylthiazol-2-yl)-2,5-diphenyltetrazolium bromide
OD	Optical density
PBS	Phosphate buffered saline
PBS-T	Phosphate buffered saline with 0.1% Triton X-100
PEGA	Polyethylene glycol polyacrylamide
PFA	Paraformaldehyde

PyBOP	Benzotriazol-1-yl-oxytripyrrolidinophosphonium hexafluorophosphate
Rce1	Ras converting enzyme 1
r_t	Retention time
rt	Room temperature
SAM	*S*-adenosyl-L-methionine
sem	Standard error of the mean
TBS	Tris buffered saline
TBS-T	Tris buffered saline with 0.05% of tween 20
TBTA	Tris(benzyltriazolylmethyl)amine
TCEP	Tris(2-carboxyethyl)phosphine
TIC	Total ion current
TIS	Triisopropylsilane
TM	Transmembrane helix
UCM	Universidad Complutense de Madrid
ZMPSTE24	Zinc metalloprotease STE24

[i] https://pubsapp.acs.org/paragonplus/submission/joceah/joceah_abbreviations.pdf
[ii] http://pubsapp.acs.org/paragonplus/submission/jmcmar/jmcmar_abbreviations.pdf

RESUMEN

RESUMEN

NUEVAS ESTRATEGIAS PARA EL TRATAMIENTO DE LA SENESCENCIA CELULAR

La senescencia celular es un proceso biológico irreversible que aparece después de una etapa de estrés celular y detiene la proliferación de células disfuncionales o dañadas. Las células senescentes se acumulan en nuestro cuerpo con la edad, por lo que la regulación de este proceso podría tener un efecto importante en la esperanza de vida y el envejecimiento. Con este fin, en el presente trabajo proponemos dos enfoques diferentes para abordar el proceso de senescencia celular. En el primero de ellos (Capítulo A), el objetivo es el desarrollo de inhibidores de la enzima isoprenilcisteína carboxil metiltransferasa (ICMT) para el tratamiento de la progeria como un modelo de envejecimiento acelerado. En la segunda aproximación (Capítulo B), teniendo en cuenta la posible influencia que los metabolitos de la microbiota humana pueden tener en el envejecimiento, proponemos una nueva estrategia para la identificación de los metabolitos de la microbiota. En particular, se pretende la puesta a punto de dicha metodología para poder abordar un proyecto más amplio que permita el estudio fenotípico en senescencia de los metabolitos identificados.

Capítulo A: Nuevos inhibidores de la enzima ICMT para el tratamiento de la progeria

El síndrome de progeria de Hutchinson-Gilford (HGPS, por sus siglas en inglés) o progeria se describió por primera vez en 1886 y es una patología causada por una mutación del gen LMNA que produce una versión aberrante de la proteína lámina A llamada progerina, que se acumula en la membrana nuclear e induce anomalías estructurales. Durante las últimas décadas, se han realizado grandes esfuerzos en la búsqueda de tratamientos para la progeria, proporcionando hasta este momento solo una eficacia moderada. En el presente trabajo hemos centrado nuestra atención en el desarrollo de inhibidores de la enzima ICMT para el tratamiento de la progeria, debido a evidencias existentes que muestran que el bloqueo genético de esta enzima mejora

tanto in vitro como in vivo el fenotipo de la progeria. Con este propósito, y sobre la base de un trabajo previo realizado en nuestro grupo de investigación dirigido al desarrollo de inhibidores de la enzima ICMT para el tratamiento de tumores dependientes de la proteína Ras, iniciamos un programa de química médica a partir del compuesto **3** (inhibidor de ICMT con capacidad citotóxica) con el objetivo de obtener nuevos compuestos que conserven la capacidad de inhibir ICMT pero que carezcan de citotoxicidad (Figura 1). En este trabajo, hemos identificado el compuesto **59**, el cual mostró una buena capacidad para inhibir la enzima ICMT, no fue citotóxico, presentó un buen perfil farmacocinético y, lo que es más importante, aumentó la viabilidad de las células progeroides de un 41% a un excelente 93%. Este compuesto se seleccionó para el estudio de su efecto sobre células progeroides humanas, en las que mostró una muy buena capacidad para mejorar la viabilidad celular, reducir el daño del ADN, estimular la proliferación celular y reducir los niveles de progerina en la membrana nuclear. Estos resultados resaltan la capacidad del compuesto **59** para mejorar las características fenotípicas de la progeria, por lo que se están realizando actualmente en nuestro laboratorio experimentos in vivo en un modelo progeroide de ratón para confirmar la eficacia del compuesto **59** y por tanto, de un inhibidor de la ICMT para tratar la progeria.

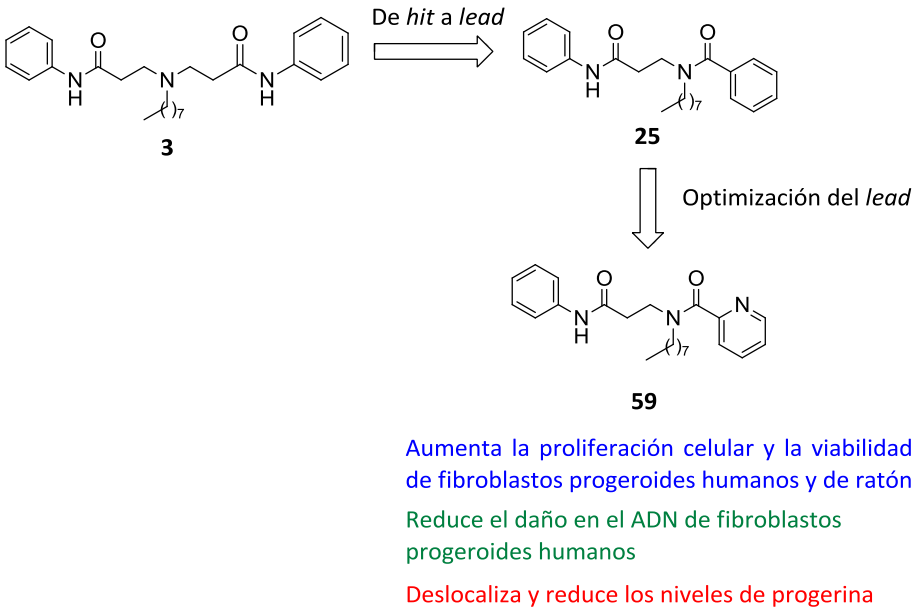

Figura 1. Programa de química médica realizado a partir del compuesto **3** para la obtención del compuesto **59**, inhibidor de la enzima ICMT para el tratamiento de la progeria.

Capítulo B: Identificación de nuevos metabolitos producidos por la microbiota humana

La microbiota humana es un complejo ecosistema de nuestro cuerpo que está constituido por múltiples microorganismos que juegan un papel importante en la salud debido a su interacción con el huésped a través de la secreción de metabolitos, que son capaces de regular funciones biológicas. Investigaciones recientes han demostrado la relación directa entre la microbiota humana y sus metabolitos con varias enfermedades como el cáncer, la diabetes, los trastornos del sistema inmunológico e incluso con la esperanza de vida y el envejecimiento. Sin embargo, debido a la complejidad del metaboloma, la mayoría de estos metabolitos no se conocen, aunque se han descrito varias estrategias en un intento de identificarlos. Estas evidencias muestran la necesidad de desarrollar nuevas estrategias para la identificación de metabolitos. Para ello, en el presente trabajo, hemos diseñado una nueva metodología que nos permitirá identificar los metabolitos producidos por la microbiota humana. Esta plataforma metabolómica se basa en el uso de precursores marcados de los metabolitos de la microbiota humana (Figura 2). La realización de esta metodología implica varios pasos: i) incubación de cepas seleccionadas de bacterias en presencia de precursores marcados para obtener metabolitos marcados; ii) aislamiento del metaboloma; iii) captura de los metabolitos marcados a través de una reacción bioortogonal con un reactivo de captura apropiado; iv) aislamiento de los metabolitos capturados, y v) elucidación estructural de estos metabolitos empleando técnicas de espectrometría de masas (EM) y resonancia magnética nuclear (RMN).

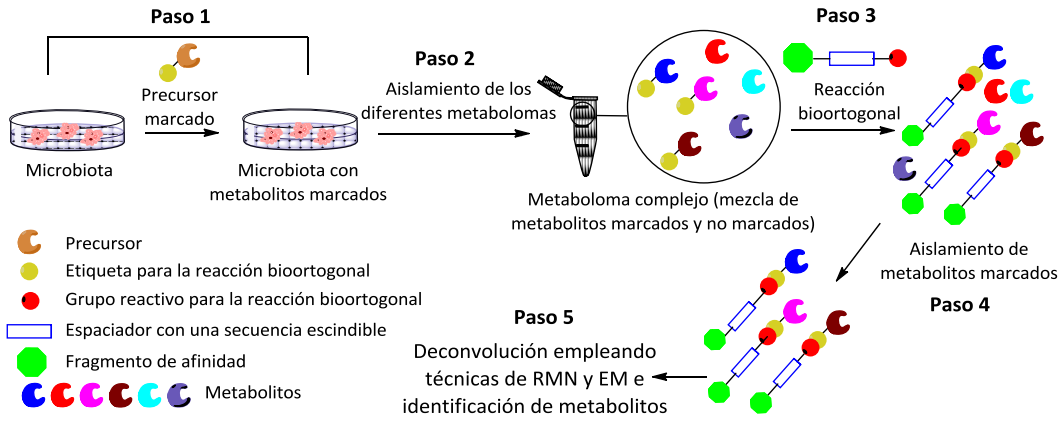

Figura 2. Estrategia diseñada para la identificación de metabolitos de la microbiota humana.

Como prueba de concepto, hemos llevado a cabo esta metodología utilizando azido azúcares como precursores marcados. La incorporación de los azido azúcares se ha evaluado en una variedad de cepas representativas de bacterias de la microbiota humana empleando técnicas de ^{1}H RMN y experimentos de citometría de flujo y análisis por microscopía confocal. Estos experimentos nos han permitido confirmar qué azúcar marcado era incorporado por qué cepa de bacterias. A continuación, para poder capturar los azido metabolitos formados, se ha utilizado una reacción de cicloadición azida-alquino catalizada por cobre (I). Para ello, se sintetizaron varias moléculas que contienen en su estructura un alquino terminal. Estos reactivos de captura poseen, además del alquino terminal, un fragmento de afinidad para aislar los metabolitos capturados y una secuencia escindible para la liberación final del metabolito. Después de optimizar el aislamiento de los diferentes metabolomas (paso 2, Figura 2), la reacción bioortogonal con el reactivo de captura (paso 3, Figura 2) y el aislamiento de los metabolitos marcados (paso 4, Figura 2), se ha abordado la identificación de los metabolitos capturados (paso 5, Figura 2). Para poder llevar a cabo este objetivo final, se ha realizado la plataforma completa a mayor escala con el fin de completar la elucidación estructural de los compuestos aislados utilizando técnicas de RMN y EM, experimentos que se están completando en la actualidad.

Este paso final constituirá la validación de la metodología propuesta para la identificación de los metabolitos producidos por la microbiota humana.

SUMMARY

SUMMARY

New strategies for the treatment of cellular senescence

Cellular senescence is a biological irreversible process that appears after cellular stress and stops the proliferation of dysfunctional or damaged cells. Senescent cells are accumulated in our body with aging, so the regulation of this process could have an important effect in healthspan and aging. Towards this end, in the present work we propose two different approaches. In the first one (Chapter A), the objective is the development of inhibitors of isoprenylcysteine carboxyl methyltransferase (ICMT) enzyme for targeting progeria as a model of accelerated aging. In the second approach (Chapter B), and taking into account the possible influence that metabolites of the human microbiota can have in aging, we propose an innovative strategy for the identification of microbiota metabolites in the framework of a broader project aimed at the phenotypic study of the identified metabolites in senescence.

Chapter A: New ICMT inhibitors for the treatment of progeria

Hutchinson-Gilford Progeria Syndrome (HGPS) or progeria was first described in 1886 and it is a pathology caused by a mutation of the LMNA gen that produces an aberrant version of Lamin A protein called progerin, which accumulates in the nuclear envelope inducing structural abnormalities. During the last decades, huge efforts have been done in the search of treatments for progeria, providing up to this moment only a modest benefit. In the present work we have focused our attention on the development of ICMT inhibitors for the treatment of progeria, due to reported evidences showing that the genetic blockade of this enzyme improves both in vitro and in vivo the phenotype of progeria. For that purpose, and based on a previous work carried out in our investigation group aimed at the development of ICMT inhibitors for targeting Ras-driven tumours, we have started a medicinal chemistry program starting from compound **3** (ICMT inhibitor with cytotoxic properties) to obtain new compounds that retain the ability to inhibit ICMT but are devoid of cytotoxicity (Figure 1). In this work,

we have identified compound **59** that showed a good percentage of inhibition of ICMT, was not cytotoxic, presented a good pharmacokinetic profile, and importantly, was able to improve the viability of progeroid cells from 41% to an excellent 93%. This compound was selected for the study of its effect on human progeroid cells, being capable of improving the cellular viability, reducing DNA damage, stimulating cellular proliferation, and reducing the levels of progerin in the nuclear membrane. These results highlight the capacity of compound **59** to ameliorate the hallmarks of progeria. Hence, its in vivo efficacy in a mouse model of progeria is currently being performed in our laboratory in order to confirm the efficacy of an ICMT inhibitor for treating progeria.

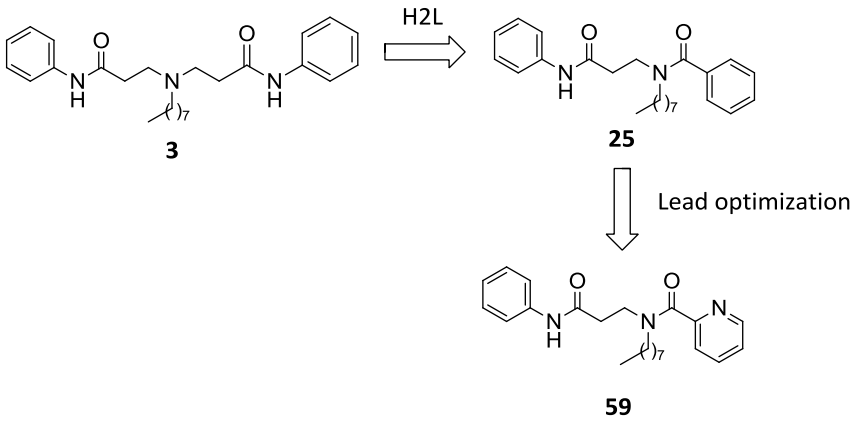

Figure 1. Medicinal chemistry program carried out starting from compound **3** to obtain compound **59** as an ICMT inhibitor for treating progeria.

Chapter B: Identification of new molecules produced by the human microbiota

The human microbiota is a complex ecosystem belonging to our body that is constituted by multiple microorganisms that play an important role in human health due to their interaction with the host through the secretion of metabolites, which are able to regulate biological functions. Recent investigations showed a direct relationship between the human microbiota and its metabolites with several diseases such as cancer, diabetes, immune system disorders, and even with healthspan and aging. However, due to the complexity of the metabolome, most of these metabolites still remain unknown, although several strategies have been performed in an attempt to identify them. This context makes clear the need of new strategies for the identificacion of metabolites. For that purpose, in the present work, we have designed a novel strategy which will allow us to identify metabolites produced by the human microbiota. This metabolomic platform is based on the use of tagged precursors of microbiota metabolites (Figure 2). The fulfillment of this methodology implies several steps: i) incubation of selected strains of bacteria in the presence of tagged precursors in order to obtain tagged metabolites; ii) isolation of the metabolome; iii) capture of tagged metabolites through a bioorthogonal reaction with an appropriate capture reagent; iv) isolation of captured metabolites, and v) structural elucidation of these metabolites by mass spectrometry (MS) and nuclear magnetic resonance (NMR).

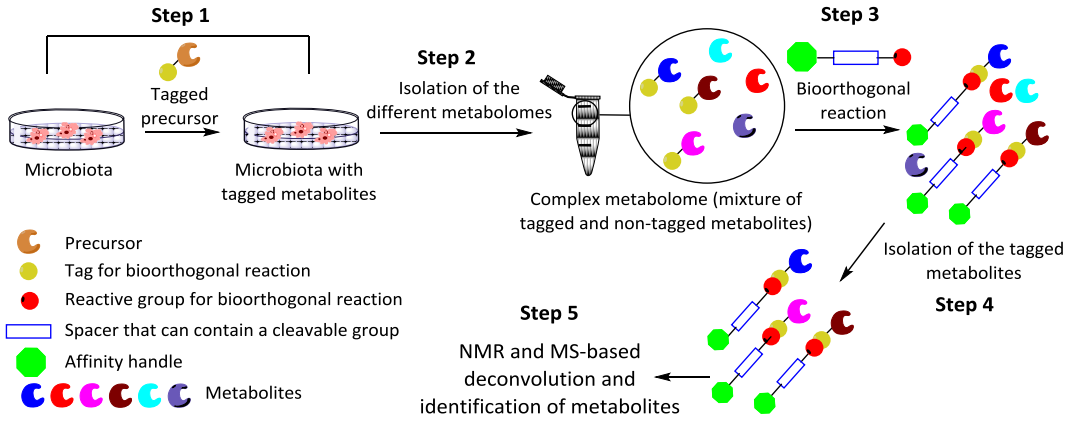

Figure 2. Innovative strategy designed for the identification of metabolites of the human microbiota.

As a proof of concept, we have set up this methodology using azido sugars as tagged precursors. The incorporation of the azido sugars has been assessed in a variety of representative strains of bacteria from the human microbiota. For that purpose, a ^{1}H NMR-based screening, and fluorescence-activated cell sorting (FACS) and confocal microscopy experiments have been carried out. These experiments have enabled us to confirm which tagged sugar was metabolized for each strain of bacteria. Then, we used the copper (I)-catalyzed azido-alkyne cycloaddition reaction to capture the azido metabolites. For this purpose, several terminal alkyne containing molecules were synthesized. These capture reagents contained, besides the terminal alkyne, an affinity handle to isolate the captured metabolites and a cleavable sequence for the final release of the metabolite. After optimizing the isolation of the different metabolomes (step 2, Figure 2), the bioorthogonal reaction between them and the capture reagent (step 3, Figure 2), and the isolation of tagged metabolites (step 4, Figure 2), we have addressed the identification of captured metabolites. This final objective required to carry out the entire platform in higher scale and complete the structural elucidation using NMR and MS techniques, experiments that are currently being completed.

This final step will constitute the validation of the proposed methodology for the identification of metabolites produced by the human microbiota.

GENERAL INTRODUCTION

GENERAL INTRODUCTION

Cellular senescence is a biological irreversible process which rises up as a response to cellular stress and stops the proliferation of dysfunctional or damaged cells. Hence, this physiological process and, consequently, its regulation, can have an important role in aging or pathologies such as cancer.[1,2] Senescent cells are accumulated in several tissues and organs with aging where they exert negative structural and functional effects due to the components they secrete.[3,4] Studies carried out by suppression of $p16^{Ink4a}$, a cyclin-dependent kinase inhibitor whose levels are increased by aging,[5] showed delayed age-dependent pathologies. These data confirmed the role of cellular senescence in accelerating aging phenotypes and support the hypothesis that healthspan and tissue dysfunction can be delayed by removal of senescent cells.[6-8] Therefore, new therapeutic approaches for the treatment of cellular senescence could represent attractive alternatives for delaying age-related diseases and enhancing healthspan. Accordingly, the development of senolytic drugs, which are compounds that induce apoptosis of senescent cells, has been a focus of research in the recent years. In this context, in our laboratory, we are following two parallel strategies towards this end (Figure 1): (i) a target-driven approach, focused on the enzyme isoprenylcysteine carboxyl methyltransferase (ICMT), whose inhibitors can delay aging, and (ii) an approach aimed at the identification of new molecules produced by the human microbiota able to stop or reverse cellular senescence.

In the first approach our objective is the development of new ICMT inhibitors for the treatment of progeria, a pathology characterized by the presence of aging symptons in children (Chapter A). Considering that the genetic mouse knockout of ICMT improves the phenotype of progeria,[9] this disease can be used as a model of accelerated aging. Cells derived from progeria patients showed increased levels of senescence markers[10]

and it is known that progerin expression is increased with aging in general population non suffering from progeria.[11] Hence, it is conceivable that ICMT inhibition cannot only improve progeria, but also delay physiological senescence.

In the second approach, we aim to develop an innovative strategy to identify metabolites produced by the human microbiota (Chapter B). The important role of microbiota and its metabolites in different (patho)physiological processes has started to emerge in the last decades including its relationship with senescence.[12-14] These findings strongly support the hypothesis that metabolites produced by the human microbiota could represent a source of new molecules endowed with interesting biological activities, and in particular in aging. However, the large complexity of the human microbiome makes the identification of microbiota metabolites a daunting task that cannot be successfully addressed by the current methodologies making necessary the development of new strategies to carry out this objective, which could constitute the first step for the development of new molecules able to stop senescent cells.

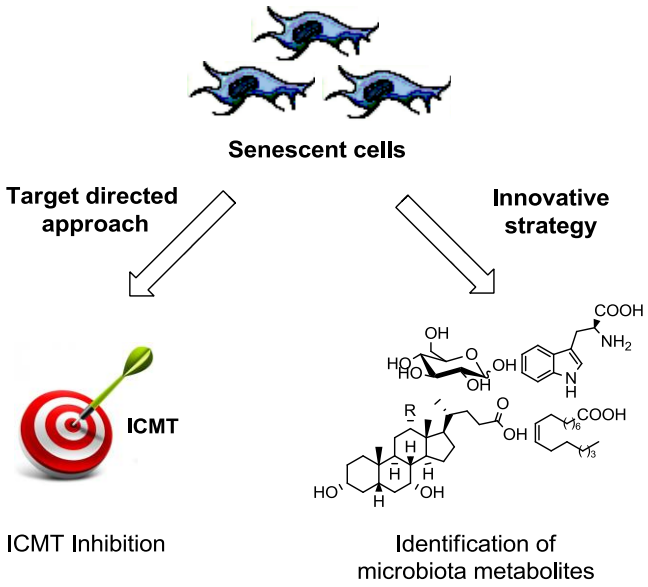

Figure 1. Proposed strategies for targeting cellular senescence.

REFERENCES

1. van Deursen, J. M., The role of senescent cells in ageing. *Nature* **2014**, *509*, 439-446.

2. Kuilman, T.; Michaloglou, C.; Mooi, W. J.*, et al.*, The essence of senescence. *Genes Dev.* **2010**, *24*, 2463-2479.

3. Rodier, F.; Campisi, J., Four faces of cellular senescence. *J. Cell Biol.* **2011**, *192*, 547-556.

4. Coppe, J. P.; Patil, C. K.; Rodier, F.*, et al.*, Senescence-associated secretory phenotypes reveal cell-nonautonomous functions of oncogenic RAS and the p53 tumor suppressor. *PLoS Biol.* **2008**, *6*, 2853-2868.

5. Krishnamurthy, J.; Torrice, C.; Ramsey, M. R.*, et al.*, Ink4a/Arf expression is a biomarker of aging. *J. Clin. Invest.* **2004**, *114*, 1299-1307.

6. Baker, D. J.; Wijshake, T.; Tchkonia, T.*, et al.*, Clearance of p16Ink4a-positive senescent cells delays ageing-associated disorders. *Nature* **2011**, *479*, 232-237.

7. Baker, D. J.; Childs, B. G.; Durik, M.*, et al.*, Naturally occurring p16(Ink4a)-positive cells shorten healthy lifespan. *Nature* **2016**, *530*, 184-189.

8. Jeon, O. H.; Kim, C.; Laberge, R. M.*, et al.*, Local clearance of senescent cells attenuates the development of post-traumatic osteoarthritis and creates a pro-regenerative environment. *Nat. Med.* **2017**, *23*, 775-781.

9. Ibrahim, M. X.; Sayin, V. I.; Akula, M. K.*, et al.*, Targeting isoprenylcysteine methylation ameliorates disease in a mouse model of progeria. *Science* **2013**, *340*, 1330-1333.

10. Gordon, L. B.; Rothman, F. G.; Lopez-Otin, C.*, et al.*, Progeria: a paradigm for translational medicine. *Cell* **2014**, *156*, 400-407.

11. Scaffidi, P.; Misteli, T., Lamin A-dependent nuclear defects in human aging. *Science* **2006**, *312*, 1059-1063.

12. Cho, S. Y.; Kim, J.; Lee, J. H.*, et al.*, Modulation of gut microbiota and delayed immunosenescence as a result of syringaresinol consumption in middle-aged mice. *Sci. Rep.* **2016**, *6*, 1-22.

13. Kim, S.; Jazwinski, S. M., The gut microbiota and healthy aging: a mini-review. *Gerontology* **2018**, *64*, 513-520.

14. Bischoff, S. C., Microbiota and aging. *Curr. Opin. Clin. Nutr. Metab. Care* **2016**, *19*, 26-30.

CHAPTER A

ICMT INHIBITORS FOR THE TREATMENT OF PROGERIA

INTRODUCTION AND OBJECTIVES

1. INTRODUCTION AND OBJECTIVES

Hutchinson-Gilford Progeria Syndrome (HGPS) or progeria is a congenital and lethal pathology characterized by the premature presence of aging symptoms in children. The genetic basis of this illness were established in 2003[1,2] although it was first originally described by J. Hutchinson[3] and H. Gilford[4] a century ago. The characteristic physical symptoms associated to this illness include alopecia, prominent eyes and ears, thin lips, small jaw, and low weight and height. Furthermore, patients suffer from phalange and clavicle osteolysis and arteriosclerosis, which finally lead to the death of the 90% of patients at the premature age of 13.[5-7]

This illness is caused by mutations in the LMNA gene, which codifies for prelamin A.[1,2] Mutations in LMNA gene are responsible of a type of illnesses called laminopathies, which include neuropathologies, muscular dystrophies, cardiomiopathies, and most progeroid syndromes due to the structural role of lamins A, B, and C in the nuclear lamin.[8] Among the different lamins, nuclear lamin A is located in the nuclear membrane and it is responsible for the form and size of the cellular nucleus. Moreover, this protein is involved in the structural stability, organization, replication and transcription of DNA.[9] Lamin A belongs to the CAAX family of proteins. They are characterized by a carboxyl terminal region that contains the CAAX box motif, where C is cysteine, A is an aliphatic residue and X is one of several different amino acids. The presence of the CAAX sequence is characteristic of a post-translational processing by which the CAAX proteins turn into their active biologically form, in this case, lamin A (Figure 1).[10] These post-translational modifications consist in the attachment of a farnesyl group to the cysteine residue by the farnesyltransferase (FTase) enzyme, proteolysis of the –AAX tripeptide by Ras converting enzyme 1 (Rce1) endoprotease, carboxymethylation of the C-terminal cysteine by isoprenylcysteine carboxyl methyltransferase (ICMT) enzyme, and enzymatic cleavage of the terminal 15 amino

acids, including the farnesylated cysteine, by Rce1 or Zinc metalloprotease STE24 (ZMPSTE24) endoprotease.

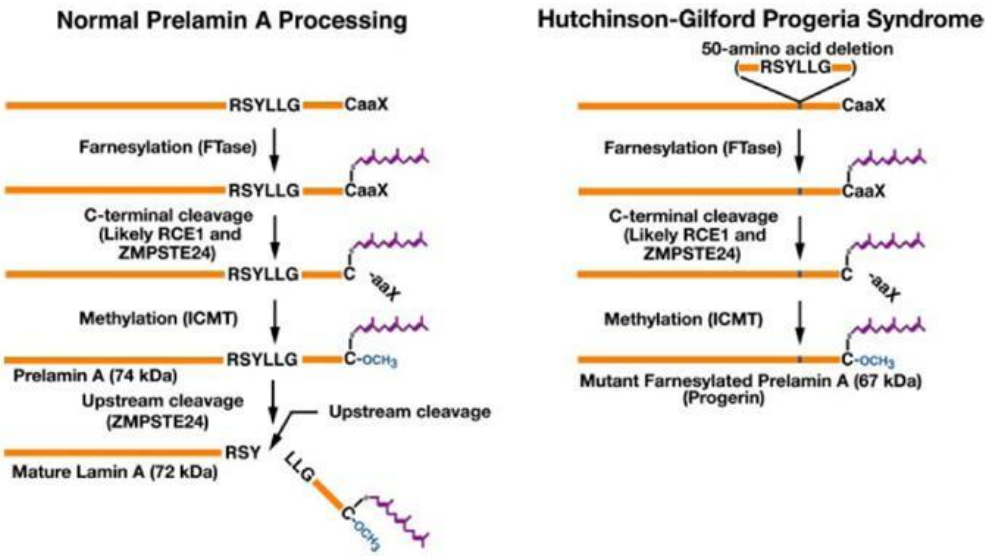

Figure 1. The nuclear prelamin A post-translational processing in normal and HGPS cells. Taken from *Annu. Rev. Genom. Hum. G*. **2009**, *10*, 153-174.

In progeria, the majority of the cases are caused by the mutation G608G, which is responsible for the substitution of a glycine coming from a GGC triplet by a glycine coming from a GGT triplet. This mutation produces a mRNA 150 nucleotides shorter. Its translation creates a mutated form of lamin A, called progerin, with 50 aminoacids less in its terminal carboxyl group that cannot be post-translationally processed in the correct manner due to the absence of the cleavage site of the terminal 15 amino acids. Therefore, this permanently farnesylated uncleaved and methylated progerin is abnormally accumulated in the nuclear membrane triggering, by yet-to-be discovered mechanisms, the many cellular and organismal symptoms of progeria.

Currently, there is only one available therapeutic treatment for progeria patients, lonafarnib (Figure 2), a farnesyl transferase inhibitor (FTI) that acts by blocking the farnesylation step, thus decreasing the levels of farnesylated mutant prelamin A. Lonafarnib monotherapy provides some improvement in vascular stiffness, bone structure, and audiological status, and is estimated to increase mean survival by 1.6 years.[11-13] However, the use of lonafarnib was previously questioned due to the evidences that FTI treatment resulted in alternative geranylgeranyltransferase mediated prenylation of prelamin A and progerin,[14] similar to the effect of FTIs on some oncoproteins in cancer therapy. Then, a trial was conducted to test the efficacy of

lonafarnib in combination with a statin (pravastatin) and a bisphosphonate (zoledronate) (Figure 2). This triple-drug therapy showed an additional improvement in bone mineral density, but there was no cardiovascular improvement compared with lonafarnib monotherapy.[15] Thus, although farnesylated progerin appears to play a major role in progeria, current therapies to prevent progerin farnesylation appear to provide only a modest benefit.[16] Hence, finding more effective therapies is still an important unmet need.[17,18]

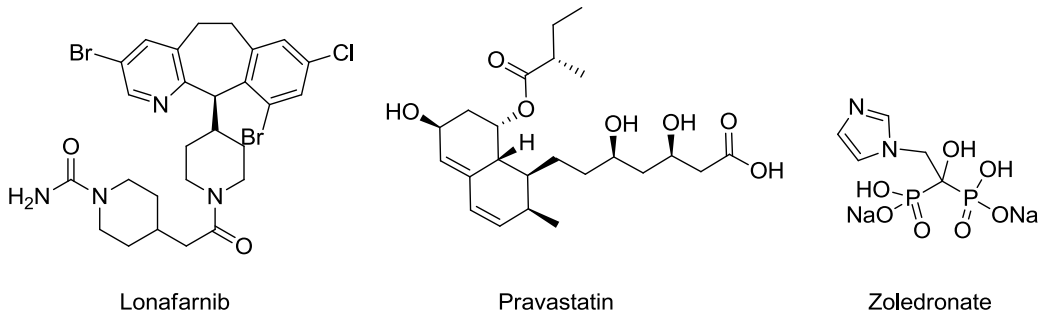

Figure 2. Main drugs used to treat progeria.

In this context, it has been recently described that inhibition of the post-translational methylation step improves progeria cellular senescence in vitro and ameliorates disease and early death in a progeroid mouse model.[19] Considering that the methylation step is catalyzed by the enzyme ICMT, this finding suggests that inhibitors of this enzyme could be useful for the treatment of progeria. Given that the efforts have been focused on the role of prenylation, the influence of methylation on the toxicity or cellular localization of progerin has not been specifically addressed. In addition, it has been shown that extremely subtle structural changes in the carboxyl terminus of progerin can be associated with major differences in the toxicity of the protein,[20] bringing about the possibility that the non-methylated form of progerin did not accumulate at the nuclear rim, was less toxic than its methylated counterpart, and improved the symptoms of the disease.

Then, the development of ICMT inhibitors could represent a promising strategy for treating this illness and would allow the validation of ICMT as a bona fide therapeutic target for the treatment of progeria. However, its clinical validation has been hampered by the lack of synthetic inhibitors and to date only one compound able to block ICMT activity, cysmethynil[21] (Figure 3), has been thoroughly characterized. This inhibitor effectively blocks the anchorage independent growth in a human colon cancer cell line[21] and impairs tumor progress in mice.[22,23] Nonetheless, its advancement towards clinical

phases has been hindered by its limited potency in vitro in some cancer cell lines[22,24] and in vivo, where doses between 100 and 200 mg/kg are usually required to observe inhibition of tumor growth.[22,23] Further efforts in the development of more efficacious ICMT inhibitors led to the identification of several structural scaffolds able to inhibit in some extent ICMT (Figure 3),[25-28] including indole derivatives,[29,30] some of them structurally similar to cysmethynil but with improved cellular antiproliferative activities,[24,31] farnesyl cysteine analogs,[32-34] and a series of tetrahydropyrane (THP) derivatives. Among them, one of these THP derivatives is the most potent ICMT inhibitor described to date, with an IC_{50} value of 1.3 nM, although this excellent in vitro value led only to a modest reduction in cell viability in different tumor cell lines.[35]

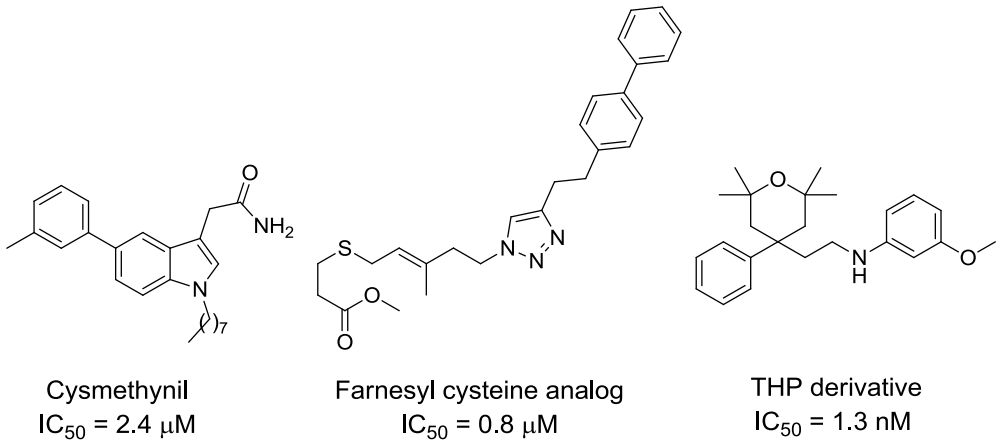

Figure 3. Representative ICMT inhibitors.

In order to identify new ICMT inhibitors with in vivo efficacy as a promising approach to anticancer drug development for treating challenging Ras-driven tumors, our research group carried out a screening of our in-house library against ICMT inhibition. This research led to the identification of compound **1** as an initial hit (Figure 4A). This compound blocked ICMT activity, albeit with moderate potency (25% inhibition of the ICMT activity at 50 μM), making necessary further optimization. As a first step in that direction, docking studies with a homology model of the human enzyme (h-ICMT) using as template the *Tribolium castaneum* enzyme (Tc-ICMT),[36] the only eukaryotic ICMT described up to date (Figure 4), were carried out.[37] Analysis of the complexes between the h-ICMT with the inhibitor cysmethynil (Figure 4B), or *N*-acetyl-*S*-farnesyl-L-cysteine (AFC), the minimal structural element recognized by ICMT (Figure 4C) showed the possibility of adding, in compound **1**, a hydrophobic tail to expand toward the membrane through the substrate tunnel, in a similar manner to the farnesyl moiety of AFC or the octyl chain of cysmethynil. Based on this model, derivative **2** was synthetized

(Figure 4D). Remarkably, this compound displayed an enhanced capacity to inhibit ICMT activity (55% inhibition at 50 μM). A closer look to the interaction model between compound **2** and the protein (Figure 4D) highlighted the presence of a cluster of aromatic amino acids in the binding site formed by Trp216 of transmembrane helix (TM) 7 and Phe243 and Phe244 of TM8. Hence, it would be conceivable that the replacement of the methyl and cyclohexyl substituents of compound **2** by phenyl rings, able to establish π-π stacking interactions, allowed for an improvement of affinity towards the protein. Consequently, we designed compound **3**, which fitted perfectly in the model (Figure 4E). One phenyl ring can fill the pocket formed by Arg174 of TM6, Tyr213 and Trp216 of TM7 and Phe243 and Phe244 of TM8. The amide group is hydrogen bonding Arg247 of TM8 and the octyl chain of the ligand fills the lipid site. The other phenyl group is placed between the TM5-TM8 crevice, while the adjacent amide group is able to establish a hydrogen bond with Ser129 on the top of TM5 (Figure 4E). Hence, compound **3** was synthesized and tested for ICMT activity, showing an excellent 93% enzyme activity inhibition at 50 μM and an IC_{50} value of 2 μM.[37,38] This compound significantly impairs the membrane association of the four Ras isoforms, leading to a decrease of Ras downstream signaling pathways. In addition, **3** induces cell death in a variety of Ras-mutated tumor cell lines and increases survival in an in vivo model of acute myeloid leukemia, which validate ICMT as a valuable target for the treatment of Ras-driven tumors.

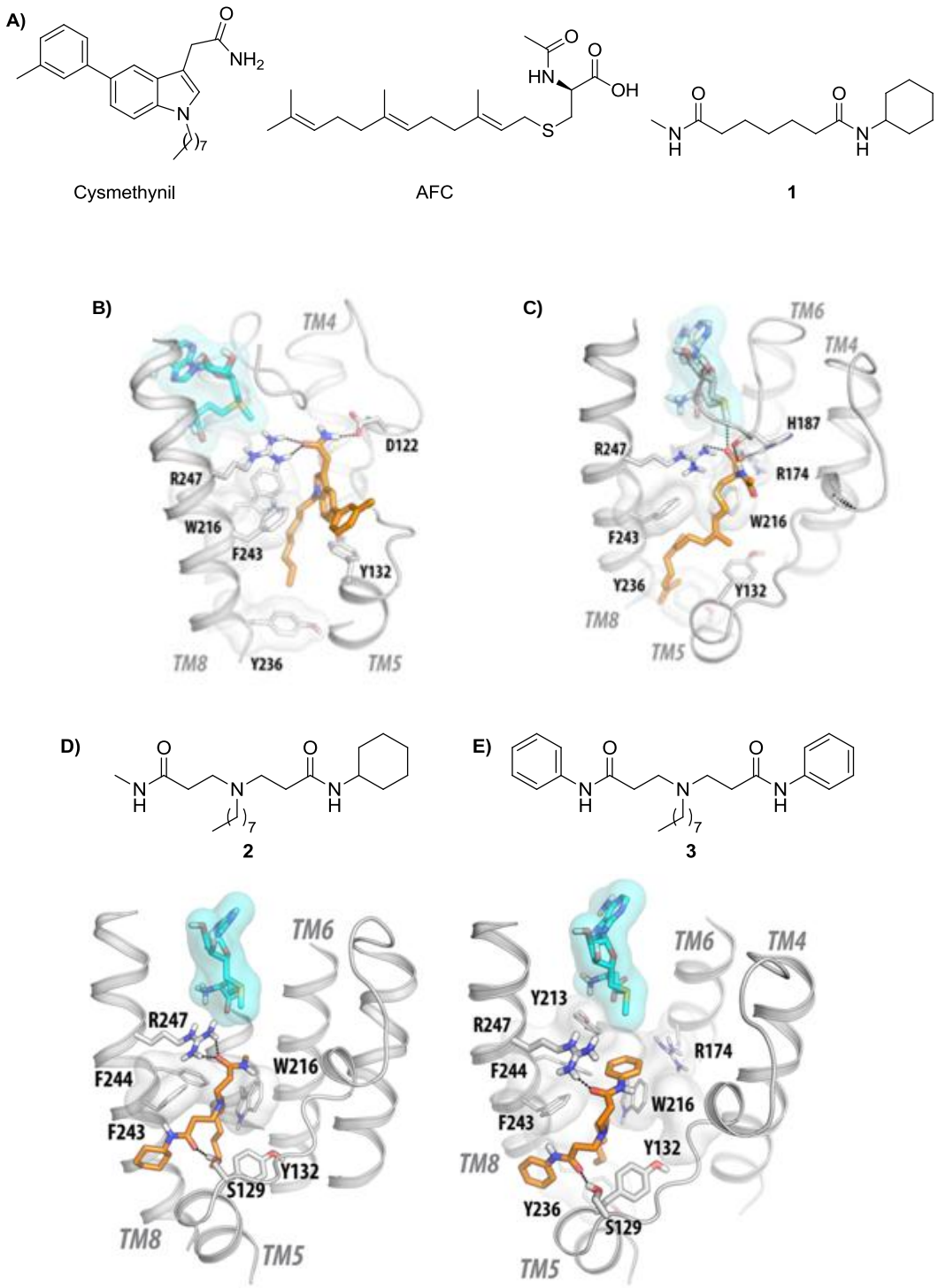

Figure 4. A) Structures of cysmethynil, *N*-acetyl-*S*-farnesyl-L-cysteine (AFC), and compound **1**. Tc-ICMT-derived homology models of h-ICMT in complex with *S*-adenosylmethionine (SAM) cofactor (cyan) and cysmethynil (B); AFC (C); compound **2** (D); and compound **3** (E). All inhibitors are represented in orange. Tc-ICMT PDB code: 5V7P.

Hence, compound **3** was selected as the initial hit to carry out a medicinal chemistry program in order to obtain compounds able to inhibit ICMT but devoid of cytotoxicity so that they can be used for improving the progeria phenotype in a cellular context and in vivo. This overall objective involves the following steps:

1. Hit to lead process
2. Lead optimization
3. Study of selected compound(s) to improve the cellular phenotype of progeria

RESULTS AND DISCUSSION

2. RESULTS AND DISCUSSION

2.1. Hit to lead process

As a first step in the search of compounds with good ICMT inhibitory activity but lacking cytotoxicity, three types of structural modifications were envisioned (Figure 5): i) modifications in the hydrophobic chain (compounds **4**-**13**), ii) changes in the secondary amides (compounds **14**-**20**), and iii) modifications in the spacer between the carbonyl groups and the central tertiary amine (**21**-**25**).

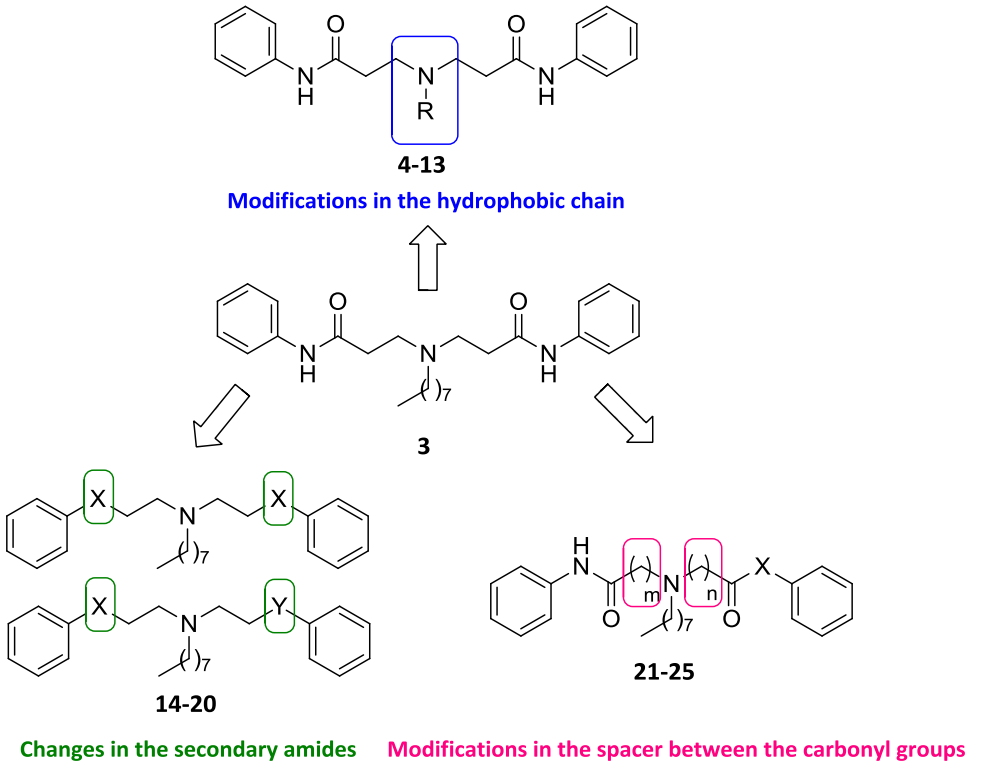

Figure 5. Compounds **4**-**25**.

2.1.1. Modifications in the hydrophobic chain

We studied the influence of the length of the hydrophobic chain and the introduction of heteroatoms in this chain. For that purpose, a new series of compounds was considered where the hydrophobic *n*-octyl chain was substituted by shorter alkyl groups (compound **4**-**6**) or its polarity was increased by introduction of oxygen or nitrogen atoms (compounds **7**-**13**). Synthesis of compounds **4**-**13** was carried out following the approach depicted in Scheme 1. Aza-Michael reaction of acrylamide **26** with the appropriate primary amines (commercial or **27**-**30**) in the presence of 1,8-diazabicyclo[5.4.0]undec-7-ene (DBU) gave final compounds **4**-**11**. The nucleophilic substitution of bromoderivative **31** with commercial 2-(4-ethylpiperidin-1-yl)ethanamine or synthesized piperazinyl amine **32** in the presence of triethylamine afforded compounds **12** and **13**.

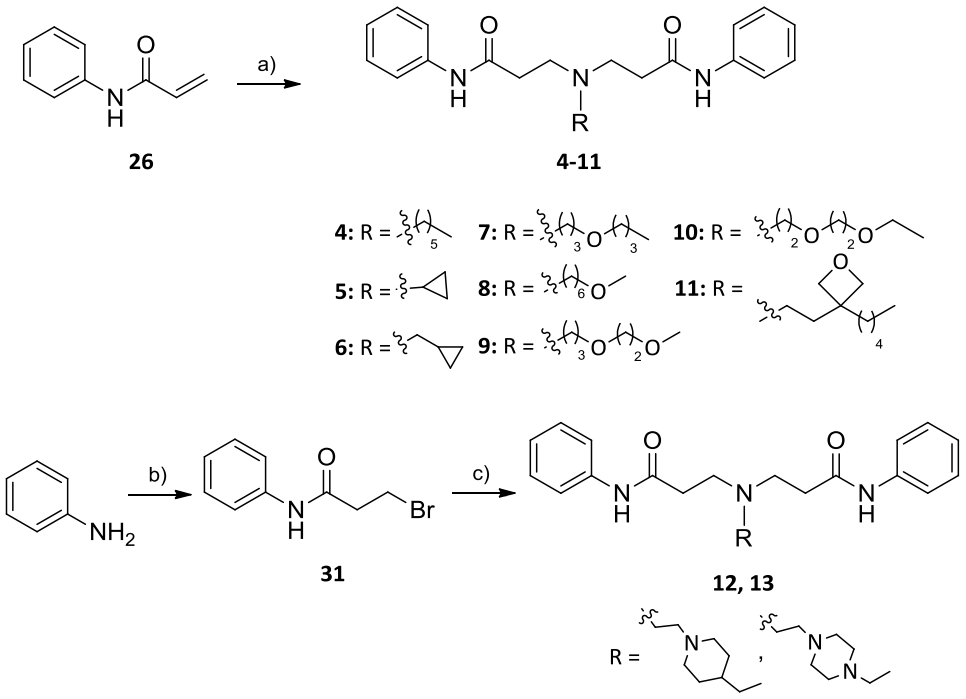

Scheme 1. Reagents and conditions: a) RNH_2 (commercial or **27**-**30**), DBU, ACN, reflux, 24 h, 21-100%; b) 3-bromopropanoyl chloride, pyridine, DCM, rt, 2 h, 92%; c) 2-(4-ethylpiperidin-1-yl)ethanamine or **32**, Et_3N, 10% KI, DCM, 60 °C, 24 h, 48-54%.

This synthetic route involved the previous preparation of non-commercial amines **27**-**30** and **32** (Scheme 2). Amine **27** was prepared using 2-methoxycyclohexanone as starting material. This ketone was transformed into the corresponding oxime **33** by reaction with hydroxylamine, and further acetylated to give intermediate **34**. Later reductive Beckman fragmentation and reduction of nitrile **35** with borane finally provided amine **27**. Synthesis of 3-(2-methoxyethoxy)propan-1-amine (**28**) was performed starting from 2-methoxyethanol, by addition of acrylonitrile in the presence of potassium hydroxide, followed by reduction of the resulting nitrile **36** with borane. 2-(2-Ethoxyethoxy)ethanamine (**29**) was prepared through Mitsunobu reaction of 2-(2-ethoxyethoxy)ethanol and phthalimide, in the presence of diisopropylazodicarboxylate (DIAD) and triphenylphosphine, followed by deprotection of **37** with hydrazine and sodium borohydride. 2-(3-Pentyloxetan-3-yl)ethanamine (**30**) was prepared by Wittig reaction between oxetan-3-one and the appropriate phosphorane followed by conjugate addition of pentylmagnesium bromide to the acrylonitrile **38** in the presence of copper (I), and further reduction of nitrile **39**. Finally, (4-ethylpiperazin-1-yl)ethanamine (**32**) was obtained through nucleophilic substitution of 1-ethylpiperazine and bromoacetonitrile in the presence of potassium carbonate, followed by reduction of nitrile **40** with lithium aluminium hydride (LAH).

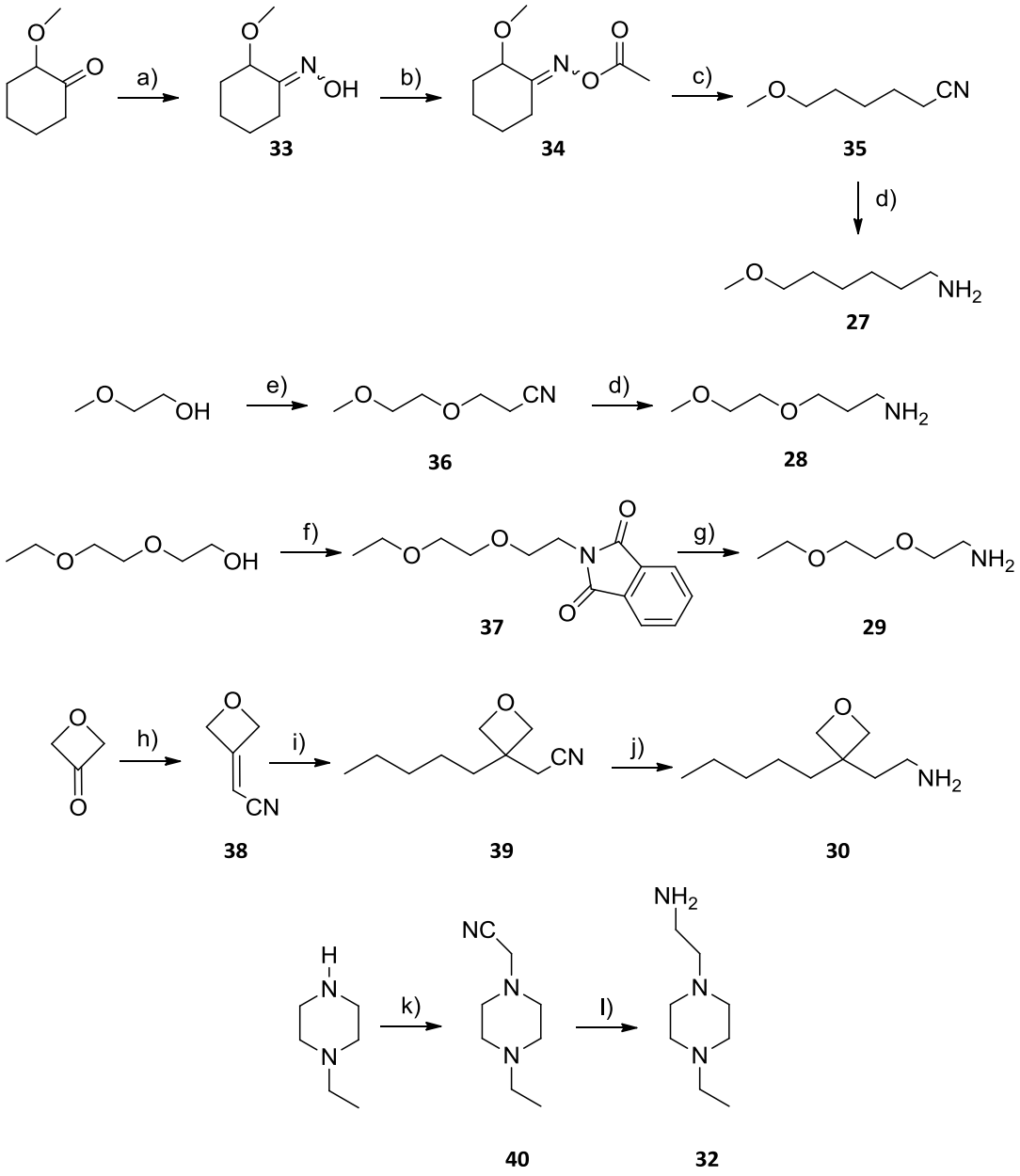

Scheme 2. Reagents and conditions: a) $NH_2OH{\cdot}HCl$, NaOAc, H_2O, MeOH, 60 °C, 24 h, 100%; b) Ac_2O, pyridine, rt, 16 h, 85%; c) Et_3SiH, $CF_3SO_3SiMe_3$, DCM, 0 °C, 6 h, 87%; d) BH_3, THF, reflux, 3.5 h, 66-89%; e) acrylonitrile, KOH, HCl, 0 °C, 1.5 h, 94%; f) DIAD, PPh_3, phthalimide, MeOH, toluene, 0 °C to rt, 16 h, 58%; g) $N_2H_4{\cdot}H_2O$, $NaBH_4$, MeOH, rt, 16 h, 71%; h) $Ph_3P{=}CHCN$, DCM, rt, 6 h, 79%; i) $C_5H_{11}MgBr$, CuI, Et_2O, 0 °C, 2 h, 26%; j) LAH, Et_2O, 0 °C, 2 h, 59%; k) $BrCH_2CN$, K_2CO_3, ACN, rt, 16 h, 100%; l) LAH, THF, 0 °C, 4 h, 86%.

The ability of synthesized compounds **4**-**13** to inhibit ICMT enzyme was determined by a radioactivity assay previously described by Baron et al.[39] The inhibitory capacity of the compounds is expressed as the percentage of inhibition of the methyl esterification step by which the tritiated methyl group of the methyl donor *S*-adenosylmethionine ([^{3}H]-SAM) is transferred to the substrate biotinyl-*S*-farnesyl-L-cysteine (BFC). The obtained results (Table 1) showed that a decrease in the length of the alkyl chain (compound **4**) or its substitution by cyclopropane or methylcyclopropane groups (compounds **5**, **6**) involved important reductions in the inhibitory activity of the compounds, ranging from 9% to 36% inhibition of ICMT at 50 µM. Neither the introduction of oxygen atoms in the alkyl chain (**7**-**11**), nor the replacement of the *n*-octyl chain by (4-ethylpiperidin-1-yl)ethane or (4-ethylpiperazin-1-yl)ethane (**12**, **13**) allowed to keep good inhibition values, compared to the 93% inhibition induced by compound **3** at the same concentration.

Table 1. ICMT inhibition values for compounds **3**-**13**.

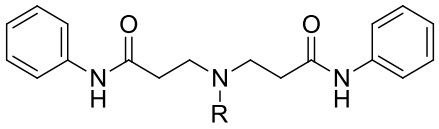

Comp.	R	ICMT Inhibition (%)[a,b]	Comp.	R	ICMT Inhibition (%)[a,b]
3		93	**9**	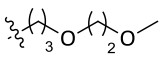	45
4		9	**10**	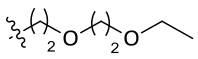	15
5		33	**11**	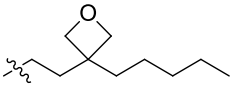	0
6	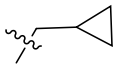	36	**12**	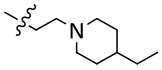	13
7	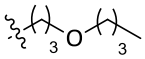	14	**13**	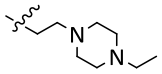	15
8	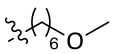	30			

[a] ICMT inhibition values were determined at 50 µM concentration of tested compounds. [b] Data are expressed as the mean from at least two independent experiments performed in triplicate. The standard error of the mean (sem) in all cases is within a 10% of the mean value.

2.1.2. Changes in the secondary amides

The previous obtained data suggested that a long hydrophobic chain attached to the nitrogen atom was needed, so we decided to keep the *n*-octyl group and continue with the structural exploration of the amide groups. Hence, the secondary amides of compound **3** were replaced by tertiary amides (**14**, **15**), sulfonamides (**16**-**19**) or an oxadiazole heterocycle (**20**), considering that the two later moieties have been reported as bioisosters of the amide group (Schemes 3 and 4).[40] For the obtention of derivatives **14**, **16**, and **17**, acrylamides **41**-**43** were treated with octylamine in the presence of DBU (Scheme 3). Synthesis of final compounds **15**, **18**, and **19** was assessed by reaction of acrylamide **26** with octylamine followed by aza-Michael reaction of the resulting secondary amine **44** with acrylamides **41-43**. The nucleophilic substitution of 2-(chloromethyl)-5-phenyl-1,3,4-oxadiazole with amine **44** afforded compound **20** (Scheme 4).

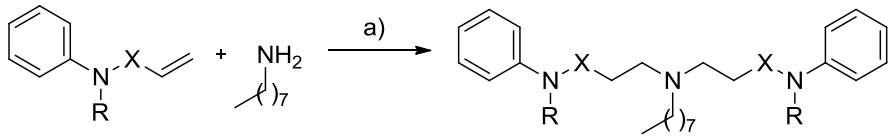

41-43 **14, 16, 17**

41: X = CO; R = Me
42, 43: X = SO_2; R = H, Me

14: X = CO; R = Me
16, 17: X = SO_2; R = H, Me

Scheme 3. Reagents and conditions: a) DBU, ACN, reflux, 24 h, 44-81%.

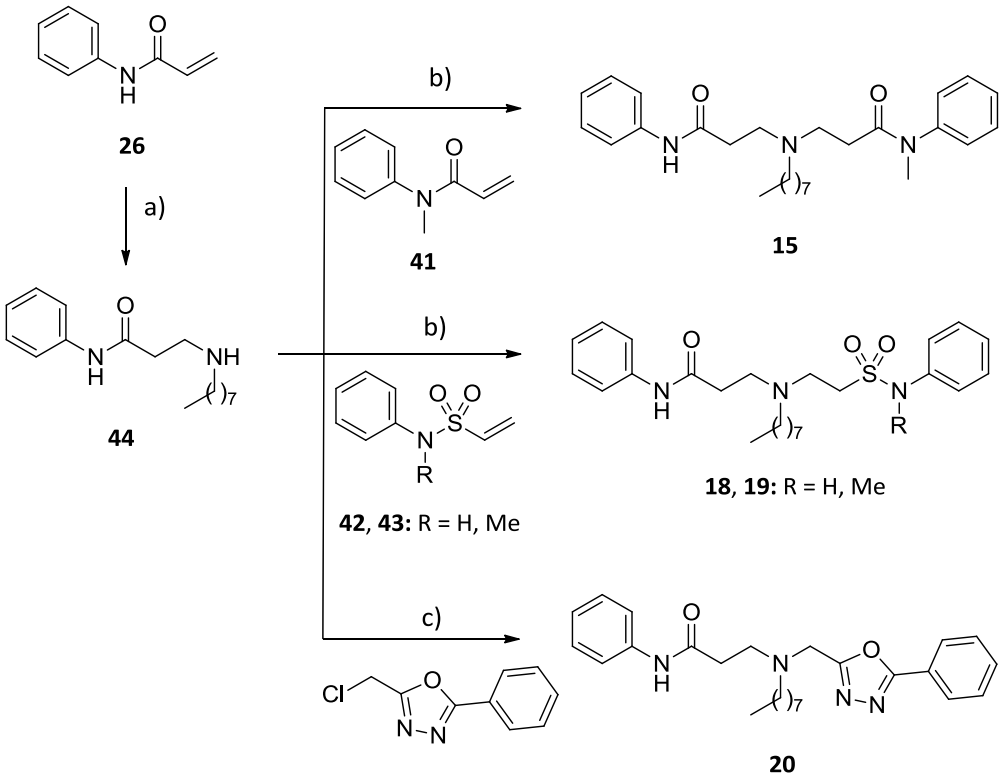

Scheme 4. Reagents and conditions: a) octylamine, DBU, ACN, 60 °C, 5 h, 76 %; b) DBU, ACN, reflux, 24 h, 12-64%; c) Et_3N, ACN, 60 °C, 24 h, 62%.

The biological evaluation of compounds **14**-**20** as ICMT inhibitors indicated that none of the modifications introduced in the amide groups improved the inhibitory capacity of these derivatives in comparison to the reference compound **3** (Tables 2 and 3) and only methylamides **14** and **15** showed moderate activity (68% and 65% inhibition, respectively).

Table 2. ICMT inhibition values for compounds **3**, **14**, **16**, and **17**.

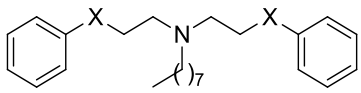

Comp.	X	ICMT Inhibition (%)[a,b]
3	NHCO	93
14	NCH_3CO	65
16	SO_2NH	34
17	SO_2NCH_3	12

[a] ICMT inhibition values were determined at 50 μM concentration of tested compounds. [b] Data are expressed as the mean from at least two independent experiments performed in triplicate. The sem in all cases is within a 10% of the mean value.

Table 3. ICMT inhibition values for compounds **3**, **15**, **18-20**.

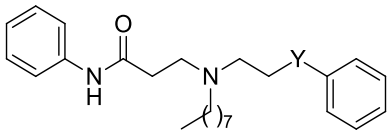

Comp.	Y	ICMT Inhibition (%)[a,b]
3	NHCO	93
15	NCH_3CO	68
18	SO_2NH	22
19	SO_2NCH_3	10
20	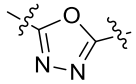	13

[a] ICMT inhibition values were determined at 50 μM concentration of tested compounds. [b] Data are expressed as the mean from at least two independent experiments performed in triplicate. The sem in all cases is within a 10% of the mean value.

2.1.3. Modifications in the spacer between the two carbonyl groups

Finally, we studied the distance between the two carbonyl groups with derivatives **21**-**25** (Scheme 5). Final compounds **21** and **22** were obtained from 2-bromo-*N*-phenylacetamide as starting material by nucleophilic substitution with octylamine. The regioselectivity of the reaction in order to obtain the dialkylated product **21** or the intermediate **45** was achieved by controlling the reaction conditions. The treatment of secondary amine **45** with 3-bromo-*N*-phenylpropanamide (**31**) provided derivative **22**. Synthesis of compounds **23**-**25** was carried out by reaction of amine **44** with the corresponding commercial haloketone (compounds **23** and **24**) or benzoic acid (diamide **25**) (Scheme 5).

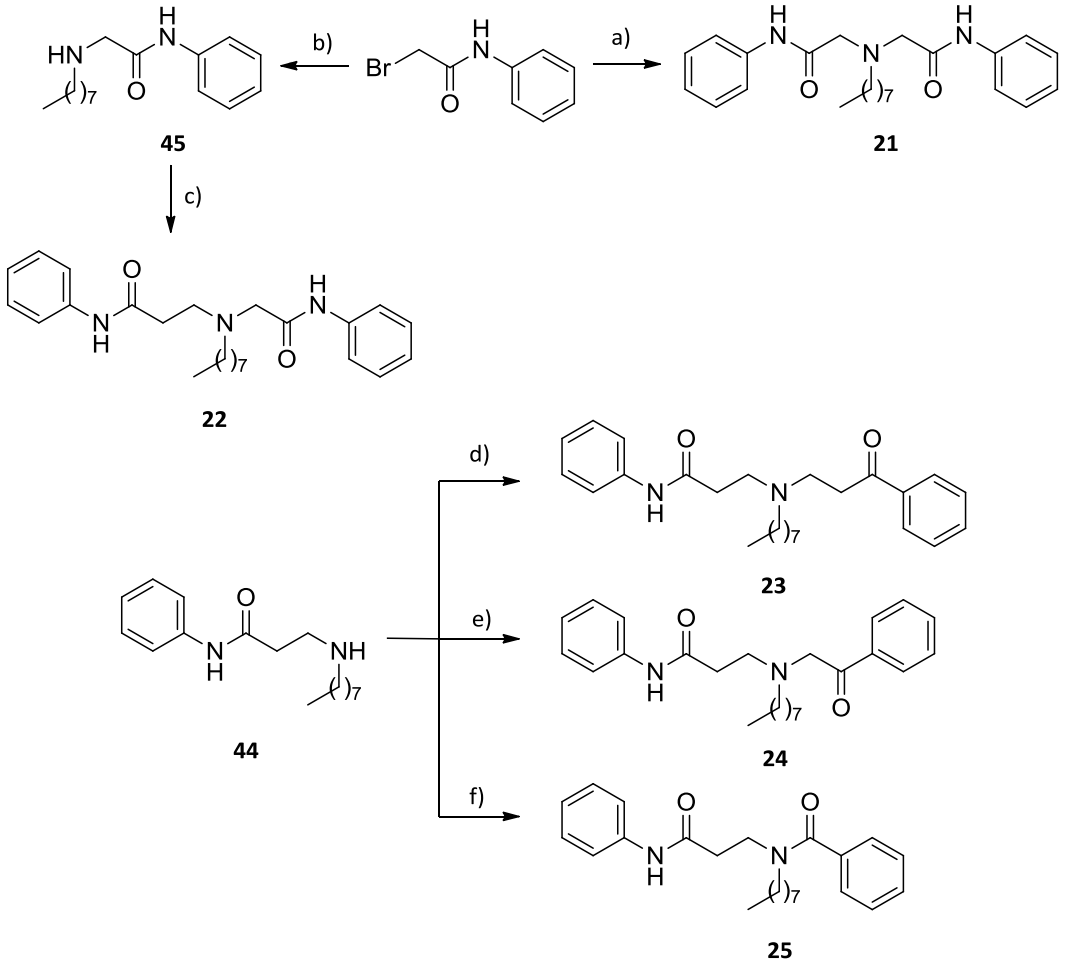

Scheme 5. Reagents and conditions: a) octylamine, DIPEA, ACN, 60 ºC, 16 h, 93%; b) octylamine, DCM, rt, 16 h, 40%; c) 3-bromo-*N*-phenylpropanamide (**31**), DIPEA, DCM, reflux, 16 h, 25%; d) 3-chloropropiophenone, $NaHCO_3$, ACN, H_2O, rt, 16 h, 43%; e) 2-bromoacetophenone, K_2CO_3, ACN, rt, 16 h, 56%; f) benzoic acid, EDC, HOBt, DCM, rt, 16 h, 72%.

Once synthesized, the ability of compounds **21-25** to inhibit ICMT enzyme was determined (Tables 4 and 5). Compounds **23** and **24** did not show enough stability for their ICMT inhibition determination. However, compound **25** showed a good percentage of ICMT inhibition (it blocked the 80% of ICMT activity at 50 µM).

Table 4. ICMT inhibition values for compounds **3**, **21**, and **22**.

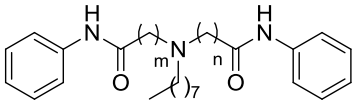

Comp.	m	n	ICMT Inhibition (%)[a,b]
3	2	2	93
21	1	1	62
22	2	1	68

[a] ICMT inhibition values were determined at 50 µM concentration of tested compounds. [b] Data are expressed as the mean from at least two independent experiments performed in triplicate. The sem in all cases is within a 10% of the mean value.

Table 5. ICMT inhibition values for compounds **3**, **23**-**25**.

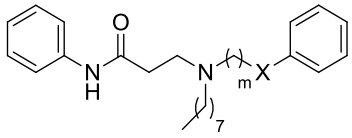

Comp.	X	m	ICMT Inhibition (%)[a,b]
3	CONH	2	93
23	CO	2	ND[c]
24	CO	1	ND[c]
25	CO	0	80

[a] ICMT inhibition values were determined at 50 µM concentration of tested compounds. [b] Data are expressed as the mean from at least two independent experiments performed in triplicate. The sem in all cases is within a 10% of the mean value. [c] Not determined.

In order to determine if any of the identified ICMT inhibitors could be a candidate for the treatment of progeria, those compounds with a percentage of ICMT inhibition higher than 60% at 50 μM were selected and their cytotoxicity was determined in AF3 fibroblasts. The evaluation of the cellular cytotoxicity was carried out by a colorimetric assay based on the metabolic reduction of 3-(4,5-dimethylthiazol-2-yl)-2,5-diphenyltetrazolium bromide (MTT) by the dehydrogenase succinate mitochondrial enzyme. After incubation of the desired compound for 48 h, the cells which remain functional are able to reduce the MTT forming a colored precipitated (formazan), which is quantified by measuring its absorbance at 570 nm. The cellular viability is expressed as the percentage of viable cells after treatment with the compound under study respect to the viability in the absence of compound. Only compound **25** showed low cytotoxicity with a percentage of cell viability of 85% with respect to 100% viability obtained in vehicle-treated cells (0.1% DMSO). Hence, we selected derivative **25** as a lead in order to continue with its optimization in the search of derivatives with improved cell viability and good capacity to inhibit ICMT enzyme.

2.2. Lead optimization

Then, we decided to introduce substituents in one phenyl ring (compounds **46**-**52**) and replace a phenyl ring by different heterocycles (compounds **53-61**) (Figure 6). All these compounds were synthesized by coupling of amine **44** with the corresponding carboxylic acids (Scheme 6).

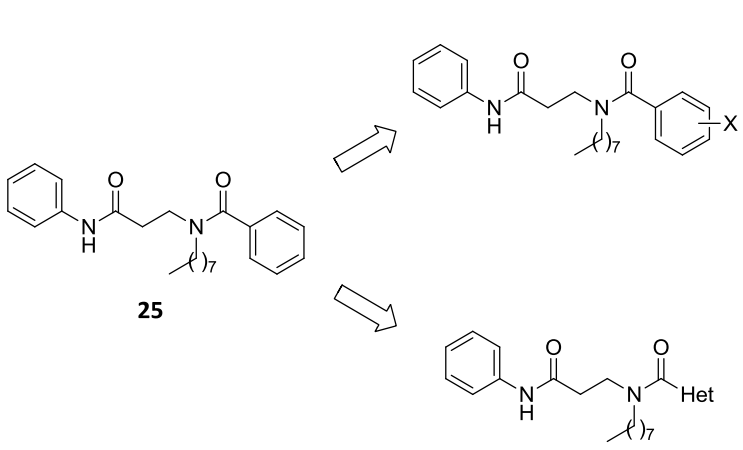

46: X = *o*-OMe
47: X = *m*-OMe
48: X = *p*-OMe
49: X = *p*-CN
50: X = *p*-F
51: X = *p*-CF_3
52: X = *p*-NHCOMe

53: Het = 2-furyl
54: Het = 3-furyl
55: Het = 2-pyrrolidinyl
56: Het = 1*H*-2-pyrrolyl
57: Het = 1*H*-3-pyrrolyl
58: Het = 1-methyl-1*H*-2-pyrrolyl
59: Het = 2-pyridinyl
60: Het = 3-pyridinyl
61: Het = 4-pyridinyl

Figure 6. Compounds **46-61**.

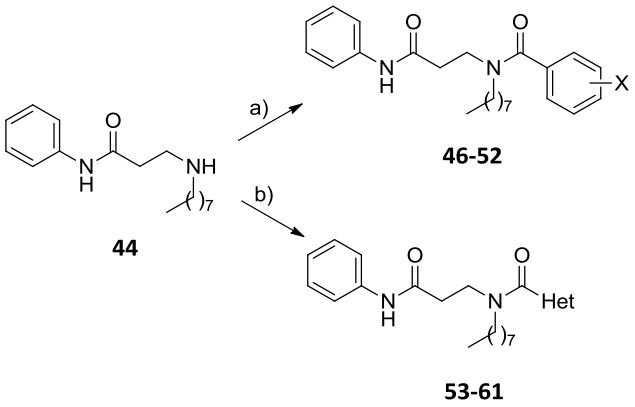

Scheme 6. Reagents and conditions: a) Ar-COOH, EDC, HOBt, DCM, rt, 16 h, 66-73%; b) Het-COOH, EDC, HOBt, DCM, rt, 16 h, 36-100%.

The ICMT inhibition data obtained for compounds **46-48** (Table 6), with a methoxy group at *ortho*, *meta*, and *para* position of one of the phenyl ring, indicated that the introduction of the substituent in *para* position yielded the best results in terms of enzymatic inhibition, so this position was kept for the rest of the studied compounds **49-52**. Nonetheless, none of the new substituents introduced in the phenyl ring improved the inhibitory capacity of initial compound **25** (80% of inhibition at 50 µM). In relationship with compounds **53-61**, their percentage of inhibition of ICMT showed that the replacement of a phenyl group by a 3-furyl ring or a pyrrol moiety (compounds **54** and **56-58**) kept the inhibitory capacity of these compounds, which showed similar ICMT inhibition percentages to the parent compound **25** (75-81% inhibition at 50 µM) (Table 7).

Table 6. ICMT inhibition values of compounds **25**, **46-52**.

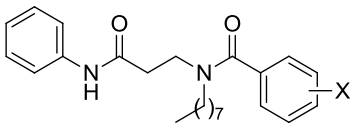

Comp.	X	ICMT Inhibition (%)[a,b]	Comp.	X	ICMT Inhibition (%)[a,b]
25	H	80	**49**	*p*-CN	59
46	*o*-OMe	32	**50**	*p*-F	42
47	*m*-OMe	26	**51**	*p*-CF_3	18
48	*p*-OMe	58	**52**	*p*-NHCOMe	10

[a] ICMT inhibition values were determined at 50 μM concentration of tested compounds. [b] Data are expressed as the mean from at least two independent experiments performed in triplicate. The sem in all cases is within a 10% of the mean value.

Table 7. ICMT inhibition values of compounds **53-61**.

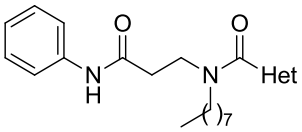

Comp.	Het	ICMT Inhibition (%)[a,b]	Comp.	Het	ICMT Inhibition (%)[a,b]
53		49	**57**		81
54		81	**58**		75
55		62	**59**		63
(*R*)-55		61	**60**		38
(*S*)-55		64	**61**		30
56		75			

[a] ICMT inhibition values were determined at 50 μM concentration of tested compounds. [b] Data are expressed as the mean from at least two independent experiments performed in triplicate. The sem in all cases is within a 10% of the mean value.

Then, those compounds with a percentage of inhibition over 60% at 50 μM were selected for the assessment of their cytotoxicity in wild type AF3 and G609G progeroid mouse fibroblasts, the cellular model of progeria as they come from the mouse model with the mutation in the LMNA gene.[41] We have also studied the pharmacokinetic profile of the selected compounds. We determined the in vitro stability of the compounds in mouse and human serum and microsomes as a model of first pass metabolism. Also, the binding to human serum albumin (HSA) was assessed. These experiments were carried out by incubation of the compounds in the presence of the corresponding serum, microsomes, or HSA and, after the appropriate incubation, the remaining compound was quantified by high performance liquid chromatography coupled to mass spectrometry (HPLC-MS) to obtain half-life values ($t_{1/2}$) in the case of serum and microsomes stabilities or affinity values in terms of dissociation constant (K_d) and bounded fraction (F_b) in the case of HSA. Also, the theoretical calculated values of the logarithm of the partition coefficient between *n*-octanol and water (clogP) and the topological polar surface area (TPSA) were determined using the ACDLabs Percepta Software as a predicted value of the lypophilicity and cellular permeability, respectively.

In terms of cellular viability, the obtained results (Table 8) showed that all compounds were not cytotoxic in wild type AF3 fibroblasts and were able to enhance the viability of progeroid cells, with the best results obtained for compound **59**, which was able to increase the viability of the progeroid cells up to 93%, compared to the 41% viability observed in the vehicle-treated cells. Regarding the pharmacokinetic profile, selected compounds exhibited moderate pharmacokinetic properties (Table 9), with $t_{1/2}$ values higher than 24 h and between 14 and 243 min in human and mouse serum, respectively, or HSA bound fractions from 72 to 100%. Furthermore, the lypophilicity and cellular permeability values were approximately in the range of expected drug-like compounds (clogP < 5, 60 < TPSA < 120 $Å^2$).[42]

Taking into account all the results obtained up to this moment, the inhibitor with the best efficacy to improve the cellular progeroid phenotype was **59**. However, their pharmacokinetic properties were slightly worse compared to the rest of compounds. Then, in an attempt to obtain an improved compound, we replaced one of the carbonyl groups by a methylene, as it has been reported that the amide bond can be, in some cases, a hydrolysis-prone group. Hence, compound **62** was synthesized by reductive amination of the intermediate secondary amine **44** with 2-pyridinecarboxaldehyde followed by treatment with sodium triacetoxyborohydride (Scheme 7).

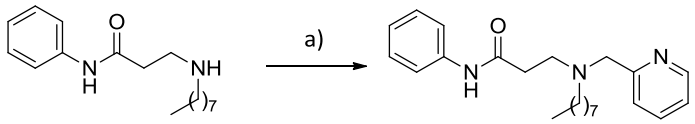

44 **62**

Scheme 7. Reagents and conditions: a) 2-pyridinecarboxaldehyde, $NaBH(OAc)_3$, DCE, rt, 16 h, 16%.

Then, we determined the cytotoxicity, effect on progeroid mouse cells, and pharmacokinetic properties of this new compound (Tables 8 and 9). The obtained results showed that the replacement of the carbonyl group next to the heterocycle by a methylene unit did not improve the viability of progeroid cells (93% viability of **59** vs 60% viability of **62**) nor the pharmacokinetic profile ($t_{1/2}$ in human microsomes decreased from 14 min for compound **59** to 2 min for derivative **62**).

Table 8. Effect of compounds **54-59** and **62** on the viability of AF3 wild type and G609G progeroid mouse fibroblasts.

Compound	Viability (%)[a]	
	AF3 wild type mouse fibroblasts	G609G progeroid mouse fibroblasts
Vehicle-treated	100	41 ± 3
54	116 ± 2	77 ± 5
55	121 ± 11	60 ± 10
(*R*)-55	114 ± 6	80 ± 7
(*S*)-55	124 ± 10	70 ± 5
56	107 ± 5	45 ± 6
57	109 ± 4	53 ± 13
58	99 ± 5	74 ± 9
59	123 ± 9	93 ± 9
62	103 ± 8	60 ± 9

[a] Cellular viability was determined by the MTT assay. Data are expressed as the means ± sem from three independent experiments performed in triplicate at a compound concentration of 2 µM. The percentage of viability is expressed considering 100% viability in vehicle-treated AF3 wild type mouse fibroblasts.

Table 9. Pharmacokinetic profile of compounds **54**-**59** and **62.**

Comp.	Stability ($t_{1/2}$, min)[a]				HSA binding[a,b] F_b (K_d, μM)	clogP[c]	TPSA (Å^2)[c]
	Serum		Microsomes				
	Human	Mouse	Human	Mouse			
54	> 1440	14 ± 1	8 ± 3	7 ± 2	98.1 (11)	5.1	62.6
55	>1440	243 ± 64	30 ± 17	17 ± 7	72.4 (240)	3.9	61.4
(*R*)-55	> 1440	112 ± 8	12 ± 1	9 ± 1	80.5 (140)	4.5	61.4
(*S*)-55	> 1440	38 ± 13	21 ± 12	4 ± 1	90.5 (62)	4.5	61.4
56	> 1440	41 ± 9	15 ± 3	4 ± 1	99.0 (1.5)	3.5	65.2
57	> 1440	58 ± 21	16 ± 2	2 ± 1	99.0 (1.6)	3.9	65.2
58	> 1440	47 ± 1	22 ± 6	11 ± 2	98.7 (8)	4.0	54.3
59	> 1440	17 ± 1	14 ± 7	3 ± 1	98.1 (7.2)	4.5	62.3
62	> 1440	26 ± 8	2 ± 1	5 ± 1	100 ($1.7 \cdot 10^{-6}$)	5.3	45.2

[a] Data are expressed as the means ± sem from five independent experiments performed in duplicate. [b] Binding to human serum albumin (HSA) is expressed as the bound fraction (F_b). Dissociation constants (K_d) are given between parentheses. Sem is in all cases within a 10% of the mean value. [c] Values obtained with the ACDLabs Percepta Software.

Taken together, these results suggested that compound **59** showed the best combination of ICMT inhibitory activity (63%), viability of progeroid cells (93%), and pharmacokinetic profile, so it was selected for further biological studies. Moreover, its excellent capacity to improve viability of progeroid cells made **59** a good candidate to confirm, as a proof of concept, the efficacy of an ICMT inhibitor to improve the progeria phenotype.

2.3. Study of the efficacy of compound 59 in human progeroid cells

As human progeroid cells are characterized by reduced viability, damaged DNA, impaired cellular proliferation, and high levels of progerin localized in the nuclear membrane, we studied whether compound **59** was able to improve or even reverse these cellular hallmarks of progeria. Hence, we determined the capacity of compound **59** to: i) increase viability of human progeroid fibroblasts; ii) reduce DNA damage; iii) stimulate cellular proliferation; and iv) delocalize progerin.

Hence, HGADFN167 fibroblasts from a progeria patient and HGFDFN168 cells from a healthy donor were obtained from The Progeria Research Foundation in order to carry out these experiments. The effect of compound **59** in the cellular viability of HGADFN167 progeroid fibroblasts was assessed by incubating the cells for 24 days in the presence of compound **59** (2 µM) or vehicle and counting the number of viable cells (Figure 7). We can observe that the cellular viability was improved around a 20% when using compound **59** in comparison with vehicle-treated cells. Next, in order to determine the efficacy of the compound in the reduction of damaged DNA, the stimulation of cellular proliferation and the delocalization of progerin, western blot or immunofluorescence experiments were carried out. Hence, HGADFN167 progeroid fibroblasts were incubated with compound **59** (2 µM) and cells analyzed at different times. In relationship with the reduction of DNA damage, the levels of phosphorylated histone 2AX (pH2AX) were measured, observing a decrease when treating with compound **59** (Figure 8A). Stimulation of the cellular proliferation pathways was assesed by determining the levels of phosphorylated Akt protein. In this case, we observed an increase when progeroid fibroblasts were treated with the compound (Figure 8B). Finally, we confirmed that selected compound **59** was able not only to delocalize progerin from the nuclear membrane but also to reduce its overall levels (Figure 9).

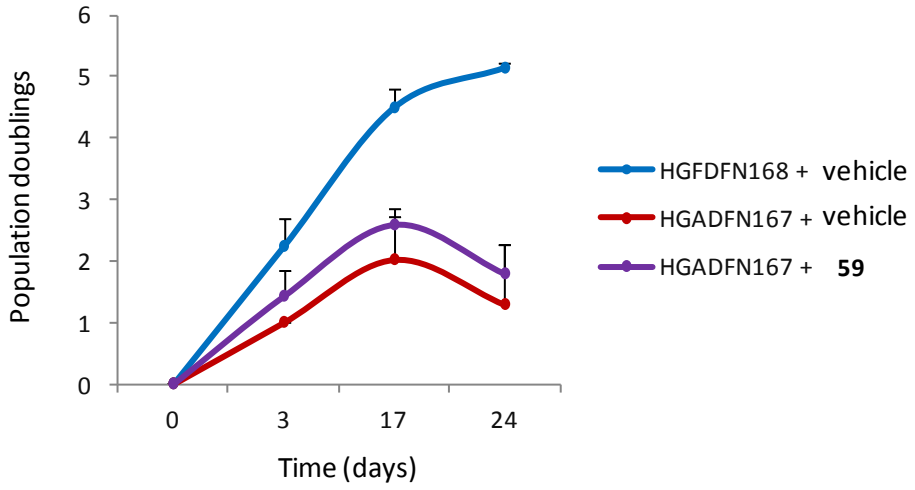

Figure 7. Viability curve at 24 days for healthy HGFDFN168 (blue) and progeroid HGADFN167 cells treated with vehicle (0.1% DMSO, red) or with compound **59** at 2 µM (purple). Data represent the mean ± sem of two independent experiments.

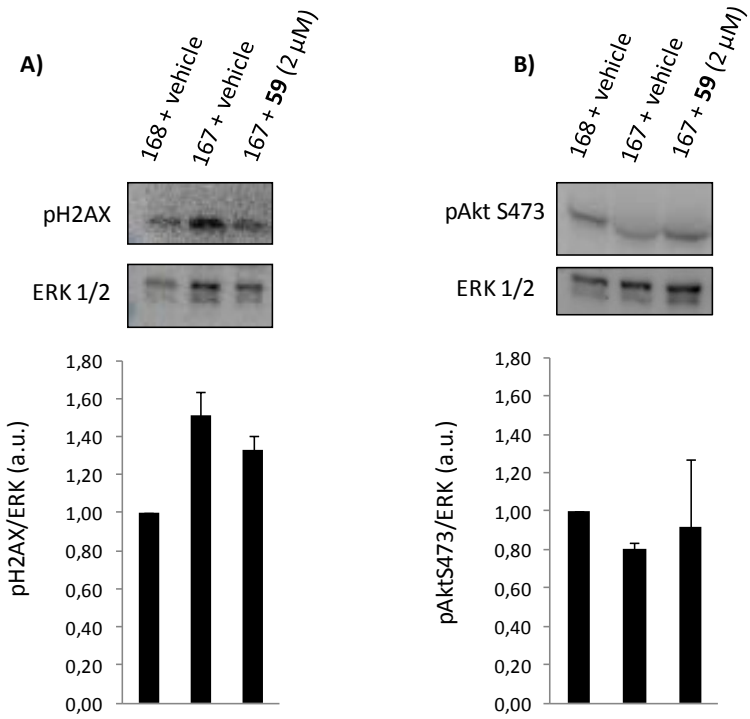

Figure 8. Representative western blots of the levels of pH2AX (A) and pAkt (B). Lysates were obtained for healthy (HGFDFN168, 168 in the figure) and progeroid (HGADFN167, 167 in the figure) cells treated with vehicle or with compound **59** after 17 and 10 days of culture for pH2AX and pAkt, respectively. The bar graphs are the mean ± sem of three different experiments and represent the optical density of the immunoreactive phosphorylated protein normalized to ERK 1/2 used as loading control, and it is expressed as relative to healthy cells treated with vehicle.

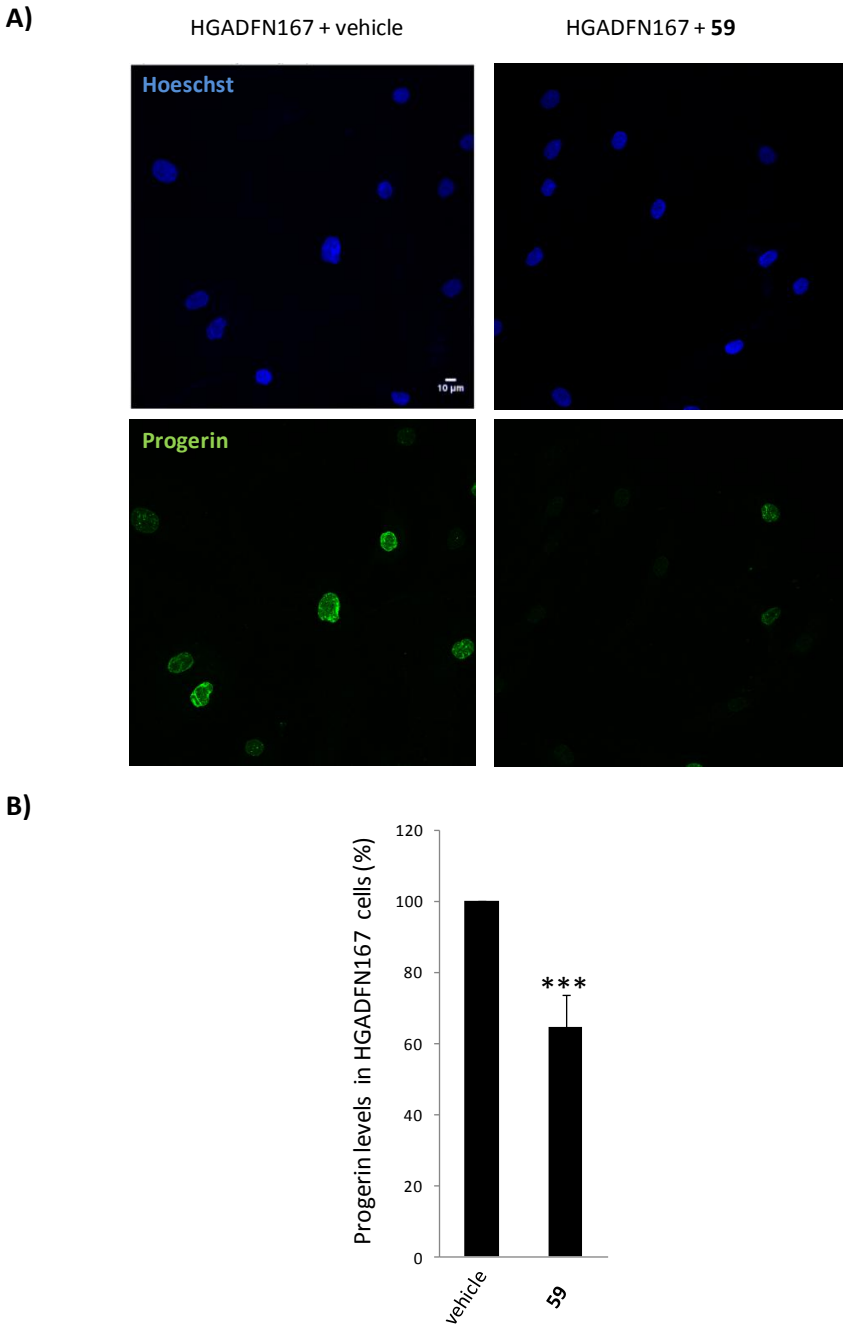

Figure 9. A) Representative confocal images of HGADFN167 fibroblasts treated with 0.1% DMSO (vehicle) or with compound **59** (2 µM) for 17 days. Cells were immunostained with an antibody against progerin (green) and imaged with an Olympus IX83 confocal microscope. Nuclei were visualized with Hoechst stain in blue. Similar results were obtained in three independent assays. B) The bar graphs represent progerin levels measured in terms of fluorescence intensity. Data correspond to the mean ± sem of two independent experiments (50 cells quantified). ***, $p < 0.0005$ (Student´s t test).

All in sum, the results obtained up to this moment indicate that compound **59** remarkably improves the viability of progeroid mouse fibroblasts. Furthemore, in human cells coming from progeria patients, this compound is able not only to increase cell viability but also to stimulate pro-proliferation pathways and to reduce DNA damage and progerin levels, and to delocalize progerin from the nuclear membrane. Accordingly, **59** is a promising compound to assay its in vivo efficacy in a mouse model of progeria, experiments that are currently ongoing in our laboratory.

CONCLUSIONS

3. CONCLUSIONS

In this work we have validated the enzyme ICMT as a new therapeutic target for the treatment of progeria. After a medicinal chemistry program starting from initial hit **3**, we have identified compound **59**, which shows the best combination of ICMT inhibitory activity (63%), viability of progeroid cells (93%), and pharmacokinetic profile. Furthermore, this compound is able to increase the viability and cellular proliferation of progeroid human fibroblasts, reduce their DNA damage and the levels of progerin, inducing its delocalization from nuclear membrane. In summary, compound **59** is an excellent candidate for in vivo efficacy testing, experiments that are currently ongoing in our laboratory.

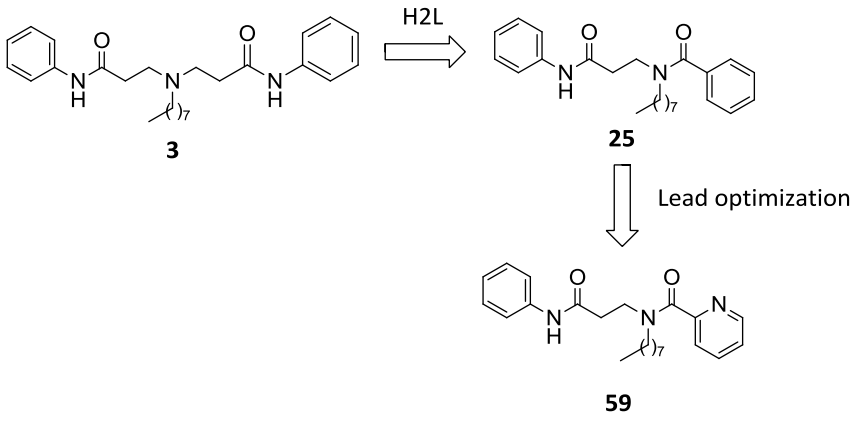

3 **25** **59**

Increases the cellular proliferation and viability of mouse and human progeroid fibroblasts

Reduces DNA damage in human progeroid fibroblasts

Delocalizes and reduces the levels of progerin

EXPERIMENTAL SECTION

4. EXPERIMENTAL SECTION

4.1. Synthesis

Unless stated otherwise, starting materials, reagents and solvents were purchased as high-grade commercial products from Sigma-Aldrich, Acros, ABCR, Fluorochem, Scharlab, Honeywell or Panreac, and were used without further purification. Tetrahydrofuran (THF), Et_2O, and dichloromethane (DCM) were dried using a Pure Solv™ Micro 100 Liter solvent purification system. Pyridine (py) and Et_3N were dried over KOH and distilled before using. All reactions in organic solvents were performed under an argon atmosphere in dry glassware. Analytical thin-layer chromatography (TLC) was run on Merck silica gel plates (Kieselgel 60 F-254) with detection by UV light (254 nm), ninhydrin solution, or 10% phosphomolybdic acid solution in ethanol. Flash chromatography was performed on a Varian 971-FP flash purification system using silica gel cartridges (Varian, particle size 50 μm) or on glass columns using silica gel type 60 (Merck, particle size 230 μm, 400 mesh). All compounds were obtained as oils, except for those whose melting points (mp) are indicated, which were solids.

Melting points (mp, uncorrected) were determined on a Stuart Scientific electrothermal apparatus. Infrared (IR) spectra were measured on a Bruker Tensor 27 instrument equipped with a Specac ATR accessory of 5200-650 cm^{-1} transmission range; frequencies (ν) are expressed in cm^{-1}. Optical rotation [α] was measured on an Anton Paar MCP 100 modular circular polarimeter using a sodium lamp (λ = 589 nm) with a 1 dm path length; concentrations (c) are given as g/100 mL. NMR spectra were recorded at room temperature on a Bruker DPX 300 (^1H, 300 MHz; ^{13}C, 75 MHz) spectrometer at the Universidad Complutense de Madrid (UCM) NMR facilities. Chemical shifts (δ) are expressed in parts per million relative to internal tetramethylsilane; coupling constants

(*J*) are in hertz (Hz). The following abbreviations were used to describe peak patterns when appropriate: s (singlet), d (doublet), t (triplet), q (quadruplet), m (multiplet), br (broad), and app (apparent). 2D NMR experiments (HMQC and HMBC) of representative compounds were carried out to assign protons and carbons of the new structures. High resolution mass spectrometry (HRMS) was carried out on a FTMS Bruker APEX Q IV spectrometer in electrospray ionization (ESI) mode at UCM's spectrometry facilities.

For all final compounds, purity was determined by high-performance liquid chromatography coupled to mass spectrometry (HPLC-MS) using an Agilent 1200LC-MSD VL instrument, and satisfactory chromatograms confirmed a purity of at least 95% for all tested compounds. LC separation was achieved with an Eclipse XDB-C18 column (5 µm, 4.6 mm x 150 mm), together with a guard column (5 µm, 4.6 mm x 12.5 mm) with a flow of 0.5 mL/min. The gradient mobile phase consisted of A (95:5 water/acetonitrile) and B (5:95 water/acetonitrile) with 0.1% formic acid as solvent modifier, indicating the gradients in Table 10. Spectra were acquired in positive or negative ionization mode from 100 to 1000 m/z and in UV-mode at four different wavelengths (210, 230, 254, and 280 nm). MS analysis was performed with an ESI source. The capillary voltage was set to 3.0 kV and the fragmentor voltage was set at 72 eV. The drying gas temperature was 350 °C, the drying gas flow was 10 L/min, and the nebulizer pressure was 20 psi.

Table 10. HPLC gradients.

Method A		**Method B**	
t (min)	% B	t (min)	% B
0	0	0	0
5	0	2	0
15	90	8	80
22	100	25	100
26	100	30	0
30	0		

The enantiomeric excess (ee) was determined by HPLC using a chiral column in reversed-phase chromatography. Chiralpak® IA (5 µm, 4.6 mm x 15.0 mm) was used as the stationary phase, equipped with an Eclipse XDC-C18 precolumn (5 µm, 4.6 mm x 12.5 mm) using a flow of 0.5 mL/min. The mobile phase consisted of A (20 mM NH_4HCO_3, pH 9) and B (acetonitrile) using an isocratic method of 80% B for 10 (chiral HPLC method A) or 30 min (chiral HPLC method B), indicated in the particular cases. HPLC traces were compared to racemic samples obtained by mixing equal amounts of the enantiopure compounds independently obtained.

4.1.1. General Procedures

4.1.1.1. Amide formation through acid chlorides

To a solution of the corresponding aniline (1 equiv) in anhydrous DCM (1 mL/mmol), acryloyl chloride (1.1 equiv) and pyridine (1.1 equiv) were added, consecutively, at 0 °C. Then, the reaction mixture was stirred for 2 h at rt and then, the reaction crude was washed with saturated aqueous solutions of $NaHCO_3$, $CuSO_4$ and NaCl, subsenquently. The organic layer was dried over Na_2SO_4, filtered, and the solvent was evaporated in vacuo to yield the corresponding compounds.

4.1.1.2. Aza-Michael reaction

A mixture of the corresponding acrylamide or sulfonamide (1.5-3 equiv), the desired amine (1.0 equiv), and DBU (1.5 equiv) in anhydrous ACN (1 mL/mmol) was heated at reflux for 24 h. Then, the solvent was removed under reduced pressure and the residue was purified by column chromatography.

4.1.1.3. Amide formation with coupling reagents

To a solution of the corresponding carboxylic acid (1.0 equiv) in anhydrous DCM (4 mL/mmol), EDC (1.0 equiv) and HOBt (1.0 equiv) were added. The reaction mixture was stirred at rt for 1 h. Then, a solution of the secondary amine **44** (1.0 equiv) in anhydrous DCM (2.0 mL/mmol) was added and the reaction mixture was stirred at rt for 16 h. The reaction crude was washed with saturated aqueous solutions of $NaHCO_3$ and NaCl, consecutively. The organic extracts were dried over Na_2SO_4, filtered, and the solvent removed under reduced pressure. The residue was purified by column chromatography obtaining the desired amides.

4.1.2. Synthesis of final compounds 4-13

● ***N*-Phenylacrylamide (26)**. Obtained following the general procedure 4.1.1.1. from aniline (500 µL, 5.0 mmol) and acryloyl chloride (500 mg, 5.5 mmol) in 63% yield (465 mg). The spectroscopic data are in agreement with those previously described.[43]

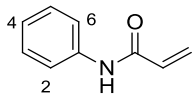

R_f (DCM/MeOH, 95:5): 0.57. Mp: 107-108 °C. (Lit.[43] 105-106 °C). ^{1}H-NMR ($CDCl_3$, δ): 5.71 (dd, *J* = 9.6, 2.0 Hz, 1H, ½CH_2), 6.31 (dd, *J* = 16.9, 9.7 Hz, 1H, CHCO), 6.42 (dd, *J* = 16.9, 1.9 Hz, 1H, ½CH_2), 7.10 (t, *J* = 7.4 Hz, 1H, H_4), 7.30 (t, *J* = 7.9 Hz, 2H, H_3, H_5), 7.60 (d, *J* = 7.9 Hz, 2H, H_2, H_6), 8.16 (br s, 1H, NH). MS (ESI, m/z): 148.1 $[M+H]^+$.

● **Amines 27-30, 32**

***N*-Hydroxy-2-methoxycyclohexylimine (33).** To a solution of sodium acetate (192 mg, 2.3 mmol) and hydroxylamine hydrochloride (163 mg, 2.3 mmol) in H_2O (5.8 mL) previously heated at 60 °C, a solution of 2-methoxycyclohexanone (150 µL, 1.1 mmol) in methanol (0.6 mL) was added. The reaction mixture was stirred overnight at 60 °C, and the crude was washed with H_2O (5.5 mL) and extracted with Et_2O. The organic phase was washed with saturated aqueous solutions of $NaHCO_3$ and NaCl, consecutively, dried over Na_2SO_4, filtered, and the solvent was removed under reduced pressure. The crude was purified by chromatography (hexane/EtOAc, 7:3) to obtain the title compound in quantitative yield (329 mg). The spectroscopic data are in agreement with those previously described.[44]

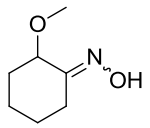

R_f (hexane/EtOAc, 7:3): 0.40. ^{1}H NMR ($CDCl_3$, δ): 1.35-1.94 (m, 5H, $2CH_2$, ½CH_2), 2.03-2.14 (m, 2H, CH_2), 3.01-3.05 (m, 1H, ½CH_2), 3.27 (s, 3H, CH_3), 3.75 (m, 1H, CH), 6.05 (br s, 1H, OH). MS (ESI, m/z): 143.9 $[M+H]^+$.

2-Methoxycyclohexanone oxime acetate (34). A solution of ketoxime **33** (166 mg, 1.2 mmol), pyridine (340 µL, 4.2 mmol) and acetic anhydride (0.7 mL, 7.2 mmol) was stirred overnight at rt. The excess of reagents was removed under reduced pressure and coevaporated with toluene. The crude was purified by chromatography (hexane/EtOAc, 7:3) to obtain the title compound in 85% yield (189 mg).

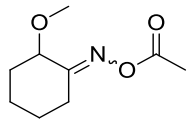

R_f (hexane/EtOAc, 7:3): 0.42. IR (ATR, cm^{-1}): 1769 (COO), 1702 (CN), 1193 (COC). ^{1}H NMR ($CDCl_3$, δ): 1.34-1.70 (m, 5H, $2CH_2$, ½CH_2), 1.73-2.02 (m, 2H, CH_2), 2.07-2.26 (m, 5H, CH_2, CH_3CO), 3.03-3.08 (m, 1H, ½CH_2), 3.30 (s, 3H, OCH_3), 3.95 (m, 1H, CH). ^{13}C NMR ($CDCl_3$, δ): 19.3 ($\underline{C}H_3CO$ diastereomer), 19.4 (CH_2 diastereomer), 19.4 ($\underline{C}H_3CO$ diastereomer), 19.6, 23.2, 25.5, 26.8, 28.0, 31.8, 32.7 ($7CH_2$ diastereomers), 56.0, 56.2 (CH_3O diastereomers), 70.1, 77.0 (CH diastereomers), 166.9, 167.4, 168.3, 168.5 (CN, CO diastereomers). MS (ESI, m/z): 125.9 $[M\text{-}OCOCH_3]^+$.

6-Methoxyhexanenitrile (35). A solution of **34** (120 mg, 0.7 mmol), trimethylsilane (120 µL, 0.8 mmol) and trimethylsilyl trifluoromethanesulfonate (TMSOTf) (12 µL, 70 nmol) was stirred at 0 °C for 6 h. Then, the solvent was removed under reduced pressure and the crude was purified by chromatography (hexane/EtOAc, 8:2) to give the title compound in 87% yield (77 mg). The spectroscopic data are in agreement with those previously described.[45]

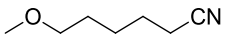

R_f (hexane/EtOAc, 8:2): 0.33. ^{1}H NMR ($CDCl_3$, δ): 1.47-1.75 (m, 6H, $(\underline{CH_2})_3CH_2CN$), 2.36 (t, *J* = 7.1 Hz, 2H, CH_2CN), 3.34 (s, 3H, CH_3), 3.39 (t, *J* = 6.1 Hz, 2H, CH_2O). MS (ESI, m/z): 113.0 $[M\text{-}CH_3\text{+}H]^+$.

6-Methoxyhexan-1-amine (27). To a solution of nitrile **35** (100 mg, 0.8 mmol) in anhydrous THF (1 mL), a solution of BH_3 (1 M in THF, 3.2 mL) was added dropwise and the mixture was stirred at reflux for 3.5 h. Once at rt, the reaction was quenched by slow addition of MeOH (1.8 mL) and concentrated HCl (0.2 mL). The product was extracted with DCM and the organic layer was dried over Na_2SO_4 and filtered. The solvent was removed under reduced pressure and the residue was purified by chromatography (EtOAc/MeOH, 9:1) to afford the title amine in 66% yield (70 mg).

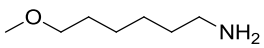

R_f (hexane/EtOAc, 1:1): 0.13. IR (ATR, cm^{-1}): 3332 (NH). ^{1}H NMR ($CDCl_3$, δ): 1.34-1.49 (m, 4H, $2CH_2$), 1.56 (qt, *J* = 6.6 Hz, 2H, CH_2), 1.79 (qt, *J* = 7.4 Hz, 2H, CH_2), 2.99 (t, *J* = 7.7 Hz, 2H, CH_2N), 3.32 (s, 3H, CH_3), 3.37 (t, *J* = 6.4 Hz, 2H, CH_2O). ^{13}C NMR ($CDCl_3$, δ): 25.7, 26.4,

27.6, 29.4 (($\underline{C}H_2)_4CH_2N$) 40.0 (CH_2N), 58.6 (CH_3), 72.6 (CH_2O). MS (ESI, m/z): 132.0 $[M+H]^+$.

3-(2-Methoxyethoxy)propanenitrile (36). A solution of 2-methoxyethanol (2 mL, 26 mmol) in acrylonitrile (15 mL, 229 mmol) was stirred at 0 °C for 10 min. Then, KOH (133 mg, 2.4 mmol) was added and the mixture was stirred at 0 °C for 1.5 h. Concentrated HCl was added and the mixture was evaporated under reduced pressure. The residue was dissolved in chloroform, filtered and the solvent was removed under reduced pressure to obtain the title nitrile in 94% yield (291 mg). The spectroscopic data are in agreement with those previously described.[46]

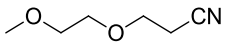

R_f (hexane/EtOAc, 7:3): 0.28. ^{1}H NMR ($CDCl_3$, δ): 2.64 (t, *J* = 6.5 Hz, 2H, CH_2CN), 3.40 (s, 3H, CH_3), 3.55-3.58 (m, 2H, CH_2O), 3.66-3.69 (m, 2H, CH_2O), 3.73 (t, *J* = 6.5 Hz, 2H, CH_2O). MS (ESI, m/z): 130.0 $[M+H]^+$.

3-(2-Methoxyethoxy)propyl-1-amine (28). To a solution of nitrile **36** (440 mg, 31.8 mmol) in anhydrous THF (41.6 mL), a solution of BH_3 (1 M in THF, 7.7 mL) was added dropwise and the mixture was stirred at reflux for 3.5 h. Once at rt, the reaction was quenched by slow addition of MeOH (73 mL) and concentrated HCl (8 mL). The product was extracted with DCM and the organic layer was dried over Na_2SO_4, filtered, and evaporated under reduced pressure to obtain the title amine in 89% yield (912 mg). The spectroscopic data are in agreement with those previously described.[46]

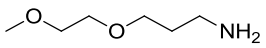

R_f (hexane/EtOAc, 9:1): 0.25. ^{1}H NMR ($CDCl_3$, δ): 1.74 (qt, *J* = 6.5 Hz, 2H, $C\underline{H}_2CH_2N$), 2.78 (t, *J* = 6.8 Hz, 2H, CH_2N), 3.38 (s, 3H, CH_3), 3.52-3.60 (m, 6H, $3CH_2O$). MS (ESI, m/z): 134.1 $[M+H]^+$.

2-[2-(2-Ethoxyethoxy)ethyl]-1*H*-isoindol-1,3(2*H*)-dione (37). To a solution of 2-(2-ethoxyethoxy)ethanol (0.5 mL, 3.7 mmol), phthalimide (549 mg, 3.7 mmol) and triphenylphosphine (977 mg, 3.7 mmol) in anhydrous toluene (11 mL), DIAD (0.8 mL, 4 mmol) was added at 0 °C. The reaction mixture was stirred at 0 °C for 50 min and at rt for an additional 1 h. Then, methanol was added (2.9 mL), the mixture was stirred on at rt and the solvents were removed under reduced pressure. Hexane was added and the

precipitate was filtered and washed with hexane (3x). The solvent was removed under reduced pressure and the residue was purified by chromatography (hexane/EtOAc, 7:3) to obtain the title compound in 58% yield (565 mg). The spectroscopic data are in agreement with those previously described.[47]

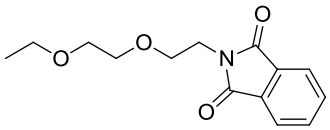

R_f (hexane/EtOAc, 7:3): 0.22. ^{1}H NMR ($CDCl_3$, δ): 1.13 (t, *J* = 7.0 Hz, 3H, CH_3), 3.45 (q, *J* = 7.0 Hz, 2H, CH_3CH_2O), 3.52-3.55 (m, 2H, CH_2N), 3.62-3.65 (m, 2H, CH_2O), 3.74 (t, *J* = 5.8 Hz, 2H, CH_2O), 3.90 (t, *J* = 5.8 Hz, 2H, CH_2O), 7.70 (m, 2H, $2H_{Ar}$), 7.84 (m, 2H, $2H_{Ar}$). MS (ESI, m/z): 264.0 $[M+H]^+$.

2-(2-Ethoxyethoxy)ethanamine (29). To a solution of **37** (295 mg, 1.1 mmol) in dry methanol (4.9 mL), hydrazine (0.1 mL, 2.2 mmol) was added and the reaction mixture was stirred at rt for 2 h. Then, $NaBH_4$ (42 mg, 1.1 mmol) and a second portion of hydrazine (0.1 mL, 2.2 mmol) were added and the mixture was stirred at rt for 16 h. The suspension was filtered and the solvent was removed under reduced pressure. The residue was dissolved in EtOAc (20 mL), warmed to 50 °C, sonicated, and filtered. The filtrate was evaporated, redissolved in Et_2O (20 mL), filtered, and the solvent was removed under reduced pressure to afford the title compound in 71% yield (104 mg). The spectroscopic data are in agreement with those previously described.[47]

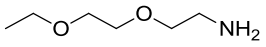

R_f (EtOAc/MeOH, 9:1): 0.35. ^{1}H NMR ($CDCl_3$, δ): 1.20 (t, *J* = 7.0 Hz, 3H, CH_3), 1.95 (br s, 2H, NH_2), 2.85 (t, *J* = 5.2 Hz, 2H, CH_2N), 3.42-3.53 (m, 4H, $2CH_2O$), 3.56-3.62 (m, 4H, $2CH_2O$). MS (ESI, m/z): 134.1 $[M+H]^+$.

(Oxetan-3-ylidene)acetonitrile (38). To a solution of oxetan-3-one (0.7 mL, 10.4 mmol) in dry DCM (3 mL), a solution of Ph_3P=CHCN (3.10 g, 10.4 mmol) in dry DCM (15 mL) was added dropwise. The mixture was stirred for 6 h at rt and the solvent was evaporated under reduced pressure. The residue was dissolved in hexane/Et_2O (3:2), filtered over a plug of silica gel and washed with Et_2O. The solvents were removed under reduced pressure and the residue was purified by chromatography (hexane/EtOAc, 8:2) to give nitrile **38** in 79% yield (780 mg). The spectroscopic data are in agreement with those previously described.[48]

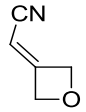

R_f (hexane/EtOAc, 7:3): 0.40. ^{1}H NMR ($CDCl_3$, δ): 5.30 (m, 1H, CH), 5.25-5.28 (m, 2H, CH_2O), 5.29-5.32 (m, 2H, CH_2O). MS (ESI, m/z): 96.0 $[M+H]^+$.

(3-Pentyloxetan-3-yl)acetonitrile (39). To a suspension of CuI (200 mg, 1 mmol) in anhydrous Et_2O (1 mL), pentylmagnesium bromide (2 M in Et_2O, 1.3 mL) was added dropwise. The mixture was cooled to 0 ºC before a solution of nitrile **38** (210 mg, 2.2 mmol) in Et_2O (4 mL) was added 15 min. The reaction mixture was stirred at this temperature for 2 h, quenched with a saturated aqueous solution of NH_4Cl, and extracted with EtOAc. The organic layers were washed with a saturated aqueous solution of NaCl, dried over Na_2SO_4 and filtered. The solvent was removed under reduced pressure and the residue was purified by chromatography (hexane/EtOAc, 8:2) to give the title compound in 26% yield (43 mg).

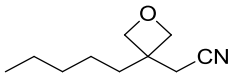

R_f (hexane): 0.20. IR (ATR, cm^{-1}): 2245 (CN). ^{1}H NMR ($CDCl_3$, δ): 0.84 (t, *J* = 6.7 Hz, 3H, CH_3), 1.16-1.29 (m, 6H, $(CH_2)_3CH_3$), 1.74 (m, 2H, CH_2C), 2.75 (s, 2H, CH_2CN), 4.43 (d, *J* = 6.4 Hz, 2H, CH_2O), 4.51 (d, *J* = 6.4 Hz, 2H, CH_2O). ^{13}C NMR ($CDCl_3$, δ): 14.0 (CH_3), 22.5, 23.9, 25.0 ($(CH_2)_3CH_3$), 31.9 (CH_2CN), 35.7 (CH_2C), 41.1 (C), 79.9 ($2CH_2O$), 118.3 (CN). MS (ESI, m/z): 168.1 $[M+H]^+$.

2-(3-Pentyloxetan-3-yl)ethanamine (30). To a suspension of LAH (96 mg, 2.5 mmol) in anhydrous Et_2O, nitrile **39** (200 mg, 1.2 mmol) was added dropwise at 0 ºC. The reaction was stirred for 2 h and the crude was quenched by adding H_2O (2.5 mL), NaOH 1 M (2.5 mL), and H_2O (5 mL). The reaction mixture was extracted with EtOAc and the organic layers were washed with a saturated aqueous solution of NaCl, dried over Na_2SO_4 and filtered. Then, the solvent was removed under reduced pressure to obtain the amine in 59% yield (121 mg).

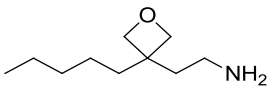

R_f (EtOAc/MeOH, 85:15): 0.10. IR (ATR, cm^{-1}): 3360 (NH). ^{1}H NMR ($CDCl_3$, δ): 0.90 (t, *J* = 6.7 Hz , 3H, CH_3), 1.18-1.35 (m, 6H, $(CH_2)_3CH_3$), 1.54 (br s, 2H, NH_2), 1.65 (app t, *J* = 7.3

Hz, 2H, CH_2C), 1.84 (app t, *J* = 8.1 Hz, 2H, CH_2CH_2N), 2.69 (t, *J* = 7.3 Hz, 2H, CH_2N), 4.40 (AB system, *J* = 5.7 Hz, 4H, $2CH_2O$); ^{13}C-NMR ($CDCl_3$, δ): 14.1 (CH_3), 22.6, 23.7, 31.0 ($(CH_2)_3CH_3$), 32.3 (C), 34.3 (CH_2CH_2N), 35.9 (CH_2C), 41.5 (CH_2N), 81.9 ($2CH_2O$). MS (ESI, m/z): 172.1 $[M+H]^+$.

(4-Ethylpiperazin-1-yl)acetonitrile (40). A mixture of 1-ethylpiperazine (0.7 mL, 5.4 mmol), bromoacetonitrile (0.4 mL, 6.0 mmol) and K_2CO_3 (1.70 g, 12 mmol) in anhydrous ACN (12 mL) was stirred overnight at rt. The crude was filtered through celite washing with ACN, and the solvent was evaporated under reduced pressure to give the title compound in quantitative yield (827 mg).

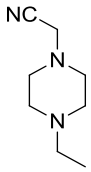

R_f (EtOAc/MeOH, 8:2): 0.28. IR (ATR, cm^{-1}): 2231 (CN). ^{1}H NMR ($CDCl_3$, δ): 1.08 (t, *J* = 7.2 Hz, 3H, CH_3), 2.42 (q, *J* = 7.2 Hz, 2H, CH_3CH_2), 2.51 (m, 4H, $2CH_2N$), 2.64 (t, *J* = 4.6 Hz, 4H, $2CH_2N$), 3.50 (s, 2H, CH_2CN). ^{13}C NMR ($CDCl_3$, δ): 11.9 (CH_3), 45.7 (CH_2N), 51.7 ($2CH_{2cyc}N$), 52.0 (CH_2N), 52.1 ($2CH_{2cyc}N$), 114.7 (CN). MS (ESI, m/z): 154.1 $[M+H]^+$.

(4-Ethylpiperazin-1-yl)ethanamine (32). A mixture of nitrile **40** (465 mg, 3 mmol) in THF (9 mL) was treated with a solution of LAH (242 mg, 6 mmol) in THF (18 mL) at 0 °C for 4 h. After completion, the reaction was quenched with $Na_2SO_4{\cdot}10H_2O$ (8.40 g, excess) and stirred for 30 min. The product was isolated by filtration through celite washing with THF. The crude was evaporated under reduced pressure to give the title compound in 86% yield (405 mg).

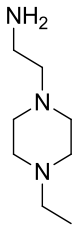

IR (ATR, cm^{-1}): 3311 (NH_2). ^{1}H NMR ($CDCl_3$, δ): 1.07 (t, *J* = 7.2 Hz, 3H, CH_3), 2.36-2.48 (m, 12H, CH_2CH_3, $4CH_2N$, $CH_2CH_2NH_2$), 2.78 (t, *J* = 6.3 Hz, 2H, CH_2NH_2). ^{13}C NMR ($CDCl_3$, δ): 12.1 (CH_3), 38.9 (CH_2NH_2), 52.4 (CH_2CH_3), 52.9 ($2CH_2N$), 53.3 ($2CH_2N$), 61.3 ($CH_2CH_2NH_2$). MS (ESI, m/z): 158.2 $[M+H]^+$.

● **3-Bromo-*N*-phenylpropanamide (31).** Obtained following the general procedure 4.1.1.1. from aniline (0.4 mL, 4.5 mmol) and 3-bromopropanoyl chloride (0.5 mL, 5 mmol) in 92% yield (939 mg). The spectroscopic data are in agreement with those previously described.[49]

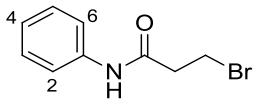

R_f (DCM/MeOH, 95:5): 0.56. Mp: 118-122 °C (Lit.[49] 123-124 °C). ^{1}H NMR ($CDCl_3$, δ): 2.96 (t, *J* = 6.5 Hz, 2H, CH_2CO), 3.65 (t, *J* = 6.5 Hz, 2H, CH_2Br), 7.10 (t, *J* = 7.4 Hz, 1H, H_4), 7.27 (t, *J* = 7.8 Hz, 2H, H_3, H_5), 7.55 (d, *J* = 7.8 Hz, 2H, H_2, H_6), 8.63 (br s, 1H, NH). MS (ESI, m/z): 143.9 $[M+H]^+$.

● **Synthesis of final compounds 4-13**

***N*^{3}-(3-Anilino-3-oxopropyl)-*N*^{3}-hexyl-*N*^{1}-phenyl-β-alaninamide (4).** Obtained following the general procedure 4.1.1.2. from acrylamide **26** (500 mg, 3.4 mmol) and hexylamine (111 mg, 1.1 mmol) in 76% yield (344 mg).

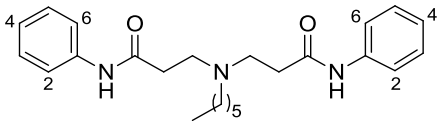

Chromatography: EtOAc/MeOH, 9:1. R_f (EtOAc/MeOH, 9:1): 0.21. IR (ATR, cm^{-1}): 3298 (NH), 1660 (CO), 1601, 1547, 1498, 1443 (Ar). ^{1}H NMR ($CDCl_3$, δ): 0.82 (t, *J* = 6.9 Hz, 3H, CH_3), 1.20-1.28 (m, 6H, $(CH_2)_3CH_3$), 1.50-1.54 (m, 2H, $CH_2(CH_2)_3CH_3$), 2.52 (t, *J* = 6.2 Hz, 6H, $2CH_2CO$, $(CH_2)_4CH_2N$), 2.83 (t, *J* = 6.2 Hz, 4H, $2NCH_2CH_2CO$), 7.02 (t, *J* = 7.4 Hz, 2H, $2H_4$), 7.19 (t, *J* = 7.8 Hz, 4H, $2H_3$, $2H_5$), 7.44 (d, *J* = 7.9 Hz, 4H, $2H_2$, $2H_6$), 9.08 (br s, 2H, 2NH). ^{13}C NMR ($CDCl_3$, δ): 14.4 (CH_3), 23.0, 27.1, 27.7, 32.1 ($(CH_2)_4CH_3$), 34.7 ($2CH_2CO$), 50.1 ($2CH_2N$), 54.0 ($(CH_2)_4CH_2N$), 120.2 ($2C_2$, $2C_6$), 124.4 ($2C_4$), 129.3 ($2C_3$, $2C_5$), 138.5 ($2C_1$), 170.9 (2CO). HRMS (ESI, m/z): Calculated for $C_{24}H_{34}N_3O_2$ $[M+H]^+$: 396.2646. Found: 369.2648.

***N*^{3}-(3-Anilino-3-oxopropyl)-*N*^{3}-cyclopropyl-*N*^{1}-phenyl-β-alaninamide (5).** Obtained following the general procedure 4.1.1.2. from acrylamide **26** (100 mg, 0.7 mmol) and cyclopropylamine (16 µL, 0.2 mmol) in 27% yield (19 mg).

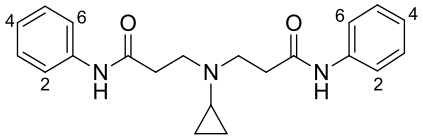

Chromatography: EtOAc/MeOH, 9:1. R_f (EtOAc/MeOH, 9:1): 0.51. IR (ATR, cm^{-1}): 3296 (NH), 1659 (CO), 1598, 1546, 1498, 1443 (Ar). ^{1}H NMR ($CDCl_3$, δ): 0.50-0.55 (m, 2H, CH_{2cyc}), 0.58-0.61 (m, 2H, CH_{2cyc}), 1.78-1.83 (m, 1H, CH_{cyc}), 2.63 (t, *J* = 6.2 Hz, 4H, $2CH_2CO$), 3.02 (t, *J* = 6.2 Hz, 4H, 2 NCH_2CH_2CO), 7.03 (t, *J* = 7.4 Hz, 2H, $2H_4$), 7.19 (t, *J* = 7.8 Hz, 4H, $2H_3$, $2H_5$), 7.41 (d, *J* = 7.7 Hz, 4H, $2H_2$, $2H_6$), 8.70 (br s, 2H, 2NH). ^{13}C NMR ($CDCl_3$, δ): 6.9 ($2CH_{2cyc}$), 34.5 ($2CH_2CO$), 37.2 (CH), 51.7 (CH_2N), 119.6 ($2C_2$, $2C_6$), 124.1 ($2C_4$), 129.0 ($2C_3$, $2C_5$), 138.1 ($2C_1$), 170.6 (2CO). HRMS (ESI, m/z): Calculated for $C_{21}H_{25}N_3O_2Na$ $[M+Na]^+$: 374.18445. Found: 374.17157.

***N*^{3}-(3-Anilino-3-oxopropyl)-*N*^{3}-(cyclopropylmethyl)-*N*^{1}-phenyl-β-alaninamide (6).** Obtained following the general procedure 4.1.1.2. from acrylamide **26** (100 mg, 0.7 mmol) and aminomethylcyclopropane (20 µL, 0.2 mmol) in quantitative yield (73 mg).

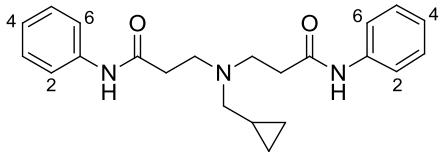

Chromatography: EtOAc/MeOH, 9:1. R_f (EtOAc/MeOH, 9:1): 0.42. IR (ATR, cm^{-1}): 3306 (NH), 1658 (CO), 1599, 1548, 1498, 1444 (Ar). ^{1}H NMR ($CDCl_3$, δ): 0.13 (q, *J* = 5.0 Hz, 2H, CH_{2cyc}), 0.49-0.55 (m, 2H, CH_{2cyc}), 0.88-0.94 (m, 1H, CH_{cyc}), 2.43 (d, *J* = 6.7 Hz, 2H, $CHCH_2N$), 2.52 (t, *J* = 6.3 Hz, 4H, $2CH_2CO$), 2.90 (t, *J* = 6.3 Hz, 4H, $2NCH_2CH_2CO$), 7.01 (t, *J* = 7.4 Hz, 2H, $2H_4$), 7.18 (t, *J* = 7.8 Hz, 4H, $2H_3$, $2H_5$), 7.46 (d, *J* = 7.7 Hz, 4H, $2H_2$, $2H_6$), 9.53 (br s, 2H, 2NH). ^{13}C NMR ($CDCl_3$, δ): 4.3 ($2CH_{2cyc}$), 8.6 (CH), 34.3 ($2CH_2CO$), 49.7 ($2CH_2N$), 58.5 (CH_2N), 119.9 ($2C_2$, $2C_6$), 124.1 ($2C_4$), 128.9 ($2C_3$, $2C_5$), 138.3 ($2C_1$), 170.7 (2CO). HRMS (ESI, m/z): Calculated for $C_{22}H_{27}N_3O_2Na$ $[M+Na]^+$: 388.20010. Found: 388.19619.

***N*^{3}-(3-Anilino-3-oxopropyl)-*N*^{3}-(3-butoxypropyl)-*N*^{1}-phenyl-β-alaninamide (7).** Obtained following the general procedure 4.1.1.2. from acrylamide **26** (336 mg, 2.3 mmol) and 3-butoxypropan-1-amine (0.1 mL, 0.8 mmol) in 25% yield (81 mg).

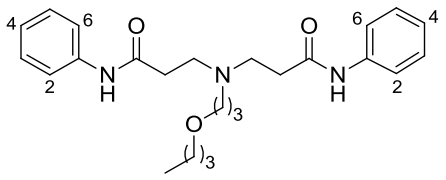

Chromatography: EtOAc. R_f (EtOAc): 0.30. IR (ATR, cm^{-1}): 3287 (NH), 1661 (CO), 1600, 1547, 1498, 1443 (Ar). ^{1}H NMR ($CDCl_3$, δ): 0.76 (t, *J* = 7.3 Hz, 3H, CH_3), 1.10-1.37 (m, 4H, $(CH_2)_2CH_3$), 1.64 (qt, *J* = 6.6 Hz, 2H, $NCH_2CH_2CH_2O$), 2.44-2.52 (m, 6H, $2CH_2CO$, $NCH_2(CH_2)_2O$), 2.75 (t, *J* = 6.3 Hz, 4H, $2NCH_2CH_2CO$), 3.13 (t, *J* = 6.6 Hz, 2H, CH_2O), 3.30 (t, *J* = 6.4 Hz, 2H, CH_2O), 6.93 (t, *J* = 7.4 Hz, 2H, $2H_4$), 7.10 (t, *J* = 7.9 Hz, 4H, $2H_3$, $2H_5$), 7.37 (dd, *J* = 8.8, 1.0 Hz, 4H, $2H_2$, $2H_6$). ^{13}C NMR ($CDCl_3$, δ): 14.4 (CH_3), 20.4, 28.3, 32.9 ($(CH_2)_2CH_3$, $NCH_2CH_2CH_2O$), 35.6 ($2CH_2CO$), 51.2 ($2CH_2N$), 51.3 (CH_2N), 69.8, 71.7 ($2CH_2O$), 121.3 ($2C_2$, $2C_6$), 125.1 ($2C_4$), 129.8 ($2C_3$, $2C_5$), 139.7 ($2C_1$), 173.4 (2CO). HRMS (ESI, m/z): Calculated for $C_{25}H_{35}N_3O_3Na$ $[M+Na]^+$: 448.25761. Found: 448.25641.

***N*^{3}-[6-(Methoxyhexyl)]-*N*^{1}-phenyl-*N*^{3}-[3-(phenylamino)-3-oxopropyl]-β-alaninamide (8).** Obtained following the general procedure 4.1.1.2. from acrylamide **26** (168 mg, 1.1 mmol) and amine **27** (60 mg, 0.5 mmol) in 21% yield (133 mg).

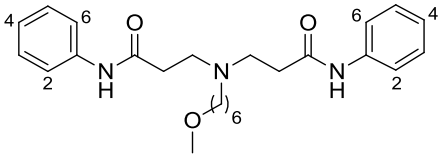

Chromatography: EtOAc/MeOH, 9:1. R_f (EtOAc/MeOH, 9:1): 0.42. IR (ATR, cm^{-1}): 3238 (NH), 1678, 1645 (CO), 1601, 1548, 1495, 1443 (Ar). ^{1}H NMR ($CDCl_3$, δ): 1.18-1.58 (m, 8H, $OCH_2(CH_2)_4$), 2.51 (t, *J* = 7.1 Hz, 2H, $(CH_2)_5CH_2N$), 2.53 (t, *J* = 5.9 Hz, 4H, $2CH_2CO$), 2.83 (t, *J* = 6.1 Hz, 4H, $2NCH_2CH_2CO$), 3.29-3.33 (m, 5H, CH_2OCH_3), 7.02 (t, *J* = 7.4 Hz, 2H, $2H_4$), 7.18 (t, *J* = 7.8 Hz, 4H, $2H_3$, $2H_5$), 7.44 (d, *J* = 7.8 Hz, 4H, $2H_2$, $2H_6$), 9.20 (br s, 2H, 2NH). ^{13}C NMR ($CDCl_3$, δ): 25.9, 26.6, 27.2, 29.5 ($(CH_2)_4CH_2O$), 34.6 ($2CH_2CO$), 50.0 ($2CH_2N$), 53.4 ($(CH_2)_5CH_2N$), 58.6 (CH_3), 72.8 (CH_2O), 119.9 ($2C_2$, $2C_6$), 124.0 ($2C_4$), 128.9 ($2C_3$, $2C_5$), 138.3 ($2C_1$), 170.7 (2CO). HRMS (ESI, m/z): Calculated for $C_{25}H_{34}N_3O_3$ $[M-H]^-$: 424.26001. Found: 424.26106.

***N*^{3}-(3-Anilino-3-oxopropyl)-*N*^{3}-[3-(2-methoxyethoxy)propyl]-*N*^{1}-phenyl-β-alaninamide (9).** Obtained following the general procedure 4.1.1.2. from acrylamide **26** (332 mg, 2.3 mmol) and amine **28** (100 mg, 0.8 mmol) in 39% yield (133 mg).

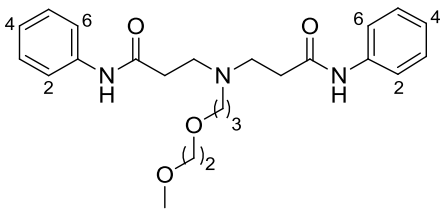

Chromatography: EtOAc/MeOH, 8:2. R_f (EtOAc/MeOH, 9:1): 0.29. IR (ATR, cm^{-1}): 3305 (NH), 1662, 1545 (CO), 1600, 1497, 1443 (Ar). ^{1}H NMR ($CDCl_3$, δ): 1.59 (qt, *J* = 5.7 Hz, 2H, $NCH_2CH_2CH_2O$), 2.51 (app t, 4H, $2CH_2CO$), 2.54 (t, *J* = 5.4 Hz, 2H, $NCH_2CH_2CH_2O$), 2.75 (t, *J* = 5.4 Hz, 4H, $2NCH_2CH_2CO$), 3.28 (t, *J* = 5.5 Hz, 2H, $NCH_2CH_2CH_2O$), 3.39-3.42 (m, 2H, CH_2O), 3.45 (s, 3H, CH_3), 3.60-3.63 (m, 2H, CH_2O), 6.98 (t, *J* = 7.3 Hz, 2H, $2H_4$), 7.11 (t, *J* = 7.7 Hz, 4H, $2H_3$, $2H_5$), 7.39 (d, *J* = 8.1 Hz, 4H, $2H_2$, $2H_6$), 8.89 (br s, 2H, 2NH). ^{13}C NMR ($CDCl_3$, δ): 27.1 (CH_2), 35.5 ($2CH_2CO$), 49.3 (CH_2N), 50.6 ($2CH_2N$), 58.9 (CH_3), 67.2, 69.4, 72.5 ($3CH_2O$), 119.8 ($2C_2$, $2C_6$), 123.6 ($2C_4$), 128.7 ($2C_3$, $2C_5$), 138.4 ($2C_1$), 171.9 (2CO). HRMS (ESI, m/z): Calculated for $C_{24}H_{34}N_3O_4$ $[M+H]^+$: 428.25493. Found: 428.25429.

***N*^{3}-(3-Anilino-3-oxopropyl)-*N*^{3}-[2-(2-ethoxyethoxy)ethyl]-*N*^{1}-phenyl-β-alaninamide (10).** Obtained following the general 4.1.1.2. from acrylamide **26** (332 mg, 2.3 mmol) and amine **29** (100 mg, 0.8 mmol) in 53% yield (181 mg).

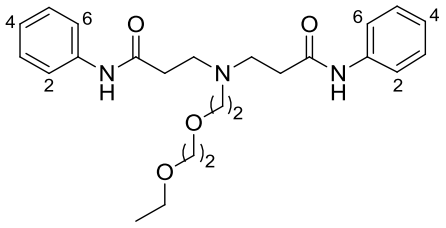

Chromatography: EtOAc/MeOH, 8:2. R_f (EtOAc/MeOH, 9:1): 0.30. IR (ATR, cm^{-1}): 3303 (NH), 1660, 1547 (CO), 1601, 1496, 1443 (Ar). ^{1}H NMR ($CDCl_3$, δ): 1.14 (t, *J* = 7.0 Hz, 3H, CH_3), 2.53 (t, *J* = 6.0 Hz, 4H, $2CH_2CO$), 2.74 (t, *J* = 4.9 Hz, 2H, NCH_2CH_2O), 2.87 (t, *J* = 6.0 Hz, 4H, $2NCH_2CH_2CO$), 3.44-3.49 (m, 4H, NCH_2CH_2O, OCH_2CH_3), 3.54-3.59 (m, 4H, $O(CH_2)_2O$), 6.98 (t, *J* = 7.4 Hz, 2H, $2H_4$), 7.13 (t, *J* = 7.8 Hz, 4H, $2H_3$, $2H_5$), 7.43 (d, *J* = 7.7 Hz, 4H, $2H_2$, $2H_6$), 9.24 (br s, 2H, 2NH). ^{13}C NMR ($CDCl_3$, δ): 15.0 (CH_3), 35.2 ($2CH_2CO$), 51.4 ($2CH_2N$), 54.7 (CH_2N), 66.6, 69.3, 69.6, 70.3 ($4CH_2O$), 120.0 ($2C_2$, $2C_6$), 123.8 ($2C_4$), 128.7 ($2C_3$, $2C_5$), 138.3 ($2C_1$), 171.0 (2CO). HRMS (ESI, m/z): Calculated for $C_{24}H_{33}N_3O_4Na$ $[M+Na]^+$: 450.23688. Found: 450.23663.

***N*^{3}-(3-Anilino-3-oxopropyl)-*N*^{3}-[(3-pentyloxetan-3-yl)ethyl]-*N*^{1}-phenyl-β-alaninamide (11).** Obtained following the general procedure 4.1.1.2. from acrylamide **26** (275 mg, 1.9 mmol) and amine **30** (98 mg, 0.6 mmol) in 21% yield (63 mg).

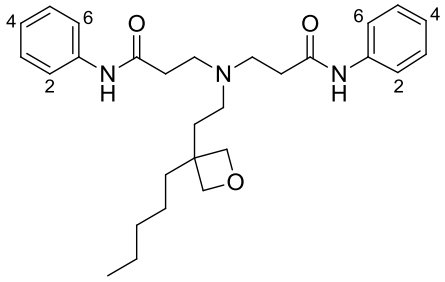

Chromatography: EtOAc/MeOH, 9:1. R_f (EtOAc/MeOH, 95:5): 0.60. IR (ATR, cm^{-1}): 3304 (NH), 1657 (CO), 1598, 1542, 1498, 1442 (Ar). ^{1}H NMR ($CDCl_3$, δ): 0.88 (t, *J* = 7.1 Hz, 3H, CH_3), 1.15-1.31 (m, 6H, $(CH_2)_3CH_3$), 1.56 (app t, *J* = 7.3 Hz, 2H, CH_2C), 1.78 (t, *J* = 7.1 Hz, 2H, CCH_2CH_2N), 2.56 (t, *J* = 5.8 Hz, 4H, $2CH_2CO$), 2.63 (t, *J* = 7.1 Hz, 2H, CCH_2CH_2N), 2.87 (t, *J* = 5.8 Hz, 4H, $2CH_2N$), 4.30 (d, *J* = 5.9 Hz, 2H, CH_2O), 4.45 (d, *J* = 5.9 Hz, 2H, CH_2O), 7.02 (t, *J* = 7.5 Hz, 2H, $2H_4$), 7.16 (t, *J* = 7.5 Hz, 4H, $2H_3$, $2H_5$), 7.38 (d, *J* = 8.1 Hz, 4H, $2H_2$, $2H_6$), 8.63 (br s, 2H, 2NH). ^{13}C NMR ($CDCl_3$, δ): 14.1 (CH_3), 22.6, 23.8 ($(CH_2)_2CH_3$), 31.6 (CCH_2CH_2N), 32.2 ($CH_2(CH_2)_2CH_3$), 35.1 ($2CH_2CO$), 36.9 (CH_2C), 41.4 (C), 49.2 (CCH_2CH_2N), 50.1 ($2CH_2N$), 80.9 ($2CH_2O$), 119.8 ($2C_2$, $2C_6$), 124.0 ($2C_4$), 128.8 ($2C_3$, $2C_5$), 138.0 ($2C_1$), 170.6 (2CO). HRMS (ESI, m/z): Calculated for $C_{28}H_{39}N_3O_2$ $[M+H]^+$: 466.3025. Found: 466.3050.

● **General procedure for the synthesis of final compounds 12 and 13.** To a solution of bromo derivative **31** (3 equiv) and the corresponding amine (1 equiv) in DCM (0.5 mL/mmol), Et_3N (2.5 equiv) and KI (0.01 equiv) were added, and the reaction mixture was stirred for 24 h at 60 °C. The solvent was removed under reduced pressure and the crude was purified by column chromatography to give the title compounds.

***N*^{3}-(3-Anilino-3-oxopropyl)-*N*^{3}-[2-(4-ethylpiperidin-1-yl)ethyl]-*N*^{1}-phenyl-β-alaninamide (12).** Obtained from **31** (218 mg, 0.9 mmol) and 2-(4-ethylpiperidin-1-yl)ethanamine (42 mg, 0.3 mmol) in 48% yield (65 mg).

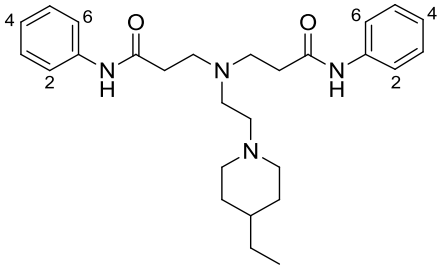

Chromatography: EtOAc/MeOH/NH_3, 9:1:0.2. R_f (EtOAc/MeOH/NH_3, 9:1:0.2): 0.43. IR (ATR, cm^{-1}): 3310 (NH), 1675 (CO), 1602, 1551, 1498, 1445 (Ar). ^{1}H NMR ($CDCl_3$, δ): 0.76 (t, *J* = 7.3 Hz, 3H, CH_3), 1.04-1.12 (m, 5H, CH_2CH_3, CH, 2x½CH_{2cyc}), 1.48 (d, *J* = 11.2 Hz, 2H, 2x½CH_{2cyc}), 1.92 (t, *J* = 11.1 Hz, 2H, 2x½CH_{2cyc}N), 2.52-2.54 (m, 6H, $N_{cyc}CH_2CH_2N$, $2CH_2CO$), 2.71 (t, *J* = 6.1 Hz, 2H, $N_{cyc}CH_2CH_2N$), 2.85 (t, *J* = 6.0 Hz, 4H, $2NCH_2CH_2CO$), 2.95 (d, *J* = 11.3 Hz, 2H, 2x½CH_{2cyc}N), 7.01 (t, *J* = 7.4 Hz, 2H, $2H_4$), 7.17 (t, *J* = 7.8 Hz, 4H, $2H_3$, $2H_5$), 7.44 (d, *J* = 7.9 Hz, 4H, $2H_2$, $2H_6$), 8.84 (br s, 2H, 2NH). ^{13}C NMR ($CDCl_3$, δ): 14.3 (CH_3), 29.2 (CH_2CH_3), 31.6 ($2CH_{2cyc}$), 35.2 ($2CH_2CO$), 37.3 (CH), 50.8 ($2NCH_2CH_2CO$), 51.5 ($N_{cyc}CH_2CH_2N$), 54.9 ($2CH_2N$), 56.8 ($N_{cyc}CH_2CH_2N$), 120.2 ($2C_2$, $2C_6$), 124.1 ($2C_4$), 128.9 ($2C_3$, $2C_5$), 138.2 ($2C_1$), 170.8 (2CO). HRMS (ESI, m/z): Calculated for $C_{27}H_{39}N_4O_2$ $[M+H]^+$: 451.30730. Found: 451.30714.

***N*^{3}-(3-Anilino-3-oxopropyl)-*N*^{3}-[2-(4-ethylpiperazin-1-yl)ethyl]-*N*^{1}-phenyl-β-alaninamide (13).** Obtained from **31** (218 mg, 0.9 mmol) and amine **32** (50 mg, 0.3 mmol) in 54% yield (73 mg).

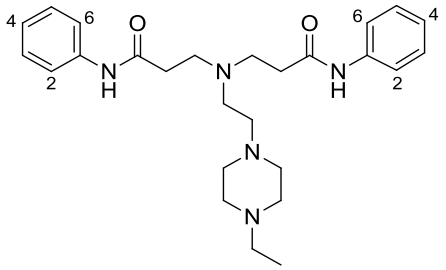

Chromatography: EtOAc/MeOH/NH_3, 7:3:0.2. R_f (EtOAc/MeOH/NH_3, 8:2:0.2): 0.22. Mp: 70-72 °C. IR (ATR, cm^{-1}): 3276 (NH), 1664 (CO), 1601, 1548, 1498, 1445 (Ar). ^{1}H NMR ($CDCl_3$, δ): 0.96 (t, *J* = 7.2 Hz, 3H, CH_3), 2.23 (q, *J* = 7.2 Hz, 2H, CH_2CH_3), 2.19-2.53 (m, 14H, $2CH_2CO$, $4CH_{2cyc}$, $N_{cyc}CH_2CH_2N$), 2.64 (t, *J* = 5.9 Hz, 2H, $N_{cyc}CH_2CH_2N$), 2.80 (t, *J* = 6.1 Hz, 4H, $2NCH_2CH_2CO$), 7.00 (t, *J* = 7.4 Hz, 2H, $2H_4$), 7.16 (t, *J* = 7.8 Hz, 4H, $2H_3$, $2H_5$), 7.44 (d, *J* = 7.7 Hz, 4H, $2H_2$, $2H_6$), 9.24 (br s, 2H, 2NH). ^{13}C NMR ($CDCl_3$, δ): 11.9 (CH_3), 34.8 ($2CH_2CO$), 50.6 ($2NCH_2CH_2CO$), 50.8 ($N_{cyc}CH_2CH_2N$), 52.2 (CH_2CH_3), 52.4 ($2CH_{2cyc}$), 53.8 ($2CH_{2cyc}$), 56.3 ($N_{cyc}CH_2CH_2N$), 120.3 ($2C_2$, $2C_6$), 124.1 ($2C_4$), 128.9 ($2C_3$, $2C_5$), 138.3 ($2C_1$), 170.7 (2CO). HRMS (ESI, m/z): Calculated for $C_{26}H_{38}N_5O_2$ $[M+H^+]$: 452.30255. Found: 452.30104.

4.1.3. Synthesis of final compounds 14, 16, and 17

● **Synthesis of acrylamides 41-43**

***N*-Methyl-*N*-phenylacrylamide (41)**. Obtained using the general procedure 4.1.1.1. from acryloyl chloride (268 µL, 3.3 mmol), pyridine (268 µL, 3.3 mmol) and *N*-methylaniline (317 µL, 3.0 mmol) in quantitative yield (484 mg). The spectroscopic data are in agreement with those previously described.[43]

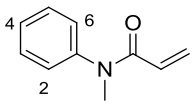

R_f (hexane/EtOAc, 7:3): 0.26. Mp: 75-76 °C. (Lit.[43] 74-76 °C). ^{1}H-NMR ($CDCl_3$, δ): 3.37 (s, 3H, CH_3N), 5.52 (dd, *J* = 10.3, 2.0 Hz, 1H, ½CH_2=), 6.08 (dd, *J* = 16.8, 10.4 Hz, 1H, CH=), 6.37 (dd, *J* = 16.8, 2.0 Hz, 1H, ½CH_2=), 7.19 (d, *J* = 7.1 Hz, 2H, H_2, H_6), 7.34 (t, *J* = 7.3 Hz, 1H, H_4), 7.42 (t, *J* = 7.4 Hz, 2H, H_3, H_5). MS (ESI, m/z): 162.1 $[M+H]^+$.

General procedure for the obtention of sulfonamides 42, 43. Over a solution of the corresponding aniline (1 equiv) and pyridine (1.1 equiv) in anhydrous acetone (2.5 mL/mmol), 2-chloroethane sulfonyl chloride (1.1 equiv) was added dropwise at 0 °C. The reaction mixture was stirred overnight at 0-10 °C and then, the solvent was removed under reduced pressure. The obtained residue was redissolved in DCM and washed with saturated aqueous solutions of $NaHCO_3$, $CuSO_4$ and NaCl, subsequently. The organic extract was dried over Na_2SO_4, filtered, and the solvent was removed under reduced pressure. The crude was purified by column chromatography to yield desired sulfonamides.

***N*-Phenylethylensulfonamide (42)**. Obtained from aniline (245 µL, 2.7 mmol), pyridine (238 µL, 3.0 mmol), and 2-chloroethanesulfonyl chloride (309 µL, 3.0 mmol) in 30% yield (148 mg). The spectroscopic data are in agreement with those previously reported.[50]

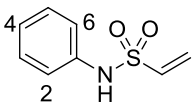

Chromatography: hexane/EtOAc, 6:4; R_f (hexane/EtOAc, 7:3): 0.29. Mp: 67-68 °C. ^{1}H-NMR ($CDCl_3$, δ): 5.94 (d, *J* = 10.0 Hz, 1H, ½CH_2=), 6.09 (d, *J* = 16.5 Hz, 1H, ½CH_2=), 6.66 (dd, *J* = 16.5, 10.0 Hz, 1H, CH=), 7.06 (tt, *J* = 6.9, 1.8 Hz, 1H, H_4), 7.21-7.32 (m, 4H, H_2, H_3, H_5, H_6), 8.69 (br s, 1H, NH). MS (ESI, m/z): 184.1 $[M+H]^+$.

***N*-Methyl-*N*-phenylethylensulfonamide (43)**. Obtained from *N*-methylaniline (300 µL, 2.3 mmol), pyridine (0.2 mL, 2.6 mmol), and 2-chloroethanesulfonyl chloride (300 µL, 2.3 mmol) in 70% yield (321 mg). The spectroscopic data are in agreement with those previously described.[50]

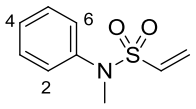

R_f (hexane/EtOAc, 8:2): 0.32. Mp: 73-74 °C. ^{1}H-NMR ($CDCl_3$, δ): 3.25 (s, 3H, CH_3), 6.02 (d, *J* = 9.9 Hz, 1H, ½CH_2=), 6.20 (d, *J* = 16.6 Hz, 1H, ½CH_2=), 6.46 (dd, *J* = 16.6, 9.9 Hz, 1H, CH=), 7.29-7.41 (m, 5H, H_2-H_6). MS (ESI, m/z): 198.1 [$(M+H)^+$].

● Synthesis of diamides 14, 16, and 17

***N*^{1}-Methyl-*N*^{3}-octyl-*N*^{1}-phenyl-*N*^{3}-{3-[phenyl(methyl)amino]-3-oxopropyl}-β-alaninamide (14).** Obtained using the procedure 4.1.1.2. from acrylamide **41** (325 mg, 2.0 mmol) and octylamine (111 µL, 0.7 mmol) in 64% yield (202 mg).

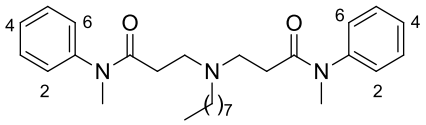

Chromatography: EtOAc. R_f (EtOAc/methanol, 9:1): 0.37. IR (ATR, cm^{-1}): 1651 (CON), 1595, 1495, 1454 (Ar). ^{1}H-NMR ($CDCl_3$, δ): 0.88 (t, *J* = 6.9 Hz, 3H, CH_3CH_2), 1.06-1.29 (m, 12H, $(CH_2)_6CH_3$), 2.09 (m, 2H, $(CH_2)_6CH_2N$), 2.14 (t, *J* = 7.6 Hz, 4H, $2CH_2CO$), 2.60 (t, *J* = 7.3 Hz, 4H, $2COCH_2CH_2N$), 3.23 (s, 6H, $2CH_3N$), 7.15 (d, *J* = 7.4 Hz, 4H, $2H_2$, $2H_6$), 7.33 (t, *J* = 7.4 Hz, 2H, $2H_4$), 7.40 (t, *J* = 7.3 Hz, 4H, $2H_3$, $2H_5$). ^{13}C-NMR ($CDCl_3$, δ): 14.5 (CH_3CH_2), 23.1, 27.3, 27.8, 29.7, 29.8, 32.1 ($(CH_2)_6CH_3$), 32.2 ($2CH_2CO$), 37.7 ($2CH_3N$), 50.1 ($2CH_2N$), 54.1 ($(CH_2)_6CH_2N$), 127.7 ($2C_2$, $2C_6$), 128.2 ($2C_4$), 130.2 ($2C_3$, $2C_5$), 144.4 ($2C_1$), 172.3 (2CO). HRMS (ESI, m/z): Calculated for $C_{28}H_{42}N_3O_2$ $[M+H]^+$: 452.3271. Found: 452.3286.

2-2´-(Octylimino)bis(*N*-phenylethanesulfonamide) (16). Obtained using the procedure 4.1.1.2. from sulfonamide **42** (140 mg, 0.8 mmol) and octylamine (42 µL, 0.3 mmol) in 44% yield (65 mg).

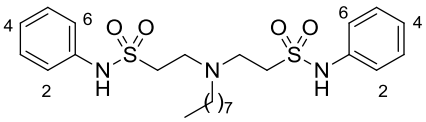

Chromatography: hexane/EtOAc, 6:4. R_f (hexane/EtOAc, 6:4): 0.50. IR (ATR, cm^{-1}): 3247 (NH), 1600, 1496 (Ar), 1340, 1148 (SO_2). ^{1}H-NMR ($CDCl_3$, δ): 0.88 (t, *J* = 6.9 Hz, 3H, CH_3), 1.02-1.37 (m, 12H, $(CH_2)_6CH_3$), 2.41 (app t, *J* = 8.0 Hz, 2H, $(CH_2)_6CH_2N$), 2.99 (t, *J* = 5.3 Hz, 4H, $2CH_2SO_2$), 3.33 (t, *J* = 5.6 Hz, 4H, $2CH_2N$), 7.11-7.19 (m, 2H, $2H_4$), 7.28-7.37 (m, 8H, $2H_2$, $2H_3$, $2H_5$, $2H_6$), 7.95 (br s, 2H, 2NH). ^{13}C-NMR ($CDCl_3$, δ): 14.1 (CH_3), 22.6, 23.0, 27.4, 29.2, 29.3, 31.8 ($(CH_2)_6CH_3$), 48.3 ($2CH_2N$), 49.4 ($2CH_2SO_2$), 50.7 (CH_2N), 119.5 ($2C_2$, $2C_6$), 124.6 ($2C_4$), 129.5 ($2C_3$, $2C_5$), 137.3 ($2C_1$). HRMS (ESI, m/z): Calculated for $C_{24}H_{36}N_3O_4S_2$ $[M-H]^-$: 494.2152. Found: 494.2173.

2,2'-(Octylimino)bis(*N*-methyl-*N*-phenylethanesulfonamide) (17). Obtained using the procedure 4.1.1.2. from sulfonamide **43** (140 mg, 0.8 mmol) and octylamine (42 µL, 0.3 mmol) in 81% yield (127 mg).

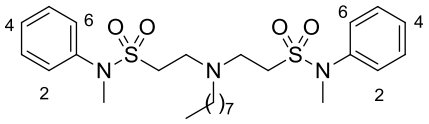

Chromatography: EtOAc. R_f (hexane/EtOAc, 7:3): 0.30. IR (ATR, cm^{-1}): 1597, 1493, 1454 (Ar), 1341, 1142 (SO_2). ^{1}H-NMR ($CDCl_3$, δ) 0.88 (t, *J* = 6.8 Hz, 3H, CH_3CH_2), 1.24-1.41 (m, 12H, $(CH_2)_6CH_3$), 2.35 (app t, *J* = 7.4 Hz, 2H, $(CH_2)_6CH_2N$), 2.85-2.90 (m, 4H, $2CH_2SO_2$), 3.07-3.12 (m, 4H, $2CH_2N$), 3.31 (s, 6H, $2CH_3N$), 7.25-7.32 (m, 2H, $2H_4$), 7.34-7.40 (m, 8H, $2H_2$, $2H_3$, $2H_5$, $2H_6$). ^{13}C-NMR ($CDCl_3$, δ): 14.2 (CH_3CH_2), 22.7, 27.1, 27.2, 29.3, 29.4, 31.8 ($(CH_2)_6CH_3$), 38.3 ($2CH_3N$), 46.8 ($2CH_2N$), 47.4 ($2CH_2SO_2$), 53.9 ($(CH_2)_6CH_2N$), 126.2 ($2C_2$, $2C_6$), 127.4 ($2C_4$), 129.4 ($2C_3$, $2C_5$), 141.2 ($2C_1$). HRMS (ESI, m/z): Calculated for $C_{26}H_{42}N_3O_4S_2$ $[M+H]^+$: 524.26112. Found: 524.25981.

4.1.4. Synthesis of final compounds 15, 18-20

***N*^{3}-Octyl-*N*^{1}-phenyl-β-alaninamide (44).** A mixture of acrylamide **26** (200 mg, 1.4 mmol), octylamine (674 µL, 4.1 mmol) and DBU (610 µL, 4.1 mmol) in anhydrous ACN (20 mL) was stirred for 5 h at 60 °C. Then, the solvent was removed under reduced pressure and the residue was purified by chromatography (hexane/EtOAc, 1:1) to obtain the desired secondary amide in 76% yield (294 mg).

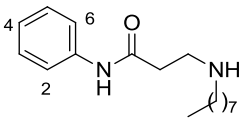

R_f (EtOAc): 0.12. IR (ATR, cm^{-1}): 3297 (NH), 1667, 1551 (CON), 1601, 1497, 1444 (Ar). ^{1}H-NMR ($CDCl_3$, δ): 0.86-0.88 (m, 3H, CH_3), 1.29 (m, 10H, $(CH_2)_5CH_3$), 1.54-1.58 (m, 2H, $CH_2(CH_2)_5CH_3$), 2.48 (t, *J* = 5.2 Hz, 2H, CH_2CO), 2.69 (t, *J* = 6.8 Hz, 2H, $(CH_2)_6CH_2N$), 2.97 (t, *J* = 5.4 Hz, 2H, $COCH_2CH_2N$), 3.48 (br s, 1H, NH), 7.06 (t, *J* = 7.3 Hz, 1H, H_4), 7.29 (t, *J* = 7.7 Hz, 2H, H_3, H_5), 7.53 (d, *J* = 7.8 Hz, 2H, H_2, H_6). ^{13}C-NMR ($CDCl_3$, δ): 14.1 (CH_3), 22.7, 27.5, 29.3, 29.5, 30.1, 31.8 ($(CH_2)_6CH_3$), 36.1 (CH_2CO), 45.5 (CH_2N), 49.3 ($(CH_2)_6CH_2N$), 119.7 (C_2, C_6), 123.6 (C_4), 128.9 (C_3, C_5), 138.8 (C_1), 171.1 (CO). MS (ESI, m/z): 277.2 $[M+H]^+$.

***N*^{3}-{3-[Methyl(phenyl)amino]-3-oxopropyl}-*N*^{3}-octyl-*N*^{1}-phenyl-β-alaninamide (15).** Obtained following the general procedure 4.1.1.2. from acrylamide **41** (87 mg, 0.5 mmol), DBU (81 µL, 0.5 mmol), and amine **44** (100 mg, 0.2 mmol) in 58% yield (102 mg).

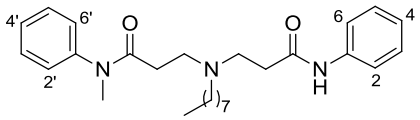

Chromatography: EtOAc/MeOH, 9:1. R_f (EtOAc/MeOH, 9:1): 0.31. IR (ATR, cm^{-1}): 3306 (NH), 1658 (CO), 1599, 1547, 1497 (Ar). ^{1}H NMR ($CDCl_3$, δ): 0.88 (t, *J* = 6.8 Hz, 3H, CH_3CH_2), 1.23 (m, 10H, $(CH_2)_5CH_3$), 1.47 (m, 2H, $CH_2(CH_2)_5CH_3$), 2.30 (t, *J* = 6.8 Hz, 2H, CH_2CO), 2.39 (t, *J* = 7.5 Hz, 2H, $(CH_2)_6CH_2N$), 2.46 (app t, 2H, CH_2CO), 2.63 (app t, 2H, NCH_2CH_2CO), 2.84 (t, *J* = 6.8 Hz, 2H, NCH_2CH_2CO), 3.18 (s, 3H, CH_3N), 7.07 (t, *J* = 7.4 Hz, 1H, H_4), 7.10 (d, *J* = 6.7 Hz, 2H, $H_{2'}$, $H_{6'}$), 7.27-7.42 (m, 5H, H_3, H_5, $H_{3'}$-$H_{5'}$), 7.50 (d, *J* = 7.9 Hz, 2H, H_2, H_6), 10.40 (br s, 1H, NH). ^{13}C NMR ($CDCl_3$, δ): 14.1 (CH_3CH_2), 22.6, 26.6, 27.6, 29.3, 29.5 ($5CH_2$), 31.5 (CH_2CONCH_3), 31.8 (CH_2), 33.9 (CH_2CONH), 37.3 (CH_3N), 49.1, 50.3 ($2CH_2N$), 53.4 ($(CH_2)_6CH_2N$), 119.8 (C_2, C_6), 123.5 (C_4), 127.1 ($C_{2'}$, $C_{6'}$), 128.0 ($C_{4'}$), 128.8 (C_3, C_5), 129.9 ($C_{3'}$, $C_{5'}$), 138.7 (C_1), 143.7 ($C_{1'}$), 170.9, 171.2 (2CO). HRMS (ESI, m/z): Calculated for $C_{27}H_{39}N_3O_2$ $[M+H]^+$: 437.3042. Found: 437.3041.

***N*^{3}-[2-(Anilinosulfonyl)ethyl]-*N*^{3}-octyl-*N*^{1}-phenyl-β-alaninamide (18).** Obtained following the general procedure 4.1.1.2. from sulfonamide **42** (150 mg, 0.8 mmol), DBU (122 µL, 0.8 mmol), and amine **44** (151 mg, 0.8 mmol) in 12% yield (44 mg).

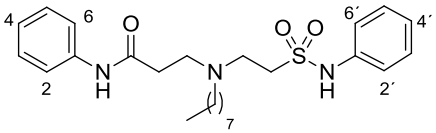

Chromatography: hexane/EtOAc, 7:3. R_f (hexane/EtOAc, 7:3): 0.35. IR (ATR, cm^{-1}): 3253 (NH), 1661, 1545 (CO), 1599, 1498, 1466 (Ar), 1376, 1148 (SO_2). ^{1}H NMR ($CDCl_3$, δ): 0.81 (t, *J* = 6.8 Hz, 3H, CH_3), 1.04-1.29 (m, 10H, $(CH_2)_5CH_3$), 1.36 (m, 2H, $CH_2(CH_2)_5CH_3$), 2.35 (app t, *J* = 7.7 Hz, 2H, $(CH_2)_6CH_2N$), 2.44 (t, *J* = 5.8 Hz, 2H, CH_2CO), 2.71 (t, *J* = 5.7 Hz, 2H, NCH_2CH_2CO), 2.96 (t, *J* = 6.5 Hz, 2H, CH_2SO_2), 3.21 (t, *J* = 6.5 Hz, 2H, $NCH_2CH_2SO_2$), 6.99-7.12 (m, 4H, H_4, $H_{2'}$, $H_{4'}$, $H_{6'}$), 7.19-7.32 (m, 5H, H_3, H_5, $H_{3'}$, $H_{5'}$, NH), 7.48 (d, *J* = 7.7 Hz, 2H, H_2, H_6), 9.12 (br s, 1H, NH). ^{13}C NMR ($CDCl_3$, δ): 14.1 (CH_3), 22.6, 26.3, 27.5, 29.2, 29.4, 31.8 ($(CH_2)_6CH_3$), 34.6 (CH_2CO), 47.4 (CH_2SO_2), 48.1 ($SO_2CH_2CH_2N$), 50.5 ($COCH_2CH_2N$), 53.7 ($(CH_2)_6CH_2N$), 119.9, 120.5 (C_2, C_6, $C_{2'}$, $C_{6'}$), 124.1, 125.0 (C_4, $C_{4'}$), 128.9, 129.6 (C_3, C_5, $C_{3'}$, $C_{5'}$), 136.9 ($C_{1'}$), 138.1 (C_1), 170.8 (CO). HRMS (ESI, m/z): Calculated for $C_{25}H_{38}N_3O_3S$ $[M+H]^+$: 460.26284. Found: 460.26383.

***N*^{3}-(2-{[Methyl(phenyl)amino]sulfonyl}ethyl)-*N*^{3}-octyl-*N*^{1}-phenyl-β-alaninamide (19)**. Obtained following the general procedure 4.1.1.2. from sulfonamide **43** (103 mg, 0.5 mmol), DBU (0.1 mL, 0.5 mmol) and amine **44** (96 mg, 0.4 mmol) in 39% yield (64 mg).

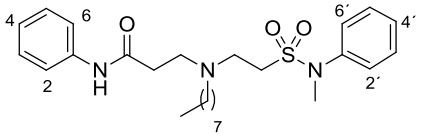

Chromatography: hexane/EtOAc, 4:6. R_f (hexane/EtOAc, 1:1): 0.38. IR (ATR, cm^{-1}): 3322 (NH), 1664, 1543 (CON), 1598, 1494, 1443 (Ar), 1342, 1143 (SO_2). ^{1}H-NMR ($CDCl_3$, δ): 0.79 (t, *J* = 6.8 Hz, 3H, CH_3CH_2), 1.15-1.22 (m, 10H, $(CH_2)_5CH_3$), 1.38-1.43 (m, 2H, $CH_2(CH_2)_5CH_3$), 2.39 (t, *J* = 5.4 Hz, 2H, CH_2CO), 2.42 (t, *J* = 7.4 Hz, 2H, $(CH_2)_6CH_2N$), 2.69 (t, *J* = 5.8 Hz, 2H, CH_2SO_2), 2.93-2.98 (m, 2H, CH_2N), 3.08-3.12 (m, 2H, CH_2N), 3.25 (s, 3H, CH_3N), 7.01 (t, *J* = 7.4 Hz, 1H, H_4), 7.18-7.33 (m, 7H, H_3, H_5, $H_{2'}$-$H_{6'}$), 7.45 (d, *J* = 7.7 Hz, 2H, H_2, H_6), 9.63 (br s, 1H, NH). ^{13}C-NMR ($CDCl_3$, δ): 14.1 (CH_3CH_2), 22.6, 26.8, 27.5, 29.2, 29.4, 31.8 ($(CH_2)_6CH_3$), 34.4 (CH_2CO), 38.3 (CH_3N), 46.1, 47.0 ($2CH_2N$), 50.5 (CH_2SO_2), 53.6 ($(CH_2)_6CH_2N$), 119.7 (C_2, C_6), 123.8 (C_4), 126.2 ($C_{2'}$, $C_{6'}$), 127.5 ($C_{4'}$), 128.9 (C_3, C_5), 129.5 ($C_{3'}$, $C_{5'}$), 138.4 (C_1), 141.1 ($C_{1'}$), 170.4 (CONH). HRMS (ESI, m/z): Calculated for $C_{26}H_{40}N_3O_3S$ $[M+H]^+$: 474.27849. Found: 474.27701.

***N*^{3}-Octyl-*N*^{1}-phenyl-*N*^{3}-[(5-phenyl-1,3,4-oxadiazol-2-yl)methyl]-β-alaninamide (20).** To a solution of 2-(chloromethyl)-5-phenyl-1,3,4-oxadiazole (117 mg, 0.6 mmol) in anhydrous ACN (2.4 mL), amine **44** (200 mg, 0.7 mmol) and Et_3N (0.1 mL, 0.7 mmol) were added and the reaction mixture was stirred for 24 h at 60 °C. Once at rt, the solvent was evaporated under reduced pressure and the crude was suspended in water and extracted with DCM. The organic layers were dried over Na_2SO_4, filtered, and the

solvent was removed under reduced pressure. The residue was purified by chromatography (DCM/EtOAc, 8:2) to yield final compound **20** in 62% yield (162 mg).

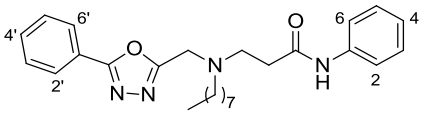

R_f (DCM/EtOAc, 8:2): 0.40. IR (ATR, cm^{-1}): 3304 (NH), 1728 (CO), 1599, 1550, 1499, 1444 (Ar). ^{1}H NMR ($CDCl_3$, δ): 0.85 (t, *J* = 6.9 Hz, 3H, CH_3), 1.25-1.30 (m, 10H, $(CH_2)_5CH_3$), 1.50-1.60 (m, 2H, $CH_2(CH_2)_5CH_3$), 2.63 (t, *J* = 6.3 Hz, 2H, CH_2CO), 2.70 (app t, *J* = 7.3 Hz, 2H, NCH_2), 3.00 (t, *J* = 6.3 Hz, 2H, NCH_2CH_2CO), 4.10 (s, 2H, NCH_2C_{het}), 7.07 (tt, *J* = 7.7 Hz, 1.8, 1H, H_4), 7.28 (t, *J* = 7.2 Hz, 2H, H_3, H_5), 7.44 (t, *J* = 7.7 Hz, 2H, $H_{3'}$, $H_{5'}$), 7.50 (d, *J* = 7.3 Hz, 1H, $H_{4'}$), 7.57 (d, *J* = 8.6 Hz, 2H, H_2, H_6), 7.93 (d, *J* = 8.6 Hz, 2H, $H_{2'}$, $H_{6'}$), 10.17 (br s, 1H, NH). ^{13}C NMR ($CDCl_3$, δ): 14.5 (CH_3), 23.0, 27.2, 27.8, 29.6, 29.8, 32.1 ($(CH_2)_6CH_3$), 34.2 (CH_2CO), 47.7 (NCH_2C_{het}), 51.0 ($COCH_2CH_2N$), 54.4 ($(CH_2)_6CH_2N$), 120.3 (C_2, C_6), 123.8 (C_4), 124.3 ($C_{4'}$), 127.3 ($C_{2'}$, $C_{6'}$), 129.3 (C_3, C_5), 129.5 ($C_{3'}$, $C_{5'}$), 132.3 ($C_{1'}$), 138.8 (C_1), 163.8 (CH_2CN), 165.9 ($C_{1'}CN$), 170.4 (CO). HRMS (ESI, m/z): Calculated for $C_{26}H_{35}N_4O_2$ $[M+H]^+$: 435.2755. Found: 435.2752.

4.1.5. Synthesis of final compounds 21-25

***N*^{2}-(2-Anilino-2-oxoethyl)-*N*^{2}-octyl-*N*^{1}-phenylglycinamide (21).** To a solution of 2-bromo-*N*-phenylacetamide (575 mg, 2.7 mmol) and octylamine (200 µL, 1.2 mmol) in anhydrous ACN (12 mL), DIPEA (600 µL, 3.5 mmol) was added at rt. The reaction mixture was stirred at 60 °C for 16 h. The solvent was evaporated under reduced pressure and the residue was purified by chromatography (hexane/EtOAc, 1:1) to yield diamide **21** in 93% yield (441 mg).

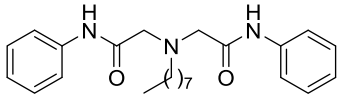

R_f (EtOAc): 0.75. IR (ATR, cm^{-1}): 3274 (NH), 1666 (CO), 1601, 1542, 1444 cm^{-1} (Ar). ^{1}H NMR ($CDCl_3$, δ): 0.85 (t, *J* = 6.7 Hz, 3H, CH_3), 1.23-1.28 (m, 10H, $(CH_2)_5CH_3$), 1.44-1.51 (m, 2H, $CH_2(CH_2)_5CH_3$), 2.66 (t, *J* = 7.4 Hz, 2H, NCH_2CH_2), 3.36 (s, 4H, $2NCH_2CO$), 7.10 (t, *J* = 7.4 Hz, 2H, $2H_4$), 7.32 (app t, *J* = 7.9 Hz, 4H, $2H_3$, $2H_5$), 7.62 (d, *J* = 7.7 Hz, 4H, $2H_2$, $2H_6$), 9.07 (br s, 2H, 2NH). ^{13}C NMR ($CDCl_3$, δ): 14.1 (CH_3), 22.6, 27.2, 27.6, 29.3, 29.4, 31.8 ($(CH_2)_6CH_3$), 56.4 (NCH_2CH_2), 59.8 ($2NCH_2CO$), 119.9 ($2C_2$, $2C_6$), 124.4 ($2C_4$), 129.0 ($2C_3$, $2C_5$), 137.7 ($2C_1$), 169.4 (2CO). HRMS (ESI, m/z): Calculated for $C_{24}H_{33}N_3O_2Na$ $[M+Na]^+$: 418.2465. Found: 418.2449.

***N*²-Octyl-*N*¹-phenylglycinamide (45).** To a solution of octylamine (3.4 mL, 21 mmol) in dry DCM (20 mL), a solution of 2-bromo-*N*-phenylacetamide (2.20 g, 10 mmol) in dry DCM (10 mL) was added dropwise at rt. The reaction mixture was stirred at rt for 16 h. The crude was washed with saturated solutions of $NaHCO_3$ and NaCl, subsequently. The organic layer was dried over Na_2SO_4, filtered, and evaporated under reduced pressure. The residue was purified by chromatography (hexane/EtOAc, 1:1) to yield secondary amine **45** in 40% yield (1.05 g).

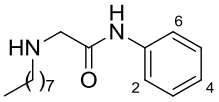

R_f (EtOAc): 0.24. IR (ATR, cm^{-1}): 3349 (NH), 1713 (CO), 1598, 1444 (Ar). ^{1}H NMR ($CDCl_3$, δ): 0.88 (t, *J* = 6.8 Hz, 3H, CH_3), 1.28-1.38 (m, 10H, $(CH_2)_5CH_3$), 1.51 (qt, *J* = 6.9 Hz, 2H, $CH_2(CH_2)_5CH_3$), 1.74 (br s, 1H, NH), 2.66 (t, *J* = 6.9 Hz, 2H, NCH_2CH_2), 3.36 (s, 2H, NCH_2CO), 7.09 (tt, *J* = 7.4, 1.1 Hz, 1H, H_4), 7.32 (app t, *J* = 7.9 Hz, 2H, H_3, H_5), 7.58 (dd, *J* = 8.7, 1.1 Hz, 2H, H_2, H_6), 9.38 (br s, 1H, NH). ^{13}C NMR ($CDCl_3$, δ): 14.1 (CH_3), 22.7, 27.2, 29.3, 29.5, 30.1, 31.8 ($(CH_2)_6CH_3$), 50.3, 53.1 ($2CH_2N$), 119.4 ($2C_2$, $2C_6$), 124.1 (C_4), 129.0 ($2C_3$, $2C_5$), 137.8 (C_1), 170.0 (CO). MS (ESI, m/z): 263.2 $[M+H]^+$.

***N*³-(2-Anilino-2-oxoethyl)-*N*³-octyl-*N*¹-phenyl-β-alaninamide (22).** To a suspension of amine **45** (195 mg, 0.7 mmol) and 3-bromo-*N*-phenylpropanamide (**31**) (340 mg, 1.5 mmol) in dry DCM (1.5 mL), DIPEA (0.40 mL, 2.4 mmol) was added and the reaction mixture was stirred at reflux for 16 h. Once at rt, the crude was washed with saturated solutions of $NaHCO_3$ and NaCl, subsequently. The organic layer was dried over Na_2SO_4, filtered and evaporated under reduced pressure. The residue was purified by chromatography (hexane/EtOAc, 1:1) to yield compound **22** in 25% yield (76 mg).

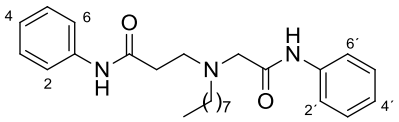

R_f (hexane/EtOAc, 6:4): 0.16. IR (ATR, cm-^{1}): 3274 (NH), 1664 (CO), 1601, 1540, 1444 (Ar). ^{1}H NMR ($CDCl_3$, δ): 0.83 (t, *J* = 6.8 Hz, 3H, CH_3), 1.18-1.23 (m, 10H, $(CH_2)_5CH_3$), 1.44 (m, 2H, $CH_2(CH_2)_5CH_3$), 2.47-2.54 (m, 4H, $NCH_2(CH_2)_6$, $COCH_2CH_2N$), 2.91 (t, *J* = 6.3 Hz, 2H, NCH_2CH_2CO), 3.15 (s, 2H, NCH_2CO), 7.08 (m, 2H, H_4, $H_{4'}$), 7.18 (t, *J* = 7.8 Hz, 2H, H_3, H_5), 7.24 (t, *J* = 7.9 Hz, 2H, $H_{3'}$, $H_{5'}$), 7.48 (d, *J* = 7.6 Hz, 2H, H_2, H_4), 7.53 (d, *J* = 7.6 Hz, 2H, $H_{2'}$,

$H_{4'}$), 8.87 (br s, 1H, NH), 9.45 (br s, 1H, NH). ^{13}C NMR ($CDCl_3$, δ): 14.0 (CH_3), 22.6, 27.2, 27.5, 29.3, 29.5, 31.8 (($\underline{C}H_2)_6CH_3$), 35.0 ($CO\underline{C}H_2CH_2N$), 51.1, 55.7 ($2N\underline{C}H_2CH_2$), 58.9 ($N\underline{C}H_2CO$), 119.7, 119.9 (C_2, C_6, $C_{2'}$, $C_{6'}$), 124.1, 124.2 (C_4, $C_{4'}$), 128.8, 128.9 (C_3, C_5, $C_{3'}$, $C_{5'}$), 137.5, 138.3 (C_1, $C_{1'}$), 170.4 (2CO). HRMS (ESI, m/z): Calculated for $C_{25}H_{35}N_3O_2Na$ $[M+Na]^+$: 432.2622. Found: 432.2615.

***N*^{2}-Octyl-*N*^{2}-(3-oxo-3-phenylpropyl)-*N*^{1}-phenyl-β-alaninamide (23)**. Over a solution of 3-chloropropiophenone (98 mg, 0.6 mmol) in ACN (3.0 mL), $NaHCO_3$ (1 M in H_2O, 0.6 mL) and a solution of amine **44** (160 mg, 0.6 mmol) in ACN (1.0 mL) were added. The mixture was stirred on at rt and then, washed with a saturated solution of NaCl. The organic extract was dried over Na_2SO_4, filtered, the solvent removed under reduced pressure and the residue was purified by chromatography (hexane/EtOAc, 1:1) to yield desired product in 43% yield (105 mg).

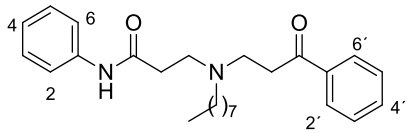

R_f (hexane/EtOAc, 1:1): 0.25. IR (ATR, cm^{-1}): 3308 (NH), 1681, 1543 (CO, CON), 1598, 1498, 1443 (Ar). ^{1}H-NMR ($CDCl_3$, δ): 0.86 (t, *J* = 6.8 Hz, 3H, CH_3), 1.21-1.27 (m, 10H, $(C\underline{H}_2)_5CH_3$), 1.55 (m, 2H, $C\underline{H}_2(CH_2)_5CH_3$), 2.53 (t, *J* = 5.5 Hz, 2H, CH_2CON), 2.60 (t, *J* = 7.5 Hz, 2H, $(CH_2)_6C\underline{H}_2N$), 2.84 (t, *J* = 5.8 Hz, 2H, $NCOCH_2C\underline{H}_2N$), 3.08 (t, *J* = 6.4 Hz, 2H, CH_2CO), 3.22 (t, *J* = 6.6 Hz, 2H, $COCH_2C\underline{H}_2N$), 7.06 (t, *J* = 7.4 Hz, 1H, H_4), 7.28 (t, *J* = 7.9 Hz, 2H, H_3, H_5), 7.46 (t, *J* = 7.6 Hz, 2H, $H_{3'}$, $H_{5'}$), 7.51 (d, *J* = 7.5 Hz, 2H, H_2, H_6), 7.58 (t, *J* = 7.4 Hz, 1H, $H_{4'}$), 7.93 (d, *J* = 7.1 Hz, 2H, $H_{2'}$, $H_{6'}$), 10.29 (br s, 1H, NH). ^{13}C-NMR ($CDCl_3$, δ): 14.2 (CH_3), 22.7, 26.8, 27.7, 29.3, 29.6, 31.9 (($\underline{C}H_2)_6CH_3$), 34.1, 35.4 ($2\underline{C}H_2CO$), 48.2, 50.8, 53.6 ($3CH_2N$), 119.8 (C_2, C_6), 123.7 (C_4), 128.1 ($C_{2'}$, $C_{6'}$), 128.8 ($C_{3'}$, $C_{5'}$), 128.9 (C_3, C_5), 133.4 ($C_{4'}$), 136.7 ($C_{1'}$), 138.6 (C_1), 170.9 (CON), 199.0 (CO). HRMS (ESI, m/z): Calculated for $C_{26}H_{36}N_2O_2Na$ $[M+Na]^+$: 431.2674. Found: 431.2666.

***N*^{2}-Octyl-*N*^{2}-(2-oxo-2-phenylethyl)-*N*^{1}-phenyl-β-alaninamide (24)**. Over a solution of 2-bromoacetophenone (110 mg, 0.6 mmol) and K_2CO_3 (229 mg, 1.7 mmol) in anhydrous ACN (2.5 mL), a solution of amine **44** (145 mg, 0.6 mmol) in anhydrous ACN (1.0 mL) was added and the mixture stirred on at rt. Then, the crude was washed with an aqueous solution of NaOH 0.1 M and the aqueous phase was extracted with EtOAc. The organic extracts were dried over Na_2SO_4, filtered, and the solvent removed under reduced pressure. The residue was purified by chromatography (hexane/EtOAc, 1:1) to give compound **24** in 56% yield (133 mg).

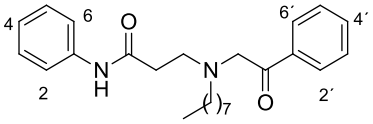

R_f (hexane/EtOAc, 1:1): 0.37. IR (ATR, cm^{-1}): 3269 (NH), 1660, 1547 (CO, CON), 1599, 1496, 1444 (Ar). ^{1}H-NMR ($CDCl_3$, δ): 0.85 (t, *J* = 6.8 Hz, 3H, CH_3), 1.20-1.27 (m, 10H, $(CH_2)_5CH_3$), 1.55 (m, 2H, $CH_2(CH_2)_5CH_3$), 2.60 (t, *J* = 5.8 Hz, 2H, CH_2CO), 2.72 (t, *J* = 7.6 Hz, 2H, $(CH_2)_6CH_2N$), 2.98 (t, *J* = 5.8 Hz, 2H, $COCH_2CH_2N$), 4.10 (s, 2H, NCH_2CO), 7.08 (t, *J* = 6.9 Hz, 1H, H_4), 7.33 (t, *J* = 7.9 Hz, 2H, H_3, H_5), 7.49 (t, *J* = 7.5 Hz, 2H, $H_{3'}$, $H_{5'}$), 7.61 (t, *J* = 7.4 Hz, 1H, $H_{4'}$), 7.77 (d, *J* = 8.2 Hz, 2H, H_2, H_6), 7.98 (d, *J* = 7.1 Hz, 2H, $H_{2'}$, $H_{6'}$), 10.81 (br s, 1H, NH). ^{13}C-NMR ($CDCl_3$, δ): 14.2 (CH_3), 22.7, 26.8, 27.4, 29.5, 29.8, 31.9 ($(CH_2)_6CH_3$), 34.3 (CH_2CO), 50.9 ($COCH_2CH_2N$), 54.4 ($(CH_2)_6CH_2N$), 60.0 (NCH_2CO), 120.2 (C_2, C_6), 123.7 (C_4), 128.0 ($C_{2'}$, $C_{6'}$), 128.9 (C_3, C_5), 129.0 ($C_{3'}$, $C_{5'}$), 133.9 ($C_{4'}$), 134.4 ($C_{1'}$), 139.0 (C_1), 170.4 (CON), 197.3 (CO). HRMS (ESI, m/z): Calculated for $C_{25}H_{35}N_2O_2$ $[M+H]^+$: 395.2698. Found: 395.2680.

***N*^{2}-Benzoyl-*N*^{2}-octyl-*N*^{1}-phenyl-β-alaninamide (25)**. Obtained using the procedure 4.1.1.3 from amine **44** (167 mg, 0.6 mmol), benzoic acid (74 mg, 0.6 mmol), EDC (94 mg, 0.6 mmol) and HOBt (81 mg, 0.6 mmol) in 72% yield (164 mg).

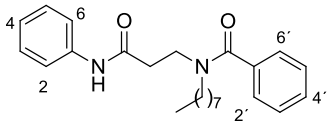

Chromatography: hexane/EtOAc, 9:1. R_f (hexane/EtOAc, 7:3): 0.28. Mp: 65-67 °C. IR (ATR, cm^{-1}): 3307 (NH), 1686 (CON), 1607, 1546, 1498, 1439 (Ar). ^{1}H-NMR ($CDCl_3$, δ): 0.85 (t, *J* = 6.9 Hz, 3H, CH_3), 1.09-1.15 (m, 10H, $(CH_2)_5CH_3$), 1.50 (m, 2H, $CH_2(CH_2)_5CH_3$), 2.75 (m, 2H, CH_2CO), 3.25 (m, 2H, $(CH_2)_6CH_2N$), 3.81 (m, 2H, $COCH_2CH_2N$), 7.04 (t, *J* = 7.4 Hz, 1H, H_4), 7.21-7.27 (m, 2H, $H_{3'}$, $H_{5'}$), 7.32-7.40 (m, 5H, H_3, H_5, $H_{2'}$, $H_{4'}$, $H_{6'}$), 7.51 (d, *J* = 7.7 Hz, 2H, H_2, H_6), 9.35 (br s, 1H, NH). ^{13}C-NMR ($CDCl_3$, δ): 14.0 (CH_3), 22.6, 26.4, 28.8, 29.0 (2C), 31.7 ($(CH_2)_6CH_3$), 36.2 (CH_2CO), 42.6 (CH_2N), 50.6 ($(CH_2)_6CH_2N$), 119.9 (C_2, C_6), 123.9 (C_4), 126.4 ($C_{2'}$, $C_{6'}$), 128.5 ($C_{3'}$, $C_{5'}$), 128.8 (C_3, C_5), 129.5 ($C_{4'}$), 136.4 ($C_{1'}$), 138.6 (C_1), 169.8, 172.7 (2CO). MS (ESI, m/z): 381.2 $[M+H]^+$.

4.1.6. Synthesis of final compounds 46-61

***N*²-(2-Methoxyphenylcarbonyl)-*N*²-octyl-*N*¹-phenyl-β-alaninamide (46).** Obtained using the procedure 4.1.1.3 from amine **44** (85 mg, 0.3 mmol), 2-methoxybenzoic acid (46 mg, 0.3 mmol), EDC (47 mg, 0.3 mmol) and HOBt (41 mg, 0.3 mmol) in 70% yield (86 mg).

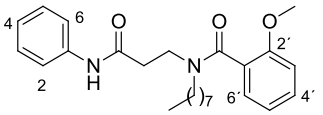

Chromatography: hexane/EtOAc, 1:1. R_f (hexane/EtOAc, 1:1): 0.42. IR (ATR, cm^{-1}): 3270 (NH), 1686, 1547 (CON), 1599, 1498, 1441 (Ar). ^{1}H-NMR ($CDCl_3$, δ): Mixture of rotamers A:B, 9:1; 0.86 (t, *J* = 7.0 Hz, 3H, CH_3CH_2), 1.08-1.31 (m, 10H, $(CH_2)_5CH_3$), 1.44-1.51 (m, 2H, $CH_2(CH_2)_5CH_3$ rotamer A), 1.52-1.73 (m, 2H, $CH_2(CH_2)_5CH_3$ rotamer B), 2.17 (m, 2H, CH_2CO rotamer B), 2.39-2.48 (m, 2H, $(CH_2)_6CH_2N$ rotamer B), 2.80-2.85 (m, 2H, CH_2CO rotamer A), 3.13-3.20 (m, 2H, $(CH_2)_6CH_2N$ rotamer A), 3.42-3.57 (m, 2H, $COCH_2CH_2N$ rotamer B), 3.67 (s, 3H, CH_3O rotamer A), 3.72-4.06 (m, 5H, $COCH_2CH_2N$ rotamer A, CH_3O rotamer B), 6.86 (d, *J* = 8.3 Hz, 1H, $H_{3'}$), 6.95 (t, *J* = 7.4 Hz, 1H, $H_{5'}$), 7.04 (t, *J* = 7.4 Hz, 1H, H_4), 7.19 (dd, *J* = 7.4, 1.7 Hz, 1H, $H_{6'}$), 7.24 (t, *J* = 8.1 Hz, 2H, H_3, H_5), 7.32 (td, *J* = 7.1, 1.7 Hz, 1H, $H_{4'}$), 7.53 (d, *J* = 7.7 Hz, 2H, H_2, H_6), 9.47 (br s, 1H, NH). ^{13}C-NMR ($CDCl_3$, δ): 14.2 (CH_3CH_2), 22.7, 26.5, 28.6, 29.1 (2C), 31.8 ($(CH_2)_6CH_3$), 36.3 (CH_2CO), 42.0 (CH_2N), 49.9 ($(CH_2)_6CH_2N$), 55.4 (CH_3O), 110.9 ($C_{3'}$), 120.0 (C_2, C_6), 120.8 ($C_{5'}$), 123.7 (C_4), 125.9 ($C_{1'}$), 127.6 ($C_{6'}$), 128.7 (C_3, C_5), 130.5 ($C_{4'}$), 138.8 (C_1), 155.2 ($C_{2'}$), 170.0, 170.5 (2CO). HRMS (ESI, m/z): Calculated for $C_{25}H_{34}N_2O_3Na$ $[M+Na]^+$: 433.2467. Found: 433.2466.

***N*²-(3-Methoxyphenylcarbonyl)-*N*²-octyl-*N*¹-phenyl-β-alaninamide (47).** Obtained using the procedure 4.1.1.3 from amine **44** (85 mg, 0.3 mmol), 3-methoxybenzoic acid (46 mg, 0.3 mmol), EDC (47 mg, 0.3 mmol) and HOBt (41 mg, 0.3 mmol) in 67% yield (83 mg).

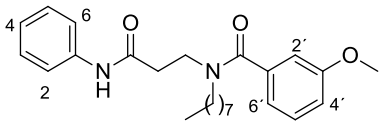

Chromatography: hexane/EtOAc, 1:1. R_f (hexane/EtOAc, 1:1): 0.48. IR (ATR, cm^{-1}): 3273 (NH), 1687, 1547 (CON), 1601, 1498, 1442 (Ar). ^{1}H-NMR ($CDCl_3$, δ): Mixture of rotamers A:B, 9:1; 0.86 (t, *J* = 6.9 Hz, 3H, CH_3CH_2), 1.12-1.27 (m, 10H, $(CH_2)_5CH_3$), 1.52 (m, 2H, $CH_2(CH_2)_5CH_3$), 2.48 (m, 2H, CH_2CO rotamer B), 2.77 (t, *J* = 6.0 Hz, 2H, CH_2CO rotamer A),

3.27 (t, *J* = 7.5 Hz, 2H, $(CH_2)_6C\underline{H}_2N$ rotamer A), 3.45 (m, 2H, $(CH_2)_6C\underline{H}_2N$ rotamer B), 3.69 (s, 3H, CH_3O), 3.81-3.92 (m, 2H, $COCH_2C\underline{H}_2N$), 6.83 (s, 1H, $H_{2'}$), 6.90 (t, *J* = 7.4 Hz, 1H, $H_{5'}$), 6.91 (d, *J* = 8.6 Hz, 1H, $H_{4'}$), 7.06 (t, *J* = 7.4 Hz, 1H, H_4), 7.23-7.29 (m, 3H, H_3, H_5, $H_{6'}$), 7.54 (d, *J* = 7.9 Hz, 2H, H_2, H_6), 9.39 (br s, 1H, NH). ^{13}C-NMR ($CDCl_3$, δ): 14.2 ($\underline{C}H_3CH_2$), 22.7, 26.5, 28.9, 29.1, 29.2, 31.8 ($(\underline{C}H_2)_6CH_3$), 36.2 ($\underline{C}H_2CO$), 42.7 (CH_2N), 50.7 ($(CH_2)_6\underline{C}H_2N$), 55.3 ($CH_3O$), 111.7 ($C_{2'}$), 115.6 ($C_{6'}$), 118.6 ($C_{5'}$), 120.0 ($C_2$, C_6), 124.0 (C_4), 128.9 (C_3, C_5), 129.8 ($C_{4'}$), 137.6 ($C_{1'}$), 138.6 (C_1), 159.7 ($C_{3'}$), 169.9, 172.6 (2CO). HRMS (ESI, m/z): Calculated for $C_{25}H_{33}N_2O_3$ $[M-H]^-$: 409.2496. Found: 409.2491.

***N*²-(4-Methoxyphenylcarbonyl)-*N*²-octyl-*N*¹-phenyl-β-alaninamide (48).** Obtained using the procedure 4.1.1.3 from amine **44** (50 mg, 0.2 mmol), 4-methoxybenzoic acid (30 mg, 0.2 mmol), EDC (20 mg, 0.2 mmol) and HOBt (23 mg, 0.2 mmol) in 73% yield (60 mg).

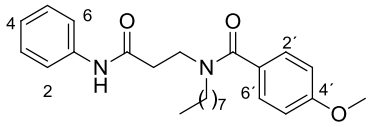

Chromatography: hexane/EtOAc, 7:3 to 3:7. R_f (hexane/EtOAc, 7:3): 0.31. IR (ATR, cm^{-1}): 3309 (NH), 1688, 1547 (CON), 1607, 1504, 1441 (Ar). ^{1}H-NMR ($CDCl_3$, δ): 0.86 (t, *J* = 6.9 Hz, 3H, $C\underline{H}_3CH_2$), 1.14-1.26 (m, 10H, $(C\underline{H}_2)_5CH_3$), 1.53 (m, 2H, $C\underline{H}_2(CH_2)_5CH_3$), 2.77 (m, 2H, CH_2CO), 3.32 (m, 2H, $(CH_2)_6C\underline{H}_2N$), 3.81-3.86 (m, 5H, $COCH_2C\underline{H}_2N$, CH_3O), 6.86 (d, *J* = 8.8 Hz, 2H, $H_{3'}$, $H_{5'}$), 7.07 (t, *J* = 7.4 Hz, 1H, H_4), 7.29 (t, *J* = 9.2 Hz, 2H, H_3, H_5), 7.30 (m, 2H, $H_{2'}$, $H_{6'}$), 7.56 (d, *J* = 7.7 Hz, 2H, H_2, H_6), 9.31 (br s, 1H, NH). ^{13}C-NMR ($CDCl_3$, δ): 14.2 ($\underline{C}H_3CH_2$), 22.7, 26.6, 28.9, 29.2 (2C), 31.8 ($(\underline{C}H_2)_6CH_3$), 36.4 ($\underline{C}H_2CO$), 42.8 (CH_2N), 50.9 ($(CH_2)_6\underline{C}H_2N$), 55.4 ($CH_3O$), 113.8 ($C_{3'}$, $C_{5'}$), 120.0 (C_2, C_6), 124.0 (C_4), 128.5 (C_3, C_5), 128.9 ($C_{2'}$, $C_{6'}$), 138.6 (C_1), 143.0 ($C_{1'}$), 160.7 ($C_{4'}$), 169.9, 172.9 (2CO). HRMS (ESI): Calculated for $C_{25}H_{34}N_2O_3Na$ $[M+Na]^+$: 433.2467. Found: 433.2450.

***N*²-(4-Cyanophenylcarbonyl)-*N*²-octyl-*N*¹-phenyl-β-alaninamide (49).** Obtained using the procedure 4.1.1.3 from amine **44** (50 mg, 0.2 mmol), 4-cyanobenzoic acid (22 mg, 0.2 mmol), EDC (20 mg, 0.2 mmol) and HOBt (23 mg, 0.2 mmol) in 68% yield (55 mg).

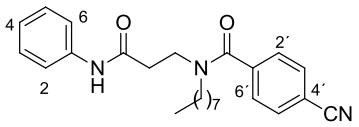

Chromatography: hexane/EtOAc, 1:1. R_f (hexane/EtOAc, 1:1): 0.30. Mp: 90-91 °C. IR (ATR, cm^{-1}): 3311 (NH), 2232 (CN), 1686, 1611, 1545 (CON), 1498, 1439 (Ar). ^{1}H-NMR ($CDCl_3$, δ): Mixture of rotamers A:B, 9:1; 0.87 (t, *J* = 6.9 Hz, 3H, CH_3), 1.10-1.27 (m, 10H, $(CH_2)_5CH_3$), 1.50 (m, 2H, $CH_2(CH_2)_5CH_3$ rotamer A), 1.66 (m, 2H, $CH_2(CH_2)_5CH_3$ rotamer B), 2.49 (m, 2H, CH_2CO rotamer B), 2.78 (t, *J* = 6.4 Hz, 2H, CH_2CO rotamer A), 3.22 (t, *J* = 7.8 Hz, 2H, $(CH_2)_6CH_2N$ rotamer A), 3.50 (m, 2H, $(CH_2)_6CH_2N$ rotamer B), 3.60 (m, 2H, $COCH_2CH_2N$ rotamer B), 3.84 (t, *J* = 6.4 Hz, 2H, $COCH_2CH_2N$ rotamer A), 7.01 (t, *J* = 7.3 Hz, 1H, H_4), 7.28 (t, *J* = 7.8 Hz, 2H, H_3, H_5), 7.42 (d, *J* = 8.1 Hz, 2H, $H_{3'}$, $H_{5'}$), 7.49 (d, *J* = 8.0 Hz, 2H, H_2, H_6), 7.65 (d, *J* = 8.1 Hz, 2H, $H_{2'}$, $H_{6'}$), 8.13 (br s, 1H, NH rotamer B), 9.02 (br s, 1H, NH rotamer A). ^{13}C-NMR ($CDCl_3$, δ): 14.1 (CH_3), 22.6, 26.4, 28.8, 29.0 (2C), 31.7 ($(CH_2)_6CH_3$), 35.8 (CH_2CO), 42.6 (CH_2N), 50.6 ($(CH_2)_6CH_2N$), 113.4 ($C_{4'}$), 118.0 (CN), 119.9 (C_2, C_6), 124.2 (C_4), 127.2 ($C_{3'}$, $C_{5'}$), 128.9 (C_3, C_5), 132.5 ($C_{2'}$, $C_{6'}$), 138.2 (C_1), 140.7 ($C_{1'}$), 169.3, 170.6 (2CO). MS (ESI): 406.3 $[M+H]^+$.

***N*²-(4-Fluorophenylcarbonyl)-*N*²-octyl-*N*¹-phenyl-β-alaninamide (50).** Obtained using the procedure 4.1.1.3 from amine **44** (85 mg, 0.3 mmol), 4-fluorobenzoic acid (42 mg, 0.3 mmol), EDC (47 mg, 0.3 mmol) and HOBt (41 mg, 0.3 mmol) in 72% yield (86 mg).

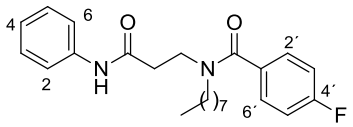

Chromatography: hexane/EtOAc, 7:3 to 3:7. R_f (hexane/EtOAc, 1:1): 0.42. Mp: 76-77 °C. IR (ATR, cm^{-1}): 3306, 3136 (NH), 1688, 1666, 1546 (CON), 1602, 1499, 1442 (Ar). ^{1}H-NMR ($CDCl_3$, δ): 0.86 (t, *J* = 6.9 Hz, 3H, CH_3), 1.11-1.26 (m, 10H, $(CH_2)_5CH_3$), 1.51 (m, 2H, $CH_2(CH_2)_5CH_3$), 2.75 (t, *J* = 5.9 Hz, 2H, CH_2CO), 3.26 (t, *J* = 7.2 Hz, 2H, $(CH_2)_6CH_2N$), 3.82 (t, *J* = 6.0 Hz, 2H, $COCH_2CH_2N$), 7.03 (t, *J* = 8.6 Hz, 2H, $H_{2'}$, $H_{6'}$), 7.07 (t, *J* = 7.4 Hz, 1H, H_4), 7.27 (t, *J* = 7.9 Hz, 2H, H_3, H_5), 7.32 (dd, *J* = 8.4, 5.5 Hz, 2H, $H_{3'}$, $H_{5'}$), 7.52 (d, *J* = 7.9 Hz, 2H, H_2, H_6), 9.29 (br s, 1H, NH). ^{13}C-NMR ($CDCl_3$, δ): 14.2 (CH_3), 22.7, 26.5, 28.9, 29.1 (2C), 31.8 ($(CH_2)_6CH_3$), 36.1 (CH_2CO), 42.8 (CH_2N), 50.8 ($(CH_2)_6CH_2N$), 115.7 ($C_{3'}$, $C_{5'}$), 119.9 (C_2, C_6), 124.1 (C_4), 128.7 (d, *J* = 8.4 Hz, $C_{2'}$, $C_{6'}$), 128.9 (C_3, C_5), 132.5 ($C_{1'}$), 138.2 (C_1), 163.3 ($C_{4'}$), 169.7, 171.8 (2CO). MS (ESI): 399.1 $[(M+H)^+]$.

***N*²-[4-(Trifluoromethyl)phenylcarbonyl]-*N*²-octyl-*N*¹-phenyl-β-alaninamide (51).** Obtained using the procedure 4.1.1.3 from amine **44** (85 mg, 0.3 mmol), 4-(trifluoromethyl)benzoic acid (57 mg, 0.3 mmol), EDC (47 mg, 0.3 mmol) and HOBt (41 mg, 0.3 mmol) in 66% yield (89 mg).

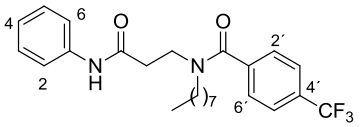

Chromatography: hexane/EtOAc, 7:3 to 1:1. R_f (hexane/EtOAc, 1:1): 0.53. Mp: 80-81 °C. IR (ATR, cm^{-1}): 3307 (NH), 1688, 1666, 1615, 1546 (CON), 1499, 1443 (Ar). ^{1}H-NMR ($CDCl_3$, δ): Mixture of rotamers A:B, 9:1; 0.88 (t, *J* = 6.9 Hz, 3H, CH_3), 1.12-1.28 (m, 10H, $(CH_2)_5CH_3$), 1.53 (m, 2H, $CH_2(CH_2)_5CH_3$ rotamer A), 1.69 (m, 2H, $CH_2(CH_2)_5CH_3$ rotamer B), 2.51 (m, 2H, CH_2CO rotamer B), 2.83 (t, *J* = 6.4 Hz, 2H, CH_2CO rotamer A), 3.26 (t, *J* = 7.5 Hz, 2H, $(CH_2)_6CH_2N$ rotamer A), 3.53 (m, 2H, $(CH_2)_6CH_2N$ rotamer B), 3.64 (m, 2H, $COCH_2CH_2N$ rotamer B), 3.88 (t, *J* = 6.4 Hz, 2H, $COCH_2CH_2N$ rotamer A), 7.10 (t, *J* = 7.4 Hz, 1H, H_4), 7.28 (t, *J* = 7.8 Hz, 2H, H_3, H_5), 7.45 (d, *J* = 8.0 Hz, 2H, $H_{2'}$, $H_{6'}$ rotamer A), 7.50 (d, *J* = 8.0 Hz, 2H, H_2, H_6), 7.64 (d, *J* = 8.1 Hz, 2H, $H_{3'}$, $H_{5'}$ rotamer A), 7.72 (d, *J* = 8.2 Hz, 2H, $H_{2'}$, $H_{6'}$ rotamer B), 8.17 (d, *J* = 8.1 Hz, 2H, $H_{3'}$, $H_{5'}$ rotamer B), 9.25 (br s, 1H, NH). ^{13}C-NMR ($CDCl_3$, δ): 14.1 (CH_3), 22.6, 26.4, 28.8, 29.0, 29.1, 31.7 ($(CH_2)_6CH_3$), 35.9 (CH_2CO), 42.8 (CH_2N), 50.7 ($(CH_2)_6CH_2N$), 120.0 (C_2, C_6), 124.2 (C_4), 125.7 (q, *J* = 3.6 Hz, $C_{3'}$, $C_{5'}$), 126.9 ($C_{2'}$, $C_{6'}$), 127.3 (CF_3), 128.9 (C_3, C_5), 131.7 ($C_{4'}$), 138.3 (C_1), 139.9 ($C_{1'}$), 169.6, 171.3 (2CO). MS (ESI): 449.2 $[(M+H)^+]$.

***N*^{2}-(4-Acetamidophenylcarbonyl)-*N*^{2}-octyl-*N*^{1}-phenyl-β-alaninamide (52).** Obtained using the procedure 4.1.1.3 from amine **44** (85 mg, 0.3 mmol), 4-acetamidobenzoic acid (54 mg, 0.3 mmol), EDC (47 mg, 0.3 mmol) and HOBt (41 mg, 0.3 mmol) in 70% yield (92 mg).

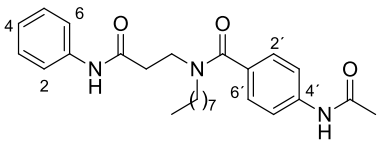

Chromatography: hexane/EtOAc, 2:8. R_f (hexane/EtOAc, 2:8): 0.19. IR (ATR, cm^{-1}): 3300 (NH), 1669, 1535 (CON), 1602, 1468, 1438 (Ar). ^{1}H-NMR ($CDCl_3$, δ): Mixture of rotamers A:B, 8:2; 0.85 (t, *J* = 6.8 Hz, 3H, CH_3CH_2), 1.16-1.29 (m, 10H, $(CH_2)_5CH_3$), 1.49-1.62 (m, 2H, $CH_2(CH_2)_5CH_3$ rotamers A and B), 1.97 (s, 3H, CH_3CO rotamer B), 2.15 (s, 3H, CH_3CO rotamer A), 2.22 (m, 2H, CH_2CO rotamer B), 2.76 (m, 2H, CH_2CO rotamer A), 3.26 (m, 2H, $(CH_2)_6CH_2N$ rotamer A), 3.45 (m, 2H, $(CH_2)_6CH_2N$ rotamer B), 3.60 (m, 2H, $COCH_2CH_2N$ rotamer B), 3.83 (m, 2H, $COCH_2CH_2N$ rotamer A), 7.07 (t, *J* = 7.4 Hz, 1H, H_4), 7.20 (d, *J* = 7.6 Hz, 2H, $H_{2'}$, $H_{6'}$), 7.27 (t, *J* = 7.8 Hz, 2H, H_3, H_5), 7.44 (d, *J* = 7.4 Hz, 2H, $H_{3'}$, $H_{5'}$), 7.53 (d, *J* = 7.7 Hz, 2H, H_2, H_6), 8.15 (br s, 1H, NH), 9.19 (br s, 1H, NH).

^{13}C-NMR ($CDCl_3$, δ): 14.2 (CH_3CH_2), 22.7 (CH_2), 24.6 (CH_3CO), 26.6, 26.7, 29.0, 29.2, 31.8 ($5CH_2$), 36.3 (CH_2CO), 42.6 (CH_2N), 50.8 ($(CH_2)_6CH_2N$), 119.7 ($C_{3'}$, $C_{5'}$), 120.1 (C_2, C_6), 124.2 (C_4), 127.6 ($C_{2'}$, $C_{6'}$), 129.0 (C_3, C_5), 131.8 ($C_{1'}$), 138.4 (C_1), 139.5 ($C_{4'}$), 169.0, 169.1, 169.9 (3CO). HRMS (ESI): Calculated for $C_{26}H_{35}N_3O_3Na$ [$(M+Na)^+$]: 460.2570. Found: 460.25833.

***N*^{2}-(2-Furoyl)-*N*^{2}-octyl-*N*^{1}-phenyl-β-alaninamide (53).** Obtained using the procedure 4.1.1.3 from amine **44** (85 mg, 0.3 mmol), 2-furoic acid (34 mg, 0.3 mmol), EDC (47 mg, 0.3 mmol) and HOBt (41 mg, 0.3 mmol) in 95% yield (106 mg).

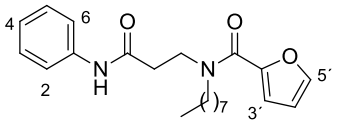

Chromatography: hexane/EtOAc, 1:1. R_f (hexane/EtOAc, 1:1): 0.40. IR (ATR, cm^{-1}): 3315 (NH), 1668 (CON), 1605 (Ar). ^{1}H-NMR ($CDCl_3$, δ): 0.87 (t, *J* = 6.6 Hz, 3H, CH_3), 1.25 (m, 10H, $(CH_2)_5CH_3$), 1.65 (m, 2H, $CH_2(CH_2)_5CH_3$), 2.75 (t, *J* = 6.3 Hz, 2H, CH_2CO), 3.61 (m, 2H, $(CH_2)_6CH_2N$), 3.83 (m, 2H, $COCH_2CH_2N$), 6.43 (m, 1H, $H_{4'}$), 6.95 (m, 1H, $H_{3'}$), 7.06 (t, *J* = 7.4 Hz, 1H, H_4), 7.27 (t, *J* = 7.8 Hz, 2H, H_3, H_5), 7.41 (m, 1H, $H_{5'}$), 7.49-7.60 (m, 2H, H_2, H_6), 9.29 (br s, 1H, NH). ^{13}C-NMR ($CDCl_3$, δ): 14.1 (CH_3), 22.6, 26.8, 29.2, 29.3, 29.7, 31.8 ($(CH_2)_6CH_3$), 36.2 (CH_2CO), 44.3 (CH_2N), 49.6 ($(CH_2)_6CH_2N$), 111.4, 116.5 ($C_{3'}$, $C_{4'}$), 119.9 (C_2, C_6), 123.9 (C_4), 128.8 (C_3, C_5), 138.5 (C_1), 144.0 ($C_{5'}$), 147.9 ($C_{2'}$), 160.5 (CON), 169.6 (CONH). MS (ESI): 371.2 [$(M+H)^+$].

***N*^{2}-(3-Furoyl)-*N*^{2}-octyl-*N*^{1}-phenyl-β-alaninamide (54).** Obtained using the procedure 4.1.1.3 from amine **44** (85 mg, 0.3 mmol), 3-furoic acid (34 mg, 0.3 mmol), EDC (47 mg, 0.3 mmol) and HOBt (41 mg, 0.3 mmol) in quantitative yield (111 mg).

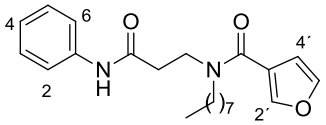

Chromatography: hexane/EtOAc, 7:3. R_f (hexane/EtOAc, 7:3): 0.14. IR (ATR, cm^{-1}): 3281 (NH), 1685 (CON), 1605, 1547, 1501, 1441 (Ar). ^{1}H-NMR ($CDCl_3$, δ): 0.88 (t, *J* = 6.7 Hz, 3H, CH_3), 1.25 (m, 10H, $(CH_2)_5CH_3$), 1.61 (m, 2H, $CH_2(CH_2)_5CH_3$), 2.76 (m, 2H, CH_2CO), 3.44 (t, *J* = 7.9 Hz, 2H, $(CH_2)_6CH_2N$), 3.82 (t, *J* = 6.6 Hz, 2H, $COCH_2CH_2N$), 6.55 (m, 1H, $H_{4'}$), 7.08 (t, *J* = 7.4 Hz, 1H, H_4), 7.29 (t, *J* = 8.3 Hz, 2H, H_3, H_5), 7.41 (t, *J* = 1.7 Hz, 1H, $H_{5'}$), 7.55 (d, *J* = 7.8 Hz, 2H, H_2, H_6), 7.68 (m, 1H, $H_{2'}$). ^{13}C-NMR ($CDCl_3$, δ): 14.1 (CH_3), 22.6, 26.6, 29.2 (3C), 31.7 ($(CH_2)_6CH_3$), 36.5 (CH_2CO), 43.2 (CH_2N), 50.1 ($(CH_2)_6CH_2N$), 110.1 ($C_{4'}$), 119.8 (C_2, C_6),

121.3 ($C_{3'}$), 124.1 (C_4), 128.9 (C_3, C_5), 138.3 (C_1), 143.1, 143.2 ($C_{2'}$, $C_{5'}$), 165.6 (CON), 169.4 (CONH). MS (ESI): 371.2 [$(M+H)^+$].

***N*²-Octyl-*N*¹-phenyl-*N*²-(pyrrolidin-2-ylcarbonyl)-β-alaninamide (55).** Following the procedure 4.1.1.3 from amine **44** (72 mg, 0.3 mmol), *N*-(tert-butoxycarbonyl)-proline (109 mg, 0.5 mmol), EDC (47 mg, 0.3 mmol), and HOBt (41 mg, 0.3 mmol), *N*²-octyl-*N*¹-phenyl-*N*²-(*N*-Boc-pyrrolidin-2-ylcarbonyl)-β-alaninamide was obtained in 44% yield (75 mg).

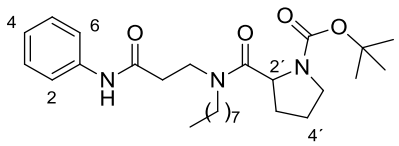

Chromatography: hexane/EtOAc, 1:1. R_f (hexane/EtOAc, 1:1): 0.27. IR (ATR, cm^{-1}): 3312 (NH), 1685, 1667 (CO), 1604, 1546, 1441 (Ar). ^{1}H-NMR ($CDCl_3$, δ): (Mixture of rotamers A:B, 2:1): 0.80-0.88 (m, 3H, CH_3CH_2), 1.17-1.28 (m, 10H, $(CH_2)_5CH_3$), 1.44-1.67 (m, 11H, $CH_2(CH_2)_5CH_3$, $C(CH_3)_3$), 1.74-1.95 (m, 2H, CH_2CH_2CH), 2.06-2.19 (m, 2H, CH_2CH), 2.31-2.51 (m, 2H, CH_2CO), 2.60-2.79 (m, 2H, CH_2NBoc, rotamer A), 3.00-3.32 (m, 2H, $NCH_2(CH_2)_6$), 3.52-3.65 (m, 2H, NCH_2CH_2CO), 3.67-3.87 (m, 2H, CH_2NBoc, rotamer B), 4.41-4.57 (m, 1H, CH), 7.01 (t, *J* = 7.3 Hz, 1H, H_4), 7.26 (d, *J* = 7.9 Hz, 2H, H_3, H_5), 7.55 (d, *J* = 7.7 Hz, 2H, H_2, H_6, rotamer A), 7.74 (d, *J* = 7.7 Hz, 2H, H_2, H_6, rotamer B), 9.13 (br s, 1H, NH, rotamer A), 9.34 (br s, 1H, NH, rotamer B). ^{13}C-NMR ($CDCl_3$, δ): 14.0 (CH_3CH_2), 22.6 (2C), 24.4, 24.7, 26.7, 27.7 ($4CH_2$, rotamers A and B), 28.5, 28.6 ($C(CH_3)_3$, rotamers A and B), 29.1, 29.3, 30.0, 30.1, 30.2, 31.7 (2C) ($4CH_2$, rotamers A and B), 37.1, 37.9 (CH_2CO, rotamers A and B), 44.9, 46.0, 47.2, 47.3, 47.9, 50.0 ($3CH_2N$, rotamers A and B), 56.1, 56.5 (CH, rotamers A and B), 80.0, 80.1 ($C(CH_3)_3$, rotamers A and B), 120.1, 120.2 (C_2, C_6, rotamers A and B), 123.8, 124.0 (C_4, rotamers A and B), 128.7 (C_3, C_5), 138.5, 139.0 (C_1, rotamers A and B), 154.7, 154.9 (NCOO, rotamers A and B), 169.6, 171.2, 172.5, 173.1 (2CO, rotamers A and B). MS (ESI): 474.3 $[M+H]^+$, 374.0 $[M\text{-Boc}+H]^+$.

To a solution of the previous *N*-Boc pyrrolidine derivative (63 mg, 0.1 mmol) in anhydrous DCM (0.5 mL), TFA (200 µL, 2.7 mmol) was added. The mixture of the reaction was stirred at rt for 1 h, basified with $NaHCO_3$ until pH ≈ 8 and extracted with DCM. The organic extract was washed with a saturated solution of NaCl, dried over Na_2SO_4, filtered, and the solvent was removed under reduced pressure, obtaining the desired final compound **55** in quantitative yield (49 mg).

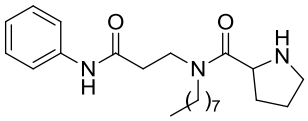

R_f (EtOAc/methanol, 7/3): 0.19. IR (ATR, cm^{-1}): 3269 (NH), 1644 (CO), 1605, 1548, 1494, 1444 (Ar). ^{1}H-NMR ($CDCl_3$, δ): (Mixture of rotamers A:B, 2:1): 0.83-0.88 (m, 3H, CH_3), 1.21-1.24 (m, 10H, $(CH_2)_5CH_3$), 1.45-2.30 (m, 6H, $CH_2(CH_2)_5CH_3$, $(CH_2)_2CH$), 2.56-3.05 (m, 4H, CH_2CO, CH_2NH), 3.15-3.34 (m, 2H, $NCH_2(CH_2)_6$), 3.55-3.76 (m, 2H, NCH_2CH_2CO), 3.91 (t, *J* = 7.5 Hz, 1H, CH, rotamer A), 4.37 (t, *J* = 7.5 Hz, 1H, CH, rotamer B), 5.10 (br s, 1H, NH), 7.05 (t, *J* = 7.3 Hz, 1H, H_4), 7.23-7.30 (m, 2H, H_3, H_5), 7.56 (d, *J* = 7.7 Hz, 2H, H_2, H_6, rotamer A), 7.61 (d, *J* = 7.7 Hz, 2H, H_2, H_6, rotamer B), 8.97 (br s, 1H, NH, rotamer A), 9.58 (br s, 1H, NH, rotamer B). ^{13}C-NMR ($CDCl_3$, δ): 14.1 (CH_3), 22.6, 25.8, 26.3, 26.8, 27.6, 29.1, 29.2 (2C), 29.3 (2C), 29.7, 30.6, 31.1, 31.7 ($(CH_2)_6CH_3$, $(CH_2)_2CH$, rotamers A and B), 36.3, 37.2 (CH_2CO, rotamers A and B), 43.2, 44.0 (NCH_2CH_2CO, rotamers A and B), 46.8, 46.9, 47.4, 48.3 ($NCH_2(CH_2)_6$, CH_2NH, rotamers A and B), 57.8, 58.2 (CH, rotamers A and B), 119.9 (C_2, C_6), 124.1 (C_4), 128.8, 128.9 (C_3, C_5), 138.4 (C_1), 168.7, 169.5, 171.4, 173.9 (2CO, rotamers A and B). HRMS (ESI, m/z): Calculated for $C_{22}H_{36}N_3O_2$ $[M+H]^+$: 374.2796. Found: 374.2802.

***N*^{2}-Octyl-*N*^{1}-phenyl-*N*^{2}-(*R*-pyrrolidin-2-ylcarbonyl)-β-alaninamide (*R*-55).** Following the procedure 4.1.1.3 from amine **44** (72 mg, 0.3 mmol), *N*-(tert-butoxycarbonyl)-D-proline (109 mg, 0.5 mmol), EDC (47 mg, 0.3 mmol), and HOBt (41 mg, 0.3 mmol), *N*^{2}-octyl-*N*^{1}-phenyl-*N*^{2}-(*N*-Boc-*R*-pyrrolidin-2-ylcarbonyl)-β-alaninamide was obtained in 74% yield (102 mg). Spectroscopic data were in agreement with those described for its racemic counterpart.

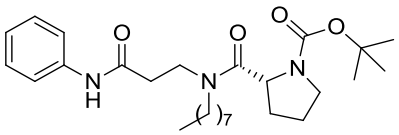

Chiral HPLC-MS, r_t (min): 6.66 (Chiral HPLC method A). ee> 99%

To a solution of the previous *N*-Boc-(*R*)-pyrrolidine derivative (63 mg, 0.1 mmol) in anhydrous DCM (0.5 mL), TFA (200 µL, 2.7 mmol) was added. The mixture of the reaction was stirred at rt for 1 h, basified with $NaHCO_3$ until pH ≈ 8 and extracted with DCM. The organic extract was washed with NaCl, dried over Na_2SO_4, filtered, and the solvent removed under reduced pressure, obtaining the desired final compound **(*R*)-55** in quantitative yield (49 mg). Spectroscopic data were in agreement with those

described for racemic compound **55**.

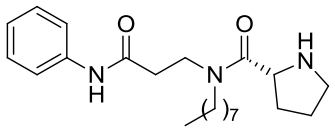

Chiral HPLC-MS, r_t (min): 5.99 (Chiral HPLC method B). ee> 99%
$[\alpha]^D_{20}$: -103.2 ° (c = 0.4, methanol)

***N*²-Octyl-*N*¹-phenyl-*N*²-(*S*-pyrrolidin-2-ylcarbonyl)-β-alaninamide (*S*-55).** Following the procedure 4.1.1.3 from amine **44** (72 mg, 0.3 mmol), *N*-(tert-butoxycarbonyl)-L-proline (109 mg, 0.5 mmol), EDC (47 mg, 0.3 mmol), and HOBt (41 mg, 0.3 mmol), N^2-octyl-N^1-phenyl-N^2-(*N*-Boc-*S*-pyrrolidin-2-ylcarbonyl)-β-alaninamide was obtained in 78% yield (107 mg). Spectroscopic data were in agreement with those described for its racemic counterpart.

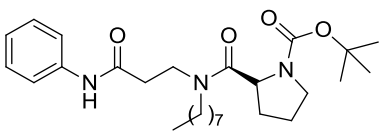

Chiral HPLC-MS, r_t (min): 7.45 (Chiral HPLC method A). ee> 99%

To a solution of the corresponding *N*-Boc-(*S*)-pyrrolidine derivative (63 mg, 0.1 mmol) in anhydrous DCM (0.5 mL), TFA (200 µL, 2.7 mmol) was added. The mixture of the reaction was stirred at rt for 1 h, basified with $NaHCO_3$ until pH ≈ 8 and extracted with DCM. The organic extract was washed with NaCl, dried over Na_2SO_4, filtered, and the solvent removed under reduced pressure, obtaining the desired final compound **(*S*)-55** in quantitative yield (49 mg). Spectroscopic data were in agreement with those described for racemic compound **55**.

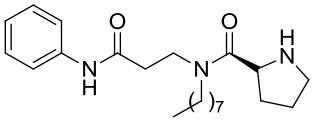

Chiral HPLC-MS, r_t (min): 10.18 (Chiral HPLC method B). ee> 99%
$[\alpha]^D_{20}$: + 99.8 ° (c = 0.4, methanol)

***N*²-Octyl-*N*¹-phenyl- *N*²-(1*H*-pyrrol-2-ylcarbonyl)-β-alaninamide (56).** Obtained using the procedure 4.1.1.3 from amine **44** (85 mg, 0.3 mmol), 1*H*-2-pyrrolcarboxylic acid (34 mg, 0.3 mmol), EDC (47 mg, 0.3 mmol) and HOBt (41 mg, 0.3 mmol) in 76% yield (84 mg).

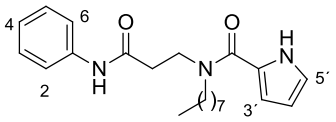

Chromatography: hexane/EtOAc, 7:3. R_f (hexane/EtOAc, 1:1): 0.40. Mp: 105-107 °C. IR (ATR, cm^{-1}): 3264 (NH), 1666 (CON), 1599, 1548, 183, 1445 (Ar). ^{1}H-NMR ($CDCl_3$, δ): 0.88 (t, *J* = 6.7 Hz, 3H, CH_3), 1.28-1.31 (m, 10H, $(CH_2)_5CH_3$), 1.71 (m, 2H, $CH_2(CH_2)_5CH_3$), 2.74 (t, *J* = 6.7 Hz, 2H, CH_2CO), 3.58 (m, 2H, $(CH_2)_6CH_2N$), 3.87 (m, 2H, $COCH_2CH_2N$), 6.25-6.28 (m, 1H, $H_{4'}$), 6.54 (m, 1H, $H_{3'}$), 6.90 (m, 1H, $H_{5'}$), 7.07 (t, *J* = 7.3 Hz, 1H, H_4), 7.28 (t, *J* = 7.8 Hz, 2H, H_3, H_5), 7.55 (d, *J* = 7.8 Hz, 2H, H_2, H_6), 8.84 (br s, 1H, NH), 9.84 (br s, 1H, NH). ^{13}C-NMR ($CDCl_3$, δ): 14.1 (CH_3), 22.6, 26.8, 28.6, 29.2, 29.4, 31.8 ($(CH_2)_6CH_3$), 36.7 (CH_2CO), 44.3 (CH_2N), 49.3 ($(CH_2)_6CH_2N$), 110.3, 112.2 ($C_{3'}$, $C_{4'}$), 119.9 (C_2, C_6), 121.3 ($C_{5'}$), 124.1 (C_4), 124.4 ($C_{2'}$), 128.9 (C_3, C_5), 138.3 (C_1), 162.5 (CON), 169.4 (CONH). MS (ESI): 370.2 $[M+H]^+$.

***N*²-Octyl-*N*¹-phenyl-*N*²-(1*H*-pyrrol-3-ylcarbonyl)-β-alaninamide (57).** Obtained using the procedure 4.1.1.3 from amine **44** (85 mg, 0.3 mmol), 1*H*-3-pyrrolcarboxilic acid (34 mg, 0.3 mmol), EDC (47 mg, 0.3 mmol) and HOBt (41 mg, 0.3 mmol) in 54% yield (60 mg).

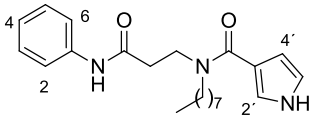

Chromatography: hexane/EtOAc, 3:7. R_f (EtOAc): 0.25. Mp: 99-101 °C. IR (ATR, cm^{-1}): 3250 (NH), 1598 (CON), 1548 (Ar). ^{1}H-NMR ($CDCl_3$, δ): 0.79 (t, *J* = 6.7 Hz, 3H, CH_3), 1.16 (m, 10H, $(CH_2)_5CH_3$), 1.54 (m, 2H, $CH_2(CH_2)_5CH_3$), 2.61 (m, 2H, CH_2CO), 3.41 (t, *J* = 7.2 Hz, 2H, $(CH_2)_6CH_2N$), 3.74 (t, *J* = 6.6 Hz, 2H, $COCH_2CH_2N$), 6.26 (m, 1H, $H_{4'}$), 6.56 (m, 1H, $H_{5'}$), 6.92 (m, 1H, $H_{2'}$), 6.97 (t, *J* = 7.4 Hz, 1H, H_4), 7.18 (t, *J* = 7.8 Hz, 2H, H_3, H_5), 7.49 (d, *J* = 7.9 Hz, 2H, H_2, H_6), 9.37 (br s, 2H, 2NH). ^{13}C-NMR ($CDCl_3$, δ): 14.1 (CH_3), 22.6, 26.7, 28.9, 29.2, 29.3, 31.8 ($(CH_2)_6CH_3$), 36.6 (CH_2CO), 43.4 (CH_2N), 49.8 ($(CH_2)_6CH_2N$), 108.6 ($C_{4'}$), 118.3 ($C_{5'}$), 118.4 ($C_{3'}$), 120.0 (C_2, C_6), 121.1 ($C_{2'}$), 123.9 (C_4), 128.8 (C_3, C_5), 138.5 (C_1), 168.4 (CON), 170.0 (CONH). MS (ESI): 370.2 $[M+H]^+$.

***N*²-[(1-Methyl-1*H*-pyrrol-2-yl)carbonyl]-*N*²-octyl-*N*¹-phenyl-β-alaninamide (58).** Obtained using the procedure 4.1.1.3 from amine **44** (163 mg, 0.59 mmol) and 1-methyl-1*H*-pyrrol-2-carboxylic acid (150 mg, 1.2 mmol) in 49% yield (111 mg).

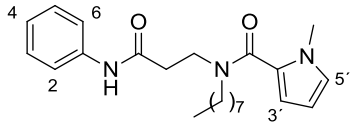

Chromatography: hexane/EtOAc, 7:3. R_f (hexane/EtOAc, 7:3): 0.44. IR (ATR, cm^{-1}): 3277 (NH), 1684 (C=O), 1602, 1543, 1473, 1439 (Ar). ^{1}H-NMR ($CDCl_3$, δ): 0.87 (t, *J* = 6.7 Hz, 3H, CH_3CH_2), 1.23-1.30 (m, 10H, $(CH_2)_5CH_3$), 1.58-1.65 (m, 2H, $CH_2(CH_2)_5CH_3$), 2.73 (t, *J* = 6.8 Hz, 2H, CH_2CO), 3.54 (t, *J* = 7.6 Hz, 2H, $NCH_2(CH_2)_6$), 3.67 (s, 3H, CH_3N), 3.80 (t, *J* = 6.8 Hz, 2H, NCH_2CH_2CO), 6.06 (dd, *J* = 3.7, 2.7 Hz, 1H, $H_{4'}$), 6.30 (dd, *J* = 3.7, 1.4 Hz, 1H, $H_{3'}$), 6.66 (t, *J* = 2.9 Hz, 1H, $H_{5'}$), 7.07 (t, *J* = 7.4 Hz, 1H, H_4), 7.28 (t, *J* = 7.8 Hz, 2H, H_3, H_5), 7.55 (d, *J* = 8.1 Hz, 2H, H_2, H_6), 9.11 (br s, 1H, NH). ^{13}C-NMR ($CDCl_3$, δ): 14.5 (CH_3CH_2), 23.0, 26.9, 29.2, 29.6 (2C), 32.1 ($(CH_2)_6CH_3$), 35.9 (CH_3N), 36.8 (CH_2CO), 43.5 (NCH_2CH_2CO), 50.6 ($NCH_2(CH_2)_6$), 107.5, 112.5 ($C_{3'}$, $C_{4'}$), 120.2 (C_2, C_6), 124.4 (C_4), 125.7 ($C_{2'}$), 126.6 ($C_{5'}$), 129.2 (C_3, C_5), 138.8 (C_1), 165.6 (CON), 170.1 (CONH). HRMS (ESI, m/z): Calculated for $C_{23}H_{34}N_3O_2$ $[M+H]^+$: 384.2646. Found: 384.2655.

***N*²-Octyl-*N*¹-phenyl-*N*²-(pyridin-2-ylcarbonyl)-β-alaninamide (59).** Obtained using the procedure 4.1.1.3 from amine **44** (85 mg, 0.3 mmol), picolinic acid (37 mg, 0.3 mmol), EDC (47 mg, 0.3 mmol) and HOBt (41 mg, 0.3 mmol) in 92% yield (105 mg).

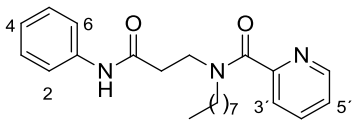

Chromatography: hexane/EtOAc, 2:8. R_f (hexane/EtOAc, 3:7): 0.30. IR (ATR, cm^{-1}): 3309 (NH), 1685 (CON), 1615, 1547, 1495, 1443 (Ar). ^{1}H-NMR ($CDCl_3$, δ): Mixture of rotamers A:B, 2:1; 0.85 (t, *J* = 6.7 Hz, 3H, CH_3), 1.11-1.25 (m, 10H, $(CH_2)_5CH_3$), 1.57 (m, 2H, $CH_2(CH_2)_5CH_3$), 2.81 (t, *J* = 6.4 Hz, 2H, CH_2CO), 3.37 (t, *J* = 7.4 Hz, 2H, $(CH_2)_6CH_2N$, rotamer A), 3.46-3.47 (m, 2H, $(CH_2)_6CH_2N$, rotamer B), 3.69-3.75 (m, 2H, $COCH_2CH_2N$, rotamer B), 3.87 (t, *J* = 6.3 Hz, 2H, $COCH_2CH_2N$, rotamer A), 7.05 (t, *J* = 7.1 Hz, 1H, H_4), 7.24-7.32 (m, 3H, H_3, H_5, $H_{5'}$), 7.54-7.56 (m, 3H, H_2, H_6, $H_{4'}$), 7.71-7.76 (m, 1H, $H_{3'}$), 8.55 (d, *J* = 4.4 Hz, 1H, $H_{6'}$), 8.64 (br s, 1H, NH, rotamer B), 8.92 (br s, 1H, NH, rotamer A). ^{13}C-NMR ($CDCl_3$, δ): 14.0 (CH_3), 22.6, 26.5, 28.8, 29.0 (2C), 31.7 ($(CH_2)_6CH_3$), 36.5 (CH_2CO), 43.2 (CH_2N), 50.0 ($(CH_2)_6CH_2N$), 119.9 (C_2, C_6), 123.1, 123.9, 124.4 (C_4, $C_{3'}$, $C_{5'}$), 128.8 (C_3, C_5), 137.0

($C_{4'}$), 138.4 (C_1), 148.5 ($C_{6'}$), 154.5 ($C_{2'}$), 169.5, 169.7 (CONH, CON). HRMS (ESI, m/z): Calculated for $C_{23}H_{31}N_3O_2Na$ $[M+Na]^+$: 404.2308. Found: 404.2276.

***N*²-Octyl-*N*¹-phenyl-*N*²-(pyridin-3-ylcarbonyl)-β-alaninamide (60).** Obtained using the procedure 4.1.1.3 from amine **44** (85 mg, 0.3 mmol), nicotinic acid (37 mg, 0.3 mmol), EDC (47 mg, 0.3 mmol) and HOBt (41 mg, 0.3 mmol) in 36% yield (41 mg).

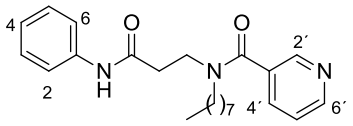

Chromatography: hexane/EtOAc, 2:8. R_f (EtOAc): 0.28. IR (ATR, cm^{-1}): 3312 (NH), 1685 (CON), 1612, 1546, 1495, 1440 (Ar). ^{1}H-NMR ($CDCl_3$, δ): Mixture of rotamers A:B, 6:1; 0.87 (t, *J* = 6.8 Hz, 3H, CH_3), 1.13-1.18 (m, 10H, $(CH_2)_5CH_3$), 1.53 (m, 2H, $CH_2(CH_2)_5CH_3$), 2.50 (m, 2H, CH_2CO, rotamer B), 2.79 (t, *J* = 5.7 Hz, 2H, CH_2CO, rotamer A), 3.28 (t, *J* = 7.0 Hz, 2H, $(CH_2)_6CH_2N$, rotamer A), 3.49 (m, 2H, $(CH_2)_6CH_2N$, rotamer B), 3.64 (m, 2H, $COCH_2CH_2N$, rotamer B), 3.86 (m, 2H, $COCH_2CH_2N$, rotamer A), 7.07 (t, *J* = 7.3 Hz, 1H, H_4), 7.24-7.32 (m, 3H, H_3, H_5, $H_{5'}$), 7.53 (d, *J* = 7.6 Hz, 2H, H_2, H_6), 7.67 (d, *J* = 7.7 Hz, 1H, $H_{4'}$), 8.64 (d, *J* = 1.4 Hz, 2H, $H_{2'}$, $H_{6'}$), 9.27 (br s, 1H, NH). ^{13}C-NMR ($CDCl_3$, δ): 14.0 (CH_3), 22.5, 26.4, 28.9, 29.0 (2C), 31.6 ($(CH_2)_6CH_3$), 35.8 (CH_2CO), 42.7 (CH_2N), 50.7 ($(CH_2)_6CH_2N$), 119.9 (C_2, C_6), 123.4 ($C_{5'}$), 124.1 (C_4), 128.8 (C_3, C_5), 132.4 ($C_{3'}$), 134.2 ($C_{4'}$), 138.3 (C_1), 147.3, 150.6 ($C_{2'}$, $C_{6'}$), 169.5, 169.8 (CONH, CON). HRMS (ESI, m/z): Calculated for $C_{23}H_{31}N_3O_2Na$ $[M+Na]^+$: 404.2308. Found: 404.2302.

***N*²-Octyl-*N*¹-phenyl-*N*²-(pyridin-4-ylcarbonyl)-β-alaninamide (61).** Obtained using the procedure 4.1.1.3. from amine **44** (85 mg, 0.3 mmol), isonicotinic acid (37 mg, 0.3 mmol), EDC (47 mg, 0.3 mmol) and HOBt (41 mg, 0.3 mmol) in 41% yield (47 mg).

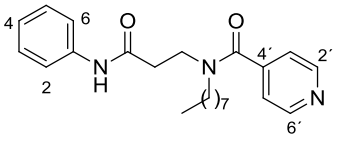

Chromatography: hexane/EtOAc, 2:8. R_f (EtOAc): 0.19. IR (ATR, cm^{-1}): 3310 (NH), 1624 (CON), 1547 (Ar). ^{1}H-NMR ($CDCl_3$, δ): (Mixture of rotamers A:B, 4:1): 0.76 (t, *J* = 6.9 Hz, 3H, CH_3), 1.02-1.07 (m, 10H, $(CH_2)_5CH_3$), 1.41 (qt, *J* = 6.9 Hz, 2H, $CH_2(CH_2)_5CH_3$), 2.40 (m, 2H, CH_2CO, rotamer B), 2.70 (t, *J* = 6.5 Hz, 2H, CH_2CO, rotamer A), 3.12 (t, *J* = 7.6 Hz, 2H, $(CH_2)_6CH_2N$, rotamer A), 3.41 (m, 2H, $(CH_2)_6CH_2N$, rotamer B), 3.50 (m, 2H, $COCH_2CH_2N$, rotamer B), 3.74 (t, *J* = 6.5 Hz, 2H, $COCH_2CH_2N$, rotamer A), 7.00 (t, *J* = 7.3 Hz, 1H, H_4),

7.11 (d, *J* = 5.8 Hz, 2H, $H_{3'}$, $H_{5'}$), 7.16-7.21 (m, 2H, H_3, H_5), 7.41 (d, *J* = 7.9 Hz, 2H, H_2, H_6), 8.55 (d, *J* = 5.7 Hz, 2H, $H_{2'}$, $H_{6'}$), 8.78 (br s, 1H, NH). ^{13}C-NMR ($CDCl_3$, δ): 14.0 (CH_3), 22.5, 26.4, 28.8, 29.0 (2C), 31.6 (($\underline{C}H_2)_6CH_3$), 35.9 ($\underline{C}H_2CO$), 42.4 (CH_2N), 50.4 (($CH_2)_6\underline{C}H_2N$), 119.8 (C_2, C_6), 120.8 ($C_{3'}$, $C_{5'}$), 124.2 (C_4), 128.9 (C_3, C_5), 138.2 (C_1), 144.1 ($C_{4'}$), 150.3 ($C_{2'}$, $C_{6'}$), 169.2, 169.9 (CON, rotamers A and B), 171.1 (CONH). HRMS (ESI, m/z): Calculated for $C_{23}H_{31}N_3O_2Na$ $[M+Na]^+$: 404.2308. Found: 404.2311.

4.1.7. Synthesis of *N*^{2}-octyl-*N*-phenyl-*N*^{2}-[(pyridin-2-yl)methyl)]-β-alaninamide (62). To a solution of the secondary amine **44** (85 mg, 0.3 mmol) in anhydrous DCE (3 mL), a solution of 2-pyridinecarboxaldehyde (50 µL, 0.5 mmol) was added and the mixture stirred for 20 min at rt. Then, the reaction mixture was cooled to 0 °C and treated with a solution of $NaBH(OAc)_3$ (135 mg, 0.6 mmol) in anhydrous DCE (5 mL), followed by stirring at rt for 16 h. The solvent was removed under reduced pressure, the residue was redissolved in EtOAc and washed with saturated solutions of $NaHCO_3$ and NaCl, consecutively. The organic extract was dried over Na_2SO_4, filtered, and the solvent was removed under reduced pressure. The residue was purified by chromatography (hexane/EtOAc, 1:1) to yield compound **62** in 16% yield (18 mg).

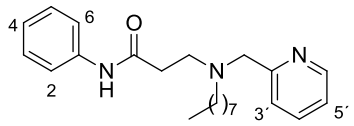

R_f: 0.15 (hexane/EtOAc, 3:7). IR (ATR, cm^{-1}): 3309 (NH), 1685 (CO), 1615, 1547, 1495, 1443 (Ar). ^{1}H-NMR ($CDCl_3$, δ): 0.85 (t, *J* = 7.0 Hz, 3H, CH_3), 1.11-1.25 (m, 10H, $(C\underline{H}_2)_5CH_3$), 1.57 (m, 2H, $C\underline{H}_2(CH_2)_5CH_3$), 2.54-2.61 (m, 4H, CH_2CO, $(CH_2)_6C\underline{H}_2N$), 2.85 (t, *J* = 5.6 Hz, 2H, $COCH_2C\underline{H}_2N$), 3.81 (s, 2H, CH_{2pyr}), 7.06 (t, *J* = 7.4 Hz, 1H, H_4), 7.15 (dd, *J* =7.2, 5.3 Hz, 1H, $H_{5'}$), 7.24-7.33 (m, 3H, H_3, H_5, $H_{3'}$), 7.59 (td, *J* = 7.6, 1.7 Hz, 1H, $H_{4'}$), 7.63 (d, *J* = 7.7 Hz, 2H, H_2, H_6), 8.50 (d, *J* = 4.2 Hz, 1H, $H_{6'}$), 10.8 (br s, 1H, NH). ^{13}C-NMR ($CDCl_3$, δ): 14.0 (CH_3), 22.8, 26.6, 27.7, 29.3, 29.8, 32.1 (($\underline{C}H_2)_6CH_3$), 34.2 ($\underline{C}H_2CO$), 50.4 (CH_2N), 54.1 (($CH_2)_6\underline{C}H_2N$), 60.1 (CH_{2pyr}), 120.4 (C_2, C_6), 122.6 ($C_{5'}$), 123.6 ($C_{3'}$), 123.7 (C_4), 128.9 (C_3, C_5), 136.7 ($C_{4'}$), 139.1 (C_1), 149.9 ($C_{6'}$), 157.9 ($C_{2'}$), 171.0 (CO). HRMS (ESI, m/z): Calculated for $C_{23}H_{33}N_3O$ $[M+H]^+$: 368.2657. Found: 368.2108.

Table 11. HPLC-MS for final compounds.*

Comp.	r_t (min)	Comp.	r_t (min)
4	19.6	**24**	13.9
5	6.7	**25**	16.5
6	6.7	**46**	10.7
7	16.3	**47**	10.8
8	8.4	**48**	10.8
9	19.0	**49**	10.7
10	20.3	**50**	10.9
11	11.5	**51**	11.6
12	13.0	**52**	9.9
13	17.4	**53**	12.7
14	8.7	**54**	10.6
15	9.6	**55**	18.7
16	9.1	**56**	11.9
17	14.2	**57**	8.6
18	8.9	**58**	24.5
19	10.3	**59**	22.9
20	10.2	**60**	23.2
21	29.1	**61**	23.5
22	25.4	**62**	18.0
23	9.7		

* All compounds have been analyzed using HPLC gradient method A with exception of compounds **16**-**19** that were analyzed with method B.

4.2. Biology

4.2.1. ICMT activity assay

The ability of synthesized compounds to inhibit ICMT enzyme was determined by a radioactivity assay previously described by Baron et al.[39] Briefly, membranes that overexpress ICMT enzyme were incubated in the presence of the compounds under study and the substrates BFC and [^{3}H]-SAM with shaking at rt. Compounds were tested at 50 µM concentration in a final volume of 50 µL of incubation buffer [Hepes 70 mM, NaCl 100 mM, $MgCl_2$ 5 mM, 1,4-dithiotreitol (DTT) 3 mM, pH 7.5] and both substrates BFC and [^{3}H]-SAM at final concentration of 5 and 2 µM, respectively. Then, the mixture was incubated for 30 min at 37 °C and the enzymatic reaction was stopped by adding 10 µL of streptavidin beads (Thermo Scientific, 10 µL of beads in 500 µL of PBS). The samples were stirred at 4 °C overnight and later filtered through fiberglass filters (Filtermat A, PerkinElmer), using a multiple filtration equipment FilterMate Unifilter 96-Harvester (PerkinElmer). The inhibition of the methylesterification reaction, in which the tritiated methyl group of [^{3}H]-SAM is transferred to the substrate BFC, was quantified by measuring the radioactivity by liquid scintillation spectrometry (Microbeta TopCount, Perkin Elmer). The percentage of this inhibition was determined with respect to the 100% activity obtained in the absence of compounds.

4.2.2. Cell lines and culture

AF3 wild type and G690G mouse fibroblasts (kindly donated by Prof. Carlos López-Otín, Oviedo University) were grown in Dulbecco´s Modified Eagle Medium (DMEM, Invitrogen) supplemented with 10% heat-inactivated fetal bovine serum (FBS, HyClone), 1% L-glutamine (Invitrogen), 1% sodium pyruvate (Invitrogen), 50 U/mL penicillin and 50 µg/mL streptomycin (Invitrogen). HGADFN167 and HGFDFN168 human fibroblasts (obtained from The Progeria Research Foundation) were grown in 15% DMEM, 50 U/mL penicillin and 50 µg/mL streptomycin. Cells were incubated in a humidified atmosphere at 37 °C in the presence of 5% CO_2.

4.2.3. MTT assay

Cells were seeded in 96-well plates at a density of 5 x 10^2 cells per well in the corresponding medium with 10% FBS for 24 h prior to treatments. The medium was then replaced by fresh medium containing different concentrations of compounds or the equivalent volume of DMSO. Cells were treated for 48 h and the medium was replaced by fresh medium with 2 mg/mL of MTT (Sigma Aldrich) and cells were incubated for 4 h at 37 °C in the dark. Then, supernatants were removed and formazan crystals formed by viable cells were dissolved in DMSO (100 µL/well) and absorbance

was measured at 570 and at 630 nm using an Asys UVM 340 microplate reader. Then, absorbance at 630 nm (background) was substracted from the absorbance at 570 nm and the cytotoxicity values were calculated from the percentage of viable cells with respect to the 100% viability of the vehicle-treated cells.

4.2.4. In vitro pharmacokinetic assays

4.2.4.1. HSA binding assay

Determination of the binding of the compound to HSA was performed by incubating a fixed concentration of the compound with different concentrations of immobilized HSA, using the TRANSILXL HSA Binding Kit (TMP-0210-2096, Sovicell). An eightwell unit of the TRANSIL assay plate was used for each compound; six wells contain increasing concentrations of HSA immobilized on silica beads suspended in PBS at pH 7.4, and two wells contain buffer only and serve as references to account for non-specific binding. The TRANSIL assay plate was thawed for 3 h at rt and centrifuged at 750*g* for 5 s. Then, 15 µL of an 80 µM stock solution of the compound in PBS (for a final concentration of 5 µM) was added to each well of the eight-well unit, and the plate was incubated on a plate shaker at 1000 rpm for 12 min at rt. After this time, the plate was centrifuged at 750*g* for 10 min, and 50 µL of the supernatants were transferred for analytical quantification by HPLC-MS using selected ion monitoring (SIM) and quantification was estimated by measuring the area under the peak ($[M+H]^+$) normalized with an internal standard. The binding percentage was calculated from the remaining free compound concentration in the supernatant of each well, using the spreadsheet and algorithms supplied with the kit.

4.2.4.2. Stability assay in mouse and human serum

Stability for selected compounds was assayed by adding 625 µL of a 2 mM solution of test compound in PBS (pH 7.4) to 1875 µL of mouse or human serum (Europa Bioproducts, EQSM-0100) pre-warmed at 37 °C. Next, solutions were incubated at 37 °C for 24 h, taking aliquots of 125 µL at different time points (0, 1, 4, 8 and 24 h). Each aliquot was quenched with 500 µL of cold ACN, vortexed, incubated for 10 min in ice and centrifuged at 39000*g* for 10 min. Supernatants were then analyzed by HPLC-MS using SIM mode. Concentrations were quantified by measuring the area under the peak ($[M+H]^+$) normalized with an internal standard and converted to the percentage of compound remaining, using the time zero peak area value as 100%.

4.2.4.3. Stability assay in mouse and human liver microsomes

Compounds were incubated at 37 °C at a final concentration of 1 or 5 µM in PBS together with a solution of nicotinamide adenine dinucleotide phosphate (NADPH) in PBS (final concentration of 2 mM) and a solution of $MgCl_2$ in PBS (final concentration of 5 mM). Reactions were initiated by the addition of a suspension of mouse liver microsomes (MLMs) (male CD-1 mice pooled, Sigma-Aldrich) or human liver microsomes (HLMs) (male human pooled, Sigma-Aldrich), respectively, at a final protein concentration of 1 mg/mL. The solutions were vortexed and incubated at 37 °C. Aliquots of 100 µL were quenched at time zero and at seven points ranging to 1 h (MLM) or 2 h (HLM) by pouring into 100 µL of ice-cold ACN. Quenched samples were centrifuged at 10000*g* for 5 min, and the supernatants were filtered through a polytetrafluoroethylene (PTFE) membrane syringe filter (pore size of 0.2 µm, 13 mm of diameter, GE Healthcare Life Sciences). The relative disappearance of the compound under study over the course of the incubation was monitored by HPLC-MS using SIM mode. Concentrations were quantified by measuring the area under the peak ($[M+H]^+$) normalized with an internal standard and converted to the percentage of compound remaining, using the time zero peak area value as 100%. The natural logarithm of the remaining percentage versus time data for each compound was fit to a linear regression, and the slope was used to calculate the degradation half-life.

4.2.5. Analysis by immunodetection of phosphorylated histone 2AX (pH2AX) and phosphorylated Akt (pAkt) levels

Progeroid HGADFN167 or healthy HGFDFN168 cells were seeded at density of 50000 cells and incubated for 24 h in DMEM medium supplemented with a 15% FBS, until reaching a 80% of confluence. Then, the culture medium was substituted by fresh medium with the compound under study at 2 µM or with vehicle (0.1% DMSO in culture media) and cells were incubated for 17 or 10 days for pH2AX and pAkt analysis, respectively. Cells were lysed with cold radioimmunoprecipitation assay buffer (50 mM Tris-HCl pH 7.4, 150 mM NaCl, 1% lgepal) with a mixture of protease and phosphatase inhibitors (Roche and Sigma-Aldrich, respectively). The lysates were immediately used or stored at -20 °C until their use. The protein concentration was determined (DC Protein Assay Kit, Bio-Rad) and samples with the same amount of protein were diluted in reductive Laemmli buffer, and denatured at 95 °C for 5 min. Samples were analyzed by electrophoresis in polyacrylamide gels (4-20% SDS-PAGE, BioRad) and the proteins transferred to nitrocellulose membranes (GE Healthcare, Amersham). After 1 h of incubation in blocking buffer (100 mM Tris-HCl pH 8.0, 150 mM NaCl and 0.05% Tween-20 (TBS-T) with 3% of bovine serum albumin (BSA)), blots were incubated overnight at 4

°C with the corresponding primary antibody [anti-phospho-histone 2AX (Ser139) (EMD Millipore, 05-636, 1:1000) and anti-phospho-Akt (Cell Signaling, 4060S, 1:1000)] for analysis of pH2AX and pAkt, respectively and anti-ERK1/2 (Cell Signaling, 9102S, 1:1000) as antibody for loading control. Then, membranes were washed (3x) with TBS-T and incubated with the corresponding secondary antibody conjugated with peroxidase (Sigma-Aldrich) for 1 h at rt. Proteins were visualized by quimioluminiscence in a Fujifilm LAS-300 imager and the bands were quantified by densitometry using the program ImageJ (NIH).

4.2.6. Progerin visualization by confocal microscopy

Progeroid HGADFN167 cells were seeded at a density of $2 \cdot 10^4$ cells/well over 12 mm diameter slide covers and were incubated for 24 h at 37 °C in 5% CO_2 atmosphere in DMEM medium supplemented with 15% FBS. Then, the culture medium was substituted by fresh one with the compound under study at 2 µM or with 0.1% DMSO and the cells were incubated for 21 days. Cells were fixed with a 4% solution of paraformaldehyde (PFA, Sigma-Aldrich) and permeabilized with PBS containing 0.1% Triton X-100 (PBS-T, Sigma-Aldrich). Then, cells were incubated with an anti-progerin antibody (Santa Cruz Biotechnology, SC-81611, 1:500) in TBS with 3% BSA at rt for 2 h. After that, cells were washed with TBS (1x) and incubated in absence of light for 1 h with the fluorophore Alexa Fluor 488 donkey anti-mouse (Thermo Scientific) diluted in TBS with 3% BSA. Later, cells were additionally washed with TBS (1x) and incubated with Hoechst 33258 (5 µg/mL, Sigma-Aldrich) for 10 min at rt in order to visualize cellular nucleus. Finally, cells were washed with PBS-T (2x) and the slide cover was carefully mounted with Immumount (Thermo Scientific). The visualization was carried out using confocal microscopy (Olympus IX83) equipped with a 60X oil inmersion lens and the appropriate excitation and emission filters at the cytometry and fluorescence microscopy UCM facilities.

REFERENCES

5. REFERENCES

1. De Sandre-Giovannoli, A.; Bernard, R.; Cau, P.*, et al.*, Lamin A truncation in Hutchinson-Gilford progeria. *Science* **2003**, *300*, 2055.

2. Eriksson, M.; Brown, W. T.; Gordon, L. B.*, et al.*, Recurrent de novo point mutations in lamin A cause Hutchinson-Gilford progeria syndrome. *Nature* **2003**, *423*, 293-298.

3. Hutchinson, J., Congenital absence of hair and mammary glands with atrophic condition of the skin and its appendages, in a boy whose mother had been almost wholly bald from alopecia areata from the age of six. *Med. Chir. Trans.* **1886**, *69*, 473-477.

4. Gilford, H., On a condition of mixed premature and immature development. *Med. Chir. Trans.* **1897**, *80*, 17-46.

5. Kieran, M. W.; Gordon, L.; Kleinman, M., New approaches to progeria. *Pediatrics* **2007**, *120*, 834-841.

6. Domingo, D. L.; Trujillo, M. I.; Council, S. E.*, et al.*, Hutchinson-Gilford progeria syndrome: oral and craniofacial phenotypes. *Oral Dis.* **2009**, *15*, 187-195.

7. Cleveland, R. H.; Gordon, L. B.; Kleinman, M. E.*, et al.*, A prospective study of radiographic manifestations in Hutchinson-Gilford progeria syndrome. *Pediatr. Radiol.* **2012**, *42*, 1089-1098.

8. Bertrand, A. T.; Chikhaoui, K.; Yaou, R. B.*, et al.*, Clinical and genetic heterogeneity in laminopathies. *Biochem. Soc. Trans.* **2011**, *39*, 1687-1692.

9. Goldman, R. D.; Gruenbaum, Y.; Moir, R. D.*, et al.*, Nuclear lamins: building blocks of nuclear architecture. *Genes Dev.* **2002**, *16*, 533-547.

10. Dechat, T.; Pfleghaar, K.; Sengupta, K.*, et al.*, Nuclear lamins: major factors in the structural organization and function of the nucleus and chromatin. *Genes Dev.* **2008**, *22*, 832-853.

11. Gordon, L. B.; Kleinman, M. E.; Miller, D. T.*, et al.*, Clinical trial of a farnesyltransferase inhibitor in children with Hutchinson–Gilford progeria syndrome. *Proc. Natl. Acad. Sci.* **2012**, *109*, 16666-16671.

12. Gordon, L. B.; Massaro, J.; D'Agostino, R. B., Sr.*, et al.*, Impact of farnesylation inhibitors on survival in Hutchinson-Gilford progeria syndrome. *Circulation* **2014**, *130*, 27-34.

13. Gordon, L. B.; Shappell, H.; Massaro, J.*, et al.*, Association of lonafarnib treatment vs no treatment with mortality rate in patients with Hutchinson-Gilford progeria syndrome. *Jama* **2018**, *319*, 1687-1695.

14. Varela, I.; Pereira, S.; Ugalde, A. P.*, et al.*, Combined treatment with statins and aminobisphosphonates extends longevity in a mouse model of human premature aging. *Nat. Med.* **2008**, *14*, 767-772.

15. Gordon, L. B.; Kleinman, M. E.; Massaro, J.*, et al.*, Clinical trial of the protein farnesylation inhibitors lonafarnib, pravastatin, and zoledronic acid in children with Hutchinson-Gilford progeria syndrome. *Circulation* **2016**, *134*, 114-125.

16. Hamczyk, M. R.; del Campo, L.; Andres, V., Aging in the cardiovascular system: lessons from Hutchinson-Gilford progeria syndrome. *Annu. Rev. Physiol.* **2018**, *80*, 27-48.

17. Piekarowicz, K.; Machowska, M.; Dzianisava, V.*, et al.*, Hutchinson-Gilford progeria syndrome-current status and prospects for gene therapy treatment. *Cells* **2019**, *8*, 1-22.

18. Santiago-Fernandez, O.; Osorio, F. G.; Quesada, V.*, et al.*, Development of a CRISPR/Cas9-based therapy for Hutchinson-Gilford progeria syndrome. *Nat. Med.* **2019**, *25*, 423-426.

19. Quigley, A.; Dong, Y. Y.; Pike, A. C. W.*, et al.*, The structural basis of ZMPSTE24-dependent laminopathies. *Science* **2013**, *339*, 1604-1607.

20. Fong, L. G.; Chang, S. Y.; Yang, S. H.*, et al.*, Absence of progeria-like disease phenotypes in knock-in mice expressing a non-farnesylated version of progerin. *Hum. Mol. Genet.* **2010**, *20*, 436-444.

21. Winter-Vann, A. M.; Baron, R. A.; Wong, W.*, et al.*, A small-molecule inhibitor of isoprenylcysteine carboxyl methyltransferase with antitumor activity in cancer cells. *Proc. Natl. Acad. Sci. USA* **2005**, *102*, 4336-4341.

22. Wang, M.; Hossain, M. S.; Tan, W.*, et al.*, Inhibition of isoprenylcysteine carboxylmethyltransferase induces autophagic-dependent apoptosis and impairs tumor growth. *Oncogene* **2010**, *29*, 4959-4970.

23. Manu, K. A.; Chai, T. F.; Teh, J. T.*, et al.*, Inhibition of isoprenylcysteine carboxylmethyltransferase induces cell-cycle arrest and apoptosis through p21 and p21-regulated BNIP3 induction in pancreatic cancer. *Mol. Cancer Ther.* **2017**, *16*, 914-923.

24. Go, M. L.; Leow, J. L.; Gorla, S. K.*, et al.*, Amino derivatives of indole as potent inhibitors of isoprenylcysteine carboxyl methyltransferase. *J. Med. Chem.* **2010**, *53*, 6838-6850.

25. Butler, K. V.; Bohn, K.; Hrycyna, C. A.*, et al.*, Non-substrate based, small molecule inhibitors of the human isoprenylcysteine carboxyl methyltransferase. *MedChemComm.* **2016**, *7*, 1016-1021.

26. Buchanan, M. S.; Carroll, A. R.; Fechner, G. A.*, et al.*, Small-molecule inhibitors of the cancer target, isoprenylcysteine carboxyl methyltransferase, from Hovea parvicalyx. *Phytochemistry* **2008**, *69*, 1886-1889.

27. Buchanan, M. S.; Carroll, A. R.; Fechner, G. A.*, et al.*, Aplysamine 6, an alkaloidal inhibitor of Isoprenylcysteine carboxyl methyltransferase from the sponge Pseudoceratina sp. *J. Nat. Prod.* **2008**, *71*, 1066-1067.

28. Buchanan, M. S.; Carroll, A. R.; Fechner, G. A.*, et al.*, Spermatinamine, the first natural product inhibitor of isoprenylcysteine carboxyl methyltransferase, a new cancer target. *Bioorg. Med. Chem. Lett.* **2007**, *17*, 6860-6863.

29. Leow, J. L.; Baron, R.; Casey, P. J.*, et al.*, Quantitative structure-activity relationship (QSAR) of indoloacetamides as inhibitors of human isoprenylcysteine carboxyl methyltransferase. *Bioorg. Med. Chem. Lett.* **2007**, *17*, 1025-1032.

30. Ramanujulu, P. M.; Yang, T.; Yap, S. Q.*, et al.*, Functionalized indoleamines as potent, drug-like inhibitors of isoprenylcysteine carboxyl methyltransferase (ICMT). *Eur. J. Med. Chem.* **2013**, *63*, 378-386.

31. Lau, H. Y.; Ramanujulu, P. M.; Guo, D.*, et al.*, An improved isoprenylcysteine carboxylmethyltransferase inhibitor induces cancer cell death and attenuates tumor growth in vivo. *Cancer Biol. Ther.* **2014**, *15*, 1280-1291.

32. Bergman, J. A.; Hahne, K.; Hrycyna, C. A.*, et al.*, Lipid and sulfur substituted prenylcysteine analogs as human Icmt inhibitors. *Bioorg. Med. Chem. Lett.* **2011**, *21*, 5616-5619.

33. Bergman, J. A.; Hahne, K.; Song, J.*, et al.*, *S*-farnesyl-thiopropionic acid (FTPA) triazoles as potent inhibitors of isoprenylcysteine carboxyl methyltransferase. *ACS Med. Chem. Lett.* **2012**, *3*, 15-19.

34. Majmudar, J. D.; Hahne, K.; Hrycyna, C. A.*, et al.*, Probing the isoprenylcysteine carboxyl methyltransferase (Icmt) binding pocket: sulfonamide modified farnesyl cysteine (SMFC) analogs as Icmt inhibitors. *Bioorg. Med. Chem. Lett.* **2011**, *21*, 2616-2620.

35. Judd, W. R.; Slattum, P. M.; Hoang, K. C.*, et al.*, Discovery and SAR of methylated tetrahydropyranyl derivatives as inhibitors of isoprenylcysteine carboxyl methyltransferase (ICMT). *J. Med. Chem.* **2011**, *54*, 5031-5047.

36. Diver, M. M.; Pedi, L.; Koide, A.*, et al.*, Atomic structure of the eukaryotic intramembrane RAS methyltransferase ICMT. *Nature* **2018**, *553*, 526-529.

37. Marín-Ramos, N. I.; Balabasquer, M.; Ortega-Nogales, F. J.*, et al.*, A potent isoprenylcysteine carboxylmethyltransferase (ICMT) inhibitor improves survival in Ras-driven acute myeloid leukemia. *J. Med. Chem.* **2019**, *62*, 6035-6046.

38. Marín-Ramos, N. I.; Ortega-Nogales, F. J.; Balabasquer-Peña, M.*, et al.*, Novel inhibitors of the enzyme isoprenylcysteine carboxyl methyltransferase (ICMT). *PCT/ES2014/070071* **2014**.

39. Baron, R. A.; Casey, P. J., Analysis of the kinetic mechanism of recombinant human isoprenylcysteine carboxylmethyltransferase (ICMT). *BMC Biochemistry* **2004**, *5*, 1-12.

40. Bostrom, J.; Hogner, A.; Llinas, A.*, et al.*, Oxadiazoles in medicinal chemistry. *J. Med. Chem.* **2012**, *55*, 1817-1830.

41. Ibrahim, M. X.; Sayin, V. I.; Akula, M. K.*, et al.*, Targeting isoprenylcysteine methylation ameliorates disease in a mouse model of progeria. *Science* **2013**, *340*, 1330-1333.

42. Gleeson, M. P., Generation of a set of simple, interpretable ADMET rules of thumb. *J. Med. Chem.* **2008**, *51*, 817-834.

43. Cvetovich, R. J.; DiMichele, L., Formation of acrylanilides, acrylamides, and amides directly from carboxylic acids using thionyl chloride in dimethylacetamide in the absence of bases. *Org. Process Res. Dev.* **2006**, *10*, 944-946.

44. Hutchins, R. O.; Adams, J.; Rutledge, M. C., Stereoselective hydride reductions of cyclic *N*-diphenylphosphinyl imines. Highly diastereoselective syntheses of protected primary amines. *J. Org. Chem.* **1995**, *60*, 7396-7405.

45. Fujioka, H.; Yamamoto, H.; Miyazaki, M.*, et al.*, Reductive Beckmann fragmentation of α-alkoxycycloalkanone oxime acetates. *Tetrahedron Lett.* **1991**, *32*, 5367-5368.

46. de Greef, T. F. A.; Nieuwenhuizen, M. M. L.; Sijbesma, R. P.*, et al.*, Competitive intramolecular hydrogen bonding in oligo(ethylene oxide) substituted quadruple hydrogen bonded systems. *J. Org. Chem.* **2010**, *75*, 598-610.

47. Jadhav, G. P.; Chhabra, S. R.; Telford, G.*, et al.*, Immunosuppressive but non-LasR-inducing analogues of the Pseudomonas aeruginosa quorum-sensing molecule *N*-(3-oxododecanoyl)-l-homoserine lactone. *J. Med. Chem.* **2011**, *54*, 3348-3359.

48. Wuitschik, G.; Carreira, E. M.; Wagner, B.*, et al.*, Oxetanes in drug discovery: structural and synthetic insights. *J. Med. Chem.* **2010**, *53*, 3227-3246.

49. Pasquinucci, L.; Prezzavento, O.; Marrazzo, A.*, et al.*, Evaluation of N-substitution in 6,7-benzomorphan compounds. *Bioorg. Med. Chem.* **2010**, *18*, 4975-4982.

50. Zhu, M.; Zhang, C.; Nwachukwu, J. C.*, et al.*, Bicyclic core estrogens as full antagonists: synthesis, biological evaluation and structure-activity relationships of estrogen receptor ligands based on bridged oxabicyclic core arylsulfonamides. *Org. Biomol. Chem.* **2012**, *10*, 8692-8700.

CHAPTER B

IDENTIFICATION OF NEW MOLECULES PRODUCED BY THE HUMAN MICROBIOTA

INTRODUCTION AND OBJECTIVES

1. INTRODUCTION AND OBJECTIVES

The human microbiota can be defined as an extremely variable and compartmentalized ecosystem of commensal, symbiotic and pathogenic microorganisms that lives in our body.[1] These populations, formed by bacteria, fungi, parasites and archaea, are more abundant than our somatic cells and contain more genes than our human genome.[2,3] About a thousand species of bacteria exist in the human body simultaneously, increasing the number of genotypes over orders of magnitude.[4] The trillions of bacteria that make up the human microbiome are believed to encode functions that are important to human health. Recent investigations showed that intestinal microbiota exerts deep effects on many aspects of human health and disease, which has led to the concept of a human meta-organism consisting on (human)microbial molecules or derivatized metabolites that integrates the communication between both prokaryotic and eukaryotic parts to achieve homeostasis (Figure 1). In particular, for many diseases, there is huge evidence that the microbiota and their metabolites can be used to explain a great percentage of variance in the relevant phenotypes for a given condition, including cancer,[5,6] liver cirrhosis,[7] diabetes,[8,9] obesity,[10] cardiovascular disease,[11] inflammatory bowel disease,[12] immune system dysfunction,[13] and aging.[14-16] Furthermore, replacement of the microbiota of a diseased individual with that of a healthy individual clearly ameliorates certain diseases.[17] These findings strongly support the hypothesis that metabolites produced by the human microbiota regulate key biological functions in the host.

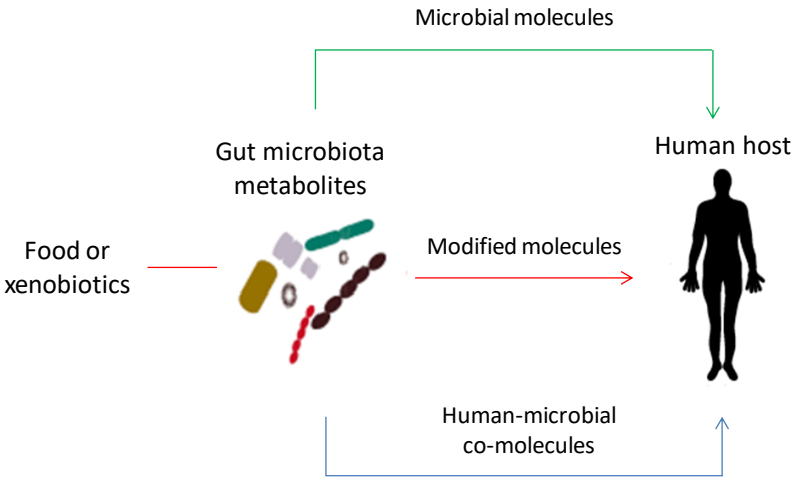

Figure 1. Relationship between the gut microbiota and the human host.

In this work, we have focused our attention on the link between microbiota metabolites and aging. The composition of human microbiota is strongly dependent on aging, and huge evidences of the differences between the gut microbiota of young and old people have been described.[18] These divergences can be associated with environmental, host, [19,20] and genetic factors.[21] In 2016, Bischoff *et al.* confirmed the presence of age-related inflammatory processes and diseases that have been linked to changes in gut bacteria.[22] Hence, alterations in the human microbiota have a direct effect in human health span and aging.

However, due to the large complexity of the human microbiome and its vast coding potential, most of the metabolites produced by the microbiota are still to be discovered, making the identification of microbiota metabolites a daunting task that has not been addressed up to date. During the last decade, huge efforts have been made to sequence isolates of the human microbiota from various body sites, and large genome programmes have been funded towards this goal.[23,24] Functional metagenomics use bioinformatics tools and genomic sequence data to infer which genes presumably codify for enzymes involved in the biosynthesis of metabolites and to predict their products based on the identification of conserved biosynthetic domains (Figure 2). The main limitation of this methodology is that it heavily relies on the development of algorithms able to identify sequence homologies and to predict the structure of the metabolites biosynthesized. In addition, this approach penalizes the identification of new gene clusters that are more likely to produce new metabolites.[25,26] On the contrary, direct metabolomic methods are specifically tailored to study the metabolites directly and are

often designed for particular compound classes that are expected to be produced by the gene(s) of interest. As this approach requires a priori knowledge of the metabolite structure, it does not enable a wide breadth of profiling coverage (Figure 2).

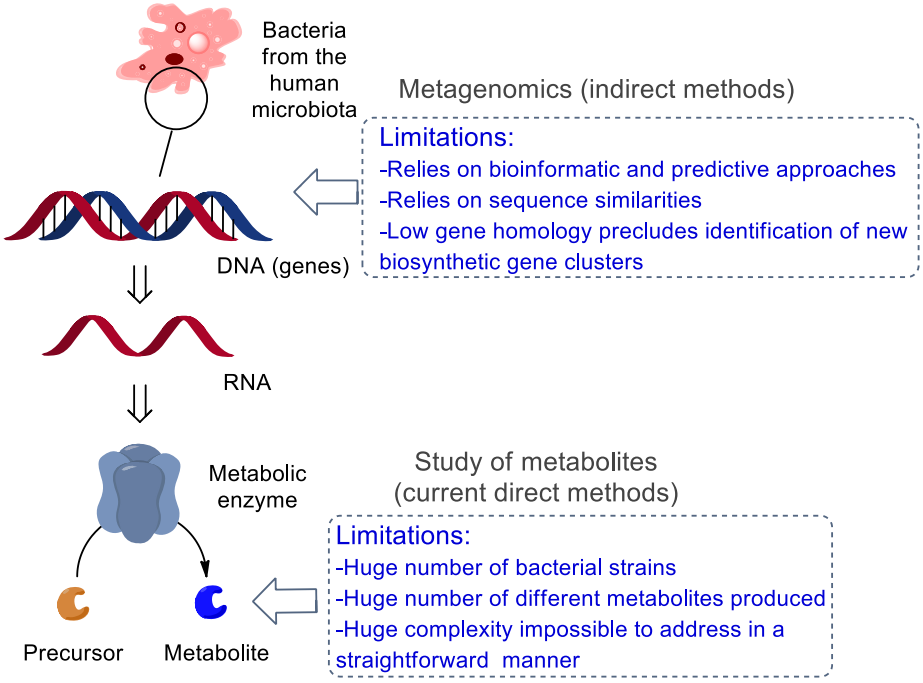

Figure 2. Current methodologies used for the identification of microbiota metabolites.

These evidences highlight the importance of the development of new strategies for the de novo identification of metabolites produced by the human microbiota. Thus, in the present work, we propose to develop an innovative methodology which will allow us to identify microbiota metabolites. This platform is based on the use of tagged precursors of metabolites of the human microbiota. A scheme of the overall platform is depicted in Figure 3.

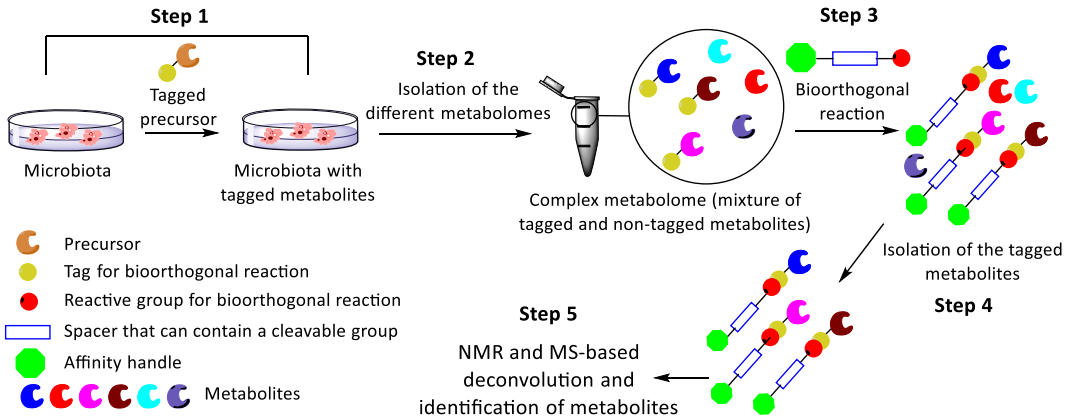

Figure 3. Platform designed for the identification of metabolites produced by the human microbiota.

The development of this strategy implies the following steps:

1. Design and synthesis of tagged precursors
2. Incorporation of tagged precursors in selected strains of bacteria

} Step 1

3. Isolation of the different metabolomes (Step 2)
4. Bioorthogonal reaction with the capture reagent (Step 3)
5. Isolation of the tagged metabolites (Step 4)
6. NMR and MS-based deconvolution and identification of metabolites (Step 5)

Then, the main objective of the present work consists on the setting up and optimization of all the steps of the platform so that we can confirm its potential to isolate and identify metabolites in complex bacterial metabolomes. If successful, this objective will provide the proof of concept for the widespread use of the platform with a variety of tagged precursors.

RESULTS AND DISCUSSION

2. RESULTS AND DISCUSSION

2.1. Design and synthesis of tagged precursors

Among the diverse precursors that have been described to be substrates of different enzymes of the human microbiota,[27-29] such as sugars, amino acids, fatty acids, or steroids, as an initial proof of concept to set up the platform, we decided to start with sugars as tagged precursors. These compounds have been selected due to the evidence that azido sugars can be recognized by the cellular machinery of some bacteria and incorporated into the metabolism.[30-35] The selection of the tag has been made considering three basic features: small size, abiotic nature, and suitability for bioorthogonal reactivity. Then, an azide group has been chosen as tag. Hence, a set of azido sugars has been designed and synthesized considering not only previously incorporated described azido sugars but also structurally diverse ones (Figure 4): glucose (**1**-**3**) and glucosamine derivatives (**4**-**6**), taking into account the preferable consumption by bacteria of glucose versus other sugars;[36-38] galactose (**7**, **8**) or galactosamine analogs (**9**, **10**), due to their not preferable but effective incorporation;[39,40] and a mannosamine derivative (**11**), based on its incorporation when used as the only source of carbon.[41,42] In addition, these amino sugars are described to be carbon or nitrogen sources for some strains of bacteria.[43-46] Finally, a representative example of a sialic acid (**12**) has also been selected due to their reported incorporation by bacteria.[47] The tag has been introduced in positions 1, 2, or 6 of the sugars in an attempt to determine the possible influence of the position of the azide in the incorporation by bacteria. Taking into account the possible differences in incorporation for peracetylated sugars compared to their free hydroxyl groups analogues, both of them have been selected.

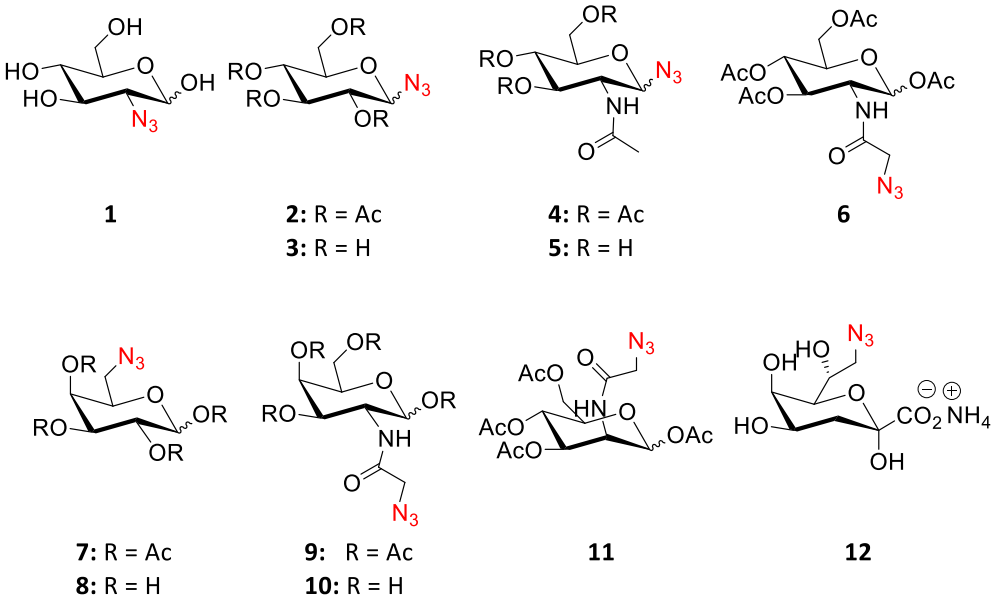

Figure 4. Azido sugars used as tagged precursors. The azide group used as tag is shown in red.

Azido sugars **2**-**8** and **11**, **12** were commercially available, whereas glucose derivative **1** and galactosamines **9** and **10** were synthesized. To obtain 2-azido-2-deoxy-D-glucopyranose (**1**), 2-glucosamine was converted into the corresponding azide using in situ prepared imidazole-1-sulfonyl azide hydrochloride as diazo-donor (Scheme 1). With respect to azido sugars **9** and **10**, their synthesis started by protection of 2-galactosamine with di-*tert*-butyl dicarbonate and further peracetylation. Its deprotection with trifluoroacetic acid (TFA), followed by reaction with chloroacetic anhydride in basic media, and nucleophilic substitution with sodium azide led to desired sugar **9**. Finally, elimination of the acetyl groups yielded the *N*-acylgalactosamine derivative **10** (Scheme 2).

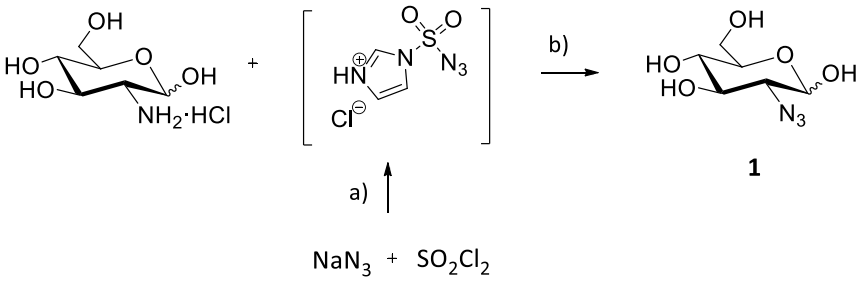

Scheme 1. Reagents and conditions: a) *i.* imidazol, ACN, rt, on; *ii.* 2 M HCl in Et_2O; b) K_2CO_3, $CuSO_4$, MeOH, rt, 6 h, 15%.

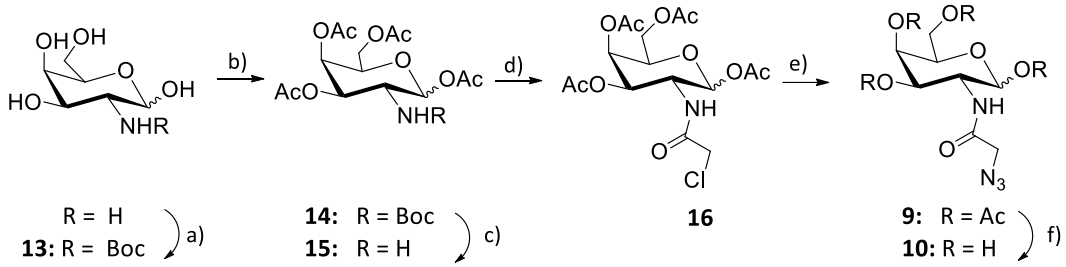

Scheme 2. Reagents and conditions: a) $(Boc)_2O$, $NaHCO_3$, dioxane/H_2O, rt, 48 h, 100%; b) Ac_2O, pyridine, DCM, rt, 18 h, 100%; c) TFA, DCM, rt, 3 h, 100%; d) chloroacetic anhydride, *N*-methyl-2-pyrrolidone, DCM, rt, 16 h, 80%; e) NaN_3, DMF, 60 °C, 3 h, 52%; f) NaOMe, MeOH, rt, 2 h, 100%.

2.2. Incorporation of tagged precursors in selected strains of bacteria

2.2.1. Screening by ^{1}H NMR

Once synthesized the tagged precursors, we needed to confirm whether bacteria from human microbiota can incorporate the selected sugars (**1**-**12**, Figure 4). For this purpose, the consumption of the tagged sugar was followed by ^{1}H NMR after 24 h of incubation with bacteria. Towards this end, the optimal concentration of the tagged sugar that could be detected in basal peptone yeast broth,[30] the culture medium used for growing the bacteria, was assesed. Since the complexity of the culture medium made difficult the determination of the signals of the azido sugars, we also analysed by ^{1}H NMR the culture medium, and then, by substraction of this spectra from the spectra of the azido sugars in medium, we were able to detect some signals coming from the analyzed sugars (see Figure 5 for a representative spectrum). The analysis of the ^{1}H NMR spectra showed that, in general, those sugars with free hydroxyl groups (**1**, **3**, **5**, and **8**) could be followed at 100 µM, whereas a concentration of 400 µM was required for the suitable detection of peracetylated sugars (**2**, **4**, **6**, **7**, **9**, and **11**), probably due to solubility issues. However, sugars **10** and **12** could not be detected under these conditions because even at the higher concentration tested, significant splitting of the signals between anomers was observed, fact that precluded a good observation of the signals in the ^{1}H NMR spectra. Therefore, sugars **10** and **12** were excluded from the NMR screening.

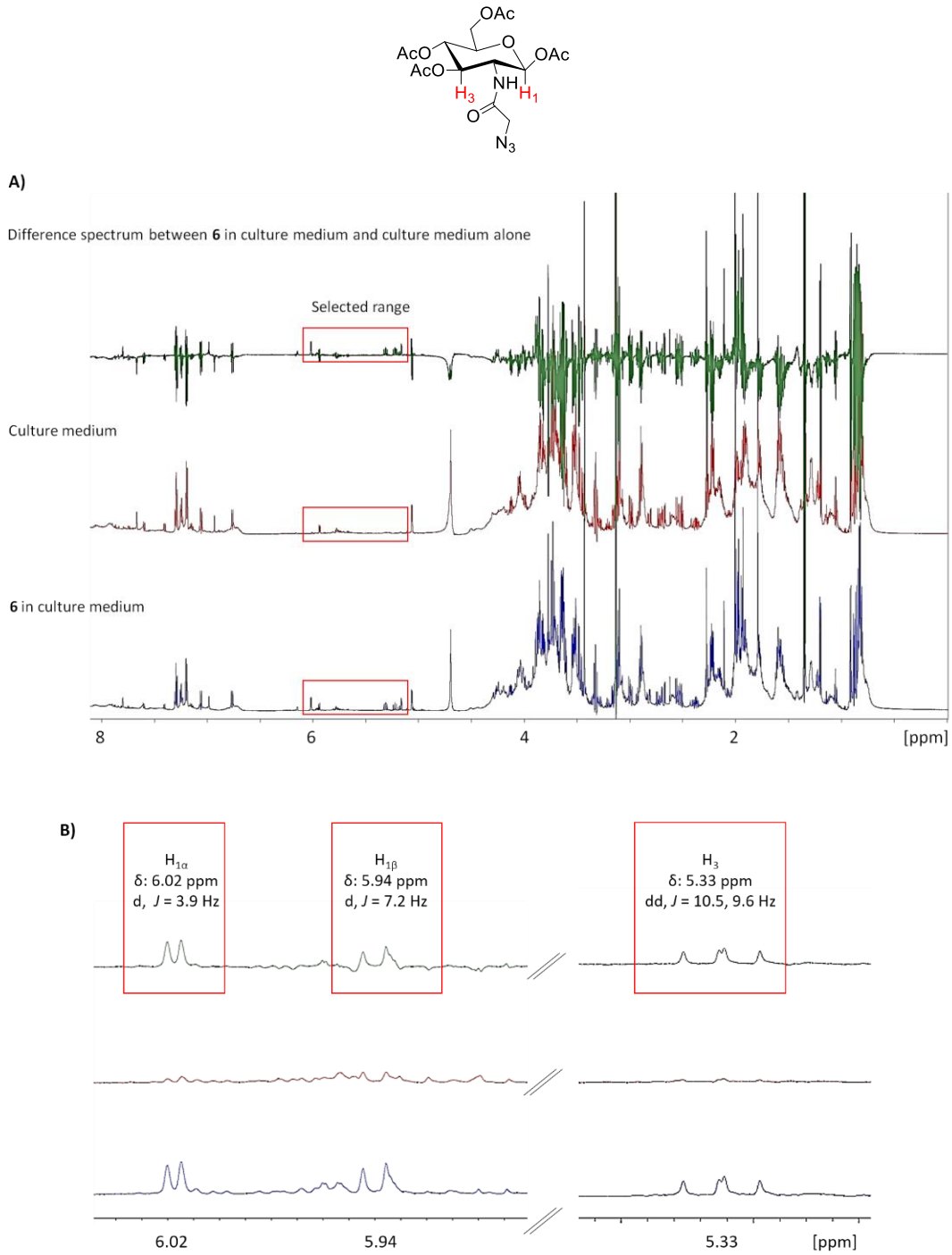

Figure 5. ^{1}H NMR spectra of azido sugar **6**. A) Full ^{1}H NMR spectrum of basal peptone yeast broth as culture medium is shown in red. Spectrum of culture medium containing 400 µM of sugar **6** is represented in blue and the difference spectrum between azido sugar **6** in culture medium and culture medium alone is indicated in green. B) Zoom of the selected range of the spectrum of panel A showing some representative signals of azido sugar **6**.

At this point, and once selected the tagged sugars and their concentration for screening (**1**, **3**, **5**, and **8** at 100 μM and **2**, **4**, **6**, **7**, **9**, and **11** at 400 μM) we needed to choose representative bacteria from the human microbiota, taking into account their high diversity and the possible differences in the incorporation process.

The most abundant bacteria found in the human body are part of four main phyla: *Firmicutes*, *Actinobacteria*, *Proteobacteria*, and *Bacteroidetes*.[48] Among them, different strains of each phyla have been described to have a role in the gut microbiota such as: i) *Bacteroides* or *Prevotella* (both belonging to phyla *Bacteroidetes*), with functions in polysaccharide decomposition, nutrients absortion, and maturation of endothelial cells,[49] ii) *Lactobacillus* (from phyla *Firmicutes*), which is in charge of the production of some short-chain fatty acids (acetic, propionic, or butyric)[49] and even in the production of neurotransmitters,[50] and iii) *E. coli* (belonging to phyla *Proteobacteria*), responsible for the production of some metabolites implicated in colorectal cancer[50] and in the decomposition of mucins. Furthermore, it has been even reported the substitution of bacteria from *Firmicutes* by *Bacteroidetes* in aging process.[51] These evidences together with previously described azido sugars incorporation,[30,31,33,35,52-54] led us to select *B. fragilis*, *B. thetaomicron*, *P. copri*, *L. rhamnosus*, and *E. coli* for our experiments.

Hence, in collaboration with Dr. Carles Úbeda (Centro Superior en Salud Pública, Valencia), selected bacteria were grown in the presence of each of the azido sugars at 37 °C in anaerobic conditions, mimicking the gastrointestinal tract. Then, aliquots from the culture media at time 0 and 24 h were taken and analyzed by ^{1}H NMR following the signals of the tagged sugars in order to determine the incorporation of the azido sugar. The obtained spectra showed that incorporation was strongly dependent on both the bacteria and the azido sugar (Table 1). Our results described for the first time the incorporation of glucose derivatives **1**-**4** in *E. coli*, azido glucose, galactose, and mannose **3**, **9**, and **11**, respectively, in *B. thetaomicron*, sugars **6**, **7**, and **9** in *P. copri*, azido galactose **8** in *L. rhamnosus,* and derivatives **6** and **11** in *B. fragilis*. The obtained results are also consistent with the previous reported incorporation results in the case of azido sugars **7**[31] and **9**[30,35] in *B. fragilis* and azido mannose **11** in *P. copri*.[30]

Table 1. Incorporation of azido sugars by selected strains of bacteria

Compound	*B. fragilis*	*B. thetaomicron*	*P. copri*	*L. rhamnosus*	*E. coli*
1					
2					
3					
4					
5					
6		ND[a]		ND[a]	ND[a]
7		ND[a]		ND[a]	ND[a]
8					
9					
11					

Green: incorporation. Red: no incorporation. [a] ND: not determined.

As representative examples, the spectra obtained for azido sugars **6**, **9**, and **11** in two different strains are represented in Figures 6 and 7. When using Ac_4GlcNAz (**6**) as azido sugar we could observe that the signals that were present at time 0 at 5.33, 5.94, and 6.02 ppm corresponding to H_3, $H_{1\beta}$, and $H_{1\alpha}$, respectively (Figure 6A), disappeared after incubation for 24 h with both *B. fragilis* (Figure 6B) and *P. copri* (Figure 6C), which indicated that azido sugar **6** was incorporated by both bacteria. In the case of Ac_4GalNAz (**9**), the incorporation took place in *B. thetaomicron* (Figure 7A) as shown by the disappearance of the signals of H_3 and H_4 at 5.37 and 5.43 ppm, respectively, in the spectrum registered after 24 h of incubation, but not in *L. rhamnosus* (Figure 7B) because these signals were still present after 24 h. When analyzing the spectra corresponding to Ac_4MnNAz (**11**), its consumption was observed in *B. fragilis* (Figure 7C), due to the disappearance, after 24 h, of the signal at 5.25 ppm corresponding to H_3, whereas this signal persists when **11** was incubated with *E. coli* (Figure 7D), indicating that azido mannosamine derivative was not incorporated in the cellular machinery.

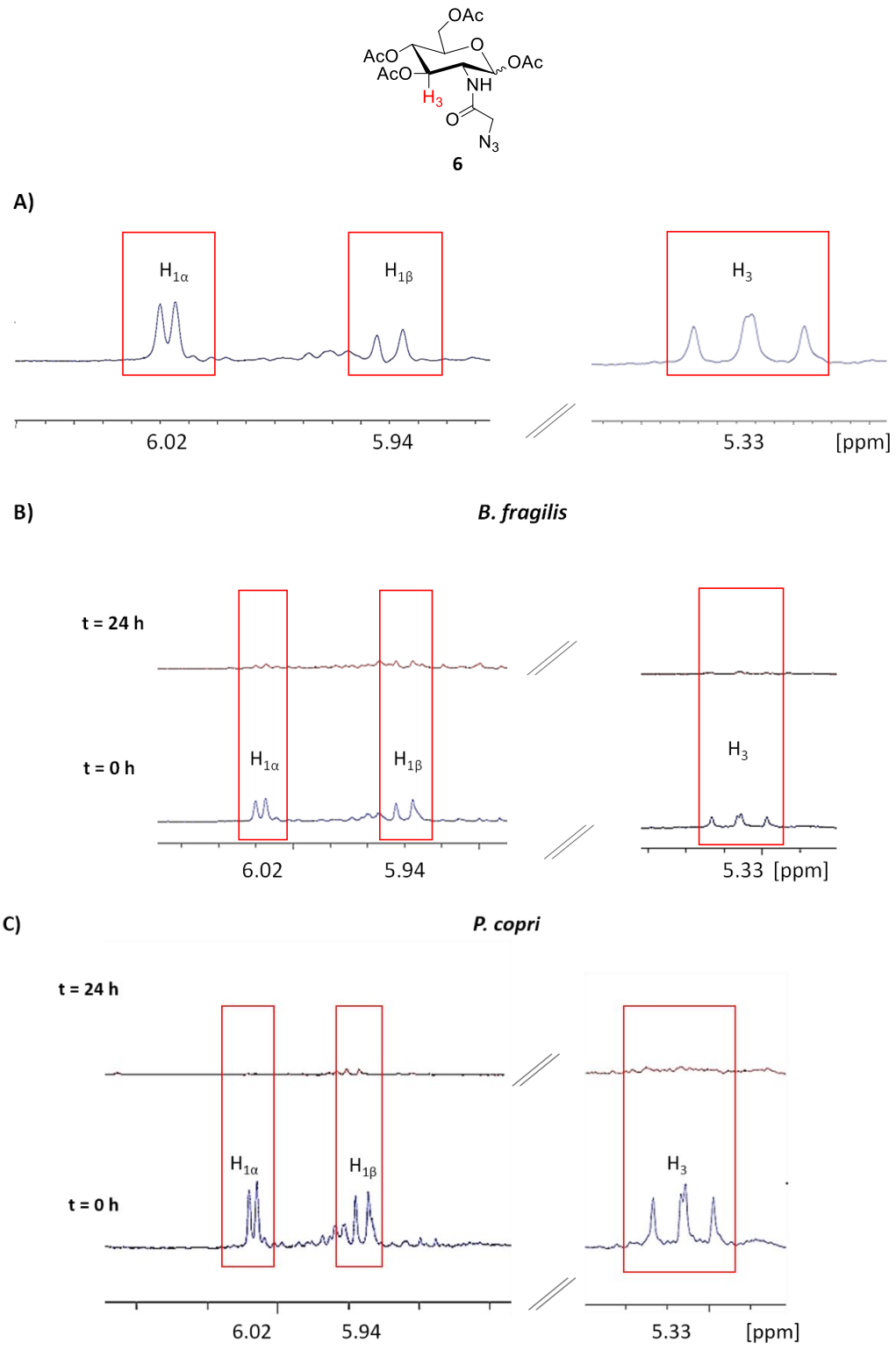

Figure 6. ^{1}H NMR spectrum of azido sugar **6** in basal peptone yeast broth (A). Overlapped spectra corresponding to times 0 and 24 h after incubation with *B. fragilis* (B), and *P. copri* (C).

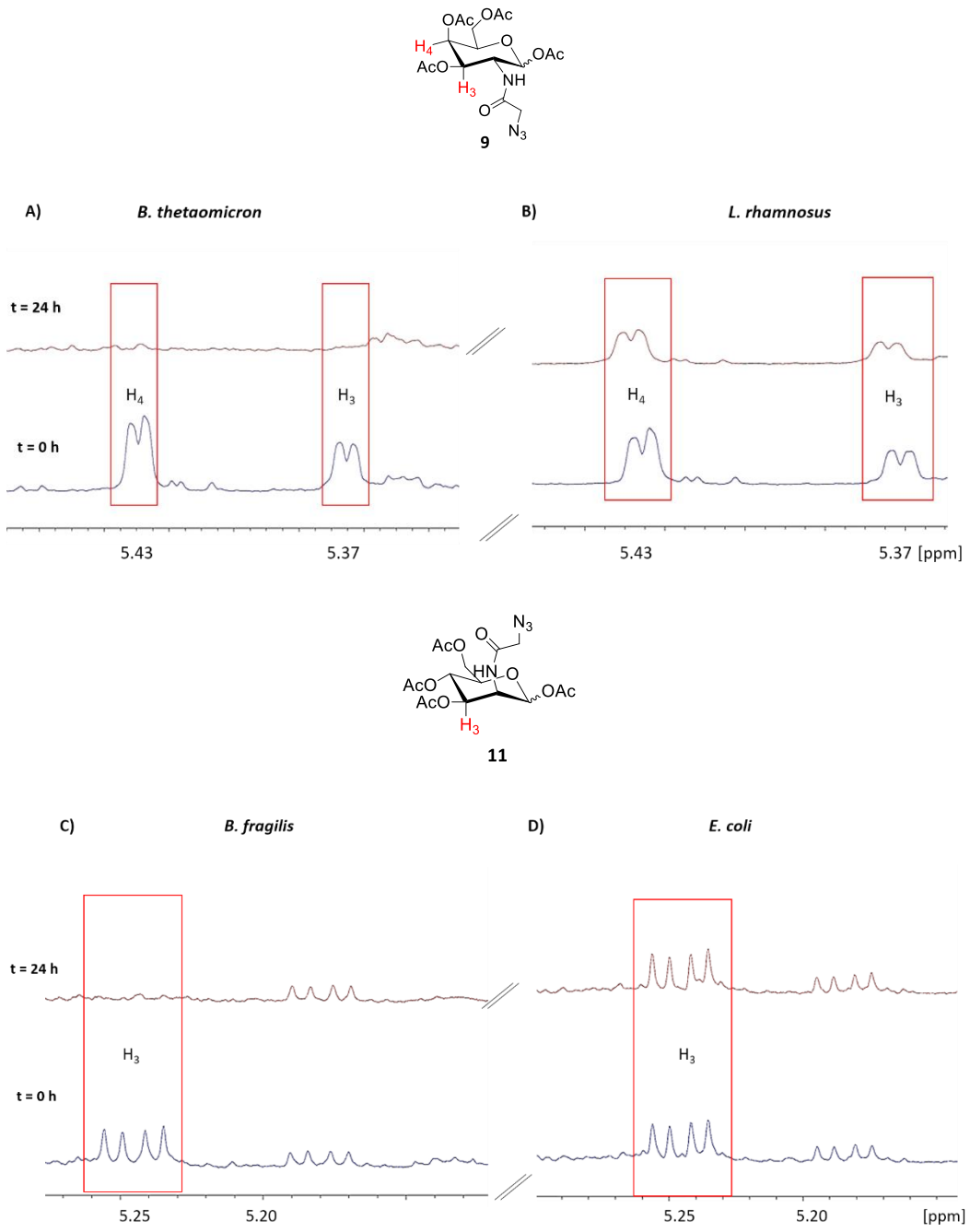

Figure 7. Representative ^{1}H NMR spectra corresponding to times 0 and 24 h for different strains and azido sugars. Ac_4GalNAz (**9**) is incorporated in *B. thetaomicron* (A), whereas incorporation does not take place in *L. rhamnosus* (B). Ac_4ManNAz (**11**) is incorporated by *B. fragilis* (C) but not in *E. coli* (D).

2.2.2. Cytometry and confocal experiments

To further confirm the results obtained from the NMR screening, the incorporation of the tagged sugars was assessed by flow cytometry and confocal experiments. Taking into account that previously described results indicate that azido sugars are at least partially incorporated in the glycoproteins of the glycocalix of bacteria, this incorporation can be detected by flow cytometry after click chemistry reaction with a fluorophore bearing a terminal alkyne. For that purpose, we have carried out these experiments using the copper free version of the azide-alkyne click chemistry reaction, trying to avoid the cytotoxicity of Cu (I) catalyst that could have a negative effect in bacteria. Hence, we selected a fluorophore with a dibenzocyclooctyne group, so that the reaction can proceed without any other catalyst with high efficiency. Thus, dibenzocyclooctyne bodipy fluorophore DBCO-FL-PEG_4-BODIPY (λ_{exc}= 503 nm, λ_{em}= 512 nm) was selected.[32] The bacteria were incubated for 24 h in basal peptone yeast broth at 37 °C, and the supernatants removed from the pellet after centrifugation. The bacterial pellet was treated with DBCO-FL-PEG_4-BODIPY, incubated with the cell-permeant dye SYTO62 (λ_{exc}= 649 nm, λ_{em}= 680 nm) and analyzed by fluorescence activated cell sorting (FACS) and confocal microscopy (Figure 8).

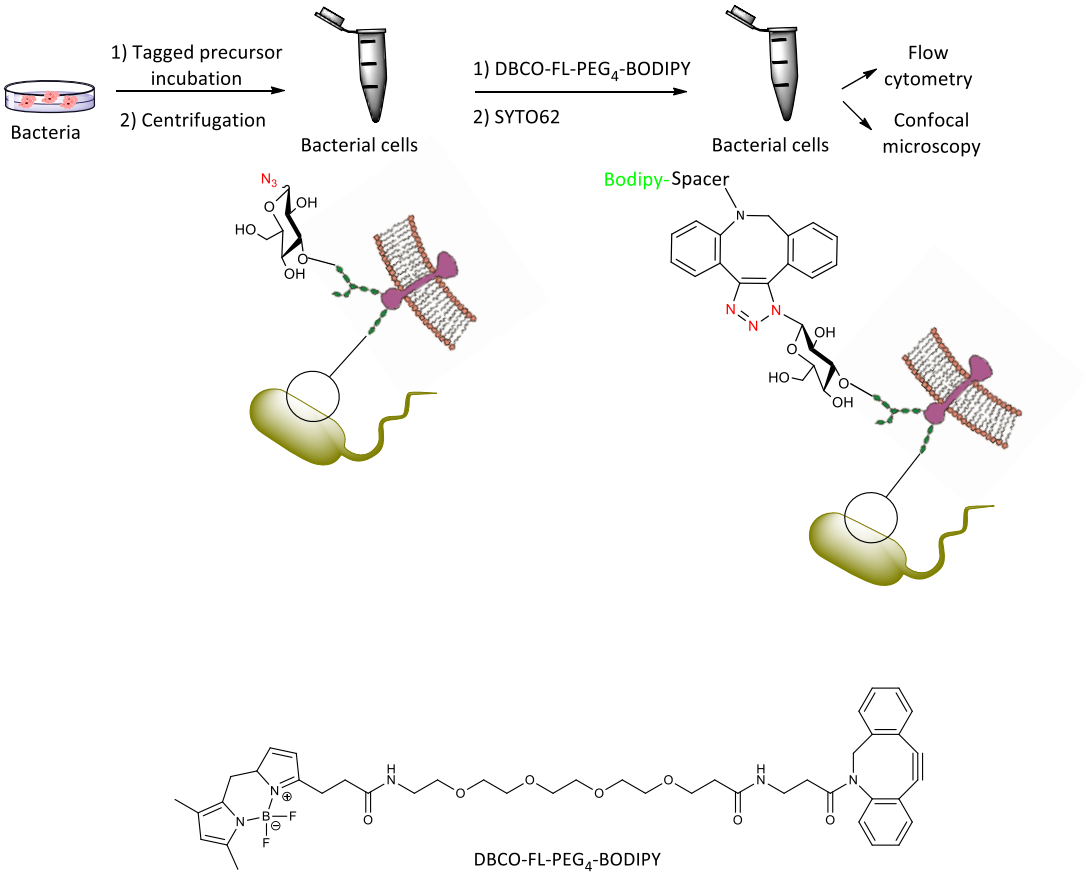

Figure 8. Study of the incorporation of azido sugars by bacteria using flow cytometry and confocal microscopy.

Representative experiments are shown in Figures **9**-**12**. In the dot plots (FL 4-H: SYTO62, FL 1-H: DBCO-FL-PEG$_4$-BODIPY) we observe that incubation of *E. coli* or *B. fragilis* in the presence of azido sugars **3** or **9**, respectively, provided a doubly positive population for both SYTO62 and bodipy (Figures 9A and 9C, upper right area), thus confirming the incorporation of these azido sugars. However, in absence of any azido sugar (Figures 9B and 9D), only SYTO62 positive cells (upper left area) were detected. The obtained results confirmed the incorporation of selected azido sugars by specific strains of bacteria.

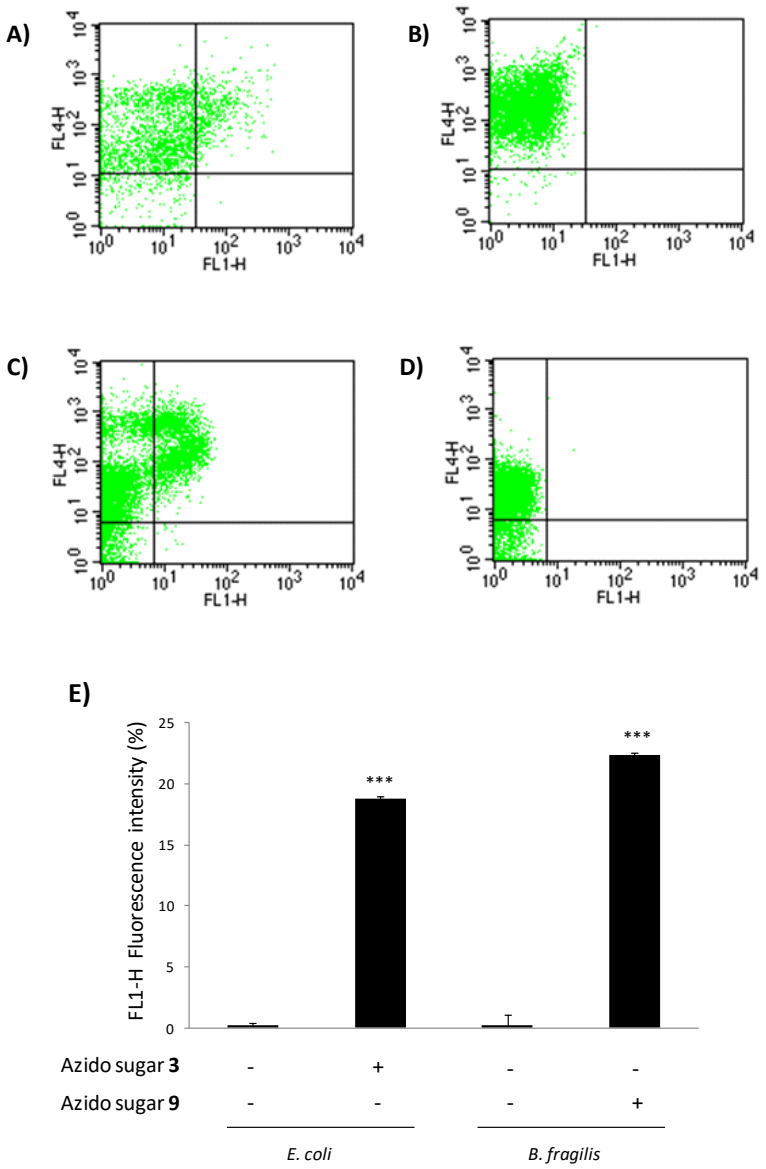

Figure 9. Incorporation of azido sugars by bacteria from the human microbiota. *E. coli* incorporates azido sugar **3** as indicated in the doubly positive population (upper right region) (A), which is not observed in the absence of azido sugar **3** (B). *B. fragilis* incorporates azido sugar **9** as indicated in the doubly positive population (upper right region) (C), which is not observed in the absence of azido sugar **9** (D). The bar graph (E) represents the percentage of fluorescence intensity of the bodipy positive cells (FL1-H) with respect to the total SYTO62 positive population after incubation of the cells in the absence or in the presence of the corresponding azido sugar. Fluorescence intensity corresponds to SYTO62 (FL 4-H) or to DBCO-FL-PEG_4-BODIPY (FL 1-H). FACS experiments were carried out in a 2FACScalibur citometer and shown data correspond to the mean ± standard error mean (sem) of two independent experiments. ***, $p < 0.0005$ (Student´s t test).

Confocal analysis also confirmed the incorporation of these azido sugars. When bacteria (*E. coli* or *B. fragilis*) were grown in the presence of azido sugars **3** or **9**, the green fluorescence appeared (Figure 10A and 10C, respectively), whereas when incubated in absence of azido sugar, only red staining corresponding to the bacterial marker SYTO62 was observed (Figure 10B and 10D).

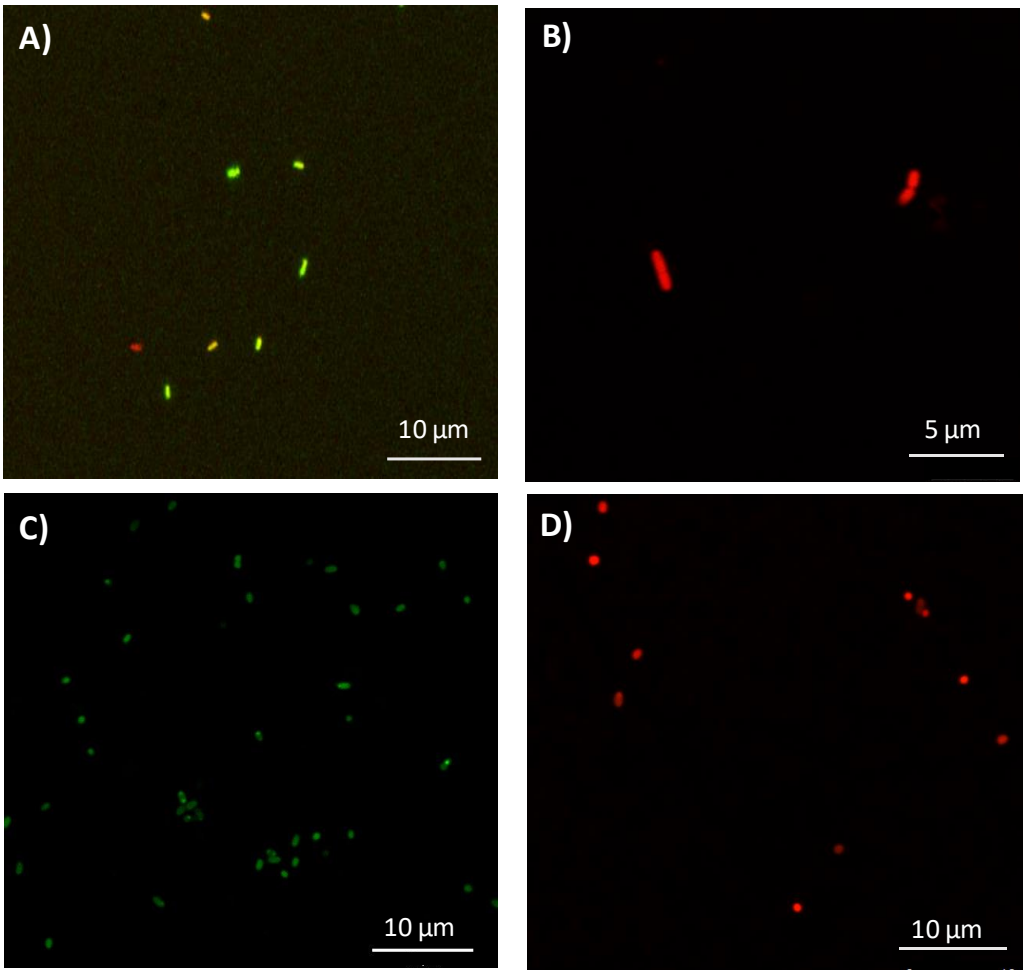

Figure 10. Azido sugars **3** and **9** are effectively incorporated by *E. coli* and *B. fragilis*, respectively. *E. coli* incorporates azido sugar **3** as pointed out by the presence of green fluorescence (A) which disappears in absence of the azido sugar **3** (B). *B. fragilis* is able to incorporate azido sugar **9** as shown by the green fluorescence (C), which is not observed in the absence of sugar **9** (D). Images were obtained in a Leica confocal microscope and are representative from two independent experiments. Bacterial cells are visualized with SYTO62 (red).

Once checked the incorporation of azido sugars in specific strains of bacteria from human microbiota, we wanted to extend the methodology in a more complex setting. Thus, human microbiota bacteria coming from a healthy individual was incubated in the absence or presence of azido sugar **3** under the conditions previously described and flow cytometry and confocal analysis were performed. The incorporation of this sugar by the human microbiota was confirmed as shown in Figures 11 and 12.

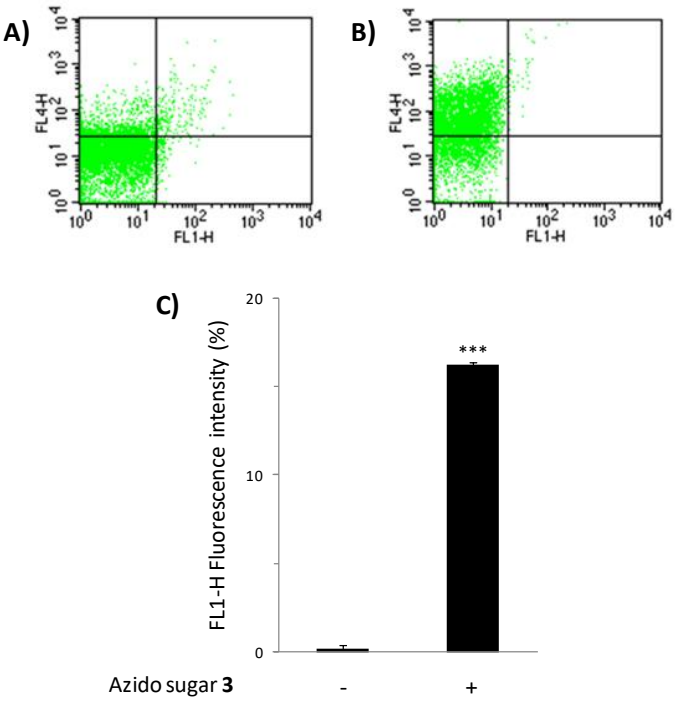

Figure 11. Incorporation of azido sugar **3** by human microbiota bacteria. Azido sugar is incorporated as indicated by the doubly positive population (upper right region) (A), which is not observed in the absence of azido sugar **3** (B). The bar graph (C) represents the percentage of fluorescence intensity of the bodipy positive cells (FL1-H) with respect to the total SYTO62 positive population after incubation of the cells in the absence or in the presence of azido sugar **3**. Fluorescence intensity correspond to SYTO62 (FL 4-H) or to DBCO-FL-PEG$_4$-BODIPY (FL 1-H). FACS experiments were carried out in a 2FACScalibur citometer and shown data correspond to the mean ± sem of two independent experiments. ***, $p < 0.0005$ (Student´s t test).

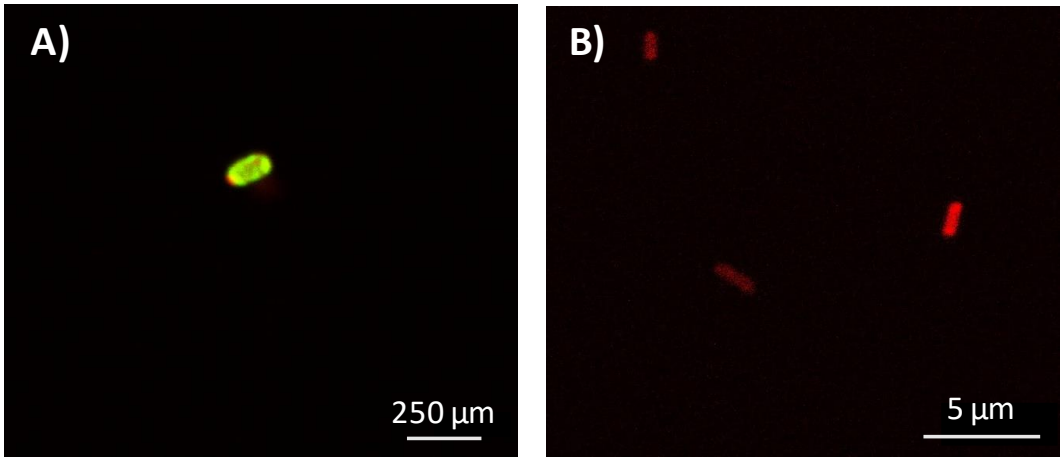

Figure 12. Azido sugar **3** is effectively incorporated by human microbiota bacteria. The green fluorescence observed in the presence of the azido sugar confirms the incorporation (A), whereas this signal disappears in the absence of azido sugar **3** (B). Images were obtained in a Leica confocal microscope and are representative from two independent experiments. Bacterial cells are visualized with SYTO62 (red).

2.3. Isolation of the different metabolomes

Due to the chemical diversity of metabolites that can be isolated from bacteria strains (polar, non-polar, secreted or non-secreted by bacteria to the medium), we designed a separation and extraction process of these metabolomes in order to obtain fractions enriched in different types of metabolites (Figure 13). First, the pellet of bacteria was separated from the culture medium by centrifugation, obtaining the first metabolome fraction (A) that contained the metabolites secreted by the bacteria to the culture medium. Then, the pellet of bacteria was extracted with a mixture of methanol/chloroform/water (2:2:1) to separate the polar and non-polar metabolites. After evaporation of the solvents of the organic phase, we obtained a second metabolome fraction (B) formed mainly by non-polar metabolites. The aqueous phase of the extraction was lyophilized to afford the last metabolome fraction (C) that contained the more polar metabolites produced by the bacteria.

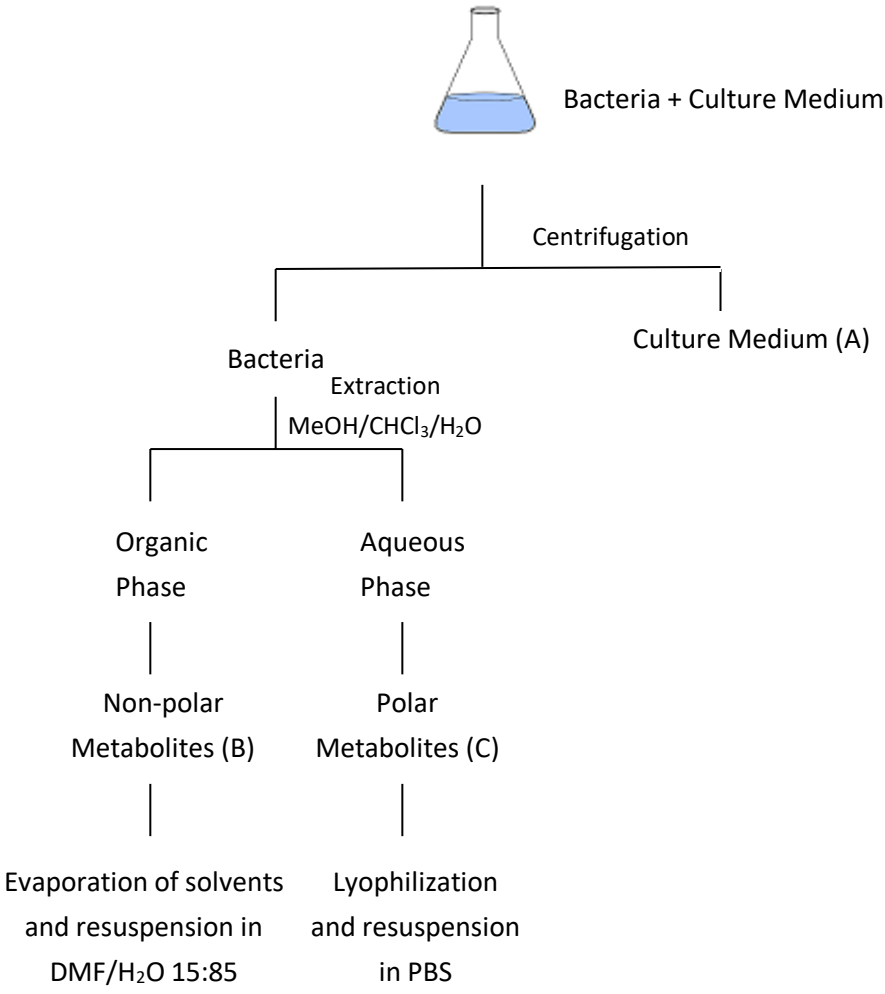

Figure 13. Schematic process of the isolation of the three different metabolomes.

2.4. Bioorthogonal reaction with the capture reagent

The next step consisted on the synthesis of the capture reagents that would allow us to capture the tagged metabolites by a bioorthogonal reaction. Taking into account the selection of an azide group as the tag, we decided to apply the copper(I)-catalyzed azido-alkyne cycloaddition[55] for the capture step. This bioorthogonal reaction can be carried out in water and in mixtures of water and miscible organic solvents and requires the presence of a source of copper (I) as catalyst that is formed in situ from Cu (II), due to the instability of Cu (I) in aqueous solutions. Hence, $CuSO_4 \cdot 5H_2O$ is used as a source of Cu (II) in the presence of a reducing agent, such as sodium ascorbate or tris(2-carboxyethyl)phosphine (TCEP). Furthermore, a stabilizing ligand such as

tris(benzyltriazolylmethyl)amine (TBTA) is used for the stabilization of the in situ Cu (I) formed. Thus, we have designed capture reagents with a terminal akyne in order to carry out this cycloaddition. For isolation of the captured metabolites we have considered either a biotin group or a resin bead, which can be pulled down using (strept)avidin beads or directly by centrifugation, respectively. Both moieties were separated by an adequate spacer that incorporates a disulfide bond as a cleavable sequence so that the metabolite can be softly released from the capture reagent. Hence, disulfide capture reagents **17** and **18** were designed (Figure 14).

A)

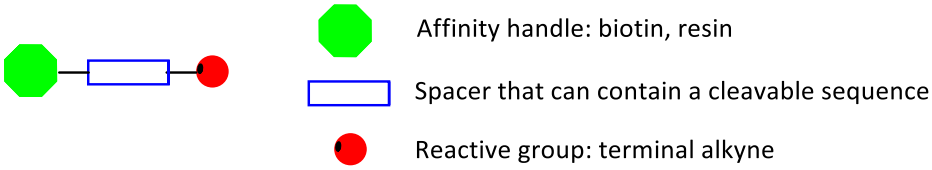

B)

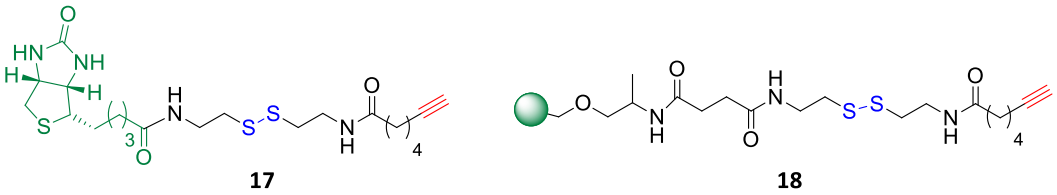

Figure 14. A) General structure of capture reagents containing an affinity handle (in green) and a reactive group (in red) separated by a cleavable spacer (in blue). B) Designed capture reagents.

The synthesis of capture reagents **17** and **18** was carried out by condensation of amine **19** with biotin or resin-supported carboxylic acid **20**, respectively (Scheme 3). The formation of **18** was checked by cleaving the resin in the presence of an aqueous solution of TFA and triisopropylsilane (TIS) and confirming the release of the corresponding free carboxylic acid **21** by high performance liquid chromatography coupled to mass spectrometry (HPLC-MS).

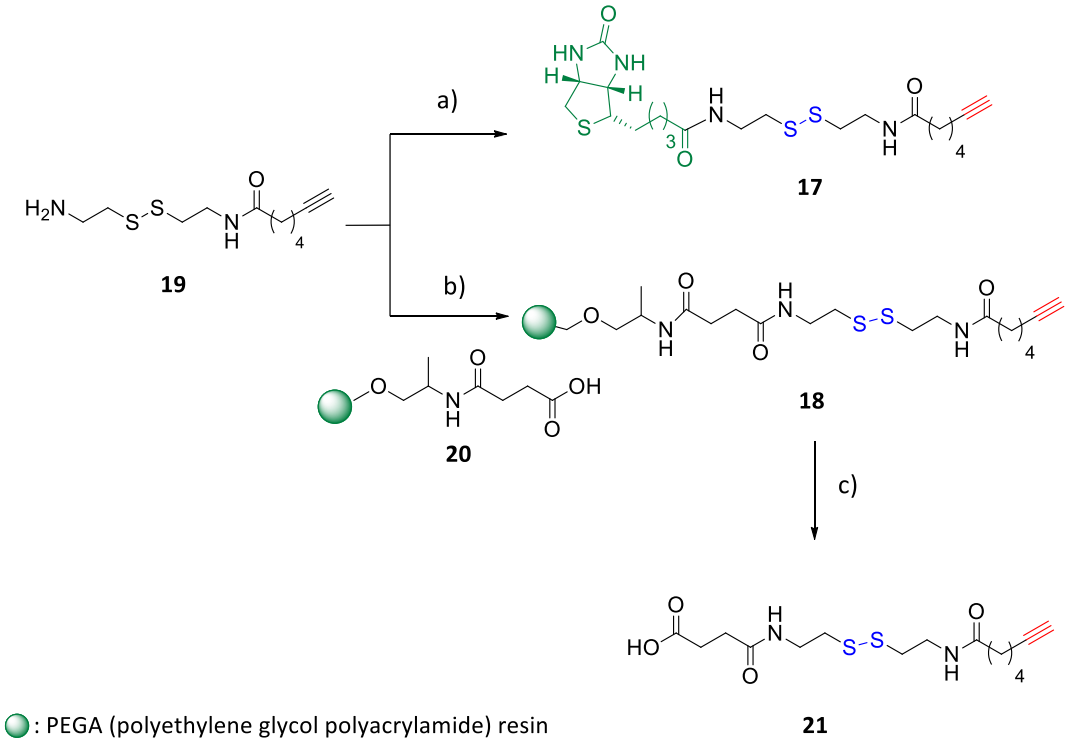

Scheme 3. Reagents and conditions: a) biotin, EDC·HCl, HOBt, DIPEA, DMF, DCM, rt, on, 31%; b) PEGA resin, PyBOP, Et_3N, DMF, rt; c) TFA/TIS/H_2O (95:2.5:2.5), rt, 60 min.

Amine **19** was obtained from commercially available cystamine dihydrochloride (Scheme 4). Its monoprotection with di-*tert*-butyl dicarbonate and further condensation with 6-heptynoic acid using 1-ethyl-3-(3-dimethylaminopropyl)carbodiimide (EDC) and hydroxybenzotriazole (HOBt) as coupling reagents led to amide **23**. Later Boc deprotection with TFA finally provided desired amine **19**. Carboxylic acid **20** was synthesized from commercially available PEGA resin and succinic anhydride (Scheme 4).

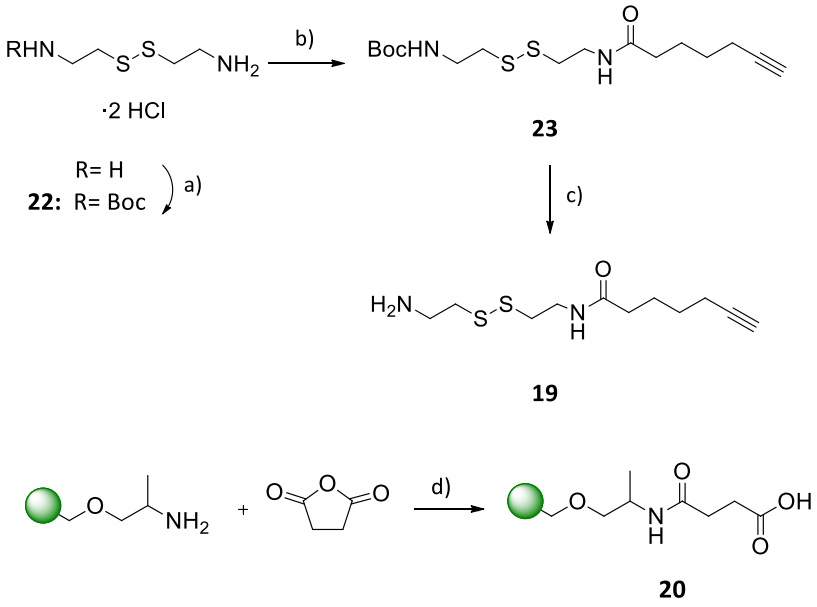

Scheme 4. Reagents and conditions: a) $(Boc)_2O$, Et_3N, MeOH, rt, 1 h, 49%; b) 6-heptynoic acid, EDC·HCl, HOBt, DCM, rt, on, 56%; c) TFA, DCM, rt, 1 h, 67%; d) DMAP, pyridine, DMF, rt, on, 100%.

The next step consisted on setting up the conditions for the click chemistry reaction between the azido sugars and the capture reagents **17**, **18** that would allow us to capture the metabolites produced by the bacteria. For this purpose, we selected 2-azidoglucose **1** as the tagged sugar for reaction with the two capture reagents. Considering that, after incubation of the corresponding tagged precursor with the bacteria, we would isolate different metabolomic fractions (A, B, and C in Figure 13) that could contain tagged metabolites, we need to carry out the click chemistry reaction in three different media (culture medium for fraction A, DMF/H_2O 15:85 for fraction B, and PBS for fraction C). Hence, the bioorthogonal reaction was optimized in the culture media (to capture the potential metabolites present in fraction A), in a mixture of solvents (DMF/H_2O, 15:85) in which the non-polar metabolites present in fraction B will be captured, and in an aqueous medium (phosphate buffered saline (PBS), pH=7.4) to capture the polar metabolites present in fraction C.

With respect to the conditions for the click chemistry reaction, we had to consider several aspects. As reducing agents, based on previous work described in the literature, we selected sodium ascorbate for those cycloaddition reactions performed in media that contain organic solvents[56,57] (fraction B, DMF/H_2O, 15:85) and TCEP for those reactions

carried out in aqueous solvents[58,59] (fractions A and C, culture medium and PBS, respectively). The equivalents of $CuSO_4 \cdot 5H_2O$ and TBTA, as well as the relative equivalents of azido sugar and alkyne (1:10), were chosen based on previously reported conditions.[30,60]

Hence, the click chemistry reaction was carried out in the three different reaction solvents during different periods of time to determine the conversion of the reaction, which was followed by the disappearance of the azide by HPLC-MS. The obtained results showed that in culture medium and with TCEP, the conversion of the reaction was higher than 90% after 3 h and this conversion was even higher in DMF/H_2O, 15:85 for the same time (>99%). However, the reaction was slower in PBS with TCEP, and 16 h were required to obtain a conversion of 95% (Table 2).

Table 2. Optimization of the click chemistry reaction with capture reagent **17**.

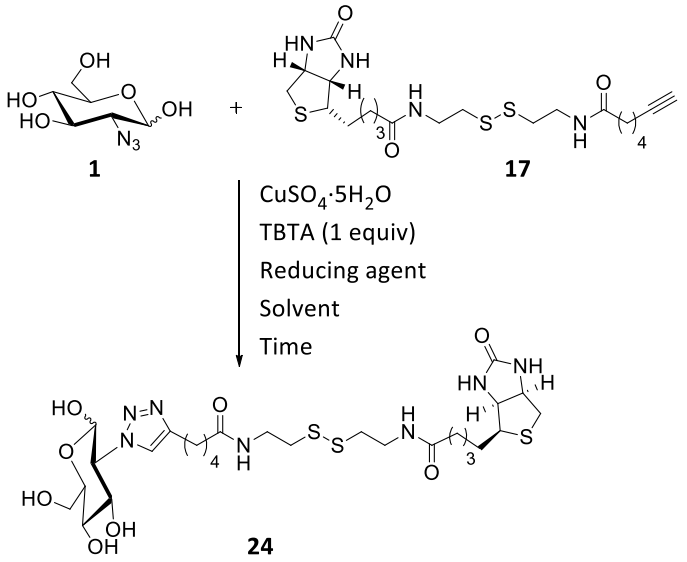

Reaction solvent	Capture reagent (equiv)	$CuSO_4 \cdot 5H_2O$ (equiv)	Reducing Agent (equiv)	Time (h)	Conversion[a] (%)
Culture medium	10	20	TCEP (20)	3 16	>90 *b*
DMF/H_2O 15:85	10	1.5	Sodium Ascorbate (1.5)	1 3 16	>99 >99 >99
PBS	10	20	TCEP (20)	1 3 16	70 70 95

[a] Determined by HPLC-MS; [b] Decomposition.

Once optimized the reaction conditions of azido sugar **1** with capture reagent **17**, we tested whether compound **18** was more efficacious than **17**. For that purpose, capture reagent **18** was reacted under the conditions previously optimized for different periods of time (Table 3). The results showed that the reactions in the culture medium or PBS maintained the high conversions obtained with capture reagent **17** (>90% after 3 h, and 95% after 16 h, respectively), whereas in DMF/H_2O, 15:85 the conversion decreased from >99% to 80% after 3 h, observing even the decomposition of the formed triazol with higher reaction times (Table 3). Hence, capture reagent **17** was selected for further experiments.

Table 3. Optimization of the click chemistry reaction using capture reagent **18**.

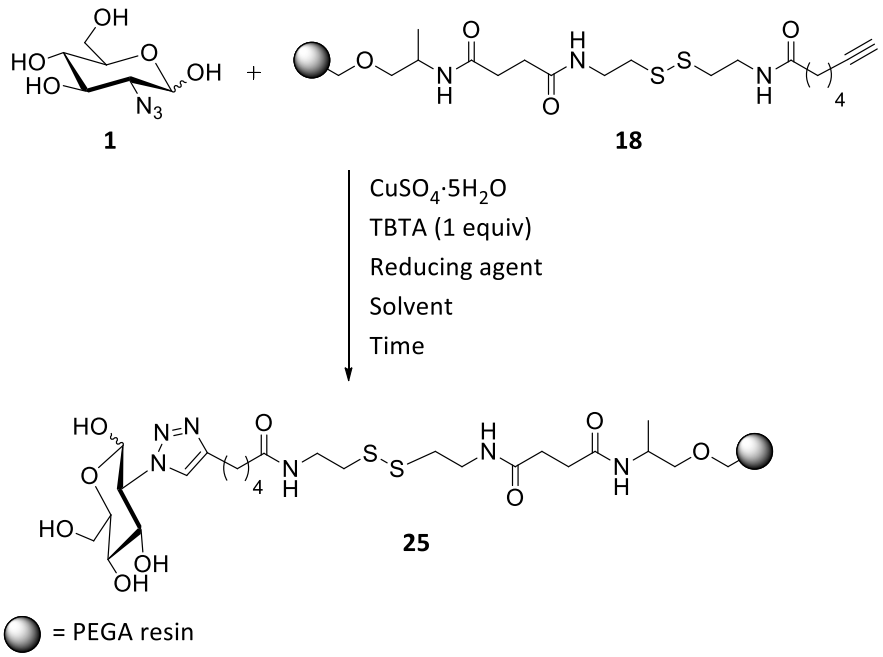

Reaction solvent	Time (h)	Conversion[a] (%)
Culture medium	3	>90
	16	*b*
DMF/H_2O 15:85	3	80
	6	80
	8	65
	16	26
PBS	1	70
	3	70
	16	95

[a] Determined by HPLC-MS; [b] Decomposition.

2.5. Isolation of the tagged metabolites

Once optimized the bioorthogonal reaction that will be carried out to capture the tagged metabolites, we performed the optimization of the isolation process of captured metabolites. The conditions for the isolation with streptavidin beads and the reduction of the disulfide bond were optimized using the resulting biotinyltriazol **24** previously obtained by the click chemistry reaction of azido sugar **1** and alkyne **17**. With respect to the isolation, we tested a variety of volumes of the aqueous suspension of commercially available streptavidin beads (100-300 µL). Hence, the resulting samples after click chemistry reaction were incubated with different volumes of streptavidin beads for 90 min, centrifuged and the supernatants analyzed by HPLC-MS quantifying the disappearance of biotinyltriazol **24**. The obtained results indicated that incubation with 250 µL of beads was enough for the complete isolation of the biotinyl compound and its disappearance of the solution. Finally, we set up the conditions for the reduction of the disulfide bond of the triazol **24** by incubation with DTT confirming the formation of the resulting thiol **26** by HPLC-MS (Scheme 5).

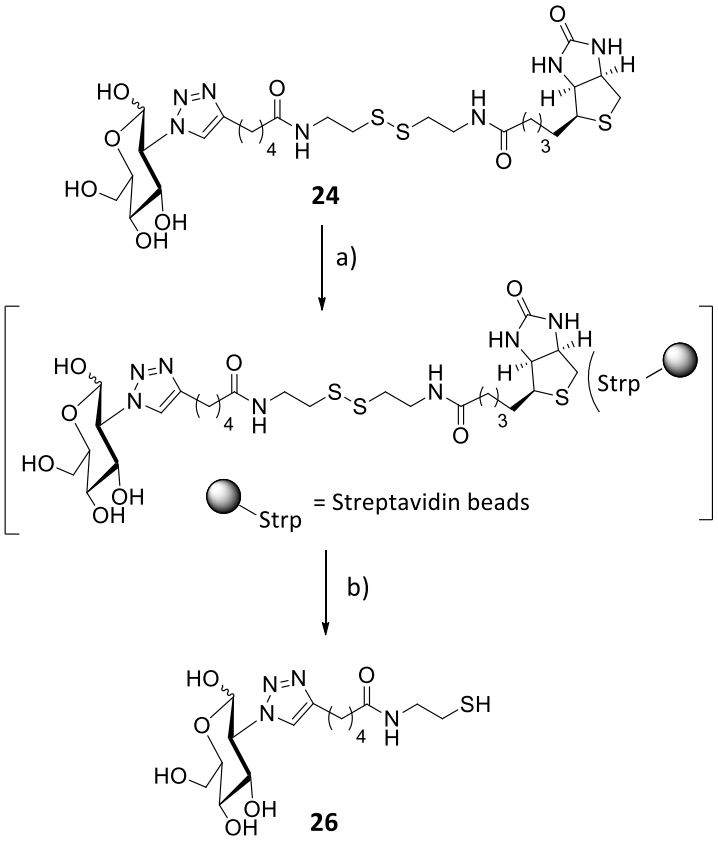

Scheme 5. Reagents and conditions: a) Streptavidin beads, rt, 90 min; b) DTT, MeOH/H_2O (1:1), rt, 60 min.

2.6. NMR and MS-based deconvolution and identification of metabolites

The final step consisted on the identification of the isolated tagged metabolites. For that purpose, we carried out the complete methodology in higher scale selecting one pair of azido sugar and strain where the incorporation took place. Hence, *E. coli* was grown in basal peptone yeast broth medium in the presence of the azido sugar **3** and after centrifugation and extraction processes, three metabolome fractions (A, B, and C, see Figure 13) were obtained. Metabolites were captured in the three different metabolome fractions using the optimized click chemistry conditions detailed in 2.4., followed by isolation with streptavidin beads, metabolite release after treatment with DTT (see 2.5.), and analysis by MS. In parallel, the same strategy was carried out growing *E. coli* without the azido sugar to discard unspecific results. The experiments aimed at the identification of the captured metabolites have been carried out during a short stay in the laboratory of Dr. Jean-Charles Portais from the Platform of Metabolomics and Fluxomics (Metatoul) in Toulouse, France, a centre with expertise in metabolomics.

To establish which peaks of the mass spectra come from the captured metabolites we checked whether they could be identified on the basis of the common fragment ion A (Figure 15).

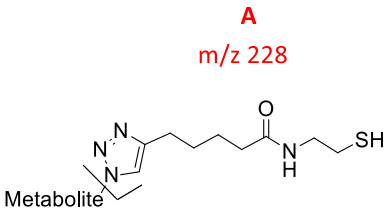

Figure 15. General structure for captured metabolites coming from azido sugars. The common fragment ion A is shown in red.

To confirm the generality of this fragmentation in this type of structures, the click chemistry reaction between azides **1**-**12** and biotinylated alkyne **17** was carried out. After isolation of the reaction products with streptavidin beads and release with DTT, MS analysis confirmed the presence of the triazol containing fragment ion $[A + H]^+$ (m/z 229) as shown by the spectra obtained for sugars **3** and **6** as representative of free and peracetylated sugars, respectively (Figure 16).

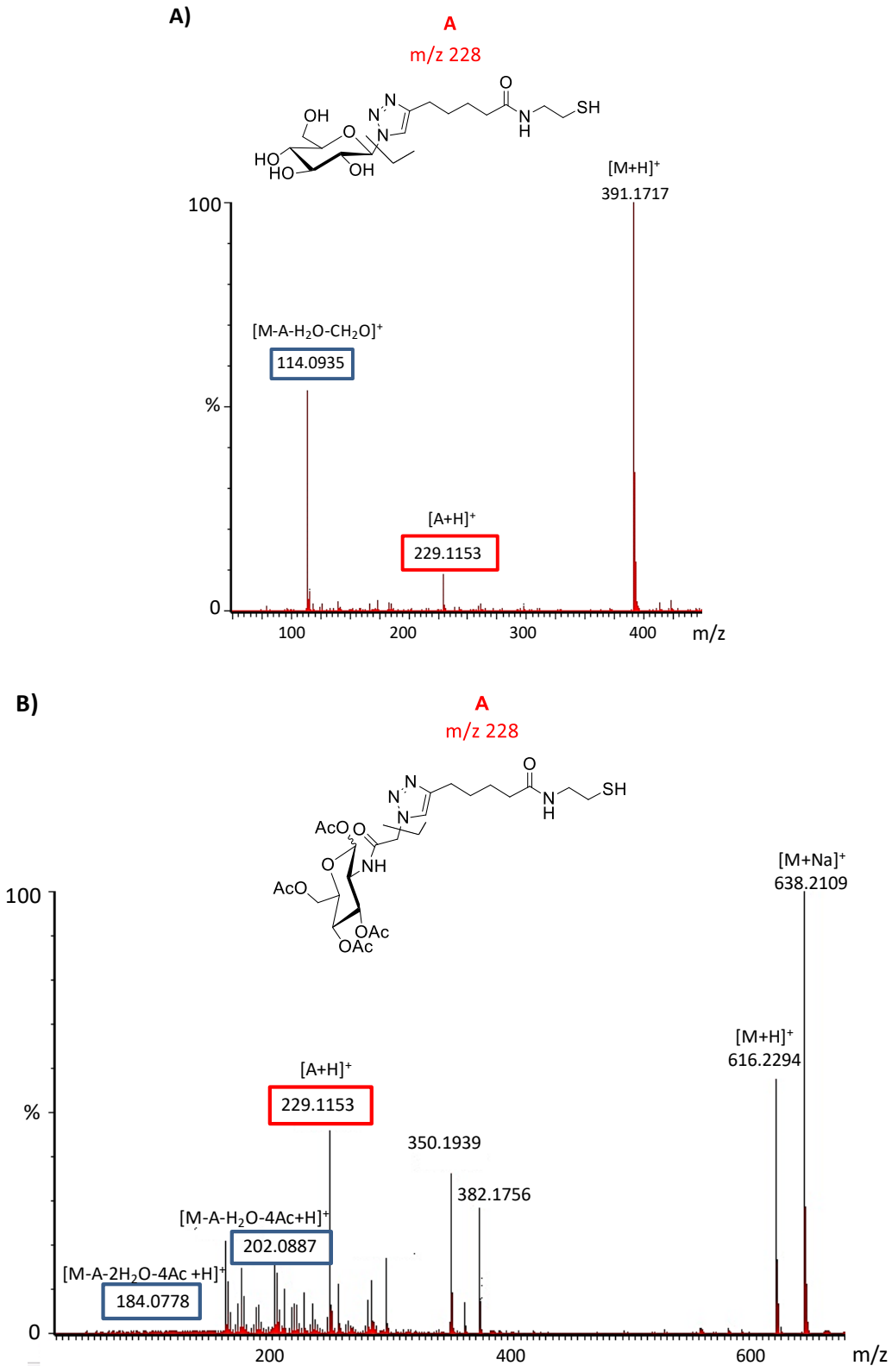

Figure 16. Mass spectra corresponding to captured azido sugars **3** (A) and **6** (B).

Then, we performed the MS/MS analysis of metabolome fractions A-C coming from the incubation of *E. coli* with azido sugar **3**, identifying those peaks that generate in their fragmentation the characteristic m/z 229 peak. For these analyses, we have used a tandem MS technique named MS^E. In MS^E, the spectometer firstly carries out a MS analysis where all the ions are transmitted from the ion source through the collision cell to the mass analyzer using low collision energy so that a minimal fragmentation occurs. Hence, a precursor ion spectrum is registered in order to identify the parental ions. Then, all the ions are transmitted from the ion source through the collision cell to the mass analyzer using higher collision energy values in order to generate the maximum information from fragment ions, providing a fragment ion spectrum. In our particular case, as we have previously checked that this type of structures fragment giving the common ion m/z 229 (Figures 15 and 16), we searched for those peaks that generate this characteristic ion in their fragmentation. As representative examples, analyses coming from metabolome fraction B of *E. coli* grown in the presence or absence of azido sugar **3** are shown in Figure 17. These chromatograms represent the total ion current (TIC) when registering the precursor and fragment ion spectra (Figure 17). When we search for those peaks containing m/z 229, we can observe the presence of two peaks with retention times of 7.77 and 9.23 that could come from captured metabolites (Figure 17A, upper pannel). When comparing with the negative control (Figure 17B, upper pannel), we discarded the peak at 9.23 min due its inespecific nature. Then, after analyzing the mass spectra from the peak at 7.77 min (Figure 18), we determined m/z 391.1717 as the molecular ion due to its high intensity in the parent ion spectrum (Figure 18A) and its almost complete disappearance in the fragment ion spectrum (Figure 18B). Analysis of these spectra and a mass of m/z 391.17 suggested the possibility of the capture of the azido sugar **3** without any transformation. This assignment was further confirmed by MS^E analysis of the product of the click chemistry reaction between compounds **3** and **17** as detailed in Figure 19. The resulting spectra (Figures 20 and 21) closely match with the ones obtained previously (Figure 18), result that suggests that the azido sugar **3** has been incorporated in *E. coli* but not metabolized, at least in an appreciable extent.

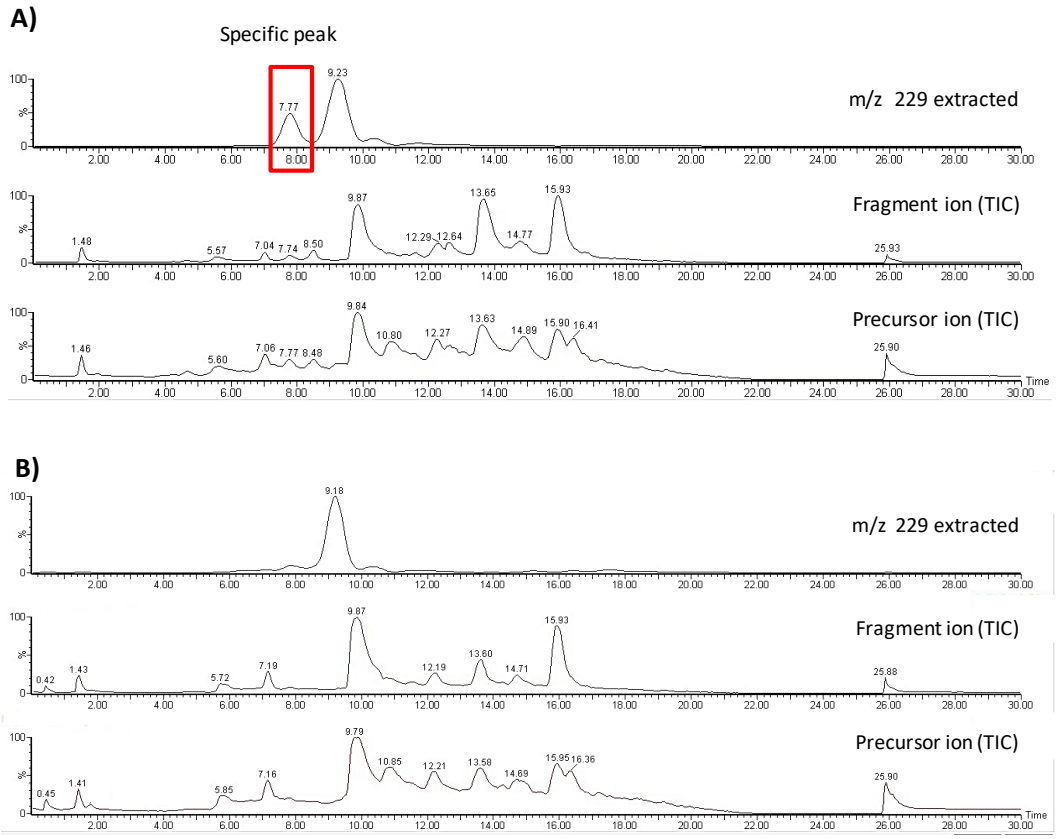

Figure 17. Chromatograms corresponding to the metabolome fraction B coming from the incubation of *E. coli* with azido sugar **3** (A) and in absence of azido sugar as negative control (B).

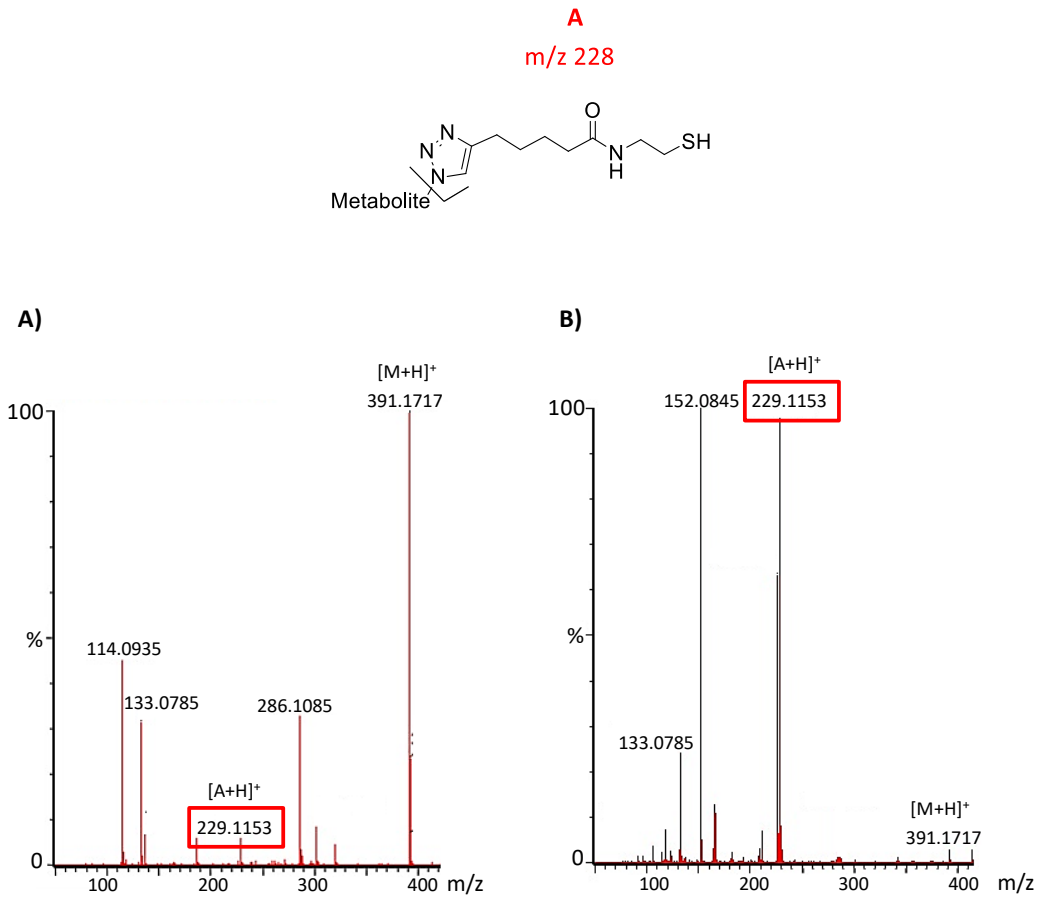

Figure 18. MS spectra corresponding to the TIC chromatograms of metabolome fraction B coming from the incubation of *E. coli* with azido sugar **3**. (A) Parent ion spectrum. (B) Fragment ion spectrum.

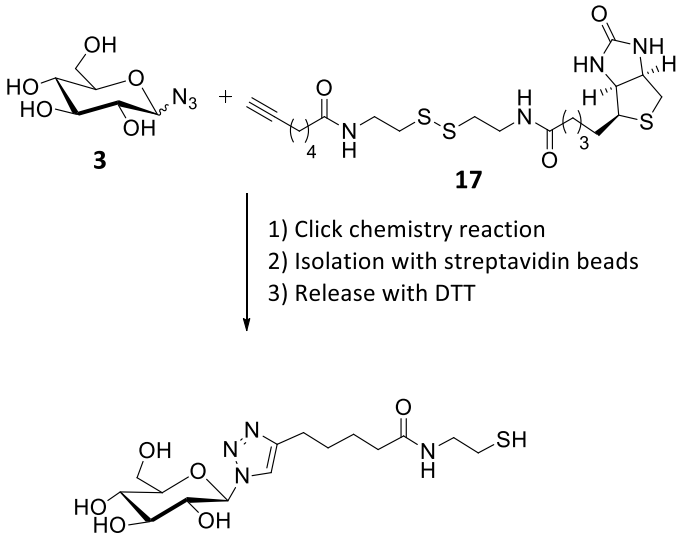

Figure 19. Schematic process of the synthesis of captured azido sugar **3**.

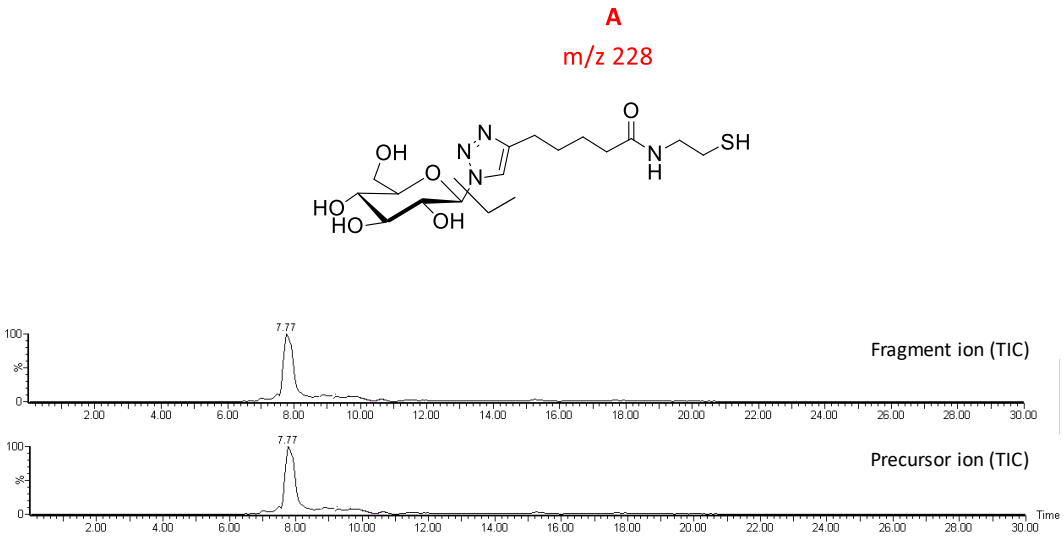

Figure 20. Chromatograms corresponding to captured azido sugar **3**.

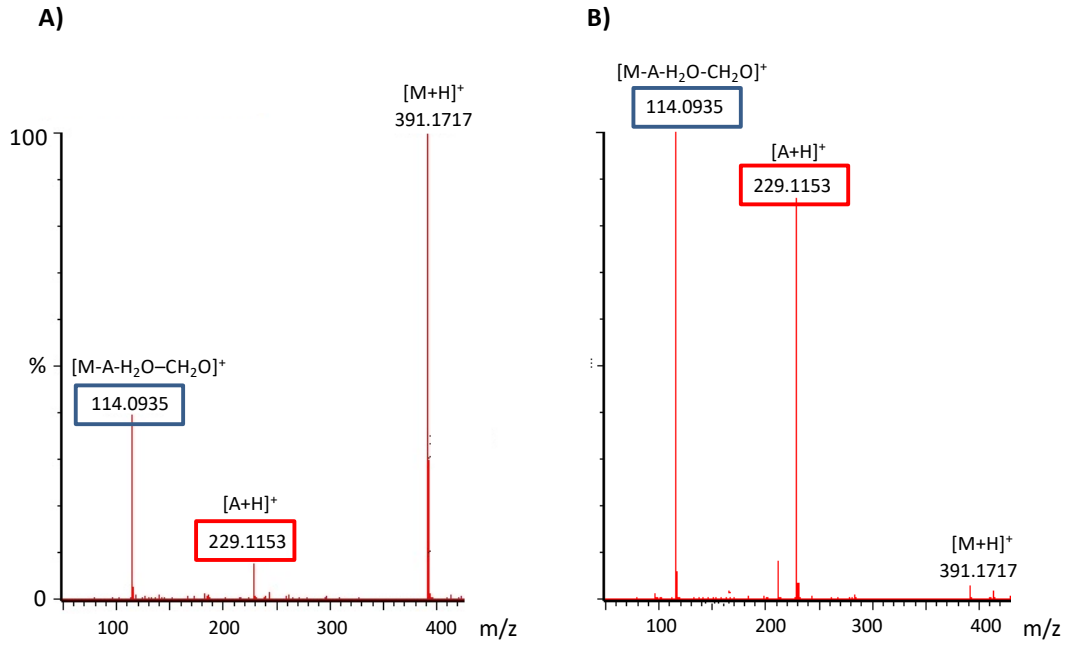

Figure 21. MS spectra corresponding to the TIC chromatograms of captured azido sugar **3**. (A) Parent ion spectrum. (B) Fragment ion spectrum.

The identification of captured azido sugar **3** in the metabolome of *E. coli* confirms that the proposed platform is suitable for the capture, isolation, and identification of tagged compounds within complex metabolomes. These results validate, as proof of concept, the proposed strategy for the identification of metabolites produced by the human microbiota. This methodology will be extended in our research group to other tagged precursors such as amino acids or fatty acids aimed at the identification of their metabolites.

CONCLUSIONS

3. CONCLUSIONS

In the present work we have developed a strategy based on the use of tagged precursors for the identification of metabolites produced by the human microbiota. Using azido sugars as tagged precursors in a variety of strains of bacteria of the human microbiota we have validated the proposed platform. These results constitute the proof of concept that the envisioned approach is suitable for the identification of tagged metabolites within complex metabolomes. This strategy is being extended in our research group to other tagged precursors (amino acids, fatty acids…) with the final objective of expediting the identification of new microbiota metabolites and their subsequent phenotypic study.

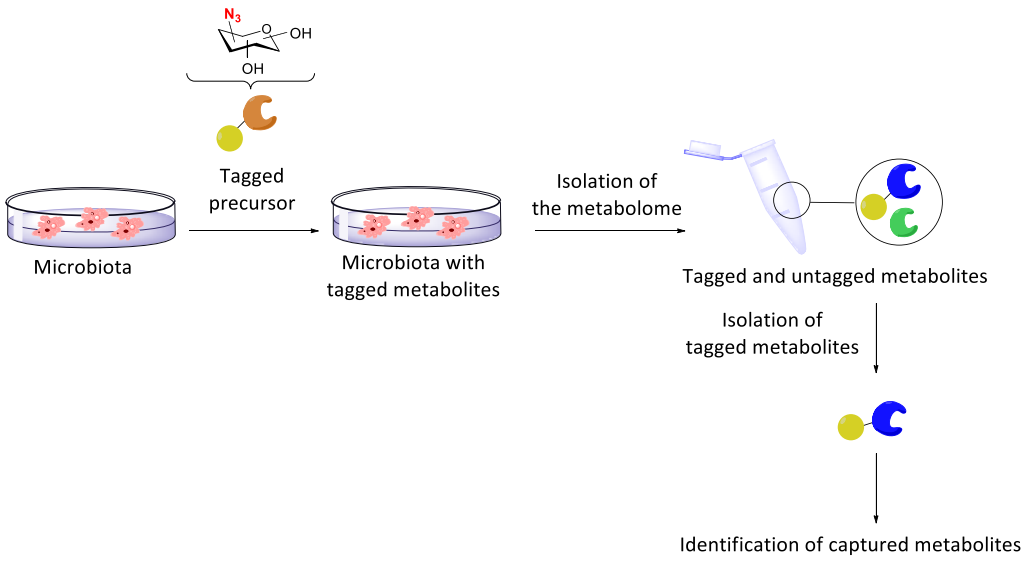

EXPERIMENTAL SECTION

4. EXPERIMENTAL SECTION

4.1. Chemistry

As far as general considerations are concerned, see section 4 of Chapter A. Additionally, specific synthetic issues related to the present chapter are detailed below.

4.1.1. Synthesis of azido sugar 1

1-(Azidosulfonyl)-1*H*-imidazol-3-ium chloride. To a suspension of NaN_3 (1.00 g, 15.4 mmol) in anhydrous ACN (15 mL), sulfuryl chloride (1.3 mL, 15.4 mmol) was added dropwise at 0 °C under and the reaction mixture was stirred on at rt. Then, a solution of imidazol (1.90 g, 29.2 mmol) was added dropwise to the ice-cooled reaction mixture and stirred at rt for 3 h. The mixture was diluted with EtOAc, washed with H_2O and saturated solutions of $NaHCO_3$ and NaCl, subsequently, dried over Na_2SO_4 and filtered. Then, a solution of HCl (2 M in Et_2O, 5.8 mL) was added dropwise to the ice-cooled filtrate with stirring, and the mixture was left stand for 10 min at 0 °C. The precipitate was isolated by filtration, washed with cold EtOAc and dried to afford the corresponding hydrochloride in 64% yield (2.10 g). The spectroscopic data are in agreement with those previously described.[61]

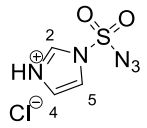

^{1}H-NMR (D_2O, δ): 7.55 (m, 1H, H_5), 7.97 (m, 1H, H_4), 9.22-9.30 (m, 1H, H_2).

2-Azido-2-deoxy-D-glucopyranose (1). To a suspensión of 2-aminoglucose hydrochloride (646 mg, 3.0 mmol), K_2CO_3 (981 mg, 7.1 mmol), and $CuSO_4 \cdot 5H_2O$ (6 mg, 40 µmol) in methanol (15 mL) at rt, 1-(azidosulfonyl)-1*H*-imidazol-3-ium chloride (755 mg, 3.6 mmol) was added and the reaction mixture was stirred at rt on. The residue was concentrated under reduced pressure, redissolved in methanol and filtered. The solvent was removed under reduced pressure to yield azido glucose **1** in 15% yield (92 mg). The spectroscopic data are in agreement with those previously described.[62]

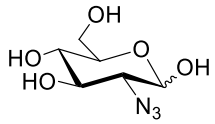

R_f (DCM/MeOH, 4:1): 0.85. ^{1}H-NMR ($CDCl_3$, δ): (mixture of anomer α/β, 1:2): 3.25 (dd, *J* = 9.2, 8.3 Hz, 1 H, $H_{2\beta}$), 3.44 (dd, *J* = 10.1, 3.2 Hz, 2H, $H_{6\alpha}$, $H_{6\beta}$), 3.45-3.49 (m, 5H, $H_{2\alpha}$, $H_{4\alpha}$, $H_{4\beta}$, $H_{6\alpha}$, $H_{6\beta}$), 3.70-3.85 (m, 4H, $H_{3\alpha}$, $H_{3\beta}$, $H_{5\alpha}$, $H_{5\beta}$), 4.69 (d, *J* = 8.1 Hz, 1H, $H_{1\beta}$), 5.33 (d, *J* = 3.6 Hz, 1H, $H_{1\alpha}$). MS (ESI, m/z): 206.1 $[M+H]^+$.

4.1.2. Synthesis of azido sugars 9 and 10

1,3,4,6-Tetra-*O*-acetyl-2-[(*t*ert-butoxycarbonyl)amino]-2-deoxy-D-galactopyranose (14). Over a solution of 2-galactosamine hydrochloride (141 mg, 0.8 mmol) in a mixture H_2O/dioxane, 1:1 (8 mL), a solution of di-*tert*-butyl dicarbonate (188 mg, 0.9 mmol) in H_2O/dioxane, 1:1 (4.5 mL) was added dropwise and the reaction mixture was stirred for 2 days at rt. The solvents were removed under reduced pressure to afford 2-[(*t*ert-butoxycarbonyl)amino]-2-deoxy-D-galactopyranose **13** in quantitative yield (350 mg), which was used in the next step without further purification. *N*-Boc protected amine **13** (310 mg, 1.1 mmol) was partially dissolved in DCM (5 mL) and pyridine (1.8 mL, 22.2 mmol) was added. The mixture was stirred at 0 °C for 30 min and Ac_2O (2.1 mL, 22.2 mmol) was added dropwise. The reaction mixture was stirred at rt observing the formation of a precipitate. After two hours of stirring, the precipitate disappeared turning into a yellow solution, and then, H_2O was added to the reaction mixture and the aqueous phase was extracted with DCM. The combined organic layers were dried over anhydrous Na_2SO_4, filtered, and the solvent was removed under reduced pressure. The obtained residue was redissolved in Et_2O and washed with a solution of $NaHSO_3$ (1 M in H_2O) and a saturated solution of NaCl. Then, it was dried over anhydrous Na_2SO_4, filtered, and the solvent removed under reduced pressure. The residue was purified by chromatography (hexane/EtOAc, 7:3) obtaining peracetylated compound **14** in 51% yield (250 mg). The spectroscopic data are in agreement with those previously described.[63]

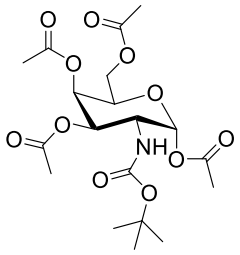

R_f (hexane/EtOAc, 1/1): 0.4. ^{1}H-NMR ($CDCl_3$, δ): 1.41 (s, 9H, $C(CH_3)_3$), 2.01 (s, 3H, CH_3), 2.02 (s, 3H, $COCH_3$), 2.16 (s, 3H, $COCH_3$), 2.17 (s, 3H, $COCH_3$), 4.07-4.14 (m, 2H, $2H_6$), 4.25 (dd, *J* = 6.7, 1.1 Hz, 1H, H_5), 4.44 (m, 1H, H_2), 5.13 (dd, *J* = 10.9, 2.5 Hz, 1H, H_3), 5.41 (d, *J* = 3.2, 1.3 Hz, 1H, H_4), 6.21 (d, *J* = 3.6 Hz, 1H, $H_{1\alpha}$). MS (ESI, m/z): 331.9 $[M\text{-}2OAc+H]^+$, 469.9 $[M+Na]^+$.

1,3,4,6-Tetra-*O*-acetyl-2-amino-2-deoxy-D-galactopyranose (15). To a solution of sugar **14** (100 mg, 0.2 mmol) in anhydrous DCM (7 mL), TFA (0.9 mL, 11.2 mmol) was added dropwise at 0 °C and the reaction was stirred within for 3 h. The solvent was removed under reduced pressure obtaining amine **15** in quantitative yield as a TFA salt (m= 114 mg). The spectroscopic data are in agreement with those previously described.[64]

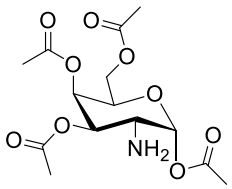

R_f (DCM): 0.35. ^{1}H-NMR (MeOD, δ): 1.91 (s, 3H, CH_3), 1.96 (s, 3H, CH_3), 2.05 (s, 3H, CH_3), 2.11 (s, 3H, CH_3), 3.98 (dd, *J* = 11.4, 3.7 Hz, 1H, H_2), 4.11 (m, 2H, $2H_6$), 5.37 (dd, *J* = 11.4, 3.2 Hz, 1H, H_3), 5.52 (dd, *J* = 3.2, 1.3 Hz, 1H, H_4), 6.36 (d, *J* = 3.6 Hz, 1H, $H_{1\alpha}$). MS (ESI, m/z): 370.1 $[M+Na]^+$.

1,3,4,6-Tetra-*O*-acetyl-2-(2-chloroacetamido)-2-deoxy-D-galactopyranose (**16**). To a solution of amine **15** (115 mg, 0.3 mmol) in DCM (3.5 mL) at 0 °C, a solution of chloroacetic anhydride (119 mg, 0.7 mmol) in DCM (10 mL) and 4-methylmorpholine (220 µL, 2.0 mmol) were added, subsequently. The reaction mixture was stirred on at rt and then diluted with Et_2O, washed with solutions of HCl (1 M in H_2O), NaOH (1 M in H_2O), and a saturated solution of NaCl, subsequently. The combined organic layers were dried over anhydrous Na_2SO_4, filtered, and then concentrated under reduced pressure to provide derivative **16** in 80% yield (111 mg).[65]

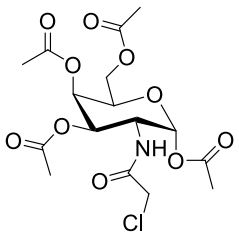

R_f (hexane/EtOAc, 1:1): 0.2. ^{1}H-NMR ($CDCl_3$, δ): 2.02 (s, 3H, CH_3), 2.03 (s, 3H, CH_3), 2.17 (s, 3H, CH_3), 2.18 (s, 3H, CH_3), 4.01 (s, 2H, CH_2Cl), 4.24 (m, 2H, $2H_6$), 4.28 (ddd, *J* = 7.6, 6.7, 0.9 Hz, 1H, H_5), 4.69 (dd, *J* = 9.1, 3.8 Hz, 1H, H_2), 5.25 (dd, *J* = 11.6, 1.1 Hz, 1H, H_3), 5.44 (dd, *J* = 3.1, 1.1 Hz, 1H, H_4), 6.23 (d, *J* = 3.8 Hz, 1H, $H_{1\alpha}$), 6.50 (d, *J* = 9.1 Hz, 1H, NH). MS (ESI, m/z): 453.0 $[M+Na]^+$.

1,3,4,6-Tetra-*O*-acetyl-2-(2-azidoacetamido)-2-deoxy-D-galactopyranose (Ac_4GalNAz) (9). To a solution of chloride **13** (500 mg, 1.1 mmol) in DMF (20 mL), NaN_3 (750 mg, 11.4 mmol) was added and the reaction mixture was stirred for 3 h at 60 °C. Then, the crude was diluted with H_2O and extracted with EtOAc. The combined organic layers were washed with a saturated solution of NaCl, dried over Na_2SO_4, filtered, and the solvent was removed under reduced pressure to yield peracetylated sugar **9** in 52% yield (250 mg). The spectroscopic data are in agreement with those previously described.[66]

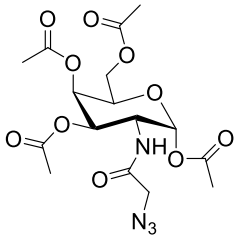

R_f (hexane/EtOAc, 1:1): 0.4. Mp: 140-142 °C. ^{1}H-NMR ($CDCl_3$, δ): 2.02 (s, 3H, CH_3), 2.03 (s, 3H, CH_3), 2.17 (s, 3H, CH_3), 2.18 (s, 3H, CH_3), 3.95 (s, 2H, CH_2N), 4.08 (m, 2H, $2H_6$), 4.25 (dd, *J* = 6.7, 1.1 Hz, 1H, H_5), 4.69 (dd, *J* = 9.1, 3.6 Hz, 1H, H_2), 5.25 (dd, *J* = 11.6, 3.1 Hz, 1H, H_3), 5.45 (dd, *J* = 3.1, 1.1 Hz, 1H, H_4), 6.21 (d, *J* = 3.6 Hz, 1H, $H_{1\alpha}$), 6.28 (d, *J* = 9.1 Hz, 1H, NH). MS (ESI, m/z): 453.0 $[M+Na]^+$.

2-(2-Azidoacetamido)-2-deoxy-D-galactopyranose (GalNAz) (10): Over a solution of peracetylated sugar **9** (150 mg, 0.4 mmol) in MeOH (3.5 mL), a solution of sodium methoxide (1 M in MeOH, 70 µL) was added dropwise. The reaction mixture was stirred for 2 h and the solvent was removed under reduced pressure to afford free hydroxyl

sugar **10** in 100% yield (m= 105 mg). The spectroscopic data are in agreement with those previously described.[67]

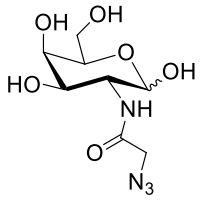

R_f (DCM/MeOH, 9:1): 0.3. ^{1}H-NMR (D_2O, δ): mixture of anomers α/β, 1:1: 3.71 (app d, *J* = 6.3 Hz, 2H, $H_{3\alpha}$, $H_{3\beta}$), 3.74 (dd, *J* = 9.9, 3.3 Hz, 2H, $H_{5\alpha}$, $H_{5\beta}$), 3.90 (dd, *J* = 9.1, 6.7 Hz, 2H, $H_{6\alpha\beta}$), 3.95 (dd, *J* = 9.9, 3.3 Hz, 2H, $H_{6'\alpha,\beta}$), 4.04 (s, 4H, $2CH_2N$), 4.05-4.11 (m, 3H, $H_{2\beta}$, $H_{4\alpha}$, $H_{4\beta}$), 4.16 (dd, *J* = 10.9, 3.7 Hz, 1H, $H_{2\alpha}$), 4.65 (d, *J* = 8.4 Hz, 1H, $H_{1\beta}$) 5.20 (d, *J* = 3.7 Hz, 1H, $H_{1\alpha}$). MS (ESI, m/z): 260.8 $[M-H]^-$.

4.1.3. Synthesis of capture reagents 17 and 18

• **Synthesis of capture reagent 17**

***tert*-Butyl-(2-[(2-aminoethyl)disulfanyl]ethyl)carbamate (22).** To a suspension of cystamine dihydrochloride (1.00 g, 4.8 mmol) in MeOH (10 mL), Et_3N (2 mL, 14.5 mmol) and a solution of di-*tert*-butyl dicarbonate (900 mg, 4.8 mmol) in MeOH (5 mL) were added. The mixture was stirred for 1 h at rt and the solvent evaporated in vacuo. To the residue, a solution of NaH_2PO_4 (1 M in H_2O, pH = 4.2) was added and the mixture was extracted with Et_2O to remove di-Boc-cystamine. The aqueous solution was basified (pH = 9) using a solution of NaOH (1 M in H_2O) and extracted with EtOAc. The combined organic layers were washed with H_2O and a saturated solution of NaCl, subsequently, dried over Na_2SO_4, filtered, and the solvent removed under reduced pressure to yield protected amine **22** in 49% yield (594 mg). The spectroscopic data agreed with those previously described.[68]

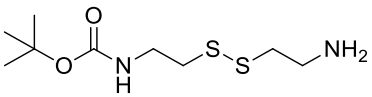

R_f (hexane/EtOAc, 3:7): 0.2. Mp: 112-113 °C (Lit.[69] 109-110 °C). ^{1}H-NMR ($CDCl_3$, δ): 1.40 (s, 9H, $3CH_3$), 2.72 (t, *J* = 5.9 Hz, 2H, $SCH_2CH_2NH_2$), 2.75 (t, *J* = 5.6 Hz, 2H, SCH_2CH_2NHCO), 2.97 (t, *J* = 6.1 Hz, 2H, CH_2NH_2), 3.40-3.42 (m, 2H, CH_2NHCO). MS (ESI, m/z): 253.1 $[M+H]^+$.

***tert*-Butyl-*N*-(2-[(2-aminoethyl)disulfanyl]ethyl)hept-7-ynamide (23).** A solution of EDC (461 mg, 3.0 mmol), HOBt (402 mg, 2.9 mmol), and 6-heptynoic acid (0.3 mL, 2.4 mmol) in anhydrous DCM (20 mL) was stirred for 1 h at rt. Then, a solution of amine **22** (500 mg, 2.0 mmol) in a mixture DCM/DMF, 1:1 (7 mL) was added dropwise and the reaction was stirred on. The reaction mixture was washed with a saturated solution of $NaHCO_3$ and the aqueous layer was reextracted with DCM. The combined organic layers were washed with a saturated solution of NaCl, dried over anhydrous Na_2SO_4, filtered, and the solvent was removed under reduced pressure. The residue was purified by chromatography (hexane/EtOAc, 6:4) to afford amide **23** in 56% yield (407 mg).

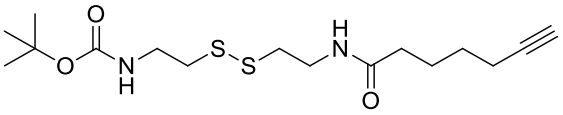

R_f (hexane/EtOAc, 1:1): 0.24. IR (ATR, cm^{-1}): 3301 (C≡CH, NH), 1696, 1652, 1533 (CONH), 640 (S-S). ^{1}H-NMR ($CDCl_3$, δ): 1.44 (s, 9H, $3CH_3$), 1.51-1.60 (m, 2H, CH_2CH_2CO), 1.70-1.80 (m, 2H, $CH_2CH_2C{\equiv}$), 1.94 (t, *J* = 2.7 Hz, 1H, CH≡C), 2.20 (td, *J* = 7.0, 2.9 Hz, 2H, $CH_2C{\equiv}$), 2.25 (t, *J* = 7.3 Hz, 2H, CH_2CO), 2.77 (t, *J* = 6.7 Hz, 2H, CH_2CH_2NHBoc), 2.83 (t, *J* = 6.1 Hz, 2H, CH_2CH_2NH), 3.44 (q, *J* = 6.7 Hz, 2H, CH_2NHBoc), 3.56 (q, *J* = 6.1 Hz, 2H, CH_2NH), 4.98 (br s, 1H, NHBoc), 6.50 (br s, 1H, NHCO). ^{13}C-NMR ($CDCl_3$, δ): 18.3 ($CH_2C{\equiv}$), 24.9 ($CH_2CH_2C{\equiv}$), 28.1 (CH_2CH_2CO), 28.5 ($3CH_3$), 36.1 (CH_2CO), 37.8 (CH_2CH_2NHBoc), 38.2 (CH_2CH_2NH), 38.7 (CH_2NH), 39.8 (CH_2NHBoc), 68.7 (C≡CH), 80.0 ($C(CH_3)_3$), 84.2 (C≡CH), 156.4 (OCONH), 172.9 (CONH). MS (ESI, m/z): 261.1 $[M\text{-Boc+H}]^+$.

***N*-(2-[(2-Aminoethyl)disulfanyl]ethyl)hept-7-ynamide (19).** To a solution of compound **23** (320 mg, 0.8 mmol) in anhydrous DCM (4 mL), TFA (1.3 mL, 16.8 mmol) was added dropwise and the reaction mixture was stirred at rt for 5 h. The solvent was removed under reduced pressure, the residue was redissolved in DCM and basified with a solution of NaOH (1 M in H_2O). The organic layer was extracted with DCM, dried over anhydrous Na_2SO_4, filtered and the solvent was removed under reduced pressure to afford amine **19** in a quantitative yield (240 mg).

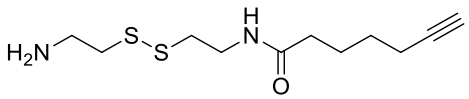

R_f (DCM/MeOH/NH_3, 8:2:0.1): 0.6. IR (ATR, cm^{-1}): 3295 (C≡CH, NH), 1648, 1552 (CONH), 638 (S-S). ^{1}H-NMR (MeOD, δ): 1.53-1.58 (m, 2H, CH_2CH_2CO), 1.70-1.80 (m, 2H, $CH_2CH_2C{\equiv}$), 2.18-2.23 (m, 3H, $CH_2C{\equiv}CH$, C≡CH), 2.25 (t, *J* = 7.3 Hz, 2H, CH_2CO), 2.88 (t, *J* = 6.8 Hz, 2H, CH_2CH_2NHCO), 3.02 (t, *J* = 6.6 Hz, 2H, $CH_2CH_2NH_2$), 3.28 (t, *J* = 6.6 Hz, 2H,

CH_2NH_2), 3.50 (t, *J* = 6.8 Hz, 2H, CH_2NHCO). ^{13}C-NMR (MeOD, δ): 18.7 ($CH_2C\equiv$), 26.0 ($CH_2CH_2C\equiv$), 29.1 (CH_2CH_2CO), 35.4 ($CH_2CH_2NH_2$), 36.5 (CH_2CO), 38.2 (CH_2CH_2NHCO), 39.3 (CH_2NH_2), 39.4 (CH_2NHCO), 69.8 (C≡CH), 84.6 (C≡CH), 176.0 (CO). MS (ESI, m/z): 261.1 $[M+H]^+$.

***N*-(2-[(2-([5-(2-Oxohexahydro-1*H*-thieno[3,4-*d*]imidazol-4-yl)pentanoyl]amino)ethyl)disulfanyl]ethyl)hept-6-ynamide (17).** A suspension of biotin (38 mg, 0.2 mmol), HOBt (21 mg, 0.2 mmol) and activated 4Å molecular sieves in anhydrous DMF (8 mL) was stirred at 77 °C until a clear solution was obtained. Once cooled to rt, a solution of EDC (27 mg, 0.2 mmol) in anhydrous DCM (3 mL) was added dropwise and the mixture stirred at rt for 3 h. Then, a solution of amine **19** (20 mg, 0.1 mmol) and DMAP (200 µg, 20 µmol) in anhydrous DCM (2 mL) was added and the reaction mixture was stirred for 24 h. Then, the crude was filtered, diluted with DCM, washed with saturated solutions of $NaHCO_3$ and NaCl, subsequently. The organic layer was dried over Na_2SO_4, and filtered. The solvent was removed under reduced pressure and the residue was purified by chromatography (EtOAc/MeOH, 9:1, 0.1% NH_3) to yield compound **17** in 31% yield (12 mg).

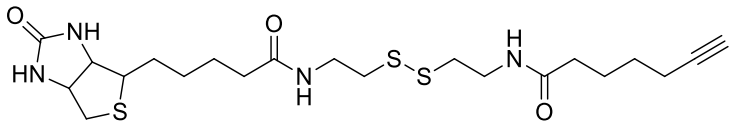

R_f (EtOAc/MeOH/NH_3, 8:2:0.1): 0.4. Mp: 217-220 °C. IR (ATR, cm^{-1}): 3301 (C≡CH, NH), 1692, 1652 (CONH). ^{1}H-NMR (MeOD, δ): 1.43-1.78 (m, 10H, $CHS(CH_2)_3$, $(CH_2)_2CH_2C\Xi$), 2.18-2.25 (m, 7H, $CH_2C\equiv$, C≡CH, $2CH_2CO$), 2.71 (d, *J* = 12.7 Hz, 1H, ½CH_2S_{biot}), 2.83 (t, *J* = 6.7 Hz, 2H, CH_2S), 2.84 (t, *J* = 6.6 Hz, 2H, CH_2S), 2.94 (dd, *J* = 12.7, 5.0 Hz, 1H, ½CH_2S_{biot}), 3.18-3.25 (m, 1H, CHS), 3.49 (t, *J* = 6.7 Hz, 4H, $2CONHCH_2$), 4.32 (dd, *J* = 7.9, 4.4 Hz, 1H, CHN_{biot}), 4.51 (dd, *J* = 7.9, 4.3 Hz, 1H, CHN_{biot}). ^{13}C-NMR (MeOD, δ): 18.5 ($CH_2C\equiv$), 25.8 ($CH_2CH_2C\equiv$), 26.5, 28.9, 29.2, 29.5 (CH_2CH_2CO, $(CH_2)_3CHS$), 36.2, 36.5 ($2CH_2CO$), 38.2, 38.3 ($2CH_2S$), 39.2, 39.3 ($2CONHCH_2$), 40.8 (CH_2S_{biot}), 56.7 (CHS), 61.4, 63.1 (2 CHN_{biot}), 69.5 (C≡CH), 84.3 (C≡CH), 164.7 (NCON), 174.7, 174.8 (2CONH). HPLC-MS (r_t, min): 15.16, method A. HRMS (ESI): Calculated for $C_{21}H_{34}NaN_4O_3S_3$ $[(M+Na)^+]$: 509.1691. Found: 509.1720.

• **Synthesis of capture reagent 18**

Solid-supported intermediate (20). Polyethylene glycol polyacrylamide (PEGA) resin (200 mg, 70 µmol, charge: 0.34 mmol/g resin) was washed with DMF and shaked for 16 h (rt, 120 rpm, THZ thermostatic shaker (Lan Technics)) with a solution of succinic anhydride (170 mg, 1.7 mmol), pyridine (20 µL, 0.3 mmol) and DMAP (8 mg, 70 µmol) in DMF (2.7 mL). Then, the resin was washed with DMF and DCM (3x). The formation of derivative **20** was checked by Kaiser´s test, which showed no presence of amino PEGA resin.

Capture reagent (18). Resin **20** (70 µmol) was swollen in DMF (700 µL) and PyBOP (181 mg, 0.3 mmol) and DIPEA (60 µL, 0.3 mmol) were added. Shaking was maintained for 20 min (rt, 120 rpm) and a solution of amine **19** (13 mg, 70 µmol) in DMF (1.4 mL) was added. The resin was shaken for 40 h (rt, 120 rpm), the reaction mixture was filtered off and the resin was washed with DMF, DCM, MeOH, and DMF (2 x 2.5 mL each) to afford capture reagent **18**. In order to check that the reaction has worked, a small amount of resin was separated and treated with a mixture of TFA/TIS/H_2O, 95:2.5:2.5 (0.2 mL) for 1 h (rt, 120 rpm). The reaction mixture was filtered, the solvent removed and the residue analized by HPLC-MS, observing the peak of m/z = 361.1, which correspond to the $[M+H]^+$ of carboxylic acid **21**.

4.1.4. NMR analysis of tagged precursors in the culture medium. The ^{1}H NMR spectra of these sugars in basal peptone broth medium* was carried out at 100, 200, and 400 µM by mixing 180 µL of the corresponding solution of the azido sugar in the culture medium with 20 µL of deuterated water and then analyzed in a 700 MHz equipment (Bruker Avance III 700 MHz).

* Basal peptone-yeast broth contains (per liter): 5 g of yeast extract, 20 g of proteose peptone, 5 g of NaCl, 5 mg of hemin, 0.5 mg of vitamin K1 and 5 g of K_2HPO_4. Hemin, vitamin K1, and K_2HPO_4 were added through a filter after the basal medium had been autoclaved.

4.1.5. Optimization of the bioorthogonal reaction and the isolation processes

4.1.5.1 With capture reagent 17

• **In culture medium.** Azido sugar **1** (2 mM in DMSO, 5 µL), capture reagent **17** (10 mM in DMSO, 10 µL), $CuSO_4 \cdot 5H_2O$ (40 mM in H_2O, 5 µL), TCEP (40 mM in H_2O, 5 µL), and TBTA (2 mM in H_2O, 5 µL), were added to 100 µL of culture medium. The samples were shaked for 3 h (rt, 120 rpm) and a suspension of streptavidin beads (250 µL) in PBS (500 µL) was added (streptavidin beads were previously centrifuged (rt, 10 min, 12000 rpm) to remove the glycerol of the commercial solution, washed with PBS (2x), and suspended in PBS). The mixture was shaked for 90 min (rt, 120 rpm), centrifuged (rt, 10 min, 12000 rpm), and the pellet of beads washed with PBS (2 x 500 µL). Then, the beads were resuspended in a solution of DTT (50 mM in MeOH/H_2O, 1:1, 100 µL), shaked for 1 h (rt, 120 rpm) and centrifuged (rt, 10 min, 12000 rpm). The supernatant was isolated, the solvent was removed and the residue was redissolved in 100 µL of MeOH and analyzed by HPLC-MS. HPLC-MS analysis was done in an Eclipse XDB-C18 column (5 µm, 4.6 mm x 150 mm), together with a guard column (5 µm, 4.6 mm x 12.5 mm) with a flow of 0.5 mL/min. The gradient mobile phase consisted of A (95:5 water/acetonitrile) and B (5:95 water/acetonitrile) with 0.1% formic acid as solvent modifier. The gradient is indicated in Table 4.

Table 4. HPLC-MS method used in the optimization of the click chemistry reaction

t (min)	% B
0	0
5	0
12	60
22	100
26	100
30	0

• **In DMF/H_2O, 15:85.** Azido sugar **1** (2 mM in DMSO, 5 µL), capture reagent **17** (10 mM in DMSO, 10 µL), $CuSO_4 \cdot 5H_2O$ (3 mM in H_2O, 5 µL), sodium ascorbate (3 mM in H_2O, 5 µL), and TBTA (2 mM in H_2O, 5 µL), were added to 100 µL of DMF/H_2O, 15:85. The samples were incubated for 1 h (rt, 120 rpm) and a suspension of streptavidin beads (250 µL) in PBS (500 µL) was added (streptavidin beads were previously centrifuged (rt, 10 min, 12000 rpm) to remove the glycerol of the commercial solution, washed with PBS (2x), and suspended in PBS). The mixture was shaked for 90 min (rt, 120 rpm), centrifuged (rt, 10 min, 12000 rpm), and the pellet of beads washed with PBS (2 x 500 µL). Then, the beads were resuspended in a solution of DTT (50 mM in MeOH/H_2O, 1:1,

100 µL), shaked for 1 h (rt, 120 rpm) and centrifuged (rt, 10 min, 12000 rpm). The supernatant was then isolated, the solvent was removed, and the residue redissolved in 100 µL of MeOH before analysis by HPLC-MS using the conditions previously described and the gradient indicated in Table 4.

• **In PBS.** Azido sugar **1** (2 mM in DMSO, 5 µL), capture reagent **17** (10 mM in DMSO, 10 µL), $CuSO_4 \cdot 5H_2O$ (40 mM in H_2O, 5 µL), TCEP (40 mM in H_2O, 5 µL), and TBTA (2 mM in H_2O, 5 µL), were added to 100 µL of PBS. The samples were shaked for 16 h (rt, 120 rpm) and a suspension of streptavidin beads (250 µL) in PBS (500 µL) was added (streptavidin beads were previously centrifuged (rt, 10 min, 12000 rpm) to remove the glycerol of the commercial solution, washed with PBS (2x), and suspended in PBS). The mixture was shaked for 90 min (rt, 120 rpm), centrifuged (rt, 10 min, 12000 rpm) and the pellet of beads washed with PBS (2 x 500 µL). Then, the beads were resuspended in a solution of DTT (50 mM in MeOH/H_2O, 1:1, 100 µL), shaked for 1 h (rt, 120 rpm) and centrifuged (rt, 10 min, 12000 rpm). The supernatant was then isolated, the solvent was removed, and the residue redissolved in 100 µL of MeOH before analysis by HPLC-MS using the conditions previously described and the gradient indicated in Table 4.

4.1.5.2. With capture reagent 18

• **In culture medium.** Azido sugar **1** (2 mM in DMSO, 5 µL), capture reagent **18** (0.3 mg, charge 0.34 mmol/g), $CuSO_4 \cdot 5H_2O$ (40 mM in H_2O, 5 µL), TCEP (40 mM in H_2O, 5 µL), and TBTA (2 mM in H_2O, 5 µL), were added to 100 µL of culture medium. The samples were incubated for 3 h (rt, 120 rpm), centrifuged (rt, 10 min, 12000 rpm) and the resulting resin was resuspended in a solution of DTT (50 mM in MeOH/H_2O, 1:1, 100 µL), shaked for 1 h (rt, 120 rpm) and centrifuged (rt, 10 min, 12000 rpm). The supernatant was then isolated, the solvent was removed, and the residue was redissolved in 100 µL of MeOH before analysis by HPLC-MS using the conditions previously described and the gradient indicated in Table 4.

• **In DMF/H_2O, 15:85.** Azido sugar **1** (2 mM in DMSO, 5 µL), capture reagent **18** (0.3 mg, charge 0.34 mmol/g), $CuSO_4 \cdot 5H_2O$ (3 mM in H_2O, 5 µL), sodium ascorbate (3 mM in H_2O, 5 µL), and TBTA (2 mM in H_2O, 5 µL), were added to 100 µL of DMF/H_2O, 15:85. The samples were incubated for 1 h (rt, 120 rpm), centrifuged (rt, 10 min, 12000 rpm) and the resulting resin was resuspended in a solution of DTT (50 mM in MeOH/H_2O, 1:1, 100 µL), shaked for 1 h (rt, 120 rpm) and centrifuged (rt, 10 min, 12000 rpm). The supernatant was then isolated, the solvent was removed and the residue was

redissolved in 100 µL of MeOH before analysis by HPLC-MS using the conditions previously described and the gradient indicated in Table 4.

• **In PBS.** Azido sugar **1** (2 mM in DMSO, 5 µL), capture reagent **18** (0.3 mg, charge 0.34 mmol/g), $CuSO_4 \cdot 5H_2O$ (40 mM in H_2O, 5 µL), TCEP (40 mM in H_2O, 5 µL), and TBTA (2 mM in H_2O, 5 µL), were added to 100 µL of PBS. The samples were incubated for 16 h (rt, 120 rpm), centrifuged (rt, 10 min, 12000 rpm) and the resulting resin was resuspended in a solution of DTT (50 mM in MeOH/H_2O, 1:1, 100 µL), shaked for 1 h (rt, 120 rpm) and centrifuged (rt, 10 min, 12000 rpm). The supernatant was then isolated, the solvent was removed, and the residue was redissolved in 100 µL of MeOH before analysis by HPLC-MS using the conditions previously described and the gradient indicated in Table 4.

4.2. Biology

4.2.1. Bacterial growth in the presence of azido sugars 1-12. Growing experiments were carried out in collaboration with Dr. Carles Úbeda (Centro Superior en Salud Pública, Valencia). *Bacteroides fragilis, Bacteroides thetaomicron, Prevotella copri, Lactobacillus rhamnosus,* and *Escherichia coli* were incubated with the corresponding azido sugar at the adequate concentration (100 µM for free hydroxyl azido sugars **1**, **3**, **5**, and **8** and 400 µM for peracetylated azido sugars **2**, **4**, **6**, **7**, **9**, and **11**) in basal peptone yeast broth (10 mL for the incorporation experiments or 100 mL for those carried out in higher scale) in an anaerobic chamber (Whitley DG250 Anaerobic Workstation) at 37 ºC. Optical density values were measured (Eppendorf Biophotometer Plus equipment) obtaining at 24 h values from 0.3 to 0.8.

4.2.2. Screening by ^{1}H NMR of the incorporation of azido sugars 1-12 in bacteria strains. Aliquots of 200 µL at time zero and 24 h were taken from the culture medium and centrifuged (4 °C, 10 min, 12000 rpm, Mikro 220R (Hettich)) to separate the supernatants from the pellets. 180 µL were taken from the supernatants and then mixed with 20 µL of deuterated water. The samples were analyzed by ^{1}H NMR in a 700 MHz NMR equipment (Bruker).

4.2.3. Analysis by flow cytometry and confocal microscopy of the incorporation of azido sugars 1-12. The pellet of bacteria after 24 h of growing in the presence of the tagged sugar was resuspended in a solution of bovine serum albumin (BSA) (0.01% in H_2O, 200 µL). Then, DBCO-FL-PEG_4-BODIPY (2 mM in DMSO, 5 µL) was added and the mixture was shaked for 16 h (rt, 120 rpm, THZ thermostatic shaker (Lan Technics)). After that time, the sample was centrifuged (rt, 10 min, 12000 rpm), the supernatant was removed and the pellet was washed with a solution of BSA (0.01% in H_2O, 200 µL, 3x).

Then, the pellet was permeabilized with a solution of PFA (3.7% in H_2O, 500 µL), and incubated for 1 h at 0 °C protected from light. After centrifugation (rt, 10 min, 12000 rpm), the resulting pellet was washed with a solution of NaCl (0.9% in H_2O, 500 µL, 3x) and resuspended in a solution of NaCl (0.09% in H_2O, 900 µL). Then, a solution of SYTO62 (50 µM in DMSO, 100 µL) was added. The samples were analyzed by FACS using a 2FACScalibur citometer at the Cytometry and Fluorescence Microscopy UCM facilities.

For confocal experiments, 20 µL of the samples prepared for flow cytometry experiments were taken, sealed in a slide cover at 0 °C for 16 h and then visualized in a confocal microscope (Leica SP-8) at the Cytometry and Fluorescence Microscopy UCM facilities.

4.2.4. Isolation of the different metabolomes fractions. The suspension of bacteria in the culture medium was centrifuged (4 °C, 10 min, 12000 rpm) and the pellet separated from the culture medium (metabolome fraction A). The pellet was homogenized in MeOH/$CHCl_3$/H_2O, 2:2:1 (200 µL), vortexed (Heidolph REAX), and centrifuged (4 °C, 10 min, 12000 rpm). The two phases were separated and after removal of the organic solvent under an argon athmosphere and lyophilization (Telstar lyophilizer, Life Science) of the aqueous phase, the two metabolome fractions corresponding to non-polar (metabolome fraction B) and polar metabolites (metabolome fraction C), respectively, were obtained.

4.2.5. Biorthogonal reaction and isolation of the tagged metabolites from azido sugars 1-12

- **Metabolome fraction A.** Capture reagent **17** (330 mM in DMSO, 150 µL), $CuSO_4 \cdot 5H_2O$ (1.7 M in H_2O, 60 µL), TCEP (1.7 M in H_2O, 60 µL), and TBTA (83 mM in H_2O, 60 µL), were added to 1 mL of the metabolome fraction A isolated as described in 4.2.4. Then, the samples were shaked for 3 h (rt, 120 rpm) and a suspension of streptavidin beads (600 µL) in PBS (1.2 mL) was added (streptavidin beads were previously centrifuged (rt, 10 min, 12000 rpm) to remove the glycerol of the commercial solution, washed with PBS (2x), and suspended in PBS). The mixture was incubated for 90 min (rt, 120 rpm), centrifuged (rt, 10 min, 12000 rpm), and the pellet of beads washed with PBS (2 x 1.2 mL). Then, the beads were resuspended in a solution of DTT (100 mM in MeOH/H_2O, 1:1, 200 µL), shaked for 1 h (rt, 120 rpm) and centrifuged (rt, 10 min, 12000 rpm). The supernatant was isolated, the solvent was removed, and the resulting residue was stored at -80 °C until further analysis for structural elucidation.

• **Metabolome fraction B.** Metabolome fraction B, isolated as described in 4.2.4., was redissolved in DMF/H_2O, 15:85 (1 mL) and capture reagent **17** (333 mM in DMSO, 150 µL), $CuSO_4 \cdot 5H_2O$ (125 mM in H_2O, 60 µL), sodium ascorbate (125 mM in H_2O, 60 µL), and TBTA (83 mM in H_2O, 60 µL), were added. Then, the samples were shaked for 3 h (rt, 120 rpm) and a suspension of streptavidin beads (600 µL) in PBS (1.2 mL) was added (streptavidin beads were previously centrifuged to remove the glycerol of the commercial solution, washed with PBS (2x), and suspended in PBS). The mixture was shaked for 90 min (rt, 120 rpm), centrifuged (rt, 10 min, 12000 rpm), and the pellet of beads washed with PBS (2 x 1.2 mL). Then, the beads were resuspended in a solution of DTT (100 mM in MeOH/H_2O, 1:1, 200 µL), shaked for 1 h (rt, 120 rpm), and centrifuged (rt, 10 min, 12000 rpm). The supernatant was then isolated and the solvent was removed under an argon atmosphere. The resulting residue was stored at -80 °C until further analysis for structural elucidation.

• **Metabolome fraction C.** Metabolome fraction C, isolated as described in 4.2.4., was redissolved in PBS (1 mL) and capture reagent **17** (330 mM in DMSO, 150 µL), $CuSO_4 \cdot 5H_2O$ (1.7 M in H_2O, 60 µL), TCEP (1.7 M in H_2O, 60 µL), and TBTA (83 mM in H_2O, 60 µL), were added. Then, the samples were shaked for 3 h (rt, 120 rpm) and a suspension of streptavidin beads (600 µL) in PBS (1.2 mL) was added (streptavidin beads were previously centrifuged to remove the glycerol of the commercial solution, washed with PBS (2x), and suspended in PBS). The mixture was shaked for 90 min (rt, 120 rpm), centrifuged (rt, 10 min, 12000 rpm), and the pellet of beads washed with PBS (2 x 1.2 mL). Then, the beads were resuspended in a solution of DTT (100 mM in MeOH/H_2O, 1:1, 200 µL), shaked for 1 h (rt, 120 rpm), and centrifuged (rt, 10 min, 12000 rpm). The supernatant was then isolated, and the solvent was removed under an argon atmosphere. The resulting residue was stored at -80 °C until further analysis for structural elucidation.

4.2.6. Analysis of captured metabolites

Analyses of captured metabolites were done by LC-MS. Metabolites were separated in a Kinetex-C18 column (1.7 µm, 150 mm x 21 mm) with a flow of 0.25 mL/min. The gradient mobile phase consisted of A (water) and B (methanol) with 0.1% formic acid as solvent modifier. The gradient is indicated in Table 5. MS analyses were carried out in a Xevo G2-XS QTof spectrometer (Waters) in positive ionization mode from 50 to 1500 m/z and in UV-mode at 254 nm. MS analysis was performed with an ESI source and a time of flight (ToF) analyzer. The capillary voltage was set to 0.5 kV and the fragmentor voltage was set at 10 or 30 eV for parent or fragment ion spectra, respectively. The

drying gas temperature was 250 °C, the drying gas flow was 10 L/min, and the nebulizer pressure was 20 psi.

Table 5. HPLC-MS method used in the optimization of the detection of captured tagged precursors

t (min)	% B
0	2
2	2
20	100
24	100
24.1	2
30	2

REFERENCES

5. REFERENCES

1. Gilbert, J. A.; Blaser, M. J.; Caporaso, J. G.*, et al.*, Current understanding of the human microbiome. *Nat. Med.* **2018**, *24*, 392-400.

2. Turnbaugh, P. J.; Ley, R. E.; Hamady, M.*, et al.*, The human microbiome project. *Nature* **2007**, *449*, 804-810.

3. Sender, R.; Fuchs, S.; Milo, R., Are we really vastly outnumbered? Revisiting the ratio of bacterial to host cells in humans. *Cell* **2016**, *164*, 337-340.

4. Locey, K. J.; Lennon, J. T., Scaling laws predict global microbial diversity. *Proc. Natl. Acad. Sci. USA* **2016**, *113*, 5970-5975.

5. Roy, S.; Trinchieri, G., Microbiota: a key orchestrator of cancer therapy. *Nat. Rev. Cancer* **2017**, *17*, 271-285.

6. Fessler, J.; Matson, V.; Gajewski, T. F., Exploring the emerging role of the microbiome in cancer immunotherapy. *J. Immunother. Cancer.* **2019**, *7*, 1-15.

7. Qin, N.; Yang, F.; Li, A.*, et al.*, Alterations of the human gut microbiome in liver cirrhosis. *Nature* **2014**, *513*, 59-64.

8. Qin, J.; Li, Y.; Cai, Z.*, et al.*, A metagenome-wide association study of gut microbiota in type 2 diabetes. *Nature* **2012**, *490*, 55-60.

9. Forslund, K.; Hildebrand, F.; Nielsen, T.*, et al.*, Disentangling type 2 diabetes and metformin treatment signatures in the human gut microbiota. *Nature* **2015**, *528*, 262-266.

10. Reijnders, D.; Goossens, G. H.; Hermes, G. D.*, et al.*, Effects of gut microbiota manipulation by antibiotics on host metabolism in obese humans: a randomized double-blind placebo-controlled trial. *Cell. Metab.* **2016**, *24*, 63-74.

11. Brial, F.; Le Lay, A.; Dumas, M. E.*, et al.*, Implication of gut microbiota metabolites in cardiovascular and metabolic diseases. *Cell Mol. Life Sci.* **2018**, *75*, 3977-3990.

12. Franzosa, E. A.; Sirota-Madi, A.; Avila-Pacheco, J.*, et al.*, Gut microbiome structure and metabolic activity in inflammatory bowel disease. *Nat. Microbiol.* **2019**, *4*, 293-305.

13. Marino, E.; Richards, J. L.; McLeod, K. H.*, et al.*, Gut microbial metabolites limit the frequency of autoimmune T cells and protect against type 1 diabetes. *Nat. Immunol.* **2017**, *18*, 552-562.

14. O'Toole, P. W.; Jeffery, I. B., Gut microbiota and aging. *Science* **2015**, *350*, 1214-1215.

15. Biagi, E.; Franceschi, C.; Rampelli, S.*, et al.*, Gut microbiota and extreme longevity. *Curr. Biol.* **2016**, *26*, 1480-1485.

16. Kim, S.; Jazwinski, S. M., The gut microbiota and healthy aging: a mini-review. *Gerontology* **2018**, *64*, 513-520.

17. Erny, D.; Hrabe de Angelis, A. L.; Jaitin, D.*, et al.*, Host microbiota constantly control maturation and function of microglia in the CNS. *Nat. Neurosci.* **2015**, *18*, 965-977.

18. Vaiserman, A. M.; Koliada, A. K.; Marotta, F., Gut microbiota: a player in aging and a target for anti-aging intervention. *Ageing Res. Rev.* **2017**, *35*, 36-45.

19. Magrone, T.; Jirillo, E., The interaction between gut microbiota and age-related changes in immune function and inflammation. *Immun. Ageing* **2013**, *10*, 1-6.

20. Cho, S. Y.; Kim, J.; Lee, J. H.*, et al.*, Modulation of gut microbiota and delayed immunosenescence as a result of syringaresinol consumption in middle-aged mice. *Sci. Rep.* **2016**, *6*, 1-22.

21. Turnbaugh, P. J.; Ley, R. E.; Mahowald, M. A.*, et al.*, An obesity-associated gut microbiome with increased capacity for energy harvest. *Nature* **2006**, *444*, 1027-1031.

22. Bischoff, S. C., Microbiota and aging. *Curr. Opin. Clin. Nut. Metab. Care* **2016**, *19*, 26-30.

23. Integrative HMP (iHMP) Research Network Consortium, The integrative human microbiome project: dynamic analysis of microbiome-host omics profiles during periods of human health and disease. *Cell Host Microbe* **2014**, *16*, 276-289.

24. Qin, J.; Li, R.; Raes, J.*, et al.*, A human gut microbial gene catalogue established by metagenomic sequencing. *Nature* **2010**, *464*, 59-65.

25. Donia, M. S.; Cimermancic, P.; Schulze, C. J.*, et al.*, A systematic analysis of biosynthetic gene clusters in the human microbiome reveals a common family of antibiotics. *Cell* **2014**, *158*, 1402-1414.

26. Medema, M. H.; Kottmann, R.; Yilmaz, P.*, et al.*, Minimum information about a biosynthetic gene cluster. *Nat. Chem. Biol.* **2015**, *11*, 625-631.

27. Wyatt, M. A.; Wang, W.; Roux, C. M.*, et al.*, *Staphylococcus aureus* nonribosomal peptide secondary metabolites regulate virulence. *Science* **2010**, *329*, 294-296.

28. Yoshimoto, S.; Loo, T. M.; Atarashi, K.*, et al.*, Obesity-induced gut microbial metabolite promotes liver cancer through senescence secretome. *Nature* **2013**, *499*, 97-101.

29. Saha, S.; Rajpal, D. K.; Brown, J. R., Human microbial metabolites as a source of new drugs. *Drug Discov. Today* **2016**, *21*, 692-698.

30. Geva-Zatorsky, N.; Alvarez, D.; Hudak, J. E.*, et al.*, In vivo imaging and tracking of host-microbiota interactions via metabolic labeling of gut anaerobic bacteria. *Nat. Med.* **2015**, *21*, 1091-1100.

31. Tra, V. N.; Dube, D. H., Glycans in pathogenic bacteria: potential for targeted covalent therapeutics and imaging agents. *Chem. Commun.* **2014**, *50*, 4659-4673.

32. Liang, Y.; Jiang, X.; Yuan, R.*, et al.*, Metabolism-based click-mediated platform for specific imaging and quantification of cell surface sialic acids. *Anal. Chem.* **2017**, *89*, 538-543.

33. Wang, W.; Zhu, Y.; Chen, X., Selective imaging of gram-negative and gram-positive microbiotas in the mouse gut. *Biochemistry* **2017**, *56*, 3889-3893.

34. Saxon, E.; Bertozzi, C. R., Cell surface engineering by a modified Staudinger reaction. *Science* **2000**, *287*, 2007-2010.

35. Clark, E. L.; Emmadi, M.; Krupp, K. L.*, et al.*, Development of rare bacterial monosaccharide analogs for metabolic glycan labeling in pathogenic bacteria. *ACS. Chem. Biol.* **2016**, *11*, 3365-3373.

36. Beisel, C. L.; Afroz, T., Rethinking the hierarchy of sugar utilization in bacteria. *J. Bacteriol.* **2016**, *198*, 374-376.

37. Denton, B. L.; Diese, L. E.; Firkins, J. L.*, et al.*, Accumulation of reserve carbohydrate by rumen protozoa and bacteria in competition for glucose. *Appl. Environ. Microbiol.* **2015**, *81*, 1832-1838.

38. Monod, J., The growth of bacterial cultures. *Annu. Rev. Microbiol.* **1949**, *3*, 371-394.

39. Ryan, C. S.; Kleinberg, I., A comparative study of glucose and galactose uptake in pure cultures of human oral bacteria, salivary sediment and dental plaque. *Arch. Oral Biol.* **1995**, *40*, 743-752.

40. Csiszovszki, Z.; Krishna, S.; Orosz, L.*, et al.*, Structure and function of the D-galactose network in enterobacteria. *MBio.* **2011**, *2*, e00053-11.

41. Sasaki, M.; Teramoto, H.; Inui, M.*, et al.*, Identification of mannose uptake and catabolism genes in *Corynebacterium glutamicum* and genetic engineering for simultaneous utilization of mannose and glucose. *Appl. Microbiol. Biotechnol.* **2011**, *89*, 1905-1916.

42. Sharma, V.; Smolin, J.; Nayak, J.*, et al.*, Mannose alters gut microbiome, prevents diet-induced obesity, and improves host metabolism. *Cell Rep.* **2018**, *24*, 3087-3098.

43. Brinkkotter, A.; Kloss, H.; Alpert, C.*, et al.*, Pathways for the utilization of *N*-acetyl-galactosamine and galactosamine in *Escherichia coli*. *Mol. Microbiol.* **2000**, *37*, 125-135.

44. Uhde, A.; Youn, J. W.; Maeda, T.*, et al.*, Glucosamine as carbon source for amino acid-producing *Corynebacterium glutamicum*. *Appl. Microbiol. Biotechnol.* **2013**, *97*, 1679-1687.

45. Moye, Z. D.; Burne, R. A.; Zeng, L., Uptake and metabolism of *N*-acetylglucosamine and glucosamine by *Streptococcus mutans*. *Appl. Environ. Microbiol.* **2014**, *80*, 5053-5067.

46. Revilla-Nuin, B.; Reglero, Á.; Martínez-Blanco, H.*, et al.*, Transport of *N*-acetyl-D-mannosamine and *N*-acetyl-D-glucosamine in *Escherichia coli* K1: effect on capsular polysialic acid production. *FEBS Lett.* **2002**, *511*, 97-101.

47. Nilsson, I.; Grove, K.; Dovala, D.*, et al.*, Molecular characterization and verification of azido-3,8-dideoxy-d-manno-oct-2-ulosonic acid incorporation into bacterial lipopolysaccharide. *J. Biol. Chem.* **2017**, *292*, 19840-19848.

48. Rinninella, E.; Raoul, P.; Cintoni, M.*, et al.*, What is the healthy gut microbiota composition? A changing ecosystem across age, environment, diet, and diseases. *Microorganisms* **2019**, *7*, 1-22.

49. Roszyk, E.; Puszczewicz, M., Role of human microbiome and selected bacterial infections in the pathogenesis of rheumatoid arthritis. *Rheumatology* **2017**, *55*, 242-250.

50. Arthur, J. C.; Jobin, C., The complex interplay between inflammation, the microbiota and colorectal cancer. *Gut microbes* **2013**, *4*, 253-258.

51. Claesson, M. J.; Cusack, S.; O'Sullivan, O.*, et al.*, Composition, variability, and temporal stability of the intestinal microbiota of the elderly. *Proc. Natl. Acad. Sci. USA* **2011**, *108*, 4586-4591.

52. Dumont, A.; Malleron, A.; Awwad, M.*, et al.*, Click-mediated labeling of bacterial membranes through metabolic modification of the lipopolysaccharide inner core. *Angew. Chem. Int. Ed. Engl.* **2012**, *51*, 3143-3146.

53. Yi, W.; Liu, X.; Li, Y.*, et al.*, Remodeling bacterial polysaccharides by metabolic pathway engineering. *Proc. Natl. Acad. Sci. USA* **2009**, *106*, 4207-4212.

54. Kaewsapsak, P.; Esonu, O.; Dube, D. H., Recruiting the host's immune system to target *Helicobacter pylori*'s surface glycans. *Chembiochem.* **2013**, *14*, 721-726.

55. Haldon, E.; Nicasio, M. C.; Perez, P. J., Copper-catalysed azide-alkyne cycloadditions (CuAAC): an update. *Org. Biomol. Chem.* **2015**, *13*, 9528-9550.

56. Himo, F.; Lovell, T.; Hilgraf, R.*, et al.*, Copper(I)-catalyzed synthesis of azoles. DFT study predicts unprecedented reactivity and intermediates. *J. Am. Chem. Soc.* **2005**, *127*, 210-216.

57. Kolarovic, A.; Schnurch, M.; Mihovilovic, M. D., Tandem catalysis: from alkynoic acids and aryl iodides to 1,2,3-triazoles in one pot. *J. Org. Chem.* **2011**, *76*, 2613-2618.

58. Baskin, J. M.; Prescher, J. A.; Laughlin, S. T.*, et al.*, Copper-free click chemistry for dynamic in vivo imaging. *Proc. Natl. Acad. Sci. USA* **2007**, *104*, 16793-16797.

59. Wang, Q.; Chan, T. R.; Hilgraf, R.*, et al.*, Bioconjugation by copper(I)-catalyzed azide-alkyne [3 + 2] cycloaddition. *J. Am. Chem. Soc.* **2003**, *125*, 3192-3193.

60. Link, A. J.; Tirrell, D. A., Cell surface labeling of *Escherichia coli* via copper(I)-catalyzed [3+2] cycloaddition. *J. Am. Chem. Soc.* **2003**, *125*, 11164-11165.

61. Goddard-Borger, E. D.; Stick, R. V., An efficient, inexpensive, and shelf-stable diazotransfer reagent: imidazole-1-sulfonyl azide hydrochloride. *Org. Lett.* **2007**, *9*, 3797-3800.

62. Zaro, B. W.; Batt, A. R.; Chuh, K. N.*, et al.*, The small molecule 2-azido-2-deoxy-glucose is a metabolic chemical reporter of *O*-GlcNAc modifications in mammalian cells, revealing an unexpected promiscuity of *O*-GlcNAc transferase. *ACS Chem. Biol.* **2017**, *12*, 787-794.

63. Stubbs, K. A.; Macauley, M. S.; Vocadlo, D. J., A selective inhibitor Gal-PUGNAc of human lysosomal beta-hexosaminidases modulates levels of the ganglioside GM2 in neuroblastoma cells. *Angew. Chem. Int. Ed. Engl.* **2009**, *48*, 1300-1303.

64. Ávalos, M.; Babiano, R.; Cintas, P.*, et al.*, Synthesis of sugar isocyanates and their application to the formation of ureido-linked disaccharides. *Eur. J. Org. Chem.* **2006**, *2006*, 657-671.

65. Fondy, T. P.; Roberts, S. B.; Tsiftsoglou, A. S.*, et al.*, Haloacetamido analogs of 2-amino-2-deoxy-D-glucose and 2-amino-2-deoxy-D-galactose. Syntheses and effects on the friend murine erythroleukemia. *J. Med. Chem.* **1978**, *21*, 1222-1225.

66. Laughlin, S. T.; Bertozzi, C. R., Metabolic labeling of glycans with azido sugars and subsequent glycan-profiling and visualization via Staudinger ligation. *Nat. Protoc.* **2007**, *2*, 2930-2944.

67. Pouilly, S.; Bourgeaux, V.; Piller, F.*, et al.*, Evaluation of analogues of GalNAc as substrates for enzymes of the mammalian GalNAc salvage pathway. *ACS Chem. Biol.* **2012**, *7*, 753-760.

68. John, J. V.; Uthaman, S.; Augustine, R.*, et al.*, Biomimetic pH/redox dual stimuli-responsive zwitterionic polymer block poly(L-histidine) micelles for intracellular delivery of doxorubicin into tumor cells. *J. Polim. Sci. Pol. Chem.* **2017**, *55*, 2061-2070.

69. Shirazi, R. S.; Ewert, K. K.; Leal, C.*, et al.*, Synthesis and characterization of degradable multivalent cationic lipids with disulfide-bond spacers for gene delivery. *Biochim. Biophys. Acta* **2011**, *1808*, 2156-2166.